Urban Land Use Modelling From Classified Satellite Imagery

T. Victor Mesev

Submitted for the degree of Ph.D in Geography at the University of Bristol, England

January 1995

DECLARATION

This thesis is the original independent work of the candidate, except where acknowledgement is given, and has not previously been submitted for a degree in this, or any other university.

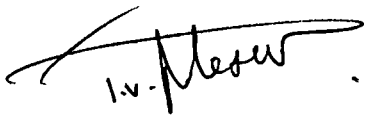

Victor Mesev
January 1995

ABSTRACT

Models derived from integrated geographical information systems (GIS) and remote sensing (RS) are fast becoming preferred vehicles for measuring and analysing complex spatial features on the Earth's surface. The appeal of these models undoubtedly lies in their ability to not only reliably detect and measure surface characteristics of large areas on a regular and consistent basis, but also to perform complex and comparative spatial analyses of these measurements. Above all, integrated GIS/RS models bring together the mapping qualities of remote sensing with the flexible analytical operations from geographical information systems.

The integrated GIS/RS framework used in this thesis is rigorously applied to the spatial interpretation of urban areas by the successful combination of satellite imagery with disaggregate surfaces of socioeconomic information held by a GIS. This approach is in the form of a 3-point image classification strategy which uses these socioeconomic surfaces as (i) a source of ancillary information for training sample selection, (ii) criteria for postclassification sorting, and (iii) a means for developing a Bayesian approach to the maximum likelihood classifier by varying prior probabilities of class occurrence. The strategy represents unique GIS/RS integration breakthroughs in the field of urban image classification by bringing together the potential of satellite imagery to capture the physical layout of built structures with the abilities of GIS to model corresponding socioeconomic attributes. Given that satellite images of urban areas suffer from severe spectral mixing caused by surface heterogeneity, this strategy is a way forward in reducing confusion between land cover types and increasing the amount of information on land use types.

The resulting classification inventory consists of a series of urban land use categories that focus on the measurement of residential density defined by discrete dwelling types. The inventory represents an improvement in classification accuracy over conventional methods, as well as providing a convenient source for subsequent urban analysis. It is this analytical framework which is explored in the second part of the thesis. Basically, classified land use patterns are used as derived data in modelling the manner in which settlements grow and the way density of land use varies within the urban area and with time. The process involves converting multitemporal classified land use coverages into binary surfaces arrayed on fine grids with resolutions of approximately 20 and 30 meters. From this, the shape and extent of urban development are determined by considering both the absolute amount of space within the total available which is filled by a land use, and the rate at which space is filled with respect to distance from the central point of the settlement. Both of these are measured in accordance with recent breakthroughs in urban spatial analysis which note that the form and growth of cities can be interpreted as exhibiting properties of a fractal nature. Attenuation in the density of land use is modelled by power functions, which are the only urban density functions that embody the essential fractal properties of self-similarity and scale independence.

The generation of thematic land use coverages by image classification and their subsequent modelling using fractal concepts are carried out on empirical data pertaining to four settlements in the United Kingdom at two time points. The benefits of the methodology lie in the ability of classified satellite data to rapidly, accurately and consistently capture urban land use patterns over wide areas, and in the abilities of fractal analysis to routinely monitor changes in urban development through a more flexible geometry of urban land use patterns.

The wider scope of this thesis can be related to the profound changes that are taking place in urban geography, particularly in the location of industrial and retail activities, and shifts in the population distribution. Only through accurate and consistent measurement and analysis of the urban fabric can these phenomena be carefully monitored and assessed, and appropriate land use policies prescribed.

ACKNOWLEDGEMENTS

I would first like to thank Paul Longley for his support and assistance in the supervision of this thesis. Special thanks also go to Mike Batty (SUNY-Buffalo) and Yichun Xie (East Michigan) for help in Chapter Four, and to Ed Thomas and Chris Kidd for support on some of the computing matters.

Last, but by no means least, I would like to thank and dedicate this thesis to Lynn and Emily, without whom this thesis would not have been as enjoyable or worthwhile. One of them read, commented and provided useful suggestions, the other kept me on my toes through most of the process.

CONTENTS

LIST OF TABLES

LIST OF FIGURES

URBAN LAND USE MODELLING FROM CLASSIFIED SATELLITE IMAGERY

Chapter One
INTRODUCTION

1.1 Introduction

The inspiration for this thesis derives from major advances in the links between the two most powerful technologies for digital spatial data collection and handling, namely, *geographical information systems* (GIS) and *remote sensing* (RS). Traditionally, remote sensing has played the role of a mere source for frequently-updated thematic information in this partnership, which some observers have claimed may have even delayed a more symbiotic integration (Marble *et al.*, 1983, Barker, 1988). However, major advances in data organisation and data matching over the last decade have led to more robust and flexible databases, this time shared by both technologies, in which the flow of data now proceeds in both directions (Ehlers *et al.*, 1989). Indeed, present achievements in the coupling of GIS and remote sensing have irrefutably outweighed inherent problems, such as data compatibility, and spatial integrity (comprehensive reviews can be found in Star *et al.*, 1991). From a user stand-point, advances in the development of proprietary *integrated GIS and image processing systems* (IGIS) have allowed data from both technologies to be processed simultaneously within a fully operational analytical framework (Zhou, 1989; Davis and Simonett, 1991; Gahegan, 1994). However, computational, statistical, and institutional issues dealing with the integration of GIS and remote sensing are far from complete or satisfactory (Ehlers *et al.*, 1991; Faust *et al.*, 1991; Lauer *et al.*, 1991). Continued research is seen widely to be essential not only for improved integration, but also for the very existence of GIS and remote sensing as leading technologies in spatial data handling.

From this starting platform, intensive focus will be given to one of the more pressing issues of GIS/remote sensing integration, that of improved classifications of spatial features (Hutchinson 1982; Mason *et al.*, 1988). The goal is to use satellite imagery and socioeconomic data within a GIS to generate detailed surfaces of urban land use and land cover that represent advances, both spatially and aspatially, in the field of urban image classification - spatially, in terms of how well image classified data correspond to real urban land cover patterns, and aspatially, in terms of how well urban land use categories are defined by socioeconomic information. These objectives are clearly mutually inter-dependent, and represent the essence of an

innovative technique in *urban image classification.* The technique stems from work pioneered by Strahler (1980) on modifications to the maximum likelihood classification algorithm through variable prior probabilities of class occurrence. As such, these modifications have been loosely related to the probability mechanics of Bayesian statistics, and in this respect the technique is frequently known as a *Bayesian-type classification*, or the *Bayesian decision rule* (Strahler, 1980; Mather, 1985; Maselli *et al.*, 1992). Statistically, the decision rule is able to link the robustness of the parametric maximum likelihood classifier with the flexibility of the non-parametric assumptions of class prior probabilities. Although the rule has been documented since just before 1980, only recently has it been applied to the classification of urban areas, most notably as a means of weighting urban classes through image segmentation (Barnsley *et al.*, 1989).

In this thesis, the decision rule will form part of an urban classification strategy that will be built around, and informed by, disaggregated surfaces of socioeconomic data. These surfaces are generated by a point-based areal interpolation algorithm developed by Bracken and Martin (1989). The classification strategy is designed to realise the potential of these surfaces to generate more detailed thematic coverages of the morphology of urban land use. Specifically, surfaces of socioeconomic data are used in image classification as a source of ancillary information for a supervised method employing training samples (Quarmby *et al.*, 1988), as criteria for postclassification sorting (Hutchinson, 1982), as well as a means for varying prior probabilities of the maximum likelihood discriminant function (Strahler *et al.*, 1978; Strahler, 1980). The strategy will attempt to embrace the ideals of GIS/remote sensing integration by bringing together the potential of satellite imagery to capture the physical layout of urban structures and the abilities of GIS to model corresponding socioeconomic attributes. The resulting classification inventory will consist of a series of urban categories that, in all but one case, are designed to measure various urban *land use* characteristics. The exception is the class, "built-up" which is widely considered a *land cover* category. A discussion of the land use/land cover dichotomy will be provided later on in this chapter as part of the review of urban definitions. However, it is important to stress that for the sake of convenience, both the title of this thesis and all other references to urban land use, will assume the inclusion of this land cover category but will fully recognise its existence as a separate definitive entity.

The generation of discrete per-pixel classifications of urban areas has always been

plagued by inherent spatial variabilities and surface heterogeneity. What the proposed classification strategy, based around socioeconomic surfaces, essentially attempts to achieve is to increase the amount of information on the selection and generation of urban spectral classes. These classifications can then either remain as inventories of urban land use, which are vital to successful urban management and planning policies, or subsequently be used as input data for urban modelling. Although the latter application will form the basis of the second part of this thesis, it is worth emphasising the importance of urban inventories generated from satellite imagery in contemporary issues such as the monitoring of urban growth by suburbanisation, and decentralisation of industrial and commercial activities. In the same way, the results of urban modelling also provide a rich source of information that can be directly used in a variety of urban monitoring and planning policies.

Classified images of urban areas will here be used as derived data in modelling the manner in which settlements grow, and the way density of land use varies within the urban area and with time. Both urban growth and density will be measured using the established statistical framework of *urban population density functions* which reproduce the well-observed feature of diminishing urban density with distance from the centre (reviews in Haggett *et al.*, 1977; Marshall, 1989; Huxhold, 1991). However, unlike established work, the formulation of urban density functions in this thesis will follow recent breakthroughs in urban analysis, which suggest that the form and growth of urban areas can be interpreted as basically exhibiting properties of a *fractal* nature. These advancements in the application of fractal models in the measurement of the extent and shape of urban areas are conveniently summarised by the works of Frankhauser (1994) and Batty and Longley (1994). Without entering into new research, fractal concepts will here be used primarily to *reformulate* urban density functions by positing the *inverse power model* is the only function which embodies the fractal properties of self-similarity and scale independence (Blackledge, 1993).

The central theme of this thesis can now be summarised as linking the generation of inventories of urban land use from integrated GIS and image classification, and their application to the modelling of urban growth and density. Furthermore, satellite data will also be assessed and evaluated in comparison with traditional sources of data used for estimating urban density functions. Comparisons should reveal that satellite data allow greater precision, cover wider areas, and arguably, are most appropriate to

fractal modelling. More appropriate in the sense that the inherent spatial irregularities associated with urban areas and assumed as fractal, are represented by classified satellite imagery of varying spatial resolutions that exhibit a similar amount of spatial irregularity (initial work by Goodchild and Mark, 1987; De Cola 1989; 1993). One other advantage of frequently gathered and updated satellite imagery over other less consistently modified data sets, involves the ability to perform regular and routine definitions and subsequent comparisons of urban form and land use density between various settlements.

Within the confines of image availability, and with respect to previous work, four settlements- Bristol, Norwich, Swindon and Peterborough, will form the basis of all empirical comparisons. Without exceeding the spectral limitations of satellite imagery, each of these urban areas will be classified into eight different categories of urban land use in order to demonstrate the successful operations of the classification strategy outlined earlier. The first four categories, "urban" (as defined by the UK Office of Population Censuses and Surveys), "built-up", "residential", and "non-residential" are established classification goals, and should present the least amount of difficulty. However, four sub-categories of residential dwellings, namely, "detached", "semi-detached", "terraced", and high-rise "apartment" blocks, which are essentially surrogates for residential density, are less discernible from standard urban spectral pattern recognition. Here, the use of many, more representative training samples, postclassification sorting, along with the potential of applying areal estimates from the Bayesian decision rule, should succeed in creating more separate spectral classes which represent each of these four dwelling types. However, it must be stressed that the inherent spectral heterogeneity associated with images of urban areas is very much a constraint on high-precision image classification. Indeed, what this classification strategy attempts to achieve, is to demonstrate the potential of disaggregate surfaces of socioeconomic data in increasing the accuracy of per-pixel urban classifications over more conventional methods.

In summary, this thesis is dedicated not solely to image classification, but also to the *role* of classified satellite imagery as potentially the most appropriate data source for the routine derivation and testing of urban density functions modelled by fractal parameters.

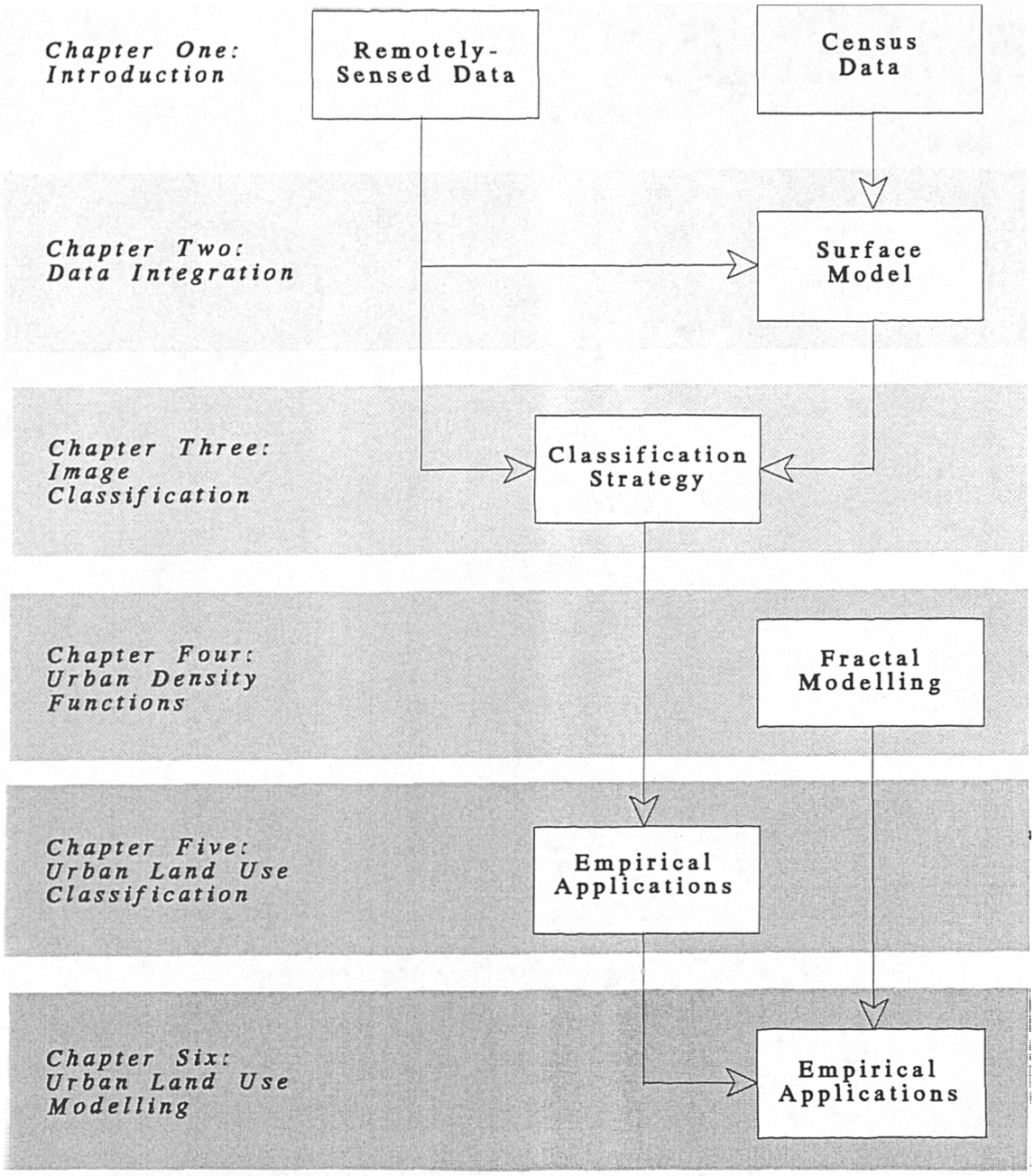

Figure 1.1 Thesis Layout

1.1.1 Thesis Outline

The thesis follows very much an inductive approach in the research of its two major fields of study:

1) Classification of satellite imagery.

2) Urban density modelling.

The results from the first essentially provide a data source for analysis in the second (Figure 1.1). The classification of satellite imagery is applied to urban landscapes, and is an exercise in the coupling of satellite imagery with census data resident in a GIS. The coupling process specifically concentrates on the development of an innovative technique for the classification of urban land and urban morphology. This technique attempts to merge spectral data from urban land cover characteristics with socioeconomic data defining land use, and is composed of three steps. The first of these involves the selection of class training statistics with the assistance of disaggregate, rasterised surfaces holding census information. Secondly, a Bayesian-type modification to the conventional maximum likelihood algorithm is developed which accepts the census information as the *a priori* probabilities of the occurrence of urban classes. Lastly, post-classification sorting is used to assist in image segmentation which is essential for the complete statistical functioning of the Bayesian decision rule.

The second direction of research involves the spatial modelling of the shape and density of these classified urban categories. The modelling process is based on fractal theory in which densities are first examined in terms of the amount of urban space filled at different distances from fixed points, and then fitted using inverse power functions. The incorporation of digital urban surfaces from classified remotely-sensed images departs from conventional urban density modelling in a number of ways. Firstly, satellite imagery allows analysis of not only urban land use, but also various sub-divisions of urban land that can be built-up, non-residential, and residential. Secondly, the frequent and relatively inexpensive cost of acquiring satellite imagery allows more consistent comparisons to be made between settlements both spatially and temporally. Furthermore, satellite technology represents data that are digital and at relatively higher resolution, allowing for a reasonable interpretation

of land surfaces, which are also amenable to rapid computer processing.

The remainder of Chapter One introduces both classification and urban modelling ideas, and provides the requisite background in the way urban land is defined, measured, classified, analysed, and modelled. The second chapter focuses on the integration of remotely-sensed data with census information resident in a GIS. Particular emphasis there is given to data and positional integration, but even more importantly to the role of census data in improving image classifications. The in-house image classification strategy, built around the use of socioeconomic surfaces, is developed in Chapter Three both conceptually and with a view to empirical implementation. The second line of research, that of urban density functions, is covered in Chapter Four. Here, concepts from fractal theory and inverse power functions are examined as a means of modelling the shape and density of urban land use. Chapter Four also includes a discussion of the urban form of Taunton in Somerset, comparing an idealised fractal model to the empirical source derived from satellite imagery. The comparison forces a reassessment of the data sources traditionally used in urban density modelling and paves the way for the incorporation of classified satellite images into the modelling process. The generation of surfaces of urban land use and land cover from empirical data of the four main settlements-Bristol, Norwich, Swindon, and Peterborough, are contained in Chapter Five, where satellite imagery, corresponding as closely as possible to the 1981 and 1991 Censuses, were obtained for each of these urban areas. Practical considerations limited the subsequent assessment of classification accuracy to Bristol, where results are generated under scenarios of variable and equal class prior probabilities. Classified urban surfaces are then exposed, in Chapter Six, to fractal modelling, density measurements and profile plots using the methods outlined in Chapter Four. Results are further contrasted with those generated by a more conventional data source, that of digitised urban boundaries from topographic source maps. Lastly, all work is summarised and discussed in Chapter Seven with a view for developing future research. A general layout of chapters and major areas of research is given by Figure 1.1.

1.1.2 Research Statements

This thesis addresses many issues and concerns in the classification and modelling of urban morphology, but concentrates on four main areas of specific research interest:

1. Exploring the potential of linking satellite data with surfaces of socioeconomic information.

2. Assessing the sensitivity of the Bayesian decision rule in urban image classification.

3. Assessing the role of classified satellite data for the application of fractal-led urban density functions.

4. Monitoring the population and density profiles of various urban categories between settlements and through time.

Before any of these areas can be fully examined, a few background clarifications are necessary in exactly what and how the urban landscape is defined, measured, classified and modelled.

1.2 Definitions of Urban

In the most general sense, *urban* has been defined as,

"...any nucleated human settlement whose inhabitants are supported chiefly by non-agricultural pursuits." (Marshall, 1989, p. 3).

However, with the rapidly receding populations engaged in agriculture in the developed world, this definition has been generally superseded by criteria based on minimum population size. Unfortunately, minimum population size is an arbitrary figure, sometimes influenced by bureaucratic boundaries, that has been interpreted quite differently between countries. For example, 2,500 is the minimum size for a settlement to be considered urban in the USA, but this threshold is as much as 30,000 in Japan, or as little as 200 in Denmark.

A discussion of the merits of various definitions of urban will not be pursued here. Instead, the physical recognition of the more objective definition of *built-form* will be mapped using satellite imagery, with labels of various types of built-up land provided by census data from the Office of Population Censuses and Surveys (OPCS). In this respect, distinctions will be made on the way *urban* land can be defined and measured

between satellite and census data. From the onset it must be stressed that satellite data are only able to measure the *physical* coverage of the earth's surface, while census data are based primarily on the way this surface is *occupied* by humans. This distinction alludes to the often confused terms of "land cover" and "land use", terms which have all too frequently been mis-defined and used interchangeably. Land cover refers to the physical layout of the landscape as it appears to someone observing the earth from a distance (e.g. in remote sensing). Land use, on the other hand, although composed of various land cover types, generally infers some anthropogenic activities not readily observable from a distance. One of the prime objectives of this thesis is to attempt to combine both definitions by incorporating land use descriptions from the Census with land cover types derived from satellite data. Image classification provides a convenient framework within which this essentially matching process will be carried out. However before image classification can be reviewed, it is important to first clarify both types of urban definitions, from the Census and from remote sensing.

1.2.1 DoE/OPCS

For this work, the definitions of all land uses pertaining to the urban environment will correspond with those used in the last two UK Population Censuses, 1981 and 1991 (OPCS, 1984; 1991; DoE, 1991). Both provide easily available census data, as well as comparable satellite imagery.

"The starting point in the definition of urban areas is the identification of areas with land use which is irreversibly urban in character..." (OPCS, 1984:9).

The above statement adopted by both the Department of the Environment (DoE) and the OPCS illustrates the first problem in matching census information with satellite data. Whereas imaged data are very much an objective measurement of physical spectral reflectance handled by statistical techniques, the definition of urban by the Census is shrouded in subjective bureaucratic decisions, for instance,

"Land included as urban comprises: permanent structures and the land on which they are situated; transport corridors (roads, railways and canals) which have built-up sites on one or both sides or which link built-up sites which are less than 50 metres apart; transportation features such as railway yards, motorway service areas, car parks as well as operational airfields and airports; mineral workings, and any area completely surrounded by built-up sites. Areas such as playing fields and golf courses are excluded unless they are completely surrounded by built-up sites." (OPCS, 1984:9).

This full definition of "urban" also states that,

"...the prerequisite for the recognition of an urban area is a continuous area of urban land extending for 20 ha. or more. Also, separate areas of urban land are linked if less than 50m apart." (OPCS, 1984:10).

However, the critical factor in the recognition of an urban area is documented as the minimum population of approximately 1000 persons. Although all parts of the OPCS definition of an urban area include some objective measurement criteria, the overall description can not be completely replicated by satellite image interpretation. Instead, less subjective definitions of urban land use are needed which can be directly related to the physical layout of urban morphology. Census data recording *residential dwelling types* represent land uses which can be more precisely defined and spatially measured. However, even this more objective land use criterion is still heavily dependent on the inference of land cover characteristics from satellite imagery. This, in turn, is heavily dependent on the statistical feasibility of spectral data and the inherent patterns of spectral classes.

1.2.2 Spectral Classes

As a contrast to activity-based definitions of urban land use, satellite sensors are limited to the observation of the physical properties of urban land cover. Instead of a land use category such as "residential", satellite data are capable only of observing the type and amount of surface materials that might constitute a residential category. These materials may be roofing tiles and brick for the building structure, and vegetation, concrete or Tarmac for gardens and driveways. Satellite sensors are able to recognise these materials by measuring the amount of incident electromagnetic energy they reflect rather than the amount they absorb and transmit. Applying the principle of conservation of energy, the interrelationship between these energy interactions can be represented as an energy balance,

$$E_I(\lambda) = E_R(\lambda) + E_A(\lambda) + E_T(\lambda) \qquad (1.1)$$

where E_I denotes the incident energy, E_R denotes the reflected energy, E_A denotes the absorbed energy, and E_T denotes the transmitted energy, with all energy components being a function of electromagnetic wavelength, λ. Most land observation satellite systems operate in the wavelength regions in which reflected energy predominates,

$$E_R(\lambda) = E_I(\lambda) - [E_A(\lambda) + E_T(\lambda)] \quad (1.2)$$

stating that reflected energy is equal to the energy incident on a given feature reduced by the energy absorbed or transmitted by that feature (Lillesand and Kiefer, 1987). The amount of reflected energy is strongly affected by the composition and geometric form of the surface feature. Water and vegetation are able to absorb more energy than denser built structures and thus less energy will be reflected back to the satellite sensor. Surface roughness is a factor in the amount of incident energy that is dispersed away from the sensor. For instance, smoother surfaces, such as flat roofs, allow the angle of reflectance to approach the angle of incidence, resulting in less dispersion and greater reflectance. As a contrast, rougher surfaces, such as heavily mixed urban building types, produce greater dispersion and less reflectance. It must be stressed, however, that surface roughness is dictated by the wavelength of incident energy and, as a rule, a surface is rough if the wavelength is much smaller than the surface height variations or the particle size that make up the surface (Jensen, 1986).

The reflectance characteristics of surface features detected by satellite images can be quantified by measuring the proportion of incident energy that is reflected. This is measured as a function of wavelength and is called spectral reflectance, $p\lambda$,

$$p\lambda = \frac{E_R(\lambda)}{E_I(\lambda)} = \frac{\text{energy of wavelength } \lambda \text{ reflected from the object}}{\text{energy of wavelength } \lambda \text{ incident upon the object}} \times 100 \quad (1.3)$$

where $p\lambda$ is expressed as a percentage.

The sensor records energy at different wavelengths to ensure the greatest amount of contrast between surfaces. Two features may be virtually indistinguishable in one wavelength range but very different in another. Wavelength bands are selected to coincide with high reflectance of specific surface features. For example, bands 1, 2 and 3 on board Landsat-5 TM are designed to distinguish, among others, the physical manifestations of human construction and settlement. Basically, the proportion of spectral reflectance received by the satellite sensor is a function of the composition and geometric form of the surface feature, as well as the area of the electromagnetic spectrum and the atmospheric conditions in which it is sensed. Over urban areas, spectral reflectance is complicated by the intricate variabilities and spatial irregularities of buildings as well as mixed land covers associated with gardens, roads,

thoroughfares, driveways, and so on. The complex nature of urban areas invariably forces many *pixels* (the smallest element of an image) to represent spectral reflectance characteristics of several land cover types. This phenomenon is known as the mixed pixel (*mixel*) problem, and is at the heart of urban classifications reproduced through remotely-sensed images.

The categorisation or classification of satellite data, based on the spectral reflectance of each discrete pixel, produces what are known as *spectral classes.* Simply put, these are groups of pixels with similar spectral values which are inherent in the image (Jensen, 1986). Spectral confusion associated with mixels of images over urban areas invariably leads to lower separability in spectral classes. It is here that external, non-spectral data are vitally needed to attempt to distinguish urban spectral classes, and improve categorisation. The inclusion of external data, known as *ancillary data*, into the spectral classification process forms the cornerstone of all supervised classification techniques. The effect is to convert spectral classes, which are based solely on land cover, into *information classes* that incorporate what we know about both land cover and land use.

1.2.3 Information Classes

The translation of spectral classes into information classes is controlled by the analyst usually within some predetermined classification scheme (see also section 1.4.2.5). An example may clarify the critical nature of the conversion. In a remotely-sensed image of an urban area, there may only be a few pure pixels representing single land cover types, typically, asphalt and Tarmac roads, concrete, brick and metal structures, tiled roofing, as well as vegetation, soil and water. Many other pixels will be composed of spectral values that are a function of the reflectance from mixtures of these cover types. A classification based purely on spectral data may produce categories such as (1) concrete, (2) vegetation, (3) mixture of concrete and vegetation, and so on. Unfortunately, few planners or administrators want to see a map labelled with such classes. They would prefer mixture classes to be renamed with more standard labels, such as single-family residential, or even detached, semi-detached or terraced residential. The translation process is essentially one of converting *measures* of land cover into *descriptions* of land use. However, descriptions of land use are open to subjective human interpretation and are also greatly influenced by the available knowledge of the study area. Fortunately, a number of standardised

classification schemes have been developed for use with remotely-sensed data (section 1.4.2.5). These schemes have been designed to aid the analyst in labelling spectral classes as well as providing a means for consistent comparisons. The definition of urban categories from remotely-sensed data is not only a matter of interpretation and description of spectral classes, but also a function of the measurement capabilities of satellite sensors and images. The scale at which sensors capture reflected energy plays an important, and limiting part in determining the proportions of materials found within the scene and within each pixel. Only if sensor and image parameters are understood, can spectral classes then be correctly re-labelled as information classes.

1.3 Urban Measurements

The previous section outlined the differences in the way in which urban attributes are defined between the Census and remotely-sensed data. Once definitions of urban land use from both data sets are established within a common framework, the next step in the outline of an integration program deals with the way each data source is able to measure the urban landscape.

Both sources of data, census and remotely-sensed, are essentially areal-based representations, subjected to some form of data aggregation to a common spatial entity. These areal units are enumeration districts (EDs) for the Census, and pixels for remotely-sensed data. However, the scale and type of measurement between the two data sets are far from similar or immediately compatible. EDs are spatially represented by zones of irregular size and shape, while digital satellite data are at a much finer spatial resolution with each pixel represented by regular raster-based structures. The objectives of the classification strategy adopted in this thesis is contingent upon an adequate spatial compatibility of census and satellite data. With this in mind, a smoothing algorithm will be examined as a means of converting census EDs into a more compatible surface of finer, regular areal units, in other words, a rasterisation of EDs. Census data in this form would then be more amenable to integration with similar raster-based data representations from satellite imagery within a GIS framework.

1.3.1 UK Population Census

The most important and most widely used source of socioeconomic and housing data in the UK is the decennial Census of Population held as *Small Area Statistics* (SAS) and *Local Based Statistics* (LBS) by the Census Division of the OPCS. A general review of the application of census data can be found in Rhind (1983) and Dale and Marsh (1993). In this thesis, census statistics will be exclusively used as supplemental data to improve the image classification of urban morphology. To this end, Chapter Two will fully review existing research into the use of census data in image classification. This chapter will also introduce the areal interpolation algorithm which will spatially represent census data in a form that will be integrated into the classification strategy in Chapter Three.

Briefly, the spatial interpolation algorithm was developed by Bracken and Martin (1989), and is essentially derived from point-based aggregated census data. The points in its spreading function are associated with the geographical coordinates of the *centre of mass*, or population-weighted ED centroids. The authors named the algorithm a *population surface model*, but as this application is predominantly based on housing data, the adapted algorithm will simply be referred to as the *surface model.*

This section will now quickly highlight those pertinent issues concerning the measurement, collection, and geographical representation of census data, which are vital to understanding and satisfying the distributional assumptions behind the surface model. The discussion particularly focuses on the problems with direct temporal comparisons between the 1981 and 1991 Censuses. These problems will need to be overcome in order for census data to be reliable and consistent elements in the classification strategy.

1.3.1.1 Collection of Census Data

Household responses are collected and aggregated into EDs, the smallest zone of census geography. EDs are defined as the area covered by a single census official, or enumerator, and typically contain 200 households or 450 to 500 persons. In order to lessen the risk of inadvertent disclosure of information in exceptionally small EDs, SAS will not be released for areas with less than 50 residents and/or 16 resident

households. Statistics for such restricted EDs are merged with a contiguous ED, provided that the total number of residents and households of the amalgamation exceed the same minimum thresholds (OPCS, 1984). Since the last Census, on the night of 21/22 April 1991, approximately 9,000 census counts (variables) have been compiled for the SAS database representing some 110,000 EDs in England. This compares with only 4,500 counts for similar areas in 1981. In addition, the 1991 LBS database provides 20,000 counts of information, but only at the local authority Ward level (UMRCC, 1989; MCC, 1992). As on previous occasions, new questions were introduced into the 1991 Census and old ones were modified in order to reflect changing social attitudes and current economic situations. For example, counts for both "central heating", and the definition of "relationship to Head of Household" had no direct comparison with the 1981 Census (Martin, 1994).

1.3.1.2 Spatial Representation of Census Data

The second, and arguably more important issue for subsequent spatial analysis, concerns the way census data are spatially represented. The term "Census geography" refers to the hierarchical scale in which aggregated census data are spatially represented, with EDs as the smallest level, nesting into wards, districts, and finally counties as the largest zone. In this thesis, all mention of census data will be referenced at the ED level of spatial aggregation. Two issues dealing with the spatial representation of EDs are particularly important, namely the zonal nature of ED aggregation, and the effects of ED boundary changes between Censuses (Martin, 1994). Both of these issues are critical to the successful implementation of the surface model, and consistent comparison between the results.

The first of these concerns the effects from the conventional practice of aggregating census data collected from individual households into areal units (EDs). Geographers have long understood the difficulties of interpreting area-based spatial representations, and the potentially misleading results associated with subsequent choropleth mapping where the value of a zone is assumed to be equal throughout its spatial extent. Any form of spatial aggregation of essentially point data commonly suffers from interpretative difficulties arising from the *ecological fallacy* and the *modifiable areal unit problem.* The ecological fallacy can be summarised by the fact that relationships observed at a particular level of aggregation do not necessarily hold for the individual observations. Similarly, the modifiable areal unit problem (MAUP)

recognises the effects on aggregation from changes in the scale of areal representation (Openshaw, 1984). Both concepts also stress that once census data are aggregated, there is no way in which the characteristics of individuals, by reference to their locations, can be retrieved as point data. This invariably means that any pattern in mapped areal data may be as much the result of the zoning system chosen for the data as of the underlying distribution of the mapped phenomenon itself (Martin, 1991). Furthermore, the spatial size and shape of EDs can vary considerably between those representing an average population of around 500 in urban areas and those with only 150 persons in rural areas (OPCS, 1991). ED boundaries are in most cases artificial but, where possible, attempt to follow logical boundaries, such as major roads, railways, and rivers. However, another problem with aggregated areal representations is the common problem of including large tracts of land that are not used for residential purposes or are not even part of an urban area. As a result, all the factors outlined in this section contribute to a less than realistic spatial distribution of population within EDs. Moreover, the ED boundaries are completely unrelated to the underlying residential distribution and the degree of distortion introduced through aggregation is both difficult to measure and control.

The second issue concerning the effect of areal representations on the geography of census data deals with the prospects for temporal comparisons between Censuses (Bracken and Martin, 1993). Being able to reliably and consistently compare changes in the socioeconomic characteristics of an area is vital for all urban monitoring and planning applications. However, inconsistencies between the 1981 and 1991 Censuses seriously limit direct and reliable comparisons. The problems with inconsistent number and definitions of census counts, already discussed, are further compounded by widespread changes in ED boundaries. Although boundaries were kept similar between the 1971 and 1981 Censuses, changes in collection policies seriously altered boundaries for the 1991 Census. The OPCS's attempt to eliminate by standardising the "difficulty" in enumerating an ED, along with rapid changes in residential developments (e.g. new estates, demolition) inevitably forced the majority of 1991 ED boundaries to be considerably different from those used in 1981.

These problems of spatial aggregation and inconsistent temporal representations of population distributions, unfortunately limit the usefulness of census data, in this form, as ancillary information in image classifications. ED information must first be converted into a more disaggregate spatial form which is both free from fixed areal

boundaries and is more representative of the real underlying population distribution. In other words, some form of spatial interpolation process is required to disaggregate EDs into finer resolution surfaces so that they are more responsive to residential land use patterns, and subsequent changes. Chapter Two will fully develop the Bracken-Martin surface model both statistically and as the vehicle for incorporating socioeconomic data into image classification. In this respect, the surface model will be used to produce data structures that can be most logically integrated with remotely-sensed imagery. Specifically, this thesis will highlight the unique abilities of this surface model to spatially represent census data by raster-based data structures at finer spatial resolutions with standardised cell dimensions.

1.3.2 Image Resolutions

Strictly speaking, the measurement of urban land from satellite imagery involves the whole process of digital thematic information extraction. However, spectral pattern recognition is dimensionalised by image resolution parameters, which directly affect thematic class discrimination. In consideration of this, it can be assumed that satellite images *recognise* urban land by the amount of spectral reflectance at various wavelengths of the electromagnetic spectrum. However, the precise *measurement* of the amount of spectral reflectance is primarily a function of the resolution of an image. *Resolution* has been defined as a

"...measure of the ability of an optical system to distinguish between signals that are spatially near or spectrally similar." (Swain and Davis, 1978:6).

There are four types of resolution: spectral, spatial, radiometric, and temporal. *Spectral resolution* refers to the dimension and number of wavelength intervals, or bands, in the electromagnetic spectrum to which the sensor is sensitive. A fine spectral resolution is considered to represent a narrow wavelength range, for example, band 3 of Landsat-5 TM, has a range from 0.63μm to 0.69μm. This band, like all others, is designed to sense specific surface characteristics, in this case chlorophyll absorption, as well as to identify certain man-made features. Both the selection and combination of spectral bands for use in image classifications are vitally important. An attempt should be made to not only maximise spectral contrast within the image by using as many bands as are available, but also to eliminate redundant data by excluding bands with similar variance. It is important to note that as reflected radiation reaches a satellite it passes through a number of components of the sensor

before being recorded. This has a smearing effect on the signal which can be determined by the *point-spread function* (PSF) of the sensor. The PSF integrates the spectral response of pixels with their surrounding neighbours to such an extent that as little as 50% of the radiation response can be attributed to a target pixel, the other 50% being drawn from surrounding pixels (Forster, 1980). Over spectrally complicated urban areas, the PSF can seriously affect the response values of minority class pixels. Finally, radiation reflected by urban surfaces tends to be weakened by higher amounts of haze or pollution in the atmosphere, particularly in larger cities (reference to these problems and possible solutions are beyond the scope of this thesis).

At any time, a sensor detects the radiation reflected and the radiation emitted from the surface within its *instantaneous field of view* (IFOV). The IFOV is determined by the instrument's optical system and the size of its detector element, and all radiation propagating toward the instrument within the IFOV contributes to the detector response at any instant. As such, the IFOV represents the dimension of the smallest unit of ground measurement which is later converted to the smallest unit of digital data, the pixel (Curran, 1985). Landsat-5 TM has most of its spectral bands at a *spatial resolution* of 30m by 30m, which means that one pixel in the image roughly represents the corresponding area of 30m by 30m on the ground. Fine spatial resolutions are able to reproduce greater detail of the earth's surface but can also limit the amount of energy reaching the sensor and hence reduce spectral contrast. The expected gains from the use of high spatial resolutions in urban mapping (Forster, 1985) have been somewhat discounted by increased intra-class variation and excessive spectral noise (Haack *et al.*, 1987). Appropriate spatial resolutions for urban areas vary substantially according to the way land is apportioned. Assuming a minimum of 4 pixels are needed from an image to identify or classify basic urban land parcels reliably. In which case, a sensor with an IFOV of 5 to 10m might be required for some parts of Asia, where urban areas are densely populated, but 30m may be adequate for some urban areas in the US, which are composed of more extensive land use parcels (Welch, 1982). As a rule the resolution of a pixel should be less than the diameter of the corresponding object to lessen mixel effects (Jensen, 1986). This however, is very difficult in urban areas where objects can vary greatly in size, orientation, and relationships with other objects.

The satellite image itself is composed of a two-dimensional array of discrete pixels.

Given an image's spectral and spatial resolutions, the intensity of each pixel corresponds to the average brightness or radiance measured electronically over the ground area corresponding to each pixel. The value of this radiance is represented by a digital number (DN) resulting from quantizing the original electrical signal from the sensor into positive integer values using a process called *analogue-to-digital* signal conversion. These DNs correspond to the average radiance measured in each pixel and are recorded over ranges which are then represented by binary computer coding scales (for example, $2^6 = 64$ radiance levels, $2^8 = 256$ radiance levels, and so on). The brightness levels of an 8-bit image are therefore 0 to 255 (256 greyscales). In other words, all the pixels in the image will have a digital number of between 0 and 255 representing black and white respectively with varying shades of grey in between. The quantifying of a continuous spectral reflectance into a discrete range is called the *radiometric resolution.* The integer values of each pixel can now be statistically manipulated, with the aid of a computer, to produce meaningful information including the categorisation of pixels into thematic, user-defined groups. This is known as image classification.

The final resolution, *temporal*, refers to how often a given sensor obtains imagery of a particular area. Many urban applications rely on the consistent multitemporal abilities of remotely-sensed data for monitoring and, where possible, for inferring processes in land use changes (Quarmby and Cushnie, 1989). However temporal comparisons of remotely-sensed data are far from routine. Even if data taken at different times are registered to precise common spatial coordinates, inconsistencies in atmospheric conditions, distortions in sensor and platform parameters, and solar illumination may all contribute to slight variations when remotely-sensed data are compared.

Once data from both the Census and remote sensing are defined and measured, the main line of statistical integration involves a categorisation of complementary entities.

1.4 Classification

The propensity to group or cluster is part of everyday life. In urban geography, the most commonly grouped phenomena include spatial representations of people, houses, industry, etc. These are usually composed of discrete categorical data, a

succinct and useful definition of which has been offered by Wrigley;

"Data which consist of counts of the number of individuals/households/places in particular categories, or of simple identifications of which category each individual/household/place belongs to, are known as categorical data" (Wrigley, 1985:4).

This section will now concentrate on the first of the two prime objectives of this thesis, that of image classification. However, before various techniques are reviewed, this section will also briefly examine the traditional and contemporary means for classifying census information. In turn, this will allow analogies to be made between the way spectral and census data are categorised. It will also act as a prelude to a full evaluation, in Chapter Two, of the role of the census as a source of ancillary data in image classification.

1.4.1 Census Classification

The Census holds information on various aspects of the socioeconomic and housing characteristics associated with a national population. Over the years, this data-rich source has been used by urban geographers to develop theories of the spatial and social structure of cities. From as far back as the 1920s a series of methodologies have attempted to classify census data categories that summarise the demographic, social, economic, and cultural characteristics of populations across space. One of the most influential which used census tract data was that of *social area analysis* developed by Shevky and Bell in 1955 (a review of which can be found in Walmsley and Lewis, 1984). The theoretical assumptions behind social area analysis were that census tracts could be classified by geographical proximity, and that population characteristics could be represented by three constructs: economic status, family status, and ethnic status.

Subsequent efforts expanded the range of socioeconomic census variables that could be considered, and led to the adoption of *factor analysis* (or *principal components analysis*) as a standard inductive method for identifying the underlying dimensions of urban social and spatial structure. Social area analysis was thus a special case of *factorial ecology* which involved the use of factor scores as summaries of the spatial variations in socioeconomic and demographic profiles (an application of factorial ecology can be found in Morris and Pyle, 1971). Researchers interested in overall spatial patterns rather than underlying social dimensions adopted grouping

procedures, such as *cluster analysis* to create a multivariate classification of social areas (Walmsley and Lewis, 1984). Both factorial ecology and cluster analysis can be directly compared with similar statistical methods in digital image processing. The essential means of reducing the dimensionality of a data set is implicit in human factorial ecology and is analogous to the use of principal components analysis in remote sensing (see section 2.2.3). In the same way, cluster analysis in image processing is simply the aggregation of similar pixels into a pre-determined number of categories, and forms the basis for all image classifications.

Much has been written about the shortcomings of this early work in social area analysis, and some writers have sought to wholly discredit it. Before attention is switched towards image classification, it is worth noting the emergence of more contemporary means and issues of building small area census-based classification systems. Along with GIS, the 1980s saw the emergence of enhanced digital abilities in the handling and analysis of spatially referenced socioeconomic data. As a result, census data came to be exploited by more practical automated applications, culminating in a rapidly growing field now referred to as *geodemographics*. Commercial applications have made full use of geodemographic systems capable of rapid retrieval and cross-referencing of census data for customer profiles, and targeting policies (Battey and Brown, 1995). Furthermore the linking of census data with address details from the *Central Postcode Directory* (CPD) or even address-point data from the Ordnance Survey, has the now the potential to target individual households (Raper *et al.*, 1992).

1.4.2 Image Classification

Briefly, urban image classifications involve the grouping of pixels with similar spectral characteristics into a pre-defined range of classes. In effect, the classification process reduces the number of spectral bands in an image to a single channel of information grouped into blocks of user-defined classes. The amount of detail associated with each class is a function of spectral purity, image resolutions, classification schemes, and most importantly from an analytical viewpoint, classifier operations. These operations are frequently distinguished both by the degree of user interaction, unsupervised and supervised, as well as by the level of classification, per-pixel and sub-pixel. A discussion of a selection from each of these techniques follows.

1.4.2.1 Unsupervised Classification

To understand the virtually automatic procedures associated with unsupervised classifications it is useful first to further clarify the assumptions behind all image classifications. Unsupervised techniques attempt to draw out natural groupings or clusters present in the image. Natural clusters in *n*-dimensional spectral space can be visualised from simple scatter graphs as a cloud of points representing pixels with similar radiance levels. Unfortunately, the automatic process means that the recognition of information classes from natural spectral groupings is *a posteriori* to the classification, and the analyst will be called upon to identify and label the classified image with the aid of reference data. Many clustering heuristics have been devised and applied in image processing. One of the most common unsupervised classification methods is the two-pass *K*-means clustering algorithm (Lillesand and Kiefer, 1987), in which the user specifies the number of clusters to be generated and the spectral distances between them. The algorithm then arbitrarily seeds or locates that number of cluster centres in multispectral space, with each pixel assigned to the cluster whose arbitrary mean vector is closest. The second pass of the *K*-means classifier relocates all pixels based on revised mean vectors and the process continues until the last iterative cycle yields no significant change in the location of class mean vectors.

Unsupervised methods guarantee that all spectrally distinct classes are recognised, and as such are sufficient to deal with broad classifications, as in urban/rural mapping. This is when suitable urban and rural classes clearly occupy distinct locations in n-dimensional space. However, problems arise when the statistical distributions of classes are far from separate, and indicate that many pixels retain spectral characteristics associated with more than one class. Serious class overlapping frequently arises from the classification of heterogeneous landscapes, of which urban morphologies provide one of the most extreme examples. In this case, pixels exhibiting low class separability and high propensity for representing multiple classes (*mixels*), are commonly associated with features in the urban landscape. Moreover, selecting the range and number of clusters can become a highly subjective matter to which little probabilistic theory can be applied. As a consequence, research in urban image classification has tended to focus on advances in techniques at reducing the effects of mixels. The result is that the classification of urban areas is usually administered by supervised methods in which the analyst has more control over the

statistical separability of spectral classes through the selection of training areas and the evaluation of class signatures.

1.4.2.2 Supervised Classification

Supervised classification techniques rely on training samples to instruct the image in the number, size and name of information classes to produce. The training process is the collection of statistics from samples of pixels that describe and represent the spectral response pattern for each land use/cover type to be classified. The selection of training areas represents the crucial stage of all supervised image classifications, in that the quality of training statistics has a direct bearing on the accuracy of the final classified image. Generating class signatures that are spectrally distinct and mutually exclusive does not pose major problems. Difficulties are confronted from overlapping spectral classes on the borders between information classes, where a significant proportion of pixels are common to different training samples. This non-exclusivity is usually reflected in a more confused classification with lower accuracy. In these situations, training sample evaluation and refinement is critical and attention should be given to sample size, spectral variances, normality and the very identity of training sets. However, it must be stressed that if samples have inherently similar spectral response patterns, very little can be done at the refinement stage to make them spectrally separable. The selection of training samples can be described as both a science and an art, and requires close interaction between the image analyst and the image data, as well as a thorough knowledge of the geographical area to which the data apply. Moreover, this knowledge is considerably enhanced if extensive and reliable ancillary reference data are available to the analyst (Hutchinson, 1982).

In this thesis, census data will be used as ancillary information in the selection of more separable training samples for the classification of urban morphologies. It will be shown in Chapter Three how the surface model is an ideal vehicle for the selection of these urban land use training samples. The model will also be examined with a view to performing sample selection within a completely automated framework which eliminates both the need for detailed local knowledge of urban areas and need for ground truth for validation. Towards this end, Chapter Five will document a series of empirical classifications and results which have been partly informed by this automated feature of the surface model.

1.4.2.3 Per-Pixel Classifications

The second distinction in image classification refers to the level of pixel discrimination- per-pixel as opposed to sub-pixel. Traditionally, image classifications have been based at the pixel level, where each pixel is assigned a single, mutually exclusive category. Classifiers at this level can further be grouped into those dealing specifically with spectral, spatial, or temporal pattern recognition. Spectral pattern recognition is based purely on the combination of DNs which are, in turn, derived from the inherent spectral reflectance and emittance properties of the Earth's surface. Algorithms, such as the maximum likelihood, minimum distance, and parallelepiped, are principally based on the spectral values of individual pixels.

Calculations associated with the conventional maximum likelihood algorithm usually involve the assignment of a single class to each pixel based on the highest probability of class membership. The maximum likelihood classifier has proved a statistically robust algorithm, but as a parametric operation, it relies on normally distributed training statistics. Unfortunately the high spectral variabilities associated with urban areas frequently produce training samples which exhibit both a multimodal distribution and a large standard deviation, leading to serious and problematic overlapping between classes (Sadler and Barnsley, 1990). Moreover, each pixel is classified independently of its neighbours, relying completely on individual spectral values and ignoring local spectral variation.

The effects of neighbouring pixels have been incorporated in spatial classifiers dealing with the contextual and textural properties of the image. For example, the spectral values of roads may be very similar to flat-topped roofs, but if roads are recognised as linear arrangements of pixels, this confusion can be lessened by a contextual decision (Harris, 1985; Gurney and Townshend, 1983). Similarly, in textural classifiers, groups of contiguous pixels may be used to characterise spectral variations, or the roughness of an image (Gong and Howarth, 1990). Examples of textural classifiers applied to urban areas have documented improvements in the detection of changes in residential development over time (Jensen and Toll, 1982), and the detection of housing density (Webster *et al.*, 1991). More recently, neural networks have been trained to infer land cover classification, including an optimised neural net technique processing both spectral signatures and textural features based on grey-level histograms (Dreyer, 1993). However, if a neural net is trained with limited

and incomplete examples of the classification, results may tend to be noisy and even unreliable (Sui, 1993).

Finally, temporal pattern recognition, based on multi-image data sets, acknowledges that the spectral and spatial properties of categories can vary according to when the image is taken, for example, growing seasons for intra-urban vegetation (Franklin and Peddle, 1990).

1.4.2.4 Sub-Pixel Classifications

More recently, techniques directed at the sub-pixel level, sometimes known as *soft* classifications, have begun to address the mixed properties of pixels in landscapes of diverse and continuously varying features, such as urban areas. Instead of attempting to classify each pixel as one class of land cover/land use, it may be preferable to predict the proportion of various cover classes that make up the mixed response. A selection of these techniques includes linear mixture modelling, fuzzy set theory, and Bayesian probability distributions.

Linear mixture models attempt to construct a linear relationship between the reflectance of a surface and the response at the sensor. This involves an equation specifying the percentage of surface cover of each pixel as a function of its constituent land cover types in each band (Forster, 1985). Coefficients are normally determined by selecting pixels with the purest parameters representing each class. The proportion of mixing for each pixel is then calculated from this linear assumption. However, the method suffers from problems of imprecise ground truth verification, the inability to construct a coherent classification, and the inherent problems arising from a model that assumes complete linearity and ultimately ignores external factors such as shadow effects and atmospheric conditions. Furthermore, the effect of a point-spread function associated with urban areas means that linear mixture models frequently require pixel weights to derive more representative class proportions for each pixel (Forster, 1985). So far, linear mixture models have mostly been applied to the recognition of spectral patterns in the natural landscape. The severe heterogeneity of urban areas invariably leads to poorly defined end-classes (pure pixels), as well as the distinct lack of a linear relationship between urban categories.

Fuzzy classifiers allow a pixel to be a member of more than one land cover class. In this respect, the fuzzy memberships of each pixel within land use categories will determine the sub-pixel proportions (Wang, 1990). Unlike the maximum likelihood algorithm, a fuzzy set approach makes no assumptions about the statistical distribution of the data. Instead of a single discrete class, mixed pixels are assigned a fuzzy set membership, ranging from 0 to 1, for each land cover type that they represent. Fuzzy set classifiers have already been applied to the physical landscapes that are composed of inherently intergrading classes, for example vegetation continua (Foody, 1992). An example of a fuzzy classifier is that of the *c-means* non-hierarchical clustering algorithm documented in urban applications by Fisher and Pathirana (1990). Their work examined the potential of the *c*-means algorithm in an iterative process, where pixels are moved to other classes in an attempt to minimize the generalized least-squared error. A classification of the suburban zone found that although urban categories exhibited typical mixed properties, classification accuracy was well within acceptable statistical significance limits.

Finally, Bayesian theory has been used to calculate the likelihood of a mixed pixel belonging to its nearest pure class (Iversen, 1984). Here, probability values are assumed to represent the proportions of each possible land cover types within mixed pixels (Foody *et al.*, 1992). Calculations resulting from Bayesian-type classifiers produce *a posteriori* probabilities, again ranging from 0 to 1, reflecting the degree to which each pixel belongs to each class (Brooner *et al.*, 1971). Both fuzzy set theory and Bayesian-type classifiers have been successfully applied to the classification of urban areas. However, unlike fuzzy set theory, the Bayesian approach is the only one which is able to accommodate additional information outside the spectral-domain. In the heavily heterogeneous and confused nature of spectral images representing urban areas, this additional information is certainly vital for reliable and accurate classification.

The strategy adopted in this thesis is developed around the application of a Bayesian-type technique. It relies on the statistical robustness of the conventional maximum likelihood algorithm combined with the flexibility of a non-parametric process of incorporating prior class probabilities generated from ancillary data (Strahler, 1980; Maselli *et al.*, 1992). Although *a posteriori* values for each class are also available, the specific requirements of subsequent urban modelling techniques depend on the generation of pixels with single class labels. This means that each pixel will be

classified according to the highest *a posteriori* class value. The full theoretical development and explanation of the technique is provided in Chapter Three, and as part of a classification strategy applied to empirical data sets in Chapter Five.

1.4.2.5 Classification Schemes

Common goals for all image classification techniques are either to produce information specific to the technique, or most likely, to produce information that conforms to an established structured scheme. The design of a structured classification scheme is primarily dependent on its intended applicability which can take a *morphological* approach, a *functional* approach, or both (Lo, 1986). The morphological, or resource-oriented approach can be traced back to Sir Dudley Stamp in the *First Land Utilisation Survey of Britain* with land cover categories such as "arable", "woodland", and "built-up" (Stamp, 1962). In contrast, the functional approach emphasises activity-oriented land use categories, such as "agriculture", "forestry" and "urban", all evident in the *US Standard Land Use Coding Manual* (SLUC) (Urban Renewal Administration, 1965). A more recent activity-oriented classification scheme is that associated with the *Land Use Change Statistics* (LUCS) collected by the Ordnance Survey and commissioned by the Department of Environment in the United Kingdom (DoE, 1992). The LUCS are frequently collected on a site-by-site basis, where selected individual plots of land are annually monitored by ground surveillance. Although the LUCS do not comprehensively cover the whole of England, they do represent a classification scheme which is highly accurate and temporally flexible.

Table 1.1 USGS Classification Scheme

Level I	*Level II*	*Level III*
1. Urban or Built-up Land -----	**11. Residential** ----------	**112. Multi-family Units**
	12. Commercial and Services	**113. Group Quarters**
	13. Industrial	**114. Residential Hotels**
	14. Transportation, Communications and Utilities	**115. Mobile Home Parks**
		116. Transient Lodgings
	15. Industrial and Commercial	**117. Other**
	16. Mixed Urban or Built-up Land	
	17. Other Urban or Built-up Land	

A scheme which recognises the potential of interpreting both land use and land cover from remotely-sensed data is the general-purpose classification scheme, designed by the *United States Geological Survey* (USGS). Although primarily resource-oriented, the USGS scheme includes many human activity-oriented categories, and is composed of four hierarchical levels representing various scales of mapping (Anderson *et al.*, 1972). Two of the USGS's many criteria are the requirements of a minimum interpretation accuracy of at least 85%, and that categories should be interpretable at all times of the year. Table 1.1 illustrates the scheme on urban land at Level II and the various categories of residential land at Level III. Level I and II categories can be interpreted from high resolution satellite sensors such as *Landsat Thematic Mapper (TM)*, and *SPOT Very High Resolution (HRV)*. The recommended scales are approximately 1:500,000 with a minimum unit size area of 150ha for Level I, and 1:62,500, and 2.5ha for Level II (Jensen, 1986). The finer detail in categories of Level III are at a scale of approximately 1:24,000 with a minimum unit size of 0.35ha, and as a result require substantial supplementary information, in addition to high-resolution satellite imagery, and high/middle aerial photography. Finer detail in Level IV (not shown here) should only be used in association with middle/low altitude aerial photography. As the classification scheme proposed in this thesis is predominantly urban oriented, it is closely related to those first three levels shown in Table 1.1. The scheme attempts to construct as many measures and definitions of urban land as are practically feasible from remotely-sensed data. It also endeavours to strike a balance between the plethora of census data available, and the confines of the spatial and spectral limitations of satellite data. It will be shown, in Chapters Three and Five, how the UK Census of Population can become a vital component in the translation of urban spectral classes into meaningful urban information classes.

1.5 Analysis

The spatial extent of urban areas rarely remains constant. Instead variable rates of growth and decline are continually changing both the spatial shape and morphological characteristics of settlements. This section will now examine the role of remotely-sensed data in the monitoring, and later modelling, of the spatial indicators of this urban dynamism.

1.5.1 Remotely-Sensed Data

The primary objective in the analysis of remotely-sensed data of urban areas is to produce inventories of land cover and land use. These are usually in the form of thematic coverages representing categories such as "urban", "built-up", "residential", "commercial", and "industrial". Although the most common data collection method involves ground surveillance, this is frequently time-consuming and expensive, with quality varying between individual collections. Instead, remotely-sensed data have now become a valuable means of collecting urban land use information more rapidly and at relatively low cost compared with ground surveillance. However, the inherently intricate spatial variability of the urban surface, along with the complex range of human activities continue to limit progress in the mapping of urban areas from remotely-sensed data. Work in this field has attempted to disentangle the mixed nature of urban landscapes and at the same time to reconcile the physical layout of buildings and structures with definitions of human activity. These difficulties have already been discussed in image classification as the mixed pixel problem and difficulties associated with the conversion of spectral classes to information classes (sections 1.4.2 and 1.2.2, respectively). Nevertheless, remote sensing remains a useful supply of data for the generation of urban inventories.

Aerial photography continues to be an important source of remotely-sensed data in the analysis of large-scale urban mapping applications (Avery, 1963; Jackson *et al.*, 1980), including the monitoring of urban growth by sequential aerial photographs (Richter, 1969; Lo *et al.*, 1984). The human interpretation of analogue aerial photographs follows standard procedures that examine the size, shape, shadow, texture, tone, pattern, site, and association of urban features (Campbell, 1987). However, aerial photography suffers from many of the problems associated with ground collection methods, especially the high costs involved in labour-intensive mapping of large-scale areal coverages at infrequent temporal intervals.

Progress in all-weather *radar* imagery has also been exploited as a potential means for urban mapping, especially when complemented by aerial photography. (Lo, 1986). Imaging radar data from the US Space Shuttle *Columbia* has a ground resolution of about 40m and a scale of 1:500,000. In urban applications, radar data are able to detect and record the surface roughness, metallic structures, and corner reflections of buildings (Lo, 1986).

However, the advent of satellite imagery has brought with it a number of advantages and improvements over other types of remotely-sensed sources. In brief, satellite imagery has facilitated wider, more repetitive areal coverages of urban areas, that allow rapid and cost-effective computerised updating. The satellite data used in this project were obtained from land observation satellites that sense reflected energy at the visible, near and middle infrared spectral wavelengths. However it is worth noting the potential of remotely-sensed data from other wavelengths, particularly the *thermal infrared* band. An urban application from such data includes the measurement of spatial distributions of population by the detection of heat energy patterns. The *Defense Meterological Satellite Program* (DMSP) of the US Air Force collects night-time images of the world in the thermal infrared band of 8-13μm at an altitude of about 830 km. A rough comparison of a DMSP image of eastern USA with a population map of the same area clearly revealed a close similarity between the two (Foster and Parkinson, 1993).

One of the more reliable earlier applications of the visible and infrared wavelengths to the mapping of population density can be traced to the work by Iisaka and Hegedus in the 1970s (first published in 1982). They recognised that the radiance levels in the four bands of *Landsat Multispectral Sensor* (MSS) data were dependent on the ground covering materials or the land use of the area. Places with low population density were shown to have more natural components, e.g. vegetation cover or bare soil, than places of higher population density where artificial structures were dominant. By using a rather coarse grid size of 500m by 500m area, the relationship between population and spectral radiance characteristics was expressed as a simple function,

$$P = Ax_1 + Bx_2 + Cx_3 + Dx_4 + E \tag{1.4}$$

where P is the population and x_1, x_2, x_3, x_4 are the spectral reflectance values of the four MSS bands. To calibrate the model, reference data of population distribution in the Tokyo census ward area for 1970 and 1975 were obtained to impute the population density in all grids. Their results confirmed most of the grid cells had values within the expected levels of estimation, while cells showing the greatest divergence were found to have non-residential land uses misclassified as residential. Later work by Forster (1980; 1983; 1993) further refined this linear relationship, this time aided by more reliable socioeconomic data. Although crude estimations of land

cover and population distributions such as this may be directly inferred from raw satellite data, the bulk of research into urban mapping is primarily based on the recognition of consistent thematic patterns observable in the image. In this respect, the classification of multidimensional digital satellite imagery is now an established means of generating extensive categorical urban inventories. However, the significance of Iisaka and Hegedus' work is still very much underscored by subsequent research in the classification of urban land use through the calibration of spectral reflectance values by socioeconomic information. However, as noted throughout this chapter, the intrinsic heterogeneous nature and complexity of urban areas is a major impediment to image classification (Forster *et al.*, 1980). Research into producing more accurate classifications has focused on either the classification algorithm (section 1.4.2) or on the incorporation of ancillary, non-spectral data sets (to be discussed fully in Chapter Two).

One other way of improving the potential of satellite imagery is by re-classifying existing images using convolved filter windows. Frequency-based re-classification techniques are designed to calculate the frequency, or occurrence of cover-types within various window sizes before being subjected to further clustering procedures (Eyton, 1993). A method developed by Barnsley *et al.* (1993) considered not only the frequency of cover types but also their spatial arrangements based on contextual decisions. Land use classes for each pixel are then inferred from comparisons between adjacency vectors with other pixels and those derived from representative sample areas of the candidate land use categories. Over urban areas, the technique was robust enough to distinguish between terraced housing (spatially represented by rows of buildings with smaller gardens) and detached or semi-detached dwellings (spatially separate buildings with larger gardens). The work by Barnsley *et al.* (1993) and Barr (1992) also examined possibilities of adopting object-based spatial re-classification procedures. Here again classification is improved through contextual decisions but this time based on objects, or classes, according to their size, shape, location and context within the whole scene. Their application in the binary segmentation of urban/non-urban land use eliminated both spurious outliers and intra-urban open space. Indeed, their case study of the town of Orpington in the London Borough of Bromley, produced an urban classification that came remarkably close to the OPCS definitions of urban land use. However, all re-classification techniques are sensitive to the initial image classifications, and most contextual decisions are approximate at best. Moreover, the elimination of intra-urban open space would not

be acceptable to the space-filling spatial analysis techniques developed here, where exclusively built-up land is considered to represent a more objective and consistent definition of urban development.

By whatever means urban inventories are eventually generated from multitemporal satellite data, they have become increasingly essential from a practical viewpoint, especially in developing forward planning policies by local government (Kent *et al.*, 1993). Some documented applications involve monitoring growth at the urban periphery (Jensen and Toll, 1982; Jensen, 1983; Quarmby and Cushnie, 1989), devising crude approximations of population density (Kraus *et al.*, 1974; Iisaka and Hegedus, 1982), road network detection (Wang *et al.*, 1992), and monitoring land use changes (Toll, 1984; Barnsley *et al.*, 1991). Other applications have addressed the potential to be gained from analysing classified images within GIS (Ehlers, *et al.*, 1989), with specific work on urban monitoring and planning regimes (Kent, *et al.*, 1983; Treitz, *et al.*, 1992; Michalak, 1993).

However, all these applications are united in the primary pursuit of the classification of images representing urban areas, which is the generation of land use inventories. For these, the classified scene is usually regarded as the end product upon which practical applications are based. Compared to the spectral domain, very little further analysis is based on the wealth of information on the *spatial form* of classified land use categories. This oversight may be partly due to the inherent spatial complexities and overall noisiness associated with images classified as urban categories. However, fractal analysis, the study of complicated phenomena manifesting self-similarity at many scales, is well-suited to the spatial analysis of these complex forms (Goodchild and Mark, 1987; De Cola, 1989; 1993; Lam, 1990; Blackledge, 1993). This thesis recognises that fractal models do have a useful role in the spatial analysis of complex patterns reproduced by the classification of urban areas. Of the current research in this sphere, the work by De Cola (1989) most closely meets the needs of this thesis. Briefly, De Cola outlined a procedure for the improvement of classification and *functional labelling* of remotely-sensed data using fractal analysis. Using the fractal dimension D and the Pareto size parameter, he provided a practical measure and description of each classified land cover type. Along with locational and spectral characteristics, and additional information, the fractal dimension of each land cover type is then input into a GIS database from which a re-classification of the original image, is attempted. This demonstrates how the analysis becomes cyclical enabling

fractal measurements to inform the conventional classification process. Although De Cola did not pursue this idea of using fractal models to actually classify an image, advances in this area are currently being researched and tentatively documented (De Jong, 1993). The direction of this thesis will not contribute to this current debate but it will consolidate and comprehensively examine the spatial analysis of classified satellite images using ideas from fractal geometry within a general urban modelling framework.

1.5.2 Urban Modelling

"...the field of urban modelling is concerned with designing, building and operating mathematical models of urban phenomena, typically cities and regions." (Batty, 1976:xx).

The second direction of analysis in this thesis involves the statistical modelling of urban phenomena. Like many models in general, those in the urban context attempt to unravel the complexities and ambiguities surrounding the mechanisms which develop and alter urban land and urban societies. The goals of these models are to explain features and processes, along with a view to prescribing actions, using a simplified understanding of the urban fabric. The field of urban modelling, however, should not be confused with urban theory, which is implicitly based upon the commonly accepted cycle of scientific method involving hypothesis formulation, observation, experiment and hypothesis refinement, but not necessarily in that order. Although urban models are based on particular hypotheses, they are largely concerned with the experiment and refinement stages of the cycle in which the theory or hypothesis is translated into a testable form. This view of the urban model as a means for testing theory through the analysis of empirical patterns in the urban environment is the one that will be most actively ascribed here. However, the empirical testing of even simple hypotheses requires vast amounts of information to be rapidly collected, stored and analysed. With this in mind, it is no exaggeration to claim that the advent and development of computer technology has facilitated a more rigorous framework for the modelling of empirical data (Batty, 1976). In the urban context, GIS and image processing systems have now become established computer frameworks within which to analyse spatially referenced data sets from various sources, including remote sensing. As already noted, classified remotely-sensed imagery will form the empirical data sets upon which this urban modelling will take place. This is in direct contrast to the more established source of data from the census which has been

traditionally used in many urban modelling methods.

The statistical framework of urban modelling used in this project centres around the measurement and monitoring of urban form and growth, and in the estimation of urban density gradients. The modelling roots of these fields can be traced back to von Thünen's theory of land use, and studies of urban spatial structure by Burgess (1925), Hoyt (1939), and Harris and Ullman (1945), all of which are summarised in Carter (1981). The success of these models stemmed from their simple assumptions and abilities to accommodate complexities in real world urban patterns. In line with these traditional strengths, models representing the form of urban areas are here assumed to exhibit simple fractal structures of self-similarity across many scales (Frankhauser 1994; Batty and Longley, 1994). Recent research by these and other authors has extensively reviewed the notion that the form and density of urban development is essentially one that embodies characteristics from fractal geometry. As such, urban density functions describing the rate and extent of urban development can best be derived through a reformulation of power functions based on fractal geometry (Batty and Kim, 1992).

As already mentioned, the severe spectral heterogeneity of satellite images over urban areas produces classified scenes of urban land use which frequently exhibit similar spatial complexities and irregularities. With this in mind, and with an established theory behind the notion of the *fractal city* (Batty and Longley, 1994; Frankhauser 1994), the remaining work will target changes in urban form and density from empirical data sets generated from the classification of satellite imagery, beginning in Chapter Four.

1.5.3 Empirical Applications

The classification and subsequent urban modelling procedures adopted in this thesis will be empirically verified and tested on four urban areas in the UK, Bristol, Norwich, Swindon, and Peterborough. The validity of these procedures will express a more accurate detection and measurement of the urban fabric of these settlements. A temporal comparison should also reveal indications of variations in the use, form, and density of each urban area. Furthermore, a vindication of the methodology proposed in this thesis opens the possibilities of systematically replicating the classification and modelling procedures for other settlements in future work. Indeed, two of the greatest

strengths of this work are full automation and virtual independence from knowledge of local characteristics of an urban area. This will allow consistent and routine generation and comparison of a typology of settlements which is considered essential for a fuller understanding the form and growth of urban areas.

1.6 Summary & Conclusions

Introductory Chapter One has outlined the main research topics, those of the measurement, classification and modelling of urban spatial features. In addition, the working definitions of relevant terminology and concepts have been presented in order to clarify the work in the chapters to come. Where possible, each section of this chapter has attempted to compare, or derive analogies in the way the urban landscape is interpreted between data from the UK Census of Population and remote sensing. Along the way, specific merits and potential pitfalls of each data source have been evaluated with respect to their role in the proposed classification and modelling of urban morphologies.

Chapter Two
DATA INTEGRATION

2.1 Introduction

"At its worst, IGIS [integrated geographical information systems] is a powerful technology that can be used to answer poorly posed questions by running misspecified models on improperly extrapolated data to generate output whose validity can never be tested. At best, the coupling of satellite measurements with other spatial data has tremendous potential for describing Earth surfaces, [and] predicting future conditions..." (Davis *et al.*, 1991:695).

The above statement emphasises the sensitive and dual-edged nature of data integration where the resulting rewards of careful synthesis far outweigh the many difficulties encountered in the process. Data integration is pivotal in the development of this thesis, amplifying the immense potential of methods which can successfully and appropriately couple seemingly incommensurable data sets. The difficult process of data integration is a troublesome feature inherent in the whole field of Geography, a sentiment which has been echoed by the following,

"The need for data integration arises because many of the questions which scientists and social scientists investigate require data from a wide range of sources which are only reported on disparate spatial bases. Data integration is especially a problem for geographers because information synthesis is at the very heart of the discipline." (Langford *et al.*, 1991:55).

This chapter will introduce established and proposed research in the integration of data from remote sensing and GIS technologies in the specific field of urban detection and measurement. Remote sensing technology is seen primarily as a source of rapidly available, multidimensional and frequently-updated data, measuring the land cover characteristics of large areas. By contrast, GIS is more of an analytical tool handling not only remotely-sensed data, but also data captured from analogue maps, aspatial attributes of both land cover and land use features, and statistics including socioeconomic data from the Census. The issues of integration pursued here are those pertaining to the merging of physical land cover data from satellite imagery, with land use socioeconomic attributes from the Population Census held by a GIS. Particular emphasis must be given to various aspects dealing with data representation, data storage, positional integrity, statistical analysis, and classification compatibility.

The second part of the chapter focuses exclusively on one specific type of data

integration, that of improving the image classification of urban areas by incorporating socioeconomic and housing data from the Census. Many of the integration techniques are evaluated in terms of how census data have been, or may be used to either instruct or constrain the image classification process. Ultimately, a classification strategy is proposed which will attempt to harness the potential of disaggregate representations of socioeconomic data in the development of inventories of intra-urban land use. However, before any form of integration is examined, the first two sections will briefly review the two integration "players" in this thesis: data from land observation satellites, and the use of GIS to handle the particular spatial interpolation method used to disaggregate the UK population census.

2.2 Remotely-Sensed Data

"Remote sensing is the science and art of obtaining information about an object, area, or phenomenon through the analysis of data acquired by a device that is not in contact with the object, area, or phenomenon under investigation." (Lillesand and Kiefer, 1987:1).

The science of remote sensing was introduced in Chapter One with a view to providing a rich source of spatial data for urban mapping applications. Specific attention was given to the abilities of remotely-sensed data to detect and measure urban surface features according to sensor resolution parameters, and statistical analyses.

In this chapter, the field of urban mapping will continue to be examined, but the focus on remotely-sensed data will be predominantly confined to represent digital satellite imagery. The goal is to extract the maximum amount of information about patterns of urban land use and morphology from satellite imagery. To this end, the field of image classification will be extensively reviewed with respect to the role of census data in informing the classification process. However, before any spectral categorisation is discussed, it is first important to draw attention to a number of pre-classification techniques which both facilitate and enhance the interpretative value of satellite imagery.

Briefly, digital satellite images are composed of pixels in matrices of irregular rows and columns, in other words, non-topological raster data structures. Each pixel represents the average radiance levels in each wavelength, given atmospheric

conditions, of the observable earth feature, expressed as digital numbers (byte data) which are a function of the spectral, spatial, radiometric, and temporal resolutions. As such, raw satellite images are simply a collection of pixel vectors, but with the aid of statistical manipulations it is possible to infer and impose meaningful information. Before a satellite image undergoes any form of categorisation, a number of techniques are available to improve both the quality and interpretation of this raw spectral data.

2.2.1 Pre-Processing

The question of improving data quality usually lies beyond the reach of most analysts, and only deserves a brief mention here. Digital raw data transmitted by a satellite and collected by a ground receiving station undergo standard processing to eliminate systematic distortions using data from platform ephemeris and knowledge of internal sensor distortions. These distortions include scan skew, mirror-scan velocity nonlinearities, panoramic distortion, spacecraft velocity, and perspective geometry (including the earth's curvature) (Bernstein, 1983). Once the image is received by users, a number of methods are available for improving its interpretative potential, including geometric rectification, contrast enhancements, and data reduction.

2.2.2 Geometric Rectification

Geometric rectification is the process by which the geometry of an image area is made planimetric to cartographic projections and coordinate systems. The process assumes common registration between identifiable pixels on the image, in rows and columns, with reliable *ground control points* (GCPs), given in northings and eastings. Normally, the most recognisable pixels are those representing features such as road intersections, rail and river bridges, but avoiding field boundaries and buildings which may not be as temporally consistent. Analogue maps have been the usual source of reference data, but most recently *global positioning systems* (GPS) have been viewed as a more reliable and rapid means, leading to improved geometric rectification accuracies. Once GCP points have been selected, confirmed and verified, a spatial interpolation process is implemented involving the transfer, or relocation, of pixel values from the original distorted image to the grid of the rectified output image. A measure commonly used to determine the accuracy of spatial interpolation is the *root-mean-square* (RMS) *error*. The RMS error is employed to measure any discrepancies between the spatial locations of the original GCPs and their new positions in the

rectified image, and is calculated for each GCP as,

$$RMS = [(x' - x)^2 + (y' - y)^2]^{0.5} \quad (2.1)$$

where, x and y are the original row and column coordinates of the GCP in the source image, and x' and y' are the computed or estimated coordinates in the output image. Once the image is spatially interpolated, the brightness values of each pixel are then recalculated using one of a number of intensity interpolation algorithms, including nearest neighbour, bilinear, or cubic convolution (Curran, 1985). The data value of the rectified pixel using a second-order, or cubic convolution interpolation, is based upon the distances between the retransformed coordinate locations (x_r, y_r) and the sixteen closest pixels in the input (source) image,

$$V_r = \sum_{i=1}^{16} \frac{(D - \Delta x_i)\,(D - \Delta y_i)}{2} \times V_i \quad (2.2)$$

where, V_r is the rectified pixel, Δx_i is the change in the x direction between (x_r, y_r) and the data file coordinates of pixel i, Δy_i is the change in the y direction between (x_r, y_r) and the data file coordinates of pixel i, V_i is the data file value for pixel i, and D is the distance between pixels (in x or y) in the source coordinate system (ERDAS, 1991).

Pre-classification processing dealing with improving the information, and hence interpretative potential of the image, can be broadly distinguished between data enhancement and data reduction techniques. Data enhancement increases radiometric contrasts of images by stretching the histogram of pixel grey level values across the full scale of available display devices, while data reduction is a means of reducing the dimensionality, or variance between spectral bands. The following section expands upon a particular data reduction technique, *principal components analysis*, providing an example and a direct analogy to uses in human geography

2.2.3 Principal Components Analysis

Remotely-sensed data, especially those representing urban areas, commonly suffer from spatial autocorrelation effects and correlation between the spectral properties of dissimilar surfaces, both of which frequently result in data redundancy. Techniques, such as principal components analysis (PCA), factor analysis, and band ratioing, are

able to alleviate correlation problems by extracting the greatest amount of radiometric variance from the most efficient combination of bands as well as significantly reducing the amount of data in the image. In keeping with data reduction techniques traditionally applied in human geography, the role of PCA has proven to be of significant value in the analysis of remotely-sensed data. Briefly, PCA may be used to compress the information content of a number of bands of imagery (3 in SPOT HRV-XS) into usually just 2 or 3 transformed principal component images. This has the effect of reducing the dimensionality (size of data) which produces images that are often more interpretable than the original scene. The PCA transformation can be conceptualised by considering a two-dimensional distribution of pixel values obtained in two SPOT bands, with the close spread or variance of the distribution of points providing an indication of correlation. The goal is to translate and/or rotate the original axes so that the brightness values on both bands are redistributed (actually projected) onto a new set of axes or dimensions. This new axis is called the first principal component, with the second component perpendicular (orthogonal) to the first. This continues with the third, fourth, and *n*th component, each containing monotonically decreasing amounts of the variance found in the data set. This reduction in variance is also able to capture and enhance broad spectral contrasts, such as the differentiation between urban and rural land cover. The work by Langford *et al.* (1991) documented a component with 40% variance that revealed the urban distinction very clearly, as well as a component that a revealed intra-urban visual contrast superior to any RBG (red-green-blue) colour composite. Another component was also able to display greater contrasts within the urban category, so much that it provided a basis for training samples to be selected.

The statistical methods outlined above are simply designed to facilitate and enhance spectral pattern recognition, or image classification. In the same way, the following section will focus on a statistical technique designed to produce appropriate spatial representations of socioeconomic data for use in image classification.

2.3 Spatial Representations of Socioeconomic Data

Socioeconomic, housing, and related data from the UK Population Census will be referred to in this thesis, as the *ancillary data* when image classifications are discussed. Although briefly mentioned in Chapter One, ancillary data, sometimes

called collateral or auxiliary data, are any forms of data that are wholly external and exclusive of the remote sensing domain. In this chapter, ancillary data will be extensively reviewed as a means of informing and enhancing the spectral classification process.

Issues dealing with the mechanics of census measurement and collection of socioeconomic characteristics of the UK population at the ED level were also covered back in Chapter One. This section will further review the specific disaggregated *surface model* representation of census data that can be efficiently handled and interrogated by a GIS, and be most amenable to the classification strategy adopted in this thesis. A fuller description of this strategy and justifications for the use of the surface method of data representation in image classification will be outlined theoretically in Chapter Three and empirically in Chapter Five.

2.3.1 Surface Models

When mapping census information, the ideal situation would be if data could be located by individual households but spatially represented by appropriate cartographic symbolism. However, the reality is that, although the census is collected by household points, census information is aggregated into areal units and cartographically represented by choropleth maps. The problems associated with the aggregation of census data by irregular areal units were raised earlier in Chapter One. In this section, and as a prelude to the Bracken-Martin model, a number of techniques in *areal interpolation* will be reviewed with reference to the way census data can be represented as a disaggregate yet smoothed surface (see Goodchild *et al.*, 1993).

A convenient distinction between areal interpolation methods made by Lam (1983) focuses on the nature of the spatial data being interpolated rather than the techniques themselves. For aggregated census data, two approaches are available. The first relies on the spatial extent of each areal unit, represented by boundary information, as the primary basis for what is commonly known as a *polygon-in-polygon* areal interpolation. Alternatively, each areal unit can be represented by a single point, which is then exposed to standard *point-based* interpolation algorithms. One of the primary distinctions between the two is that, unlike the latter, the former is said to preserve the correct volume under the surface. A more detailed review may highlight this and other distinctions. Polygon-in-polygon areal interpolation techniques arise in

situations where the target units are much larger than the source units. A simple decision function, preferably by a GIS, would estimate target zone values from the sizes of the overlapping regions. The result is the generation of a more continuous surface, commonly represented either by the existence of a smooth density function using, what is known as a pycnophylactic method, or by a polygon overlay (Wagner, 1989). An interesting variation on the latter by Langford *et al.* (1991) enabled areal interpolation to be informed by the distribution of land cover types, as inferred from a classified Landsat TM image, in both the source (Census Wards) and target (regular grid) units.

The other group of areal interpolation methods use point data as surrogate values for aggregated areal units. For population mapping, these points can be census zone centroids which are then subjected to conventional point interpolation methods. However, this practice does not preserve the total volume of the data interpolated. The next section will review the surface model as a point interpolation technique used to create continuous surfaces of socioeconomic data while conserving the total number of people, in other words, preserving this total volume of data.

2.3.2 Bracken-Martin Model

The Bracken-Martin (1989) surface model is essentially a smoothing technique which is able to transform spatial data based on irregular zonal units into regular units at finer levels of spatial disaggregation. In this thesis, the model is predominantly applied to housing attributes extracted from the UK Population Census and recorded by ED zonal units. The problem of preserving the total volume of data (households) within the surface is overcome by adopting a spreading function which allocates people to neighbouring cells. These cells are then represented by a regular grid with an optimum spatial resolution of approximately 200m by 200m (Martin, 1989). Figure 2.1 is an example of the graphical output of the model. It shows a disaggregate representation of unemployment levels in South Wales, and illustrates in particular, the linear spatial arrangement of settlements along the Mid Glamorgan valleys. Using a GIS, complementary measurements of administrative boundaries, area of study and frequency distributions are also possible.

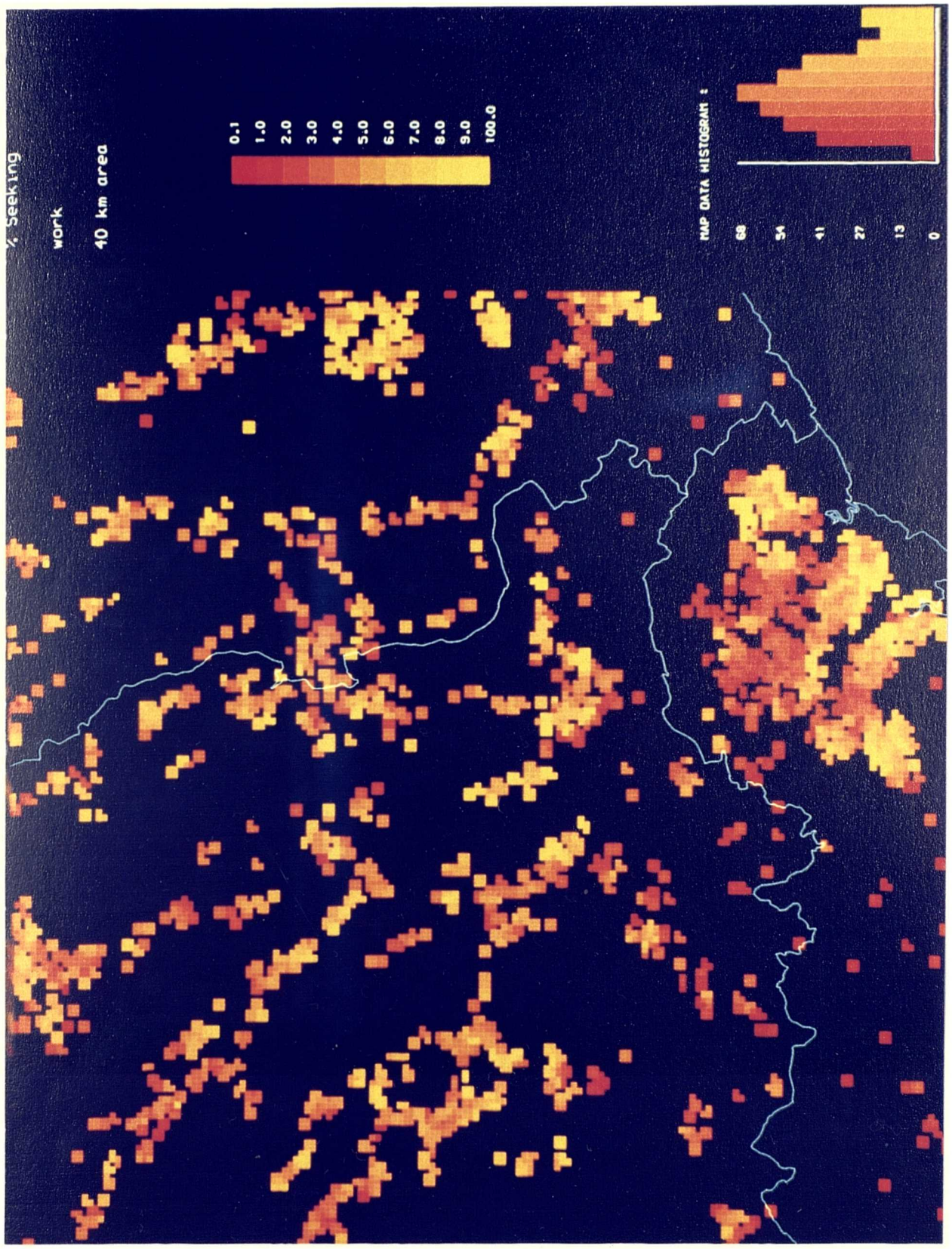

Figure 2.1 Bracken-Martin Surface Model

As mentioned in the previous section, the whole process of point-based areal interpolation is dependent on the use of centroids. In the surface model, centroids from the EDs are generated by the OPCS according to their *centre of mass*, or population-weighting, using the following criterion:

"...the centroid was selected to be as near as possible to the centre of population of the enumeration district. This was carried out by manual examination of the Ordnance Survey 1:10000 and 1:10560 maps used for enumeration district planning." (OPCS, 1984:4).

The OPCS also stresses that the identification and referencing of a single building is more important than recognising the centre of population. This guarantees that ED centroids will represent land that is built, rather than the geographical centre of population which may not always be located within the settlement. For the 1981 Census, ED centroids are referenced to OS coordinates with 100m precision, but spatial redefinitions in 1991 reduced this error to only 10m. However, research by Dunn and Boyle (1991) have pointed to further errors and suggested that all coordinates should be systematically changed by 50m in both easting and northing directions. Given the limitations of centroid referencing, the census surfaces can be created in the following manner.

Overall, the surface model is essentially an estimation procedure with a weighting factor based on intercentroid distances. The census value associated with each ED centroid is distributed spatially according to a basic model of distance-decay, implemented by centring, in turn, a moving window (kernel) over the cells containing each centroid. The distance-decay model is then used to compute the probability of each local (within window) cell containing a proportion of the count (census value). For any cell i, the variable Y_i is allocated as,

$$Y_i = \sum_{j=1}^{c} A_j \; Z_{ij} \qquad (2.1)$$

where Y_i is the estimated value in the ith cell of the output surface, A_j is the value of the variable assigned to the jth centroid (where c is the total number of centroids in the model area), and Z_{ij} is a unique weighting of cell i relative to centroid j (based on the distance-decay assumptions). Cell i will not receive counts or populations from every centroid location but only from any centroids in whose kernel it falls (Z_{ij} will be zero for all other cell-centroid combinations). At each location, the kernel is initially

defined as a circle of radius r, and is locally adjusted according to the density of other centroids falling within distance r of that location j. Weights are then assigned to every cell whose centre falls within the adjusted kernel, according to the distance decay function,

$$Z_{ij} = f(d_{ij} / r_j) \tag{2.2}$$

where f is the distance decay function, d_{ij} is the distance from cell i to centroid j, and r_j is the radius of the adjusted kernel defined as,

$$r_j = \frac{\sum_{l=1}^{k} d_{jl} \quad (j=1)}{k} \tag{2.3}$$

where $l = 1, 2, ..., k$ are the other points in the initial kernel window of radius z. If there are no other points with $d_{ij} < z$ (i.e. k=0), then the window size z_j remains set equal to z. This sets the dispersion of the count from point j to a maximum in the case where there are no other points within the entire window. In effect, the value r determines the maximum extent to which the count will be distributed from a given location. Where $k > 0$, a greater clustering of points around point j (smaller radius r_j) will result in a smaller window and hence greater weights being assigned to cells falling close to j (Martin, 1988).

The goal of the model is to generate surfaces of census data that are more disaggregate than conventional zonal-based representations. In this way, the model attempts to circumvent some of the effects of the modifiable areal unit problem (Openshaw, 1984) by producing output areal cells that are of standard size. Furthermore, by concentrating on population-weighted points, the model is able, to a certain degree, to reconstruct the residential geography of settlements by preserving unpopulated areas. However, as with any model, the algorithm is still very much a simplification of real spatial patterns. Its accuracy is sensitive to parameter estimations, including the distance-decay assumptions of its spreading function.

Nevertheless, the surface model has particular merits that will be fully exploited in this thesis. First of all, from a computational point of view, the model is able to produce surfaces that can be represented by raster-based data structures. This enables

surfaces, holding census information, to be fully incorporated into a GIS and interrogated by standard analytical functions (Martin and Bracken, 1991; Bracken, 1994). As a raster surface, each cell can be visualised as a single discrete entity capable of representing all available census data, and open to standard GIS functions, including overlay, proximity searches, and neighbourhood operations. Furthermore, as the model is generally based on population-weighted centroids and not on conventional areal units, it should be able to facilitate consistent temporal comparisons of socioeconomic data between Censuses, regardless of changes in ED boundaries (Bracken and Martin, 1993; Martin, 1994). Both of these qualities make the surface model amenable to logical integration with other similar spatial structures from disparate sources, including satellite sensors (see Sadler and Barnsley, 1990). In Chapter Three a full outline of the model's potential for integrating census data with satellite imagery will be explored with respect to refining image classification, with a special reference to the notion of informed training samples where surface cells are used to directly supervise a classification. The remainder of the chapter will address some issues of data integration, concluding with a general discussion on research into the incorporation of census data into image classification.

2.4 Integration of Satellite Data with Census Data

The two data sets used extensively in this thesis are satellite imagery and census data held by a GIS. This section will review some of the methodologies and pitfalls of integrating these two data sets, eventually paving the way for a discussion on integration issues dealing specifically with image classification.

2.4.1 GIS/Remote Sensing Integration

The integration of satellite imagery with census data is only part of a wider field of research that has gained momentum during the dramatic rise of remote sensing and GIS over the last twenty years. Remote sensing is a powerful technology in the collection and analysis of multitemporal images of the earth taken at various portions of the electromagnetic spectrum. GIS is capable of collecting large volumes of spatial data derived from a variety of sources, including remote sensors, and to efficiently store, retrieve, manipulate and display these data according to user-defined specifications (Marble and Peuquet, 1983).

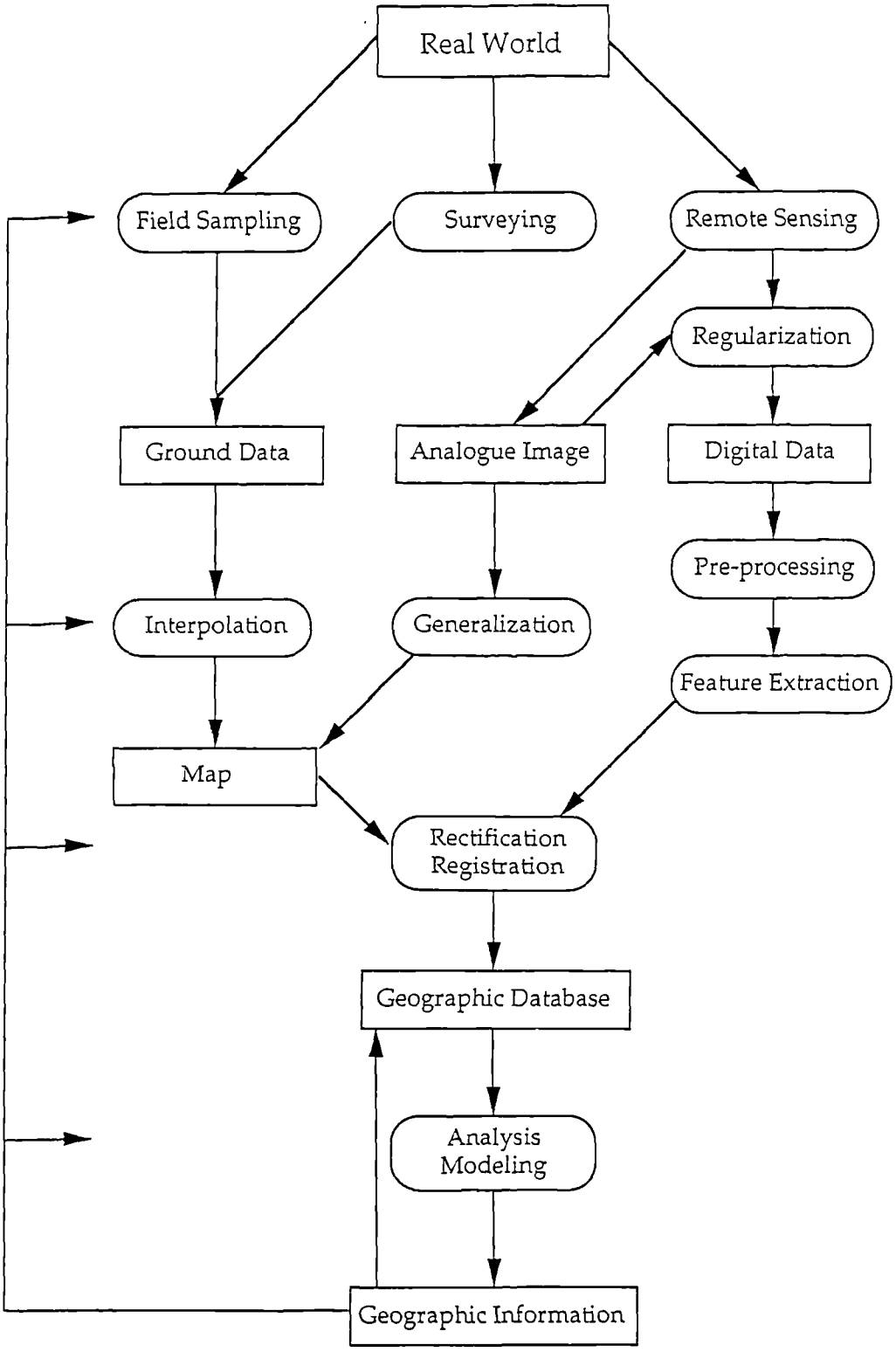

Figure 2.2 Conceptual diagram of data processing and information flow during integrated analysis of GIS and remote sensing data. Processes are enclosed in ellipses and products in boxes (after Davis *et al.*, 1991)

Many observers feel that integration is the only way that the full potential of both technologies can be realised (Shelton and Estes, 1981; Star *et al.*, 1991). The integration of remotely-sensed data with GIS, however, is not without its problems and it has taken over two decades to develop operational methodologies. These generally adhere to the conceptual representations of data processing and information flow designed by Davis *et al.* (1991) (Figure 2.2). Presently, many proprietary software packages are based around an integrated GIS and image processing rationale, with the most popular ones summarised in Table 2.1.

Table 2.1 Selection of GIS/RS Proprietary Software Packages

Software	*Producer*	*GIS/RS Integration Capabilities*
Arc/Info	ESRI Inc.	Vector-based GIS with *GRID* module allowing some elementary image processing
Intergraph MGE	Intergraph Corp.	Object-oriented and relational spatial analysis with a unique raster analysis capability which links raster files to an RDBMS
ERDAS & Imagine	ERDAS Inc.	Raster-based image processing system with standard GIS abilities, as well as a "Live link" with Arc/Info
SPANS	Tydac Technologies	Complete integration of vector, raster and quadtree data with a fully topological data structure
GRASS	US Army Corps Eng.	Raster-based image processing system with good support of spatial statistical analysis
MIPS & TNTMIPS	MicroImages Inc.	Raster and vector, also CAD information as well as some image processing capabilities
IDRISI	Clark University	Raster-based with many advanced GIS functions, including good import/export capabilities, and some image processing
Laser-Scan	Laser-Scan Ltd	Object-oriented GIS with good raster-vector integration
GENAMAP	Genasys Ltd	Topological vector-based GIS, with *Genacell* module for raster/grid modelling
GisPlus	Caliper Corp.	Integrated spatial database manager allowing full-featured vector-based GIS as well as supporting raster images
InfoCad	Digital Matrix Services	Vector-based GIS which can incorporate raster imagery as a backdrop
MapGrafix	ComGrafix Inc.	GIS with limited raster-based data handling

Some of the software systems in Table 2.1 also have well-developed import/export facilities for communicating with each other. The ERDAS 7.5 and Imagine 8.1

systems used extensively in this project were not only selected for their abilities in image processing and GIS but also their expediency in handling urban boundary data represented by arc coverages from Arc/Info. Incidentally, urban boundary data in vector form will provide important comparisons with classified remotely-sensed data in Chapter Six.

It is worth noting in passing that *artificial intelligence* (AI) and *expert systems* (ES) show promise in the integration of non-image spatial data with image data by virtue of their increased flexibility, generality, and intuitive appeal (Bolstad and Lillesand, 1992).

This section will exclusively focus on the problems of integrating remote sensing and socioeconomic data. For a more general and comprehensive coverage of GIS/remote sensing integration see NCGIA (*National Centre for Geographic Information and Analysis*) Initiative 12 (Star *et al.*, 1991). The discussion here will be grouped under five general headings, data and data storage, institutional issues, positional accuracy, statistical analysis, and the compatibilities of the classification scheme (Marble, 1981). Integration designed exclusively for the image classification of urban areas will be further and entirely the subject of the following section.

2.4.2 Data and Data Storage

For successful GIS/RS integration to be even attempted, it is first important to assess what each technology is measuring and how measurements are to be stored. Digital remote sensing methods employ electromagnetic energy as the means of detecting and measuring land cover characteristics, such as buildings and roads. The most common form of data storage for digital remote sensing is the creation of two-dimensional raster data sets composed of multispectral pixel vectors. Data managed by a GIS, on the other hand, can represent not only physical land cover information, but also aspatial attributes dealing with activity-based land uses. Unlike remote sensing, GIS normally contain data from secondary sources, usually digitised vectors from existing maps, or derived from raster remotely-sensed data. The abilities of GIS to accommodate both vector and raster data structures has recently been accompanied by rapid and fairly efficient conversions from one type to the other (see again Table 2.1). There are no major technical obstacles to providing procedures that allow ease of movement between various physical implementations of spatial data (Piwowar *et*

al., 1990). The main issue is providing users with efficient and accessible means to do so, which operate with known effects on data accuracy and precision. One way to achieve this has involved the use of high level (declarative) languages supporting queries and operations regardless of storage formats. A database management system (DBMS) capable of handling various types of data representations would spare the user repetitive data conversions and data transferences (Ehlers *et al.*, 1991).

Both remotely-sensed data and census data, suitably adapted by the surface model, are stored in raster-based structures, where each pixel or cell is a discrete spatial entity holding one or more attributes. There are no major technical impediments for integrating both within a GIS. Potential problems should be more evident during positional, institutional, analytical, and classification integration. However, it is worth noting that data content and data quality, which are somewhat beyond the scope of this analysis, are the key to successful integration in these other areas.

2.4.3 Institutional Issues

This section covers all non-analytical aspects related with the integration of GIS and remote sensing, especially data availability, data and equipment marketing and costs, standards and practices, education and training, and organisational infrastructures (Lauer, *et al.*, 1991). Institutional issues can be viewed as the enabling issues bridging the process from data acquisition to data processing. The objectives are to eliminate, or at least minimise, institutional impediments to a better integration of remote sensing and GIS techniques. Indeed, the development of both GIS and remote sensing technologies, like all breakthroughs in science, is plagued by constraints to immediate adoption and implementation. These problems are most acute in the availability, marketing and costs of spatial data used in GIS analyses. *The Federal Geographic Data Committee* (FGDC) in the US has concluded that it is usually more cost effective, or at least more expedient, to digitise data from maps than to search for and assess suitable existing digital cartographic databases (Lauer, *et al.*, 1991). In other words, data duplication is considered a commercially feasible, indeed preferable, means of developing a digital database. The whole idea of data sharing has been grossly hampered by many problems directed towards product awareness, product descriptions (including error measures), inflated costs, transfer standards, and legal issues dealing with freedom of information. Only the largest programs in digital cartography, such as those conducted by the US Geological Survey (USGS) and the

US Bureau of Census, currently provide an adequate product awareness policy. Even access to data from the UK Population Census, and the Central Postcode Directory (CPD) still requires authorised user registration with copyright restrictions heavily discriminating against commercial applications. Furthermore, although address-point data from the UK Ordnance Survey (OS) are only now becoming available, they are still likely to prove prohibitively expensive for geographically extensive areas unless national licensing agreements can be reached.

The availability of satellite data seems to be more widely available, although for extensively detailed mapping requirements there is a distinct lack of images at or below the 1m by 1m spatial resolution (Jensen, 1989). Even the general availability of coarser resolution data is only realised at exceptional costs, which have spiralled over the last decade to such an extent that some countries, such as China and Indonesia, may no longer consider remotely-sensed data economically feasible (He, 1989). The 1980s saw the price of digital tapes of Landsat TM data, for instance, increase by almost 200 per cent to a staggering $3,960 per scene in 1990 (EOSAT, 1990). Fortunately discounts on the price of digital imagery are available for academic research in the UK from sources such as *The Combined Higher Education Software Team* (CHEST) and even research funding councils. Satellite data used in this thesis have been obtained from local archives at Bristol University.

2.4.4 Positional Integrity

Full integration requires a means of relating information from one data set to another in explicitly spatial terms. Positional integration within a GIS critically depends on the precise spatial registration of disparate data sets to common cartographic projections and georeferenced coordinate systems. Locational integrity is essential if a truly coherent integration and subsequent statistical analysis between spatial data sets from different sources is even to be attempted. However, the assimilation of data sets into common spatial units is probably the most difficult of all integration issues. Errors inherent in singular data layers are frequently perpetuated and compounded when merged with other layers. An application of conditional probability theory suggests that errors associated with map overlays are a function of the number of map layers, their accuracy and reliability, and the coincidence of errors at the same position from several data sets (Newcomer and Szajgin, 1984). The result of compounded errors frequently contributes towards potential locational discrepancies,

which can be viewed as the spatial displacement of the same earth feature from one data set to another (Goodenough, 1988). The numerical assessment of the locational accuracies of satellite data is commonly reported as the root-mean-square error (RMSE). This is derived from the georeferencing algorithms used to rectify images to map coordinates (section 2.2.2). However, the positional integrity of data sets held by a GIS are not as easily reported. Most are derived by digitising existing analogue maps which may or may not include details of displacement errors. Moreover the digitisation process is heavily affected by human subjectivity and commonly introduces further errors (Peuquet and Boyle, 1990). Presently, the most accurate, and unfortunately most time consuming way of examining locational accuracy is by means of a ground survey with differential ground positioning systems (GPS).

The conventional means of disseminating census data is by aggregating household information into EDs, spatially represented by zonal units. However, the use of the surface model, outlined earlier in this chapter, eliminates the need for spatial boundaries. Instead, disaggregate cells are generated by a smoothing algorithm based on a distance decay function drawn from population-weighted intercentroid distances. In this respect, the location of ED centroids, not boundaries, are the subject of accuracy assessments. Indeed, ED centroids are assigned to the central location of the largest populated area by human judgement, which is invariably open to subjective bias (Dunn and Boyle, 1991).

However, the method of integration adopted in this thesis does not require perfect positional integrity between satellite imagery and census data. Instead, census data are treated as approximations of the residential geography of urban areas. Chapter Three will reveal that the process of generating training samples relies not on the absolute accuracy of point-based ancillary data but on area-based surface cells from within which training samples are drawn. An extensive review of the various methods in which census data may be incorporated into image classification will follow the brief discussion of statistical frameworks for analysing satellite imagery and census data.

2.4.5 Statistical Analysis

Statistical analysis involves the exploration of relationships between data variables and subsequent inferences that may be made. Many current GIS software packages

provide limited options for rigorous statistical analysis essential for comprehensive data integration. However, inexperienced users frequently return blind default options in menu-based systems which may not be sufficiently adequate for their application or indeed may not fulfil all of the assumptions of specific statistical techniques. As a result, relationships between remotely-sensed data and census data are frequently analysed using established GIS functions, such as vertical analysis from map overlays, spatial proximity calculations, neighbourhood operations, and time-based analysis (Burrough, 1986; Tomlin, 1990; Faust *et al.*, 1991). Raster-based data sets, such as digital imagery, and population surface models, are most amenable to vertical analysis stemming from simple overlays, where raster cells at the same position from the two data sets are exposed to logical and arithmetic operators. Error propagation due to vertical analysis (Newcomer and Szagin, 1984) can be monitored and quantified using a variety of overlay benchmark algorithms (Wagner, 1989).

It was Forster (1980) who initially employed multiple regression models based on vertical analysis techniques to reveal relationships between remotely-sensed data and socioeconomic variables simply because of the absence, in his view, of a methodology to classify urban land use. He states:

"Residential areas in large cities are typically heterogeneous and as such are not amenable to classification by cluster or discriminant analysis" (Forster, 1980).

Since his statement in 1980, increases in sensor resolutions, and development of more elaborate classification models have re-opened the role of satellite imagery in urban mapping. Furthermore, the fractal modelling application adopted in this thesis relies heavily on the wide coverage, and temporal frequency and consistency most associated with satellite data. However, Forster's 1980 work enabled other non-classification techniques to be applied to urban recognition. First of all, multiple regression models were used to examine the relationships between Landsat digital data and the percentage of urban cover types (buildings, concrete, roads, trees, grass, water and soil) at the pixel level for metropolitan Sydney (Forster, 1980). A similar approach (Forster, 1983) was later used to examine the relationships between Landsat data and a number of urban measurements, including surface cover proportions, housing density relative average house values and a residential quality index. The most significant relationship (only $r^2 = 0.76$) was found to be with residential quality index as the dependent variable. In later work, the development of a texture measure using neighbourhood operations was based on the standard deviation of the spectral

data within a 5 x 8 pixel window. Results of this method substantially increased the explained variation for regression models employing housing density and average house size as the dependent variables (Forster, 1983). However, it must be stressed that spatial data commonly violate assumptions of independence for measured parameters and error variance. As a result, multicollinearity may present a problem in multivariate regression modelling techniques where variance estimates for regression weights, derived from ordinary least squares, are inflated, leading to possible unstable values (Lunetta *et al.*, 1991). Another multiple regression technique by Langford *et al.* (1991) avoids using reflectance values from individual pixels. Instead their work attempts to derive linear relationships between land use categories, classified from satellite data, and population figures aggregated at the ward level. Their work essentially produces both what are known as *dasymetric* and *isarithmic* representations of residential development by projecting socioeconomic characteristics onto the physical layout of the urban areas (Langford *et al.*, 1989a; 1989b). In this respect, their technique parallels some of the classification objectives of this thesis. However, whereas this thesis focuses primarily on the role of census data in the modification of image classifiers, the works of Langford *et al.*, rely on an existing classified image as essentially a spatial constraint in census inference.

Various other statistical techniques are employed at different stages in the analysis of this project. Among them, the implementation of the Bayesian decision rule classifier relies on standard overlay functions as well as the generation of probability distributions for each cell of the surface model. Other techniques, including proximity analysis and neighbourhood operations, are applied to classified images which are subsequently exposed to a suite of programs measuring density and shape parameters based fractal geometry. Detailed discussions of all of these will be provided in Chapters Three and Four.

2.4.6 Classification Compatibility

Data categorisation is a means of reducing or partitioning, in most cases, continuous data into discrete classes, and is usually responsible for a loss of some information (Wrigley, 1985). Unless natural breaks in the data are apparent, the process can be very subjective leading to class distributions that may be biased, and sometimes highly insensitive to comparisons. Indeed, image classifications of spectrally complex landscapes, such as urban areas, frequently suffer from poorly defined

classes reflecting high user bias and scene-specific characteristics. As a result, inappropriate and non-standardised classification schemes represent the major sources of difficulties in the integration of remotely-sensed data with other spatial data sets from a GIS. Classification incompatibility is also a problem in the integration of census data with classified imagery. Here, difficulties arise when satellite data measuring land cover is combined with predominantly land use categories from the Census. The land cover/land use dichotomy was spelled out in Chapter One as part of the definition, measurement, and classification of urban land. Chapter Five will develop an appropriate classification scheme that is acceptable to both remotely-sensed imagery and census data, as well as feasible within the statistical processing limits of each data set. The following section outlines research into the classification of urban land by satellite imagery which is heavily regulated by census data. Virtually all work in this field adopts satellite imagery as the base data delineating spatial units of land cover. Census information is then utilised in either directing image categorisation or in superimposing land use information onto these spatial units of land cover. In this instance, satellite data is viewed as providing the more reliable spatial depiction of urban areas with census data providing the aspatial socioeconomic attributes.

2.5 Image Classification of Urban Areas Using Census Data

Numerous studies have investigated the problems and inaccuracies of classifying urban areas from primarily spectral methods (among these Forster, 1985; Gong and Howarth, 1990), an issue already set out in Chapter One. As a result of these problems, supervised classifications have further capitalised on the benefits of using non-spectral information from ancillary data sets, such as administrative boundary maps, elevation models, as well as population related data from the census, in an effort to improve classification accuracy (Marble *et al.*, 1983). The collection and handling of ancillary data, and their subsequent integration with digital imagery, are most efficiently dealt with by geographical information systems. The use of ancillary data for image classification improvement occurs at one of three points: incorporating these data before, during, or after spectral classification, through stratification, classifier operations, or post-classification sorting, respectively (Hutchinson, 1982) (Figure 2.3). Techniques employed at each of these stages are discused next, with special attention paid to the use of census data for urban image classifications.

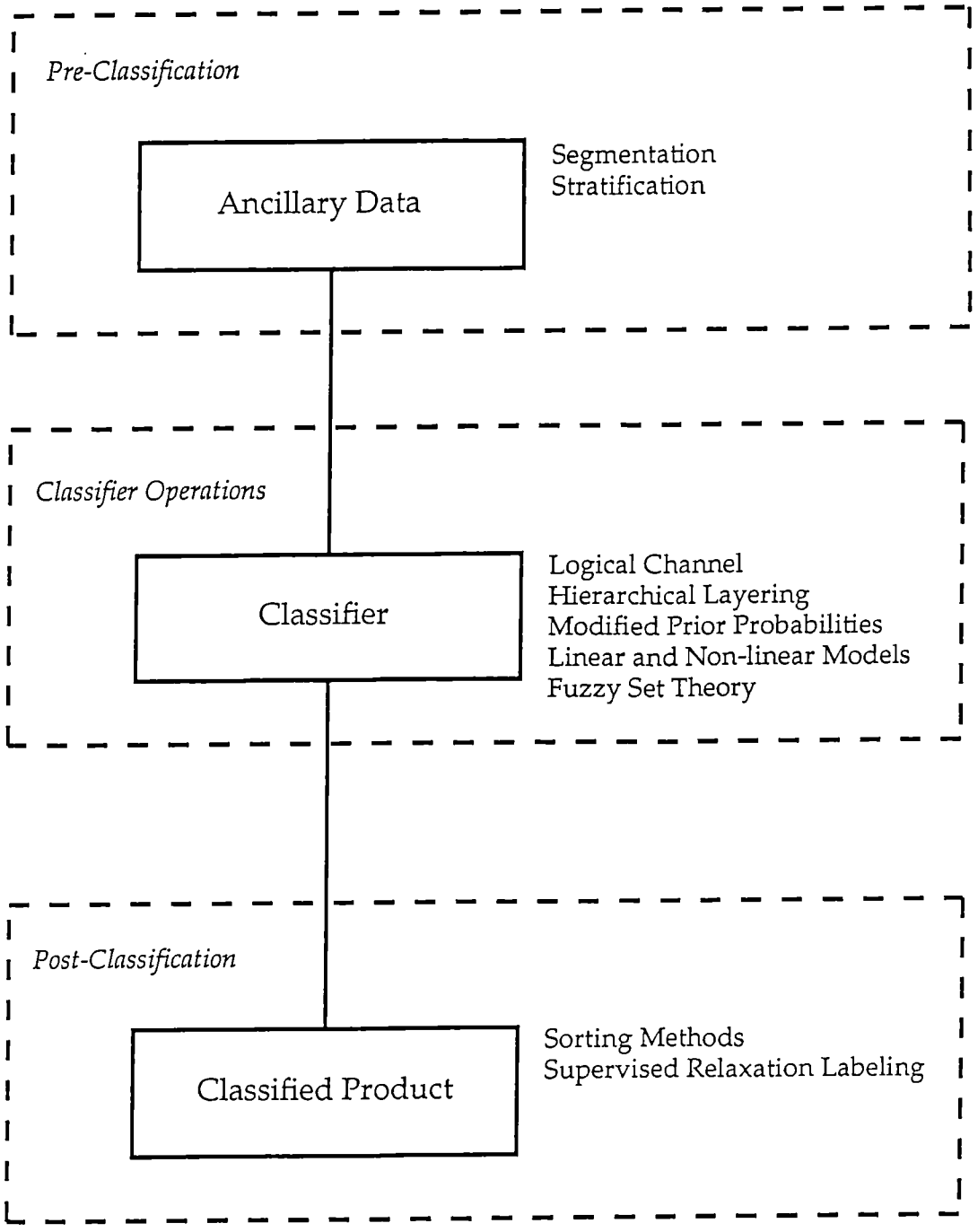

Figure 2.3 Techniques for Incorporating Ancillary Data into Image Classification by Stage

2.5.1 Pre-Classification

Scene stratification, or *segmentation*, involves a division of the study area into smaller, more manageable subsets *prior* to image classification. This may be an overriding practical consideration especially in large studies (Mason *et al.*, 1988). Classification accuracy is improved by reducing the spectral variation of the region in order to distinguish between spectrally similar land covers. It has already been observed that as variance increases, the likelihood of confusion between spectrally similar objects also increases (Bryant *et al.*, 1979). For instance, in urban areas the similar spectral characteristics of various buildings may be more discernible if first partitioned within urban/rural segments through the use of statutory planning boundaries (Barnsley *et al.*, 1989). Stratification may also be used to directly separate spectrally similar land covers. Low density residential land use and bare soil share very strong spectral similarities. In this case, census data may be used to segment the scene into exclusively residential land before classification is attempted. Stratification is a conceptually simple technique for using ancillary data to prepare the image for classification, although it does assume a thorough local knowledge of the scene. Other limiting factors are its relative insensitivity to subtle distinctions, and the assumption that differences between land uses are absolute and abrupt. The latter is a particular problem in urban morphologies where building types are regularly intermixed. In addition, because stratification is performed before classification, incorrect criteria can be perpetuated throughout the classification process, invalidating intermediate as well as final results.

2.5.2 Classifier Operations

The use of ancillary data *during* classification, employing established numerical algorithms, has sparked the greatest proliferation of research. Several approaches have been used to date. The first is simply to increase the number of input layers into the classification process, which is referred to as the *logical channel* approach (Strahler *et al.*, 1978). For example, population count, household size, and housing type from the Census might represent three additional layers that could be included along with the three spectral bands from a SPOT-HRV XS satellite image. However, work by Aronoff (1982) suggests that the simple annexation of non-spectral layers adds very little to classification accuracy, and can actually create problems in developing class statistics, as well as increase computer time.

Campbell (1983), on the other hand, advocates a hierarchical method called *layered classification* in which ancillary data dictate a series of separate decision rules. For example, population variables, such as large household sizes, high number of persons per room, and possibly rented accommodation, could be used to threshold areas on the image that have high housing density.

Alternatively, the *modified priors* concept, or *Bayesian-type classifier*, was developed by Strahler (1980) who reported an increase in the overall classification accuracy of forest cover types from 58% to 77%. This method stems from an alteration of the maximum likelihood classifier which involves varying the prior probabilities of class occurrence. The technique is sufficiently versatile to allow prior weighting of output classes based on their anticipated sizes, the merging of continuously varying measurements (multispectral signatures) with discrete collateral information, and, in temporal situations, the output of one classification to be used as the prior information in a later one. In urban mapping, statutory planning boundaries have been used to first segment scenes into urban and non-urban zones, within which urban class prior probabilities have then been estimated (Barnsley, *et al.*, 1989). The modified priors and layered approaches are both probabilistic and thus have been seen as having the greatest potential for making efficient use of ancillary data and improving classification accuracy. However, because they are based on statistical parameters, many samples must be drawn to characterise relationships between spectral and ancillary data. As such, they require an extensive level of sampling that is somewhat beyond what is normally conducted in normal spectral classifications.

Another major area of image classification where ancillary data has improved accuracy is in the selection of training samples. In urban analysis, the application of population density surfaces provides a means of informing the selection of more appropriate and representative training areas (see especially Quarmby *et al.*, 1988; Sadler and Barnsley, 1990).

Finally, ancillary data can also be used to assist in the final stages of cluster labelling rather than as a feature in the classification process. Simple socioeconomic variables may be employed as a reference source in deciding the land cover categories of different clusters, and even determining when to collapse clusters into one class (Mesev, 1992).

2.5.3 Post-Classification

Post-classification techniques rely on the influence of ancillary data *after* an image has been classified. Attention is normally paid to those individual pixels that exhibit extraneous patterns or are a part of identified problem spectral classes. Prior testing would first determine these classes and questionable pixels may then be re-assigned to their appropriate class using collateral information. In certain circumstances, sources of ancillary data can be determined and incorporated after the image classification has been performed (Mesev, 1991). The approach and techniques of post-classification sorting using ancillary data are derived from methods for overlay analysis found in grid-based GIS (Hutchinson, 1982). However, overlay analysis is heavily dependent on the close spatial integration of a classified image and ancillary data. Where spatial compatibility is adequately achieved, attention can then be given to those potentially misclassified pixels (Janssen *et al.*, 1990).

The use of contextual decision rules to improve the quality of classified images was already raised in Chapter One. A method which incorporates ancillary data to determine the spatial relationships of neighbouring pixels was developed by Richards *et al.* (1982). The technique, based on *probabilistic label relaxation* procedures, is used for embedding spatial context data with image-labelling problems in existing classifications, and strikes a balance between the spectral, spatial, and ancillary data sources of information. A more recent spatial re-classification technique by Eyton (1993) was applied to urban areas, examining the relationships between cover-type frequencies from a classified image and socioeconomic variables from the Census. High correlations were found for both the average age and average value of dwellings against relative counts of the cover-type frequencies. All these techniques at the post-classification stage can be crude and deterministic in the way selected pixels are re-classified. Nonetheless, these methods can be relatively rapid, easy to implement, and, to a certain degree, efficient in that they only deal with problem classes. Furthermore, it is relatively simple to include several types of ancillary data in developing decision rules. But above all, because they are performed after image classification, errors made in rule selection can be corrected easily as opposed to those made prior to classification using scene stratification (Mason *et al.*, 1988).

2.6 Summary and Conclusions

Chapter One outlined the way data from two disparate sources, the Census and remote sensing, define and are used to measure, classify and analyse urban spatial attributes. It was argued that both data sets possess specific qualities that, when combined, will improve our abilities to detect and measure, through image classification, the spatial layout of urban morphologies.

This chapter began with further discussions in the processing of satellite imagery and, even more importantly, the development of surface-based representations of census data. This led to a through review and assessment of the Bracken-Martin surface model as a potential means of accommodating socioeconomic and housing data into the image classification process. Specific attributes of the model included spatial disaggregation of census data, temporal consistency between Censuses, and a raster-based data structure capable of allowing census information to be completely handled by a GIS. The goal of improved urban classifications was then further advanced by explaining how satellite and census data can be integrated analytically, institutionally, and most importantly, combined within image classification frameworks.

An overriding concern raised in this chapter which must not be overlooked pertains to the critical and sensitive nature of the integration of information from different sources and representations. Although huge benefits may be realised from successful integration, careful acknowledgement of all potential incompatibilities are essential for both accurate and reliable results. In the particular realm of classification integration, special attention should be given to the initial accuracy and manner in which ancillary data are to be presented to image classification. Taken together, Chapter One and Chapter Two have established a framework which accents the joint qualities of both remotely-sensed and census data in the definition and detection of urban morphology, as well as highlights the advantages of merging both sets. The next chapter will fully develop the classification strategy that is able to accommodate census information with the aid of the Bracken-Martin model.

Chapter Three
IMAGE CLASSIFICATION

3.1 Introduction

The objective of this chapter is to outline how thematic coverages of urban land use are generated by the digital processing of satellite images. The method of extracting these coverages is known as image classification or spectral pattern recognition, and can be simply viewed as a process of deriving meaningful information from raw multispectral digital numbers. Formally, image classification is when pixels of similar values are grouped into definitive information classes using pre-defined parameters. The subject of image classification was introduced in Chapter One, and analysed as part of the integration of GIS and remote sensing in Chapter Two. In this chapter, a specific urban classification strategy, based on the integration of spectral data with census information is explored in detail. The strategy is composed of three elements, each of which may be adapted to allow socioeconomic information to be accommodated into the classification process. The elements are,

1) Training sample selection (*Before Classification*)

2) Bayesian-type classification (*During Classification*)

3) Postclassification sorting (*After Classification*)

Notice that these components represent the three sequential stages - before, during and after (discused in Chapter Two) - at which ancillary data may be incorporated into image classification (Hutchinson, 1982). Once developed theoretically, the strategy will subsequently be demonstrated, in Chapter Five, with the empirical classification of eight different land use categories from four settlements in the United Kingdom. Finally, in Chapter Six, the results of these classifications will then be assessed by a series of density modelling measurements based on space-filling properties and ideas from fractal geometry. By then, the work involved in the detection and modelling of urban morphologies will result in a clearer understanding of the way urban areas fill and occupy their available space.

Chapter Two introduced a surface model designed to produce a representation of

census data which is spatially more disaggregate than conventional zonal representations. The model's ability to generate a continuous density surface composed of a fine regular grid from an arbitrarily-partitioned map, will potentially be the most beneficial aspect in each of the three components of the classification strategy. This feature of the model provides the image analyst with a tool for disentangling the confused spectral patterns associated with urban areas. Disaggregated cells are able to inform training sample selection and direct postclassification sorting. The latter is important for image segmentation which will, in turn, facilitate the statistical operations of the Bayesian-type classifier. Although training sample selection and postclassification sorting are vital to the overall functioning of the strategy, they are considered as the more established and routine techniques in remote sensing, and will be discussed as part of the implementation procedure at the end of this chapter. The bulk of the chapter will be devoted to the theoretical development of the Bayesian decision rule, which is both much rarer in urban classification work, and is statistically more challenging (Mesev, 1993).

Essentially, the Bayesian decision rule is derived by modifying the *a priori* probabilities of the maximum likelihood classifier by considering and including census information. The conventional maximum likelihood discriminant function is based on Gaussian principles and assumes that each class has an equal probability of occurrence. The Bayesian decision rule lifts this equal probability assumption by adopting a modification which is based on Bayesian concepts and principles, specifically the notion of prior probabilities of class occurrence. In this thesis, prior probabilities of urban classes are estimated from the UK Population Census, and as such represent, for the first time, the application of socioeconomic prior probabilities to the classification of urban morphologies. There are three good reasons why the Bayesian decision rule should be used in the classification of urban areas:

1) It allows discrete non-spectral ancillary data (eg. census) to be merged with continuous spectral data.

2) It allows closely-related spectral classes of typically heterogeneous urban landscapes to be more separated.

3) It allows the coupling of the parametric maximum likelihood discriminant function, with the nonparametric modification of using prior probabilities. This coupling can

be translated into the harnessing of a statistically robust maximum likelihood classifier with the area preservation properties of prior probabilities.

Before the maximum likelihood discriminant function is examined in detail, it is first important to briefly review some principles of Bayesian statistics that will be used in its modifications.

3.2 Bayesian Statistics

Although the classification decision rule adopted in this thesis is labelled *Bayesian*, the use of Bayesian statistics basically involves only a simple and intuitive adaptation of Bayes' theorem (Bayes, 1763). Nevertheless, it is still helpful to quickly review the mechanics and assumptions behind Bayesian statistics in order to derive some statistical comparisons and analogies with the decision rule.

The main use of Bayesian statistics is to apply conclusions from known data in samples to populations for which data are not known, and as such it is a form of data extrapolation (detailed discussions in Bayes, 1763; Schmitt, 1969; Berger, 1985). Any form of extrapolation carries with it some uncertainty, and in Bayesian statistics uncertainty is represented by *a priori* and *a posteriori* probabilities. It would be fair to say that uncertainty is an unavoidable part of complex real life situations and the concept of probability is a convenient vehicle for expressing likelihood about populations and quantities that are truly uncertain. Bayesian statistics have recently emerged as an alternative to classical hypothesis testing and confidence interval estimation, and their primary advantage over classical statistics lies in their ability to incorporate information gathered over a series of experiments or over time. In this way, prior information is constantly updated and becomes more reliable after successive cycles, allowing the updated posterior probabilities to assume the role of prior probabilities after each complete iteration. Another advantage of Bayesian statistics over classical methods is their ability to yield valuable information from relatively small sample sizes. In addition, for the many social scientists who have a limited background in mathematics and statistics, Bayesian techniques provide a framework for data analysis nearly as conceptually simple as the standard maximum likelihood estimation approach.

3.2.1 Laws of Probability

The *empirical* view of probabilities, sometimes called *frequentist* probabilities or *objective* probabilities, will aid in the understanding of the classification of data in this research. Empirical probabilities are long-term relative frequencies or *proportions*. In this project, information from the Population Census provides established relative frequencies of socioeconomic attributes. On the other hand, *subjective* probabilities, dealing with more personal, non-repetitive, biased uncertainty, along with the *necessary*, or *logical* concept of probability, do not have any bearing on the approach taken in this work.

In this review of probability theory, the probabilities of all classes, variables and observations will be represented by brackets immediately following the letters *Pr*. Probabilities express likelihood on a continuous interval scale that ranges between 0 and 1 inclusive,

$$0 \leq \Pr(w|x) \leq 1 \tag{3.1}$$

where 0 is interpreted as impossible and 1 as certainty. $\Pr(w|x)$ is the *conditional probability* of class w, given the conditions of the observation pixel x. Conditional probabilities indicate the likelihood of an event happening given some observed measurement, with the *Law of Conditional Probability* stating that,

$$\Pr(w|x) = \Pr(x,w) / \Pr(x) \tag{3.2}$$

where, $\Pr(x,w)$ is the *joint probability* of x and w, which describe the likelihood of x and w occurring jointly. However, it is important to assess whether these variables are independent. Event x is independent of w if,

$$\Pr(w|x) = \Pr(w) \quad \text{or} \quad \Pr(x|w) = \Pr(x) \tag{3.3}$$

which means the likelihood of w happening given that x has occurred is just the value of w happening. This means that knowledge of the value of one, w or x, does not affect knowledge of the other as the two events do not influence each other at all. This will be true if all conditional distributions are the same, and if conditional distributions equal the marginal distribution. When x and w are independent, their

joint probability, that is the likelihood of both events occurring, is the product of their individual (marginal) values,

$$\Pr(x,w) = \Pr(x) \times \Pr(w) = \Pr(w,x) \tag{3.4}$$

But if they are dependent, their joint probability is,

$$\Pr(x,w) = \Pr(w|x) \Pr(x) \quad \text{or} \quad \Pr(w,x) = \Pr(x|w) \Pr(w) \tag{3.5}$$

Finally, *normalisation* is the process of making sure all probabilities for a single observation, class or variable sum to 1.

3.2.2 Bayes' Theorem

Using empirical prior probabilities, the Bayesian decision rule in image classification can be directly compared with the statistical structure of Bayes' theorem. Very briefly, this theorem is the formal derivation of the equality among certain probabilities (developed by Bayes, 1763, summarised by Iversen, 1984). It is based on the notion that the joint probability of two events w and x is the product of the probability of one of the events and conditional probability of the second event, given the occurrence of the first event (Iversen, 1984), and begins by recalling that,

$$\Pr(w,x) = \Pr(w) \Pr(x|w) \tag{3.6}$$

and,

$$\Pr(x,w) = \Pr(x) \Pr(w|x) \tag{3.7}$$

Since the left sides of equations (3.6) and (3.7) are equal, the right sides must also be equal. Equating these and rearranging, Bayes' theorem is developed as,

$$\Pr(w|x) = \frac{\Pr(x|w) \Pr(w)}{\Pr(x)} \tag{3.8}$$

If the experiment becomes multivariate with several different, mutually exclusive and exhaustive w's (w_1, w_2, .. , w_K), then the probability of the denominator is a weighted

sum of the conditional probabilities $\Pr(x|w_k)$, where the weights are $\Pr(w_k)$,

$$\Pr(w_k|x) = \frac{\Pr(x|w_k)\,\Pr(w_k)}{\Sigma_K \Pr(x|w_k)\,\Pr(w_k)} \qquad \text{where, } k = 1,...K \tag{3.9}$$

Assuming that w represents a spectral class, and x stands for observed pixel data, the left side of Bayes' theorem is then the probability of dealing with class w_k given the observed data x (the posterior probability of class w_k). $\Pr(x|w_k)$ represents the probability of the observed data x, given that it comes from class w_k (known as the likelihood of x). Finally, $\Pr(w_k)$ is the probability of class w_k before any data are known (the prior probability of class w_k). The denominator makes sure all probabilities sum to 1. Bayes' theorem can also be expressed simply as,

$$\text{Posterior Pr} \propto \text{Likelihood X Prior Pr} \tag{3.10}$$

where the posterior probability is proportional to the product of the likelihood and prior probability. This means that the same multiplier (the normalisation constant) is to be applied to every alternative under consideration.

Bayes' theorem is a simple, undisputable consequence of standard probability axioms and is not controversial. However, when used as the basis for an inference system, the theorem has been the source of much disagreement among statisticians (Berger, 1985). Here, the theorem is used to demonstrate the power and development of conditional prior probabilities solely in the modification of the maximum likelihood classifier as used in remote sensing. To this end, prior probabilities are seen as the key to more accurate classifications.

3.2.3 Prior and Posterior Distributions

Prior probabilities $\Pr(w_k)$, derived from available, existing information about a population are critical in Bayesian statistics and are used in all methods employing Bayesian techniques. The degree to which a prior distribution is known varies with the amount of information that is available. Noninformative priors indicate little prior information or opinion and are commonly characterised by rectangular distributions where the probability of a class lies between a wide range of values. Each of the probabilities within this range has an equal chance of occurring. As more data and

opinion becomes available the distribution becomes increasingly informative and takes on a more revealing form. As research is often cumulative, the most common method of increasing the amount of prior information is by expressing knowledge from early research as informative prior distributions in subsequent research. In this method of pragmatically updating information, the posterior distributions of earlier experiments become the prior distributions of later work (for a remote sensing example refer to Strahler, 1980). The most informative prior distribution is one that assigns either a zero or a value of 1 to a class, as both values express certainty.

Discovering prior distributions depends on whether they are generated probabilistically or deterministically. Most Bayesian methods rely on probabilistic prior distributions, which use samples to extrapolate for the whole population. Alternatively, if the prior distribution reflects the whole population, deterministic methods are employed and provide more informative, objective and accurate prior probabilities. The Population Census provides information which can be regarded as representative of the whole population.

The appearance of the prior distribution depends on whether the observation data are discrete or continuous variables. Prior distributions generated from discrete variables are usually called *probability mass functions* and do not present major difficulties. Each individual state of a variable has a corresponding probability value. An example of such a variable would be housing type, where each house falls into one of a number of discrete, mutually exclusive categories, for instance, detached, semi-detached, terraced, or purpose-built apartments. Continuous variables, such as urban populations, are represented by *probability density functions.* Here, the prior distribution is drawn as a continuous curve, and Bayes' theorem would need to use the mathematical function for that curve to derive the posterior distribution.

3.2.4 Prior & Posterior Probabilities

Extreme values of prior probabilities can virtually force a classification regardless of the values of the observation. A zero prior probability effectively eliminates a class completely, and similarly, a probability of 1 eliminates alternative classes. This can be seen in the numerator of Bayes' theorem (equation 3.9) where a zero prior probability $\Pr(w_k)$ renders the product of the whole numerator as zero causing the posterior probability to be zero also.

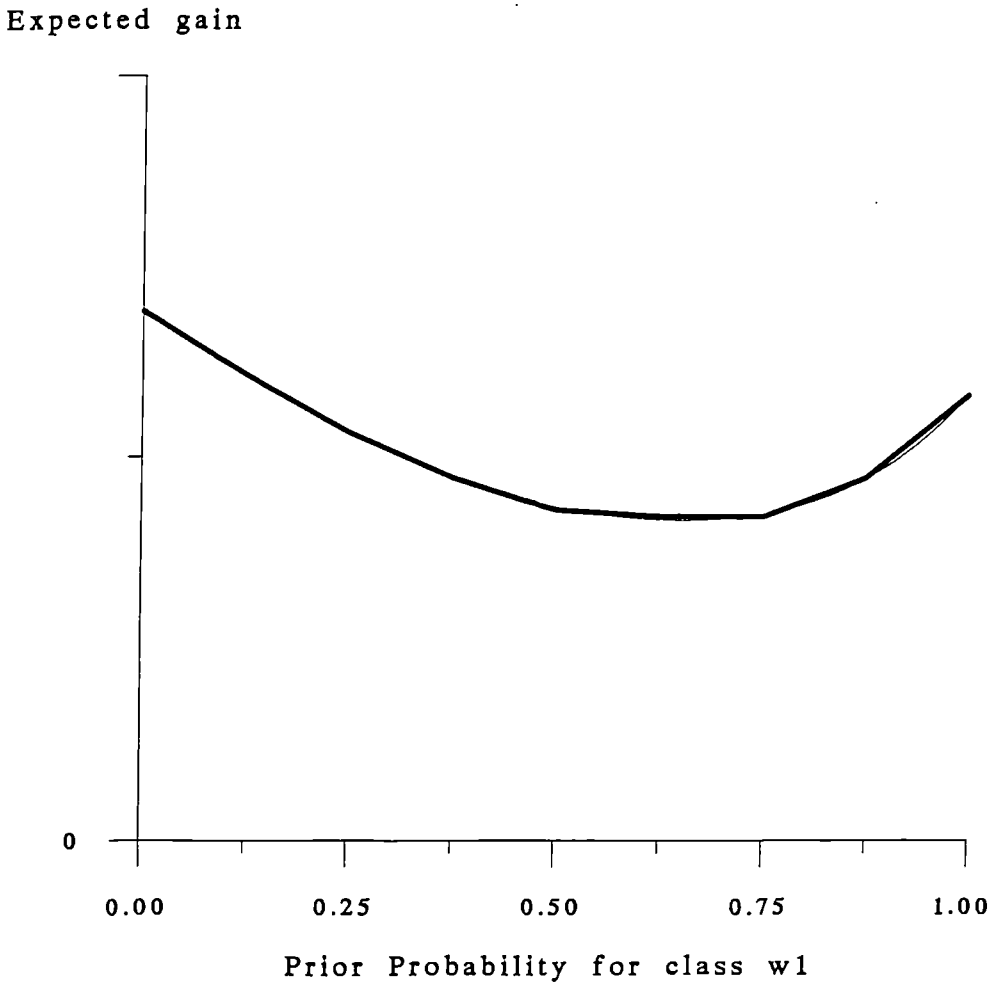

Figure 3.1 Expected Gain Function for a Two-Category Classification

As the prior probability for class w1 becomes 1, the prior certainty reflects itself in an *a posteriori* certainty which makes expected gain high.

When the prior probability for class w1 becomes 0, the prior probability for class w2 becomes 1 and the situation is similar.

For prior probabilities between 1 and 0, the situation is less certain and the expected gain must be less than the end cases.

The shape of the function is guaranteed to be convex.

Only in exceptional cases where a class is completely and unequivocally absent may a zero probability be appropriate. Conversely, when priors are equal, or are unknown and are assumed equal, they have no effect and the observation values determine the classification (Figure 3.1). In Bayes' theorem, equal priors would simply cancel out in the numerator and denominator, equating posterior probabilities with the observed data probabilities.

Prior probabilities are very influential in Bayesian analyses. However, the exact shape of the posterior distribution is influenced by both the prior distribution and the observed data. Extreme prior probabilities will have major effects on posterior probabilities only if the data samples are small, or have large variances. The principle of *stable estimation* states that even a somewhat informative prior distribution has very little effect on the posterior distribution given a large sample of observed values expressed in the likelihood function (Iversen 1984).

The preceding sections outlined the components which will modify the maximum likelihood discriminant function. However, before this modification is examined in more detail, a review of the statistical mechanics of the *conventional maximum likelihood classifier* need to be first addressed.

3.3 Maximum Likelihood Classifier

The maximum likelihood classifier has been in use in the social sciences since the late 1940s. Based on multivariate normal distribution theory it provides a convenient probabilistic method for recognising similarities between individual measurements.

3.3.1 Introduction

In remote sensing, the advent of multispectral digital images from aircraft and satellites has seen maximum likelihood classification emerge as the most favoured per-pixel method for generating thematic coverages. As a parametric classifier, each training sample is represented by a Gaussian probability density function, completely described by the mean vector and variance-covariance matrix using all available spectral bands. Given these parameters, it is possible to compute the statistical probability of a pixel vector being a member of each spectral class. Usually, a pixel is

assigned to one class, the class for which the probability value is the greatest. Research into the maximum likelihood classifier has centred on computational improvements, particularly hash-table look-up methods to reduce calculation repetition (Schlien and Smith, 1975; Mather, 1985). Further in-depth analysis of the maximum likelihood discriminant function may be found in Swain and Davis, (1978), Hord (1982), Schowengerdt, (1983), and Thomas *et al.* (1987).

Table 3.1 Symbols and Notation for All Classifications

x	pixel
$\boldsymbol{X}_i$	measured vector for ith pixel over all bands
w	spectral class
k	spectral class index
K	total number of spectral classes
a, b	ancillary variable
h, j	ancillary variable indices
Y_i	value of surface cell i
n	total number of spectral bands
m, l	band indices
q_k	total number of pixels in class w_k sample
$\Pr(x_{im}\|w_{km})$	probability of ith pixel in the mth dimension of feature space being a member of class w_k given that class w_k has been previously defined in that dimension
$\Pr(\boldsymbol{X}_i\|w_k)$	probability of pixel vector $\boldsymbol{X}_i$ over all bands being a member of class w_k [known as the maximum likelihood estimator, $F_k(\boldsymbol{X}_i)$]
$\Pr(w_k)$	prior probability of class w_k
$\Pr(w_k\|\boldsymbol{X}_i)$	posterior probability of class w_k given observation $\boldsymbol{X}_i$
u_{km}	mean for class w_k over band m
v_{kmm}	variance for class w_k over band m
v_{kmn}	covariance for class w_k between bands m and n
$\boldsymbol{U}_k$	mean vector for class w_k over all bands
$\boldsymbol{V}_k$	variance/covariance matrix for class w_k over all bands
$\|\boldsymbol{V}_k\|$	determinant of the variance/covariance matrix
$\boldsymbol{V}_k^{-1}$	inverse of the variance/covariance matrix
$(\boldsymbol{X}_i - \boldsymbol{U}_k)^T$	column vector, by the transpose of the row vector $(\boldsymbol{X}_i - \boldsymbol{U}_k)$

The maximum likelihood classifier has been widely regarded as the most advanced per-pixel discriminant function (Estes *et al.*, 1983). As long as the assumptions of multinormality are satisfied, the classifier guarantees optimum performance and relative robustness towards distributional anomalies even with limited number of training pixels. However, as many researchers have shown, the algorithm shows

much reduced classification performances when spectral distributions of cover types are very far from normal, as in the case of complex heterogeneous urban environments (Skidmore and Turner, 1988; Maselli *et al.*, 1990). Another drawback of parametric classifiers is the frequent deficiency in preserving area estimates, particularly noticeable when cover types are very different in extent. In attempts to overcome some of the problems associated with the maximum likelihood classifier, research has led to the development of entirely nonparametric methods (Skidmore and Turner, 1988), as well as hybrid methods which preserve the benefits from both parametric and nonparametric approaches (Maselli *et al.*, 1992). These modifications, and their underlying assumptions, will be examined in more detail later.

3.3.2 Discriminant Function

Before the maximum likelihood discriminant function can be modified, its precise mathematical and statistical mechanisms must first be examined. All subsequent analysis are based on the symbols and notation in Table (3.1).

For the single-dimensional case in band m, the probability that a pixel x_i will be classified into class w_k is given by,

$$\Pr(x_{im}|w_{km}) = \{(2\pi)^{0.5}\, s_{km}^{-1}\}\ \exp[-0.5\{(x_{im} - u_{km})^2 / v_{kmm}\}] \tag{3.11}$$

where,

$$u_{km} = 1/q_k \sum_{i=1}^{q_k} x_{im} \tag{3.12}$$

and

$$v_{kmm} = 1/(q_k - 1) \sum_{i=1}^{q_k} (x_{im} - u_{km})^2 \tag{3.13}$$

u_{km} and v_{kmm} are the best estimates for the true values (Swain and Davis, 1978). If equation (3.11) is extended over n-dimensions, it then becomes $\Pr(\boldsymbol{X}_i|w_k)$, the probability that pixel vector $\boldsymbol{X}_i$ will be classified into class w_k. This becomes the standard multivariate maximum likelihood function, $F_k(\boldsymbol{X}_i)$, and is expressed as,

$$F_k(X_i) = (2\pi)^{-n/2} |V_k|^{-0.5} \exp[-0.5(X_i - U_k)^T V_k^{-1} (X_i - U_k)] \quad (3.14)$$

where,

$$X_i = \begin{bmatrix} x_{i1} \\ x_{i2} \\ \vdots \\ \vdots \\ x_{im} \\ \vdots \\ \vdots \\ x_{in} \end{bmatrix} \qquad U_k = \begin{bmatrix} u_{k1} \\ u_{k2} \\ \vdots \\ \vdots \\ u_{km} \\ \vdots \\ \vdots \\ u_{kn} \end{bmatrix}$$

$$V_k = \begin{bmatrix} v_{k11} & v_{k12} & \cdots & v_{k1n} \\ v_{k21} & v_{k22} & \cdots & v_{k2n} \\ \cdot & \vdots & \cdots & \vdots \\ \cdot & \vdots & v_{klm} & \vdots \\ v_{kn1} & v_{kn2} & \cdots & v_{knn} \end{bmatrix} \quad (3.15)$$

and where,

$$u_{km} = 1/q_k \sum_{i=1}^{q_k} x_{im} \qquad m = 1, 2, ..., n \quad (3.16)$$

and,

$$v_{klm} = 1/(q_k - 1) \sum_{i=1}^{q_k} (x_{il} - u_{kl})(x_{im} - u_{im}) \quad l = 1, 2, ..., n; \quad m = 1, 2, ..., n \quad (3.17).$$

The exponent of equation (3.14) is equal to one half of the negative Mahalanobis distance, with its quadratic product represented as a χ^2 variate with n degrees of freedom,

$$\chi^2 = (X_i - U_k)^T V_k^{-1} (X_i - U_k) \quad (3.18)$$

Equation (3.18) can be described as a squared distance function, which measures the distance between an observation and the class mean, scaled and corrected for covariance in the class. Variations on this function include the log form of observed means, variances, and covariances (Strahler, 1980),

$$\ln[F_k(X_i)] = -0.5n \ln \pi - 0.5 \ln |V_k| - 0.5(X_i - U_k)^T V_k^{-1} (X_i - U_k) \quad (3.19)$$

In this case, since the log of the probability is a monotonic increasing function of the probability, the decision can be made by comparing values for each class as calculated from the right hand side of the equation. Another variation (Tatsuoka, 1971) eliminates the constants and minimises the following objective function.

Choose k which minimises,

$$F_k^{\#}(X_i) = \ln |V_k| + (X_i - U_k)^T V_k^{-1} (X_i - U_k) \quad (3.20)$$

Here $\ln |V_k|$ and V_k^{-1} do not vary from one X_i to another, and so need only be calculated once (Mather, 1985).

3.3.3 Numerical Example

A hypothetical example may clarify the mathematical operations of the maximum likelihood estimator. As always, assuming each sample class is from a Gaussian distribution, the mean vectors and variance-covariance matrices can be manipulated in the following way:

Consider two classes, w_1 and w_2 in three-dimensional space.

$$U_1 = [3\ 1\ 2] \qquad U_2 = [1\ 2\ 5]$$

$$V_1 = \begin{bmatrix} 1 & 1 & 1 \\ 0 & 1 & 1 \\ 0 & 0 & 1 \end{bmatrix} \qquad V_2 = \begin{bmatrix} 1 & 2 & 3 \\ 0 & 2 & 3 \\ 1 & 2 & 4 \end{bmatrix} \quad (3.21)$$

$$|V_1| = 1 \qquad |V_2| = 2 \quad (3.22)$$

$$V_1^{-1} = \begin{bmatrix} 1 & -1 & 0 \\ 0 & 1 & -1 \\ 0 & 0 & 1 \end{bmatrix} \qquad V_2^{-1} = \begin{bmatrix} 1 & -1 & 0 \\ 3/2 & 1/2 & -3/2 \\ -1 & 0 & 1 \end{bmatrix} \quad (3.23)$$

Assuming a random pixel vector, $X_{2,1,3}$ in three spectral bands, the quadratic product (equation 3.18) for class w_1 would be,

$$\chi^2_1 = [1\ 0\ -1] \times \begin{bmatrix} 1 & -1 & 0 \\ 0 & 1 & -1 \\ 0 & 0 & 1 \end{bmatrix} \times \begin{bmatrix} 1 \\ 0 \\ -1 \end{bmatrix} = [1] \quad (3.24)$$

and the maximum likelihood function (equation 3.14) would then be,

$$F_1(X_{2,1,3}) = (2\pi)^{-3/2} |1|^{-0.5} \exp[-0.5 \times 1] = 0.145 \quad (3.25)$$

For class w_2, the quadratic product would be,

$$\chi^2_2 = [-1 \;\; 1 \;\; 2] \times \begin{bmatrix} 1 & -1 & 0 \\ 3/2 & 1/2 & -3/2 \\ -1 & 0 & 1 \end{bmatrix} \times \begin{bmatrix} -1 \\ 1 \\ 2 \end{bmatrix} = [4] \quad (3.26)$$

with the maximum likelihood function as,

$$F_2(X_{2,1,3}) = (2\pi)^{-3/2} |2|^{-0.5} \exp[-0.5 \times 4] = 0.128 \quad (3.27)$$

Therefore, pixel vector $X_{2,1,3}$ has a higher probability of belonging to class w_1 and, under assumptions of equal *a priori* probabilities, would be classified as w_1.

Monitoring the behaviour of the maximum likelihood discriminant function under unequal class conditions will form the basis for the rest of this chapter. The addition of class variability, where information external to the spectral domain is introduced into the maximum likelihood function invokes the Bayesian decision rule in image classification.

3.4 Bayesian Decision Rule

The Bayesian decision rule is an image classification technique developed by linking the maximum likelihood discriminant function with concepts of variable prior probabilities. Image classifications using the conventional maximum likelihood classifier assume all classes have an equal probability of occurrence. However, it would seem intuitively more sensible to suggest that some classes are more likely to occur than others. For example, spectral classes representing dwelling type can be weighted according to expected relative proportions from sources such as the Census of Population. In other words, the spectral classes generated from the maximum likelihood discriminant function could be weighted according to their expected areal proportions. Furthermore, the use of unequal prior probabilities in the maximum likelihood classifier has shown that, where classes are well-separated the effect of including prior probability estimates is negligible. However, where classes are closely-related, as in typically heterogeneous urban morphologies, then the choice of

prior probability estimates can have a considerable effect (Mather, 1985).

Prior probabilities can be visualised as a means of shifting decision boundaries to produce larger volumes in *n*-dimensional measurement space for classes that are expected to be large and smaller volumes for classes that are expected to be small. Figure 3.2a is a diagrammatic representation of the basic problem in spectral pattern recognition where areas of overlap are frequently observed between class distributions. The use of prior probabilities in Figure 3.2b has had the effect of reducing areas of confusion by determining corrected class distributions based on their prior probabilities.

Once the classification is completed, the logical result of a technique that employs *a priori* probabilities is the generation of *a posteriori* probabilities. In this instance, each pixel is assigned a probability value based on the degree to which that pixel belongs to each possible class, and is hence a measure of exclusivity.

Figure 3.3 illustrates the effect of posterior probabilities in areas of spectral confusion. Here some pixels are exhibiting the classical symptoms of the mixel problem by representing spectral properties derived from two classes. Foody *et al.* (1992) have outlined the potential of using these *a posteriori* measures, generated from either a conventional or modified maximum likelihood algorithm, as direct indications of the inherent spectral intergrading of natural continuums, such as vegetation cover. The same continuous degree of spectral variations and spatial arrangements of surface phenomena are not, however, part of urban landscapes, which are more composed of irregular, and haphazard mixtures of different surface features. As such, the use of posterior probabilities in the classification of urban morphologies are restricted to simple measures of class exclusivity.

A large part of this chapter will therefore be dedicated to the development of prior probabilities and their effect on the classification of discrete thematic coverages of urban land use. However, before specific classification procedures are developed, it is first important to assess the statistical linkages between the maximum likelihood method and the use of prior probabilities. The maximum likelihood classifier is a parametric method of supervised image classification, while prior probabilities frequently require nonparametric assumptions. Benefits from both statistical methods can be derived from linkages through the Bayesian decision rule.

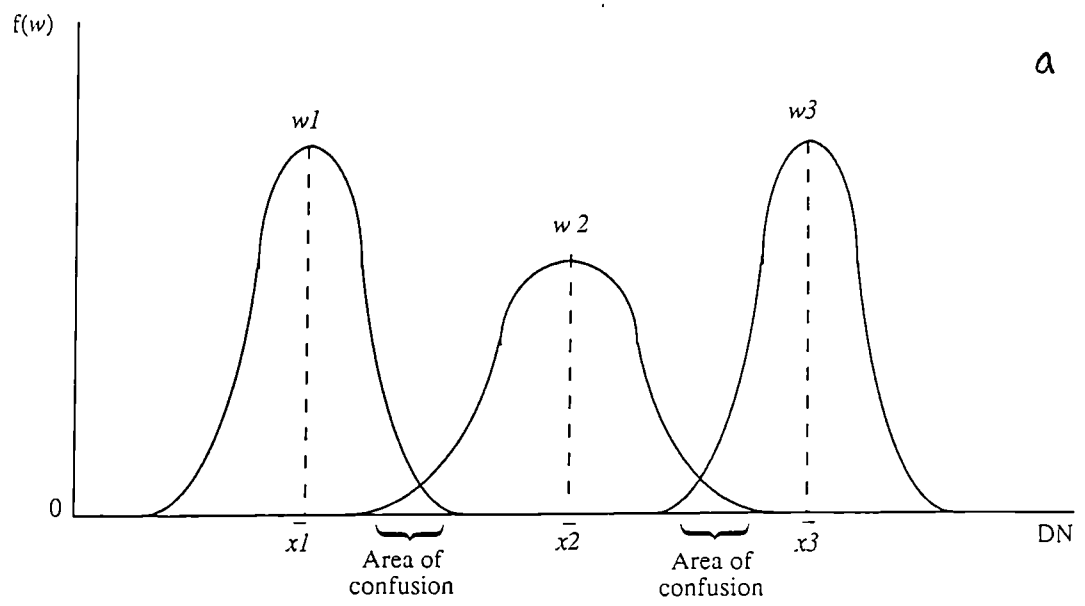

The basic problem in spectral pattern recognition. An example with three classes (*w1, w2,w3*) in a 1-dimensional decision boundary. Areas of overlap represent potential classification error

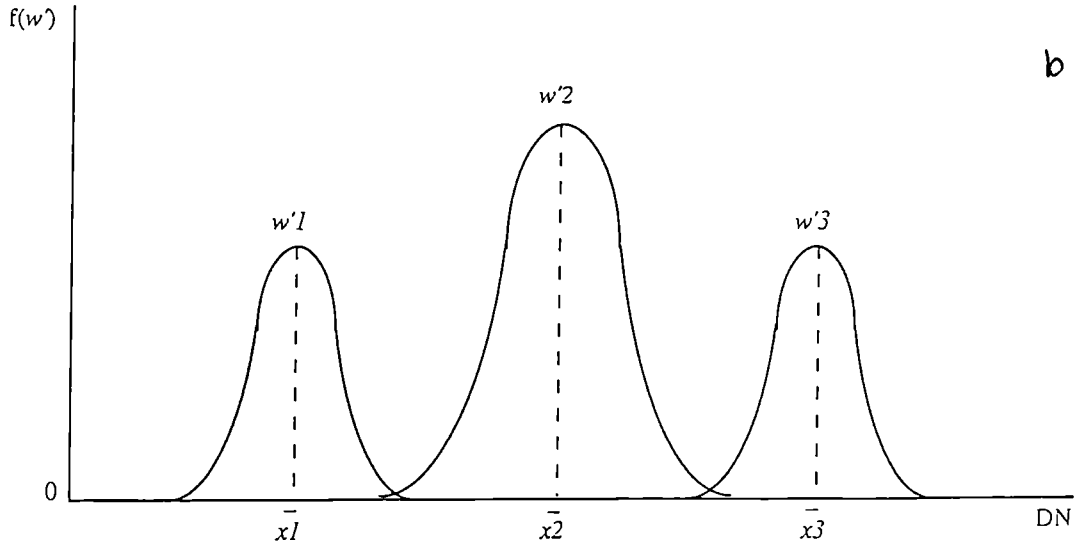

The use of Census prior probabilities (for new classes, *w'1, w'2, w'3*) has the effect of reducing areas of confusion. In this example, prior probabilities for class w2 has meant more pixels have been assigned to *w'2*

Figure 3.2 The Effect of Prior Probabilities on Class Histograms

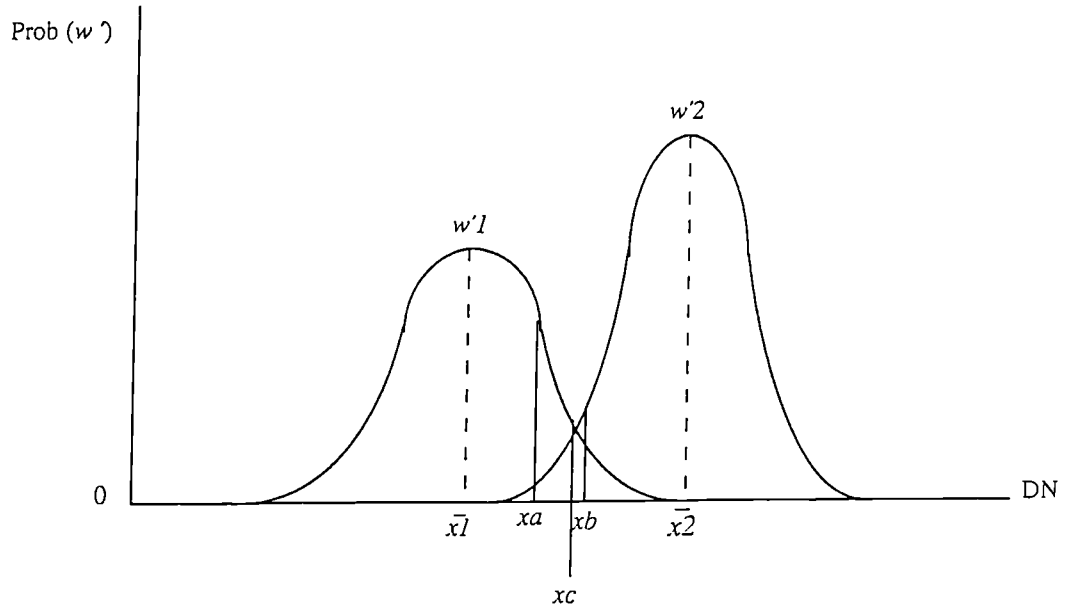

Posterior Probabilities. Pixel at *xa* the ratio of class densities is roughly 5:1 in favour of class *w'1*. Pixel at *xb* belongs to class *w'2* but only at a ratio of 4:3. Pixel at *xc* has equal posterior probabilities.

Figure 3.3 Assessing Posterior Probabilities of Class Histograms

3.4.1 Linking Parametric and NonParametric Classifiers

The maximum likelihood classifier is considered one of the most accurate and efficient discrimination procedures (Curran, 1985). Parametric classifiers, such as the maximum likelihood, take into account not only the marginal properties of the data sets, but also their internal relationships through the standardisation on the inverse of the variance-covariance matrix of each class. This is one of the prime reasons for the technique's great robustness but also its relative insensitivity to distribution anomalies. If the spectral distributions of each class deviate greatly from the normal, the procedure shows poor performances, and if no information about the actual dimension of the group is available, area estimates tend to be highly inaccurate. The problems encountered with the conventional parametric maximum likelihood classifier have been, to a certain extent, circumvented by nonparametric algorithms. One algorithm developed by Skidmore and Turner (1988), documented a 14 to 16 per cent overall accuracy improvement in the classification of forest cover types. Their classifier relies on the extraction of class probabilities from the grey-level frequency histograms, which are computed as,

$$Pr = F_r / F_n \tag{3.28}$$

where F_r is the number of pixels in a class at pixel vector, and F_n is the sum of counts of all the classes at pixel vector. Skidmore and Turner found that classifier performance was increased in most cases even when spectral distributions of cover types were not intrinsically Gaussian. Further improvements from their decision rule documented by Dymond (1993) are possible if each class histogram is normalised by dividing by the mean frequency (excluding zero frequency in the mean), instead of dividing by the number of training pixels in the class. Moreover, Skidmore and Turner's method also allows direct estimation of the probability of correct assignment to a class (Green *et al.*, 1993). However, nonparametric classifiers have been shown to be extremely sensitive to the presence of biased training samples. Also, the lack of assumptions regarding the shape of data distributions opens up the risk of over-reliance on erroneous distributions that are not statistically representative of the entire population (Dillon and Goldstein, 1984). Both of these problems are particularly evident when training samples are composed of only a small number of pixels.

The classification proposed in this thesis is based on this theory of the insertion of

prior probabilities into the maximum likelihood estimation process, and is fully developed in the works by Swain and Davis (1978), Strahler (1980), Haralick and Fu (1983), Mather (1985), Maselli *et al.* (1992), as well as Skidmore and Turner (1988). The initial substantive work on the use of per-pixel prior probabilities in maximum likelihood classifications can be attributed to Strahler (1980). His example involved the improvement in the accuracy of classified natural vegetation in Doggett Creek, California. Informative probabilistic priors were calculated from 85 sample points using aerial photographs and slope and aspect generated from a USGS terrain image at the 1:250,000 scale. Elevation as a single ancillary variable increased classification accuracy from 58% (spectral only) to 71%, and when combined with slope this boosted accuracy to 77%. However, the small number of sample points was a major hindrance to the classification, as they were more likely to predict the rank order of the magnitudes rather than the values of the magnitudes. More recent work by Maselli *et al.* (1992), again applied to rural management, documented equally favourable results from parametric classifiers employing non-parametric prior probabilities. They also revealed that the conventional maximum likelihood classifier showed a general tendency towards inaccurate areal estimates, whilst the non-parametric classifier left wide areas unclassified completely, especially when trained on small samples. Work in the urban sphere seems to have been virtually neglected, simply because of the severe heterogeneity of urban land use. One notable exception is that of Barnsley *et al.* (1989), who noted a 4% improvement in urban classification accuracy by using statutory planning map data to first segment and then assign prior probabilities to a selection of broad urban categories.

In this thesis, the employment of prior probabilities in the urban context will be pursued and evaluated. The work will involve, for the first time, the use socioeconomic data from the Census as prior probabilities in the classification of residential dwelling types. Furthermore, the problems of small training sample sizes, evident in earlier work, will be avoided by utilising the full potential of the spatially extensive population surface model. Discussion of the precise implementation operations will precede the in-depth examination of the mechanics of the Bayesian decision rule along with a look at the generation of census prior probabilities.

3.4.2 Discriminant Function

As noted earlier, the Bayesian decision rule adopts the basic principles of Bayes'

Theorem (equation 3.9),

$$\Pr(w_k|x_i) = \frac{\Pr(x_i|w_k)\ \Pr(w_k)}{\Sigma_K \Pr(x_i|w_k)\ \Pr(w_k)} \quad \text{where } k = 1,...,K \tag{3.9}$$

where $\Pr(w_k|x_i)$ is the posterior probability of class w_k given observation x_i, $\Pr(x_i|w_k)$ is the likelihood of pixel x_i being a member of class w_k, and $\Pr(w_k)$ is the prior probability of class w_k. Assuming the likelihood can be derived from the maximum likelihood function (equation 3.14),

$$F_k(\boldsymbol{X}_i) = (2\pi)^{-n/2}\ |\boldsymbol{V}_k|^{-0.5}\ \exp[-0.5(\boldsymbol{X}_i - \boldsymbol{U}_k)^{\mathrm{T}}\ \boldsymbol{V}_k^{-1}\ (\boldsymbol{X}_i - \boldsymbol{U}_k)] \tag{3.14}$$

the Bayesian decision rule is expressed as

$$\Pr(w_k|\boldsymbol{X}_i) = \frac{F_k(\boldsymbol{X}_i)\ \Pr(w_k)}{\Sigma_K F_k(\boldsymbol{X}_i)\ \Pr(w_k)} \tag{3.29}$$

Operationally within an image processing system, this modification can be inserted into the maximum likelihood classifier as,

$$F_k(\boldsymbol{X}_i)' = (2\pi)^{-n/2}\ |\boldsymbol{V}_k|^{-0.5}\ \exp[-0.5(\boldsymbol{X}_i - \boldsymbol{U}_k)^{\mathrm{T}}\ \boldsymbol{V}_k^{-1}\ (\boldsymbol{X}_i - \boldsymbol{U}_k)]\ \mathrm{X}\ \Pr(w_k) \tag{3.30}$$

where the decision rule now states that the *i*th pixel is a member of the class *k* for which the probability value is the greatest given its prior probability.

Using again the Tatsuoka (1971) variation of the maximum likelihood function (equation 3.20), prior probabilities would be inserted and the objective function becomes,

Choose *k* which minimises,

$$F_k^{\#\#}(\boldsymbol{X}_i) = \ln|\boldsymbol{V}_k| + (\boldsymbol{X}_i - \boldsymbol{U}_k)^{\mathrm{T}}\ \boldsymbol{V}_k^{-1}\ (\boldsymbol{X}_i - \boldsymbol{U}_k) - 2\ln\Pr(w_k) \tag{3.31}$$

The decision rule in this instance is influenced by prior probabilities in the following way. If the prior probability $\Pr(w_k)$ is very small, then its natural log will be a large negative number and when multiplied by -2 it will become a large positive number and thus $F_k^{\#\#}$ for the class will not be minimised. A zero probability will effectively

remove a class from the output classification. As the prior probability approaches 1, its log will go towards zero and $F_k^{\#\#}$ will approach $F_k^{\#}$ (equation 3.20) for that class. However, as this probability when combined with those for alternative classes must sum to 1, the remaining classes will have small priors and hence a small output representation. In general, the more extreme the values of the prior probabilities, the less important are the actual observation pixel values.

3.4.3 Numerical Example

A simple numerical example can clarify this modification of the maximum likelihood function into the Bayesian decision rule. Consider the same two classes that were used in the numerical example for the maximum likelihood classifier, w_1 and w_2 in three-dimensional space. This time, prior probabilities of occurrence are unequal and assumed for each class as follows,

$$\Pr(w_1) = 0.4, \quad \text{and} \quad \Pr(w_2) = 0.6 \tag{3.32}$$

The probability density function adjusted for prior probabilities is then

$$F_k(\boldsymbol{X}_i) \Pr(w_k) \tag{3.33}$$

and using the likelihood values, $F_k(\boldsymbol{X}_{2,1,3})$, calculated by equations (3.25) and (3.27), the Bayesian decision rule for class w_1 becomes,

$$F_1(\boldsymbol{X}_{2,1,3}) = 0.145 \times 0.4 = 0.0580 \tag{3.34}$$

and for w_2,

$$F_2(\boldsymbol{X}_{2,1,3}) = 0.128 \times 0.6 = 0.0768 \tag{3.35}$$

The complete decision rule (equation 3.29) makes sure all probabilities sum to 1.0, and provides the actual modified maximum likelihood classifier $F_k(\boldsymbol{X}_i)'$ (equation 3.30),

$$F_k(\boldsymbol{X}_i)' = \Pr(w_1|\boldsymbol{X}_{2,1,3}) = 0.0580 / (0.0580 + 0.0768) = 0.43 \tag{3.36}$$

and,

$$F_k(X_i)' = \Pr(w_2|X_{2,1,3}) = 0.0768 / (0.0580 + 0.0768) = 0.57 \quad (3.37)$$

Table 3.2 Numerical Bayesian Decision Rule Example

w_k	$\Pr(w_k)$	$F_k(X_{2,1,3})$	$F_k(X_{2,1,3})\ \Pr(w_k)$	$\Pr(w_k\|X_{2,1,3})$
w_1	0.4	0.145	0.0580	0.43
w_2	0.6	0.128	0.0768	0.57
	---		---	---
Σ	1.0		0.1348	1.000

Prior probabilities have now made class w_2 more appropriate to the random pixel vector $X_{2,1,3}$. This is contrary to the results calculated under the assumptions of equal class probability in section 3.3.3. The results are summarised in Table 3.2.

3.5 Implementation

The UK Census of Population provides the ancillary data to be used to calculate prior probabilities in the Bayesian decision rule, as well as the information for the surface model used in the selection of training samples and postclassification sorting. These procedures form a classification strategy that is flexible enough to be easily and routinely applied to various data sets. But before this is discussed, a short review of census prior distributions will be provided.

3.5.1 Census Prior Distributions

Prior probabilities of occurrence for any census variable pertaining to urban land use or land cover are extracted from probability distributions. The term probability distribution, or probability function, refers to a graph of all values of a variable and their corresponding probabilities. Variables may be discrete or continuous depending on the level of measurement, and are either drawn from samples or represent entire populations. All empirically derived variables extracted from the UK Population Census are considered certain within the limits of the study area, because they represent entire populations. In this respect, the relative frequency distributions

associated with these variables will produce the appropriate deterministic probability distributions. Discrete census variables, such as dwelling type, and household size are represented by probability mass functions where each discrete state or value of a variable has a corresponding probability, similar to a frequency histogram. For continuous variables, probabilities are calculated from specified areas underneath a density function. Population size is commonly treated as continuous, simply because of its large range of values.

Census data will be represented in this work as probability values at two levels. The first relates to the entire population within the area of study. Each census variable a, composed of J states or values will have corresponding probabilities of occurrence based on their absolute frequencies, and assuming,

$$0 \leq \Pr(a_j) \leq 1 \qquad j = 1, 2, \ldots, J$$

$$\Sigma_J \Pr(a_j) = 1 \tag{3.38}$$

Probabilities associated with such global variables a_j will be used directly in the Bayesian decision rule as weights for each spectral class (see section 3.5.4).

The second level refers to individual cells of the population surface model. Here estimated probabilities for a_j are allocated to each surface cell, Y_i again assuming,

$$0 \leq \Pr(Y_i) \leq 1$$

$$\Sigma_I \Pr(Y_i) = 1 \tag{3.39}$$

These local probabilities associated with single discrete surface cells will be used at both the training sample stage (section 3.5.2), as well as in postclassification sorting (section 3.5.3).

3.5.2 Training Area Selection

Before examining the ways census prior probabilities may be used at the training stage it is important to first discuss the salient assumptions behind the selection of training areas from satellite imagery.

Recall from Chapter One that the supervised classification procedure relies on the abilities of the analyst to develop training statistics for all spectral classes, constituting each information class, to cover the whole image. The exact number, size and location of each training sample are handled by the analyst within the objectives and scale of the classification. To take an extreme example, the classification of "buildings" requires a large selection of pixels covering a broad range of radiance levels. However, a class such as "detached dwellings" will need more restrictive samples, with more selective radiance levels. For both scenarios, it is important to analyse the location of several training sites throughout the scene in order to increase the chances of capturing the pixels that are most representative of all the variations in the class. A general rule for the minimum number of pixels for a sample is $n+1$, where n is the number of spectral bands (Lillesand and Kiefer, 1987). Particularly in parametric classifiers, such as the maximum likelihood, this minimum number rule guarantees the calculation of the inverse of the covariance matrix. There is, however a trade-off between having a sufficiently large sample size to ensure accurate statistical parameters used by classifiers, and restrictive enough to ensure class separability. In other words, it is essential not to exclude any important pixels that would contribute to the representation of the class, but it is equally important not to include redundant pixels in the classification from a computational standpoint. There needs to be a balance between sample size and sample error (Curran and Williamson, 1986). Moreover, the development of representative training statistics is sometimes more important for obtaining accurate classifications than the selection of classifier algorithms (Hixson *et al.*, 1980). As a consequence, the quality of training statistics are frequently evaluated and refined prior to classification.

Training samples are evaluated in terms of their spectral homogeneity, uni-modal distributions, and spectral separability. These criteria are essential to generate training statistics that are unique representations of the information classes. Evaluation may be aided graphically and quantitatively. Histograms and coincidence plots are quick visual methods for observing the shape of training sample distributions. These are supplemented by calculations of sample means and variances, as well as a class divergence parameter based on a covariance-weighted distance between class means. In general, the larger the divergence, the greater the statistical distance between training samples and the higher the probability of correct classifications. Preliminary evaluation also allows extraneous pixels to be deleted, additional ones to be selected in poorly represented samples, and the merging of

samples to reduce data redundancy.

Generating training statistics for spectral classes that are spectrally distinct and mutually exclusive does not pose major problems. Difficulties arise when spectral classes overlap on the borders between information classes. Classes are said to overlap, in the sense that a significant proportion of pixels are common to training samples from different classes. This non-exclusivity is usually reflected in a more confused classification with lower accuracies. In these situations, training sample evaluation and refinement is critical and attention should be given to sample size, spectral variances, normality and the very identity of training sets. However, it must be stressed that when samples have inherently similar spectral response patterns, very little can be done at the refinement stage to make them spectrally separable.

The inherent heterogeneity of spatial patterns of urban land cover and urban land use has meant that classification by digital imagery has always been plagued by spectral confusion, frequently leading to poor overall accuracy. As a result, ancillary data are commonly incorporated into the classification process (Chapter Two) in an attempt to increase the amount of information available, and thereby reduce spectral confusion. In this work, the population surface model, as outlined in Chapter Two, provides the basis for generating and labelling more separable spectral training statistics. Broadly speaking, the model is a surface smoothing technique that has allowed census data to be represented in a more disaggregate form. The surface model is a means of representing ancillary data in a manner which facilitates a more efficient selection of training samples, both in spatial integration as well as sample information. The process is comparable with the work of Quarmby *et al.* (1988) who also used population information to produce significant improvements in the classification accuracy of housing density from a SPOT image.

It is argued here that although the spatial resolutions between the satellite data and the surface model are different, their mismatch aids in generating sensible training statistics. The following line of argument may clarify this. Satellite data from Landsat TM images are commonly represented at a 30m spatial resolution, while the surface model produces cells with an optimal 200m by 200m resolution (Martin and Bracken, 1991). This means that, when spatially integrated, a single surface cell will cover just over 44 Landsat TM pixels. As training samples are generated from contiguous groups of pixels representing *areas* of the image, not points, this

resolution imbalance is more of a benefit than a hindrance. Training samples of land cover characteristics can be collected within the spatial limits of surface cells representing census information. However, as noted in Chapter Two, the surface model is only an approximation to the residential geography of an urban area. As such, the analyst should not rely on generating training samples from single surface cells, but should use the model as a framework within which to base sampling decisions.

Moreover, the question of which surface cells to use for which land cover samples is determined by the frequencies of corresponding census variables. Each cell of the surface model is assigned a probability value of occurrence associated with a census variable. The probability value is derived from the smoothing effects of the surface model directly generated from the population-weighted centroids of each enumeration district. An example may clarify this. Consider the census variable, "dwelling type" with four possible alternatives, detached, semi-detached, terraced, and purpose-built apartments. Each enumeration district contains the aggregated totals of each of these four dwelling types. Probability values for each type based on simple frequency proportions can be easily assigned to each population-weighted centroid. Once the surface model is calibrated, these probability values are disaggregated throughout the scene, replicating the spatial patterns of residential land use. Most of the surface cells will contain non-zero probability values for each of the dwelling types, representing the mixed properties of urban residency. However, there will also be a large number of surface cells that contain exceptionally high probabilities of only one dwelling type. These are the cells that are the most useful in the selection of training samples. The process can be repeated up to the maximum number of surface cells exhibiting high probabilities of individual dwelling types. It has already been shown (Mesev *et al.*, 1995) that many cells will exhibit high probabilities (frequently over 0.9) for one of the four major dwelling types (detached, semi-detached, terraced, and high-rise apartments).

However, the actual selection of training areas is still a somewhat subjective process of relating surface cells with homogeneous spectral groupings in the image. Fortunately, the high number of potential training areas associated with high probability cells will reduce this subjectivity. A similar approach by Sadler and Barnsley (1990) employed a smoothed 3-D population surface, again based on ED centroids, to inform the selection of training samples. They documented an overall

accuracy improvement of almost 20% when population density data were incorporated into an urban classification, with specific reductions in the confusion between residential classes. However, spectral confusion was still evident between bare soil and residential land use. Even this confusion should be resolved using a more robust surface model as well as through postclassification sorting, which will be discussed in the next section.

3.5.3 Postclassification Sorting

Postclassification sorting is simply the resolution of potentially misclassified pixels. As documented in Chapter Two, these problem pixels can be reassigned to a more appropriate spectral class by using ancillary map data (Hutchinson, 1982). The only role of the surface model in postclassification sorting is to verify the classification of the "residential" land use category. In other words, pixels classified as residential will be validated by reference to the surface model.

In this role, the surface model closely follows theoretical assumptions in the use of contextual model-based approaches in the segmentation of satellite imagery (Mason *et al.*, 1988). Because postclassification sorting will only play a small and rather polishing part in the overall classification strategy, brief attention will be given to the development and implementation of such model-based techniques. The essential reasoning of these approaches is primarily based on the ability to incorporate context more formally into the interpretation of a scene. Model-based systems which exploit ancillary data include the *SPAM* system of McKeown *et al.* (1985). This scheme uses map and domain-specific knowledge in a rule-based system for interpreting airport scenes. The authors basically conclude that map knowledge can be used to decide where in the image to look and what to look for, and that this may provide sufficient context for inherently weak methods of feature extraction to be effective. Rather than looking for perfect segmentations, their approach extracts segments characterised as "islands of reliability" for some particular class of object. These local regions are then further analysed by modules that bring to bear more object-specific knowledge which confirms or refutes the initial hypothesis.

Model-based approaches can be highly reliable yet elaborate means of image segmentation and classification. However the method proposed within this classification strategy involves the use of the surface model as a simple, spatially

approximate device for "weeding out" potentially misclassified pixels. As the surface model is based on census attributes pertaining to residential land use, problem pixels will be interrogated as to whether they belong to the "residential" spectral class, or not. Although this type of postclassification sorting is rather crude, the surface model still upholds the contextual, rule-based principles of model-based approaches in scene verification.

The actual implementation of the postclassification sorting procedure relies on the spatial integration of the classified scene with the surface model. Acting very much as a template, cells of the model are then used to determine if pixels classified as residential fit within the spatial pattern of the model. If classified pixels clearly do not conform to the spatial extent of the model, they are then labelled as potentially misclassified pixels, and will either await further verification (e.g. ground survey, topographic maps or aerial photographs) or they will simply be eliminated. However, the approximate nature and coarse spatial resolution of the model invariably restricts the utility of this procedure to classified areas on the urban periphery. Nevertheless, postclassification sorting will still be of value, especially to distinguish those spectrally similar pixels representing bare soil and particular urban surfaces.

3.5.4 Bayesian Decision Rule

As already outlined, the Bayesian decision rule is derived by modifications of the *a priori* probabilities of the conventional maximum likelihood classifier. So far in this chapter, the conceptual development of the rule has resulted in the values of these prior probabilities being dealt with hypothetically. However, the degree to which one class should be favoured over another needs to be inferred from the empirical criteria extracted from additional, non-spectral information. The reader may refer back to Chapter Two where additional, or ancillary data, were used to improve supervised classifications.

The formula for the Bayesian decision rule can be adapted to incorporate ancillary variables from the Census. Consider a as an ancillary variable with states, a_1, a_2, ... , a_J. The objective is then to find the probability that a random pixel will be a member of a spectral class w_k, given its vector of observed measurements X_i, in n-band space and the fact that it belongs to ancillary class a_j, described as,

$$\Pr(w_k|\boldsymbol{X}_i,a_j) \tag{3.40}$$

It is also assumed that the effects of a_j are external to the original generation of the mean vector and variance-covariance matrix of w_k. As a result the likelihood function $F_k(\boldsymbol{X}_i)$ is unaltered by the introduction of a_j, but is simply modified by the conditional probability,

$$\Pr(w_k|a_j) \tag{3.41}$$

This is a process of identifying the association between *spectral class* w_k with *census variable* a_j. For example, the spectral class labelled as "detached dwellings" or "low density residential" would be directly associated with the census variable of "detached dwellings". In effect, w_k is weighted by the probability of a_j, producing the prior probability of class w_k. The Bayesian rule can now be represented as,

$$\Pr(w_k|\boldsymbol{X}_i,a_j) = \frac{F_k(\boldsymbol{X}_i)\ \Pr(w_k|a_j)}{\Sigma_K\ F_k(\boldsymbol{X}_i)\ \Pr(w_k|a_j)} \tag{3.43}$$

In effect, $\Pr(w_k|a_j)$ is a weighting of the class w_k, and within ERDAS this is implemented in exactly the same way as equation (3.30), i.e $F_k(\boldsymbol{X}_i)'$, except that the derivation of the prior probability of w_k has been augmented by a single corresponding census variable.

The procedure may be expanded to include more than one census variable. The following assumes a three-way Bayesian-type classification with an additional ancillary census variable b with states, $b_1, b_2, \ldots, b_H$, inserted as,

$$\Pr(w_k|\boldsymbol{X}_i,a_j,b_h) \tag{3.44}$$

stating the probability that an observation pixel is a member of w_k given its measurement vector $\boldsymbol{X}_i$ in n-bands, and that it belongs to ancillary variable a_j *and* ancillary variable b_h. The Bayesian decision rule now becomes,

$$\Pr(w_k|\boldsymbol{X}_i,a_j,b_h) = \frac{F_k(\boldsymbol{X}_i)\ \Pr(w_k|a_j,b_h)}{\Sigma_K\ F_k(\boldsymbol{X}_i)\ \Pr(w_k|a_j,b_h)} \tag{3.45}$$

The likelihood function, $F_k(X_i)$ is again unchanged, but the prior probability term $\Pr(w_k|a_j,b_h)$ has expanded to include the additional conditioning variable b_h. In effect, $\Pr(a_j,b_h)$ is the prior probability of class w_k. Operationally, statistical packages would first calculate the joint probability of the two ancillary variables before relating them to the spectral class w_k. As all ancillary variables are obtained from the surface model, the calculation of $\Pr(a_j,b_h)$ should proceed routinely with the aid of a GIS. Once again, this weighting within ERDAS is implemented as equation (3.30), except that the prior probability of w_k has now been augmented by two conditioning ancillary variables.

3.5.4.1 Numerical Example

Working through a simplified numerical example will illustrate the calculations needed in a Bayesian decision rule using census prior probabilities. Consider two spectral classes w_1 and w_2, and a single conditioning census variable a, labelled as "Detached Dwellings", under two scenarios, a_1 (equal priors) and a_2 (unequal priors).

From the Census, it is possible to determine the proportion of detached dwellings within a defined residential area. However, for this example, consider two separate scenarios where the prior probabilities for detached dwellings are weighted to each of the two spectral classes w_1 and w_2 in the following way (Table 3.3).

Table 3.3 Detached dwellings prior probabilities

Probability	a_1	a_2
$\Pr(w_1)$ $\Pr(w_2)$	0.5 0.5	0.2 0.8
Σ	1.0	1.0

Under the first scenario a_1, both spectral classes, w_1 and w_2 have an equal probability of being conditioned by the ancillary variable and as such prior probabilities will have no effect. However, under a_2, class w_1 is assumed to be more likely to be detached housing, given its likelihood function. Using the probability density functions $F_1(X_i)$ and $F_2(X_i)$ that were calculated in equations (3.25) and (3.27) respectively, the component terms for the Bayesian decision rule (equation 3.43) are in Table 3.4.

Table 3.4 Results from Numerical Example

	$\Pr(w_k)$	$F_k(X_i)$	$\Pr(X_i\|w_k)\ \Pr(w_k)$	$\Pr(w_k\|X_i,a_j)$
$\Pr(w_1,a_1)$	0.5	0.145	0.0725	0.53
$\Pr(w_2,a_1)$	0.5	0.128	0.0640	0.47
	---		---	---
Σ	1.0		0.1365	1.00
$\Pr(w_1,a_2)$	0.2	0.145	0.0290	0.22
$\Pr(w_2,a_2)$	0.8	0.128	0.1024	0.78
	---		---	---
Σ	1.0		0.1314	1.00

The following steps will illustrate how the actual conditional probabilities $\Pr(w_k|X_i,a_j)$ are reached. First, under the equal prior probabilities of a_1, w_1 would be,

$$\Pr(w_1|X_i,a_1) = \frac{F_1(X_i)\ \Pr(w_1|a_1)}{F_1(X_i)\ \Pr(w_1|a_1) + F_2(X_i)\ \Pr(w_2|a_1)} \tag{3.46}$$

$$= \frac{0.145\ (0.5)}{0.145\ (0.5)\ +\ 0.128\ (0.5)} = \frac{0.0725}{0.1365} = 0.53 \tag{3.47}$$

and then for w_2,

$$\Pr(w_2|X_i,a_1) = \frac{F_2(X_i)\ \Pr(w_2|a_1)}{F_1(X_i)\ \Pr(w_1|a_1) + F_2(X_i)\ \Pr(w_2|a_1)} \tag{3.48}$$

$$= \frac{0.128\ (0.5)}{0.145\ (0.5)\ +\ 0.128\ (0.5)} = \frac{0.0640}{0.1365} = 0.47 \tag{3.49}$$

Under the unequal prior probabilities of a_2,

$$\Pr(w_1|X_i,a_2) = \frac{F_1(X_i)\ \Pr(w_1|a_2)}{F_1(X_i)\ \Pr(w_1|a_2) + F_2(X_i)\ \Pr(w_2|a_2)} \tag{3.50}$$

$$= \frac{0.145\ (0.2)}{0.145\ (0.2)\ +\ 0.128\ (0.8)} = \frac{0.0290}{0.1314} = 0.22 \tag{3.51}$$

and for w_2,

$$\Pr(w_2|\boldsymbol{X}_i,a_2) = \frac{F_2(\boldsymbol{X}_i)\Pr(w_2|a_2)}{F_1(\boldsymbol{X}_i)\Pr(w_1|a_2) + F_2(\boldsymbol{X}_i)\Pr(w_2|a_2)} \tag{3.52}$$

$$= \frac{0.128\ (0.8)}{0.145\ (0.2) + 0.128\ (0.8)} = \frac{0.1024}{0.1314} = 0.78 \tag{3.53}$$

In summary, under equal prior probabilities represented by a_1, the posterior probability $\Pr(w_k|\boldsymbol{X}_i,a_j)$ for spectral class w_1 is higher. It can be noticed that under these conditions of equal prior probabilities, the posterior probabilities are proportional to the likelihood function $F_k(\boldsymbol{X}_i)$. However, under unequal prior probability assumptions in the case of a_2, the posterior probability now greatly favours spectral class w_2, even with the same likelihood function. For both cases, it is worth noting that a sensitivity analysis of the complete effects from marginal variations in prior probability values may be found in Mather (1985).

The theoretical development of a modified maximum likelihood classifier using *a priori* probabilities produces by definition *a posteriori* probabilities, and this was briefly discussed earlier in this chapter. However, for the purposes of the specific fractal modelling assumptions used in this thesis (Chapter Four), each land use category will only be classified as either present or absent, denoted by either a 1 or 0 respectively. Thus, each pixel will be assigned to a single discrete, category by selecting the maximum probability, $L_k(\boldsymbol{X}_i)$ of a pixel $\boldsymbol{X}_i$ belonging to category w_k, with the following decision,

$$L_k(\boldsymbol{X}_i) = \begin{cases} 1, \text{ in land use category } w_k \text{ if max } F_k(\boldsymbol{X}_i)' \\ 0, \text{ otherwise.} \end{cases} \tag{3.54}$$

In this respect, the modified maximum likelihood classifier produces conventional discrete thematic coverages. However, this simplification should not devalue the role of prior probabilities, because they also determine the degree to which a pixel belongs to a class as determined by accuracy assessments (section 3.5.5).

At this stage it is essential to emphasise the importance of specifying a correct spatial framework within which prior probabilities are applied. In other words, the spatial

extent of a satellite image needs to completely and exclusively accommodate the full range of prior probabilities for each spectral class. For instance, in the classification of dwelling types, each set of prior probabilities associated with each dwelling type needs to correspond with a satellite image that is constrained by the full and exclusive delineation of residential land use. This requirement is vital to the correct statistical assumptions of the Bayesian decision rule which relies on an exact partitioning of a finite decision space between all possible classes. Statistically, this is shown in the denominator of the decision rule (equation 3.29) which forces the set of prior probabilities to sum to 1.

With this in mind, the Bayesian-type classification approach adopted in this thesis will proceed along three consecutive lines of analysis. To begin, the entire decision space is first defined by a *segmentation* of a satellite image into regions of exclusively residential land use. Next, prior probabilities for all dwelling types within this segmented image are generated on the basis of their known relative areal proportions. Finally, these prior probabilities are entered into the conventional maximum likelihood classifier. This approach basically follows the work of Strahler (1980). However, Barnsley *et al.* (1989) have expressed concern over the lack of a suitable, objective rationale for assigning prior probabilities. In this work, sets of prior probabilities for various land categories were processed within discrete segmented portions of the image to avoid situations where a frequently occurring individual class with a large prior probability virtually eliminates minority classes. To address this particular concern, only four dwelling types will be considered to ensure that no one type dominates an image. It is expected, however, that the apartments category will be noticeably smaller than other groups, and as such will have a small associated prior probability.

3.5.5 Accuracy Assessment

The overriding objective of all image classifications is to produce a meaningful map that is both consistent with user-defined specifications and, more importantly, relates to the real world as closely as possible. Accuracy assessments entail testing a classified image against reference data that are considered the "truth". Whether the reference data are completely accurate is a matter of how it was collected and interpreted. Selecting the ideal number of sample pixels to be tested can be determined from a formula based on the binomial probability theory (Fitzpatrick-

Lins, 1980).

$$N = 4\,(p)(q^{\sim}) / E^2 \qquad (3.55)$$

where, N is the number of test points (pixels) to be sampled, p is the expected percent accuracy, $q^{\sim}$ is the difference between 100 and p, and E is the allowable error. For a situation where the expected accuracy meets the Anderson *et al.* (1972) guidelines of 85% at an allowable error of 5%, the sample size would be,

$$N = 4\,(85 \times 15) / 5^2 = 204 \qquad (3.56)$$

Assuming the analyst has complete confidence in the truth data, the usual practice is to select common samples from both the classified image and the reference data and to generate measurements of accuracy in terms of how closely they agree. The basic measure of agreement is overall accuracy, which is simply the proportion of pixels, in all categories, correctly classified. Previous studies have underlined the volatile nature of image classification, perhaps reflecting the low precision of the reference data as well classifications that are very much scene-specific. On a regional scale the classification of similar land covers from different studies have yielded accuracies of between 50% and 90% (Hill and Megier, 1988; Shimoda *et al.*, 1988).

Overall accuracy assessments evaluate the agreement between the classified image and the truth map in total area in each category. They usually do not elucidate compensating errors that occur in the various categories. For this reason, Aronoff (1982) suggests that the comparative analysis of site-specific error matrices may provide a better method of comparing land-use classification techniques than a simple comparison of overall estimated map accuracy. These site-specific assessments produce measurements in errors of omission and errors of commission. Errors of omission reflect the number of pixels assigned to incorrect categories, while errors of commission indicate the number of incorrect pixels assigned to each category. Both the overall and site-specific assessments should be tested as to whether the classified map exceeds the 85% Anderson criterion. For an overall accuracy, the 95% one-tailed lower confidence limit for a binomial distribution can be obtained from the equation derived from Snedecor and Cochran (1967, p.211),

$$p = p^{\sim} - \{1.645\,[(p^{\sim})(q^{\sim})/n]^{0.5} + (50/n)\} \qquad (3.57),$$

where p is the accuracy of the map expressed as a percentage, $p\tilde{}$ is the overall accuracy as a percentage, $q\tilde{}$ is simply 100 - $p\tilde{}$, and n is the sample size. If $p\tilde{}$ exceeds the 85% criterion (Anderson *et al.*, 1972) at the lower confidence limit, it is fair to state, with 95% confidence, that the classified map meets or exceeds the accuracy standards. For site-specific assessments requiring a two-tailed test,

$$p = p\tilde{} \text{ + or - } \{1.96\,[(p\tilde{})(q\tilde{})/n]^{0.5} + (50/n)\} \quad (3.58)$$

However, the benchmark that has become the standard in image classification over the last decade, although it was first developed by Cohen (1960), is known as the *Kappa Coefficient of Agreement.* Unlike the accuracy measures already outlined, the estimate of Kappa (K) uses all cells in the matrix, not just diagonal elements, and can be defined as the proportion of agreement after chance agreement is removed from consideration. It is expressed as,

$$K = (y_o - y_c) / (1 - y_c) \quad (3.59),$$

where y_c is the proportion of units for expected chance agreement (overall accuracy percentage), and y_o is the proportion of classes which agree. $K = 0$ when obtained agreement equals chance agreement, and perfect agreement or perfect classification results in a value of $K = 1.00$. The Kappa technique is one which is accountable to intra-class correlation coefficients by using information in the classification error matrix resulting from errors of commission and omission (Rosenfield and Fitzpatrick-Lins, 1986). All of the accuracy measurements mentioned in this section will be used to assess classifications generated in Chapter Five.

3.6 Summary and Conclusions

Chapter Three has provided a detailed discussion of the role of census data within an urban image classification strategy. It has been shown how the Bracken-Martin surface model can be used to incorporate data from the UK Population Census into urban image analysis in a three stage strategy: training sample selection, postclassification sorting, and classification by the Bayesian decision rule. All three were able to capitalise on the unique abilities of the surface model in combining aspatial attributes from the Census with the power of satellite imagery to detect the

physical spatial properties of urban areas. Specifically the surface model was found to be able to represent numerous potential sites for both training sample selection and postclassification sorting. However, the bulk of Chapter Three was given to the theoretical development of the Bayesian decision rule as the most innovative technique in the classification strategy. Bayes' theorem was shown to be a straightforward derivation of the formula for calculating conditional probability, and it was contrasted with the maximum likelihood estimator, of which it is a modified case. In addition to setting out the complex notation used in the formulation of the decision rule, Chapter Three also showed how the concepts of prior and posterior probabilities would be operationalised, and provided numerical examples to illustrate the conventional maximum likelihood discriminant function, and the Bayesian-type classifier. The chapter concluded with a synopsis of standard accuracy assessment measurements.

This chapter has established a workable framework within which census data pertaining to all aspects of socioeconomic and housing characteristics can be used to inform and improve the image classification of urban morphology. In Chapter Five this improved classification strategy will be applied to, and tested on empirical data sets representing four settlements in the United Kingdom. However, the next chapter, Four, will first examine the development of urban density functions using fractal concepts, with which all classifications will be analysed in Chapter Six.

Chapter Four
URBAN DENSITY FUNCTIONS

4.1 Introduction

The last two chapters have been almost completely dedicated to the theoretical foundations for the generation of urban land use inventories through the coalescing of data from observation satellites and population censuses. Many of the practical applications that could benefit from using these inventories have been listed, and tend to relate to urban management and planning policies, both by public authorities and private development agencies. These previous chapters have established a sound measurement framework from which physical and activity based analyses of urban densities can now be covered. In this chapter, the analysis of urban systems will begin by summarizing current research into urban growth, urban form, and the formulation of urban density functions based on concepts derived from fractal geometry (Longley *et al.*, 1991; Batty and Kim, 1992; Arlinghaus, 1993; Frankhauser, 1994; Batty and Longley, 1994). Particular attention will also be given to the fractal properties of simple urban growth models and the development of urban gradients based on the fractal reformulation of conventional density functions. However, the main contribution of this chapter will not be the actual statistical estimations, but an account of the quality and representation of empirical data from which density functions are derived. This is in direct response to the established, but deficient, process of fitting urban density functions by elaborate models which were usually based on low quality, highly aggregated source data. Incidentally, source data here are all forms of information pertaining to the delineation of urban land use, as well as associated attributes including, but not limited to, population, employment, and housing land use. This chapter will also attempt to assess the limitations and paucity of source data used in previous work, and from there will present the case for the role of data derived from classified satellite imagery in urban density modelling.

The chapter begins with a brief review of the development of urban density functions as modelled using negative-exponential and inverse power functions. The latter model will further be evaluated as an appropriate vehicle for demonstrating the fractal property of self-similarity considered by some to be a fundamental characteristic of urban form and density. Finally, traditional and present data sources used in the testing of urban density functions are assessed in terms of accuracy and consistency,

as well as the cartographic technique from which their values are derived.

4.2 Development of Urban Density Functions

Urban density functions are defined as mathematical formulations which describe the relationship between distance from a city centre (or other growth focus) and density measures of some facet of the urban environment, often population, buildings, or economic activity. The development of these functions is based on the widely-observed phenomenon in urban systems of density decline with distance from their historic sites of first development.

Often credited as the earliest land use model, von Thünen's (1826) spatial organisation of agricultural land use, and subsequent interpretations (see Lloyd and Dicken, 1977), described both existing and optimal agricultural location patterns. In this model, land nearest the farm or market centre commanded higher rent per unit area because of the associated decreased transportation costs. In agricultural terms, this land was more often intensely cultivated.

The extension from agricultural land use to urban land use is well-developed in classical location theory by Haig (1926), Isard (1956), and Alonso (1964). Basically, land closest to the city centre commands higher rent per parcel, in much the same way as in the agricultural framework. Reduced transportation costs and other advantages of central accessibility also encourage activity to concentrate around the core, while land-extensive activities tend to locate further out (Evans, 1985). Because of the established infrastructure, the minimisation of the cost and maximisation of access to transportation, as well as simple inertia (Muth, 1969), we typically see higher urban density at the core, and observe that rent per unit space is higher in these dense areas (Alonso, 1964).

However, the effects of suburbanisation, such as outlying business districts and suburban shopping centres, have resulted in changes to the gradients of metropolitan density profiles (Mills and Tan, 1980; Edmonston *et al.*, 1985; Batty *et al.*, 1989; Alperovich and Deutsch, 1992), as well as in regional spatial structures (Parr, 1985a; 1985b). Interest in explaining the suburbanisation phenomenon accounts for some of attention paid to density gradients. The influences of increased household incomes

and improved transportation infrastructures are among the causes investigated for affecting residential density (Evans, 1985; Anas and Kim, 1992). However, apart from founding works by Mills (1970) and Sibley (1971), the application of strictly statistical density functions to non-residential activities has been relatively neglected despite the marked decentralisation of a range of urban activities during the last two decades. The location of new and relocation of existing firms and functions, due in part to economic restructuring, has seen manufacturing, large and small scale retailing, wholesaling and other commercial activities move further away from the city centre. In addition, the increased traffic congestion in the city centre, along with transportation improvements in the form of motorways, has also seen new "mini-cores" spring up on the outskirts, especially at the intersections of major roadways.

Today, however, urban density is still observed to basically decline with distance from the urban core, though not strictly monotonically, despite major shifts in population to the suburbs over the last century, most notably in North America.

Before moving on to the statistical developments of density functions, it is worth clarifying the working definition of density.

4.2.1 Urban Density

For all the various references to the concept of "density" used in geographical studies, its definition remains simply a measure of the number of attributes or items (people, workers, buildings, traffic, etc.) per unit area of land. This means that density values are clearly affected by fluctuations and inconsistencies in the measurement definitions of both urban attributes and parcels of land. Fluctuations in both sides of the ratio inevitably lead to the modifiable areal unit problem (MAUP), which was already discussed in Chapter Two. In this chapter, density, as used in urban density functions, will be assessed in terms of the level of accuracy and consistency in data measurements for both urban attributes and land parcels. However, this raises the question of what exactly urban density is measuring, for example, "resident (or night time) population", "buildings", "economic activity", "land uses", or some other attributes of the urban fabric. Most of the previous works in the estimation of urban density are heavily dependent upon national population censuses, which are spatially aggregated and are represented in areal tracts for which the census data were initially collected. Density is, therefore, a measure of any socioeconomic or housing attribute

available from the census per unit area of census tract, most usually represented by a choropleth map. As a result, density may be considered a gross value, where the measure of land area includes land in all uses, not just in residential use. Moreover, gross density is in effect an average which is assumed to fill the entire area of the census tract. In reality, this is clearly not the case. Observed densities are likely to vary within zones, and a record of an attribute occurring in a tract does not presume an even within-tract distribution. As a result, data sources that represent the actual physical layout of the urban space contain information about single land uses, such as industrial and commercial, as well as various types of residential. Here, density based on single, discrete land use types extracted from sources such as digital databases and remote sensing, can be viewed as "net density" where actual land use patterns are measured.

However, the statistical formulations of urban density functions are frequently based on the measurement of density by standard areal units, commonly arranged in concentric zones radiating out from the urban core. As a result, empirical areal data are frequently resampled into standard sized grid cells. Standardisation is merely a cosmetic process and does not, in any respect, standardise the quality of data from the various sources. Data quality and cartographic representations employing gross density and net density estimations, along with intermediary variations, will be extensively examined later in this chapter. Before their specific roles are assessed, it is first important to briefly review the theoretical and statistical foundations of conventional urban density functions, as well as those based upon fractal concepts.

Table 4.1 General Chronology of Conventional Models Related to Urban Population Densities (from Zielinski, 1980)

Year	*Model*	*Proponent*
1947	linear	Stewart
1951	negative-exponential	Clark
1960	normal	Sherratt
1961	normal	Tanner
1963	inverse-power	Smeed
1968	gamma	Aynvarg
1969	quadratic negative-exponential	Newling
1969	quadratic negative-exponential	Muth
1972	normal gamma & quadratic gamma	Amson
1973	equilibrium models	Amson
1977	negative-exponential (random coefficient model)	Kau and Lee

4.2.2 Statistical Foundations

As already outlined, traditional notions in the growth of settlements have tended to be described by a basic, essentially geographical, process of distance decay, which was implicit as far back as the works of von Thünen. However, only since the 1940s, 1950s and the subsequent culmination of the so-called quantitative revolution in the social sciences, have a range of more elegant mathematical functions been developed and applied (Table 4.1).

By far the model most widely adopted in quantitative urban analysis is the negative-exponential (Clark, 1951). It assumes that population density $p(R)$ at distance R from the centre of the city (where $R = 0$) declines monotonically according to the following negative-exponential,

$$p(R) = K \exp(-\lambda R) \tag{4.1}$$

where K is a constant of proportionality which is equal to the central density $p(0)$ and λ is a rate at which the effect of distance attenuates. If λ is large, density falls off rapidly; if it is small, density falls off slowly. Clark's objectives for developing a statistical function were strongly motivated by a desire to analyse suburbanisation systematically. The model was also formulated in a manner consistent with laws of strict utility-maximisation associated with urban economic theory (Muth, 1969), while the development of discrete choice theory also made widespread use of such functions (Anas, 1982). Even by the late 1970s, exponential density functions had already been estimated for many metropolitan areas in many countries. The appeal of the function may lie in its analytical convenience in problems of economic optimisation, as well as the elegance of the mathematical forms that it produces. Detailed statistical analyses of the model are given in Zielinski (1979; 1980), and Batty and Kim (1992).

In contrast to the negative exponential, inverse-power functions have also been widely applied in social physics, such as in gravitational models of traffic flow, rank-size relations, as well as to population density (Smeed, 1961).

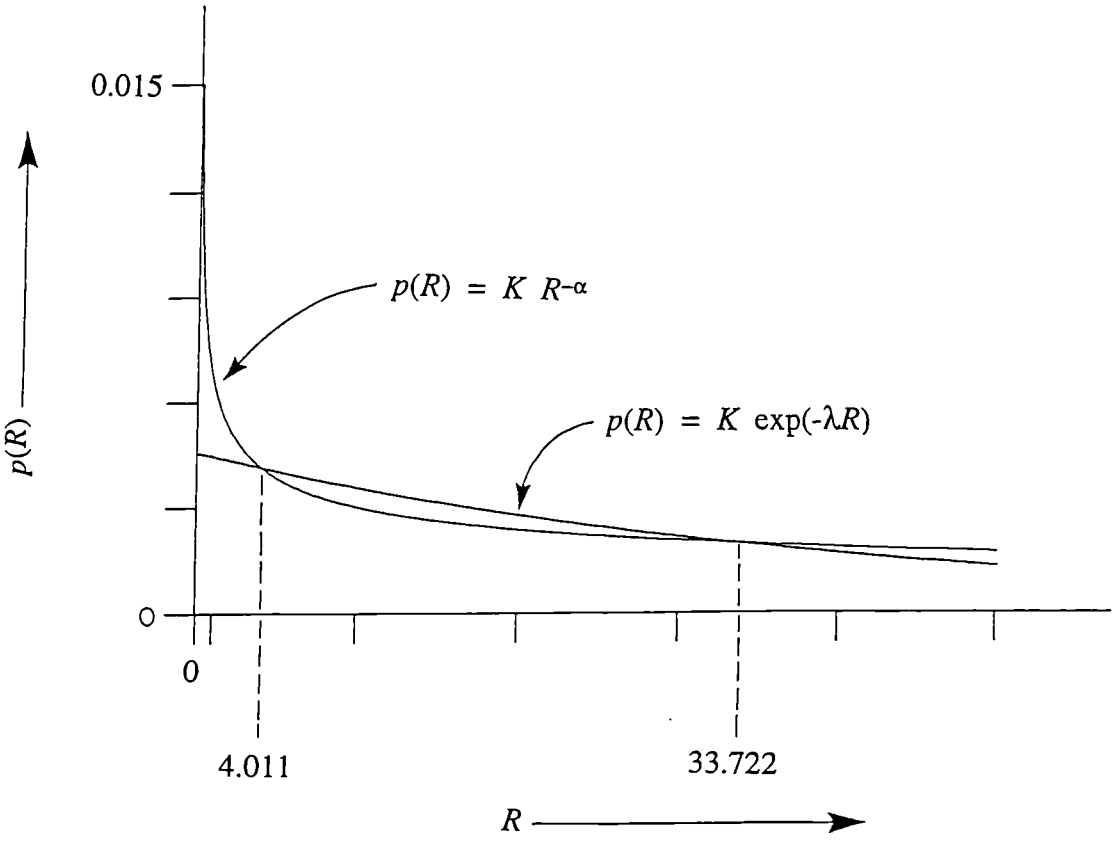

Figure 4.1 A Comparison of the Negative Exponential and Inverse Power Functions (after Batty and Kim, 1992)

The inverse-power function can be expressed as,

$$p(R) = K\ R^{-\alpha} \tag{4.2}$$

where K is the constant of proportionality as in equation (4.1), but not defined where $R = 0$, and α is the parameter on distance.

A comparison of the two functions on urban population density made by Batty and Kim (1992) revealed both to be poor predictors at central densities (Figure 4.1), partly because of the imprecision of censuses (Zielinski, 1980). However, the inherent flexibility of the inverse-power function produced a less steep fall-off at the periphery, reflecting the suburbanisation process in Western cities. Batty and Kim also contend that the negative-exponential function is fundamentally flawed when used to measure urban systems. They argue that its α parameter is scale dependent whereas urban systems exhibit a degree of scale independence in terms of the extent to which development fills the space available. There are strong connections between urban density, as modelled by power functions, and the processes of allometric and fractal growth (Nordbeck, 1971). Before the inverse power function is developed further, there now follows a discussion of the role of fractal geometry in areas of urban growth, density, and form.

4.3 Urban Growth and Urban Form

In most discussions, urban growth invariably means an increase in the net population (natural increase and net migration) of a settlement, and/or an increase in the spatial extent of a continuously built-up area. There is no single cause which is responsible for the growth of particular cities. Instead, a set of causes, ranging from resource availability to agglomeration economies, have been associated with urban expansion rates. By contrast, the shape of urban areas has not attracted as much research, and has not been a part of many theories of urban dynamics. Urban form was traditionally considered an assumption of analysis, a given, never a consequence of the processes at work (Batty *et al.*, 1989). During the last fifteen years, however, there have been major developments in the science of form, especially within physics and mathematics. In particular, the physical processes of growth have been linked to form based on the emergence of a geometry of the irregular, termed *fractal geometry* by

Mandelbrot (1983). Fractal measurements of boundaries, exhibiting intrinsic self-similarity, have been observed from coastlines, river systems, fine particles, and other dendritic forms (Vicsek, 1989). Here, fractal geometry is applied to the measurement of urban morphologies, and closely follows works by Batty and Longley (1987; 1994), Fotheringham *et al.* (1989), Longley *et al.* (1991), Dendrinos (1992), and Frankhauser (1994).

4.3.1 Fractal Settlements

Fractal geometry is essentially a geometry of the irregular where, with regard to linear features, the length of a boundary is a function of the scale at which it is measured. Mandelbrot (1967) demonstrated that the dimension (D) of geometrical objects may be viewed as existing along a continuum, with the Euclidean dimensions of points, lines, areas and volumes (0, 1, 2, 3 respectively) being special cases along this continuum. Fractal dimensions which lie between 1 and 2 are deemed to provide an index of line ruggedness or irregularity.

The foundations of a fractal theory of settlements now exists which has the potential to unify many ideas from location theory with those of spatial form (Batty and Longley, 1994). However, the notion that settlements exhibit self-similarity in their functions has been widely cited in urban theory for over a century. Examples include relations such as the rank-size rule, hierarchical differentiation of service centres in central place theory, transportation hierarchies and modes, and in the area and importance of different orders of hinterland (Arlinghaus, 1985; 1993). Each of these relations, which are the cornerstones of urban geography, can be now be explicitly tied together in a fractal geometry of the irregular, a geometry of the real world (Batty and Longley, 1994). Moreover, whatever approach to urban analysis is taken, at some stage cities need to be visualised in terms of their geometric form. In urban economics and related fields such as transportation, models are used to describe, explain and predict in spatial terms, often ascribing geometric terminology to the shape of urban land use and the manner in which it spreads.

Recall that the measurement of fractal dimensions of urban areas has generally followed the Mandelbrot interpretation and assigned only values lying between 1 and 2. This assumes that settlements fill more than the linear extent of the two-dimensional space in which they exist (where $D = 1$), but less than the entire space (D

= 2). The reasons are that most city landscapes are perforated with undeveloped land, not only by physical constraints on what can and cannot be built upon, but also by the very processes of development at the micro level which take place slowly and incrementally, with little coordination in terms of physical contiguity. It is also theoretically possible to allow urban development to become three-dimensional in the vertical axis, in which case D might lie between 2 and 3, although this notion will not be pursued here. However, despite problems in both the definition of urban development and the quality of urban data, as well as variations in the methods of fractal estimation, there is a wide agreement that settlements spread out in the plane and hardly touch the third dimension. Examples of fractal dimensions that lie between 1 and 2 can be found in Table 4.2, along with a selection of data from which these dimensions were measured.

Table 4.2 Fractal Dimensions of Selected Settlements

Settlement	*Dimension D*	*References*	*Data Source*
Albany (USA) 1990	1.494	Batty and Xie (1994b)	Digital Line Graphs
Beijing (China) 1981	1.93	Frankhauser (1994)	Census Tracts
Berlin (Germany) 1980	1.73	Frankhauser (1994)	Census Tracts
Buffalo (USA) 1990	1.729	Batty and Xie (1994b)	Digital Line Graphs
London (UK) 1981	1.864	Longley *et al.* (1991)	Digital Boundary Data
Los Angeles (USA) 1981	1.93	Frankhauser (1994)	Census Tracts
Paris (France) 1981	1.66	Frankhauser (1994)	Census Tracts
Pittsburgh (USA) 1990	1.775	Batty and Xie (1994b)	Digital Line Graphs
Pittsburgh (USA) 1981	1.59	Frankhauser (1994)	Census Tracts
Seoul (South Korea) 1981	1.682	Batty and Kim (1992)	Cadastral Map

The most noticeable feature of Table 4.2 is the various source data used in empirical applications and the rather erratic range of dimensions generated. It is likely that inconsistencies in source data heavily restrict direct comparisons of fractal measurements between settlements. Indeed problems in measurement have been and still are a recurrent difficulty in human geography (Haggett, 1977). What is needed is a data source that is readily available, highly consistent, and can be rapidly analysed. This thesis postulates that the processing of satellite imagery can fulfil this need most successfully. Urban data from satellite imagery, as well as the other sources listed in Table 4.2, will be reviewed extensively later in this chapter, and in Chapter Six where direct comparisons will be made between dimensions generated from these data

sources and those from classified satellite imagery.

However, empirical examples from all data sources can also be compared with theoretical models of fractal growth. These are models in which simple random growth, constrained by the geometry of the system in which the growth is occurring, generate highly ordered fractal structures. Known as *Diffusion-Limited Aggregation* (DLA) models, they can act as baseline measures against which results of empirical applications are compared.

4.3.2 Diffusion-Limited Aggregation Processes

The first DLA models were suggested by Witten (1981), and Witten and Sander (1981). Briefly, using an urban analogy, DLA models generate urban structures through the process of random accretion, or aggregation, of points, representing developed urban land. Initially, a central point, or urban core, is defined within an isotropic grid of a given radius. Points are then allowed to randomly enter the plane from the circumference and either to join the urban structure or to leave the grid. The process continues until a predetermined number of points have joined the structure, or the radius of the grid has been breached. Although the form of these structures is highly idealised, it replicates the dendritic pattern and preserves the fractal property of self-similarity, argued here as the basis for the form of real urban areas. The structure also exhibits the cardinal feature of urban density functions, that of declining density with distance from the centre. However, the most important conclusion that can be drawn from generating models by DLA processes is the efficient demonstration of how urban growth and form are inextricably linked (Batty *et al.*,1989). Several independent estimations of the fractal dimensions of DLA simulations suggest that the value for D should invariably fall between 1.66 and 1.71 (Witten and Sander, 1981; Sander, 1987; Meakin and Tolman, 1989; Vicsek, 1989; Batty and Longley, 1994).

Though this section may not have contributed to the advancement or re-working of fractal simulation theory, it has, nonetheless, set out to establish a baseline model from which comparisons both with, and between empirical applications may be attempted. The DLA model's ability to reproduce a space-filling regime which is fractal is here presented as the appropriate baseline model with which to perform these comparisons.

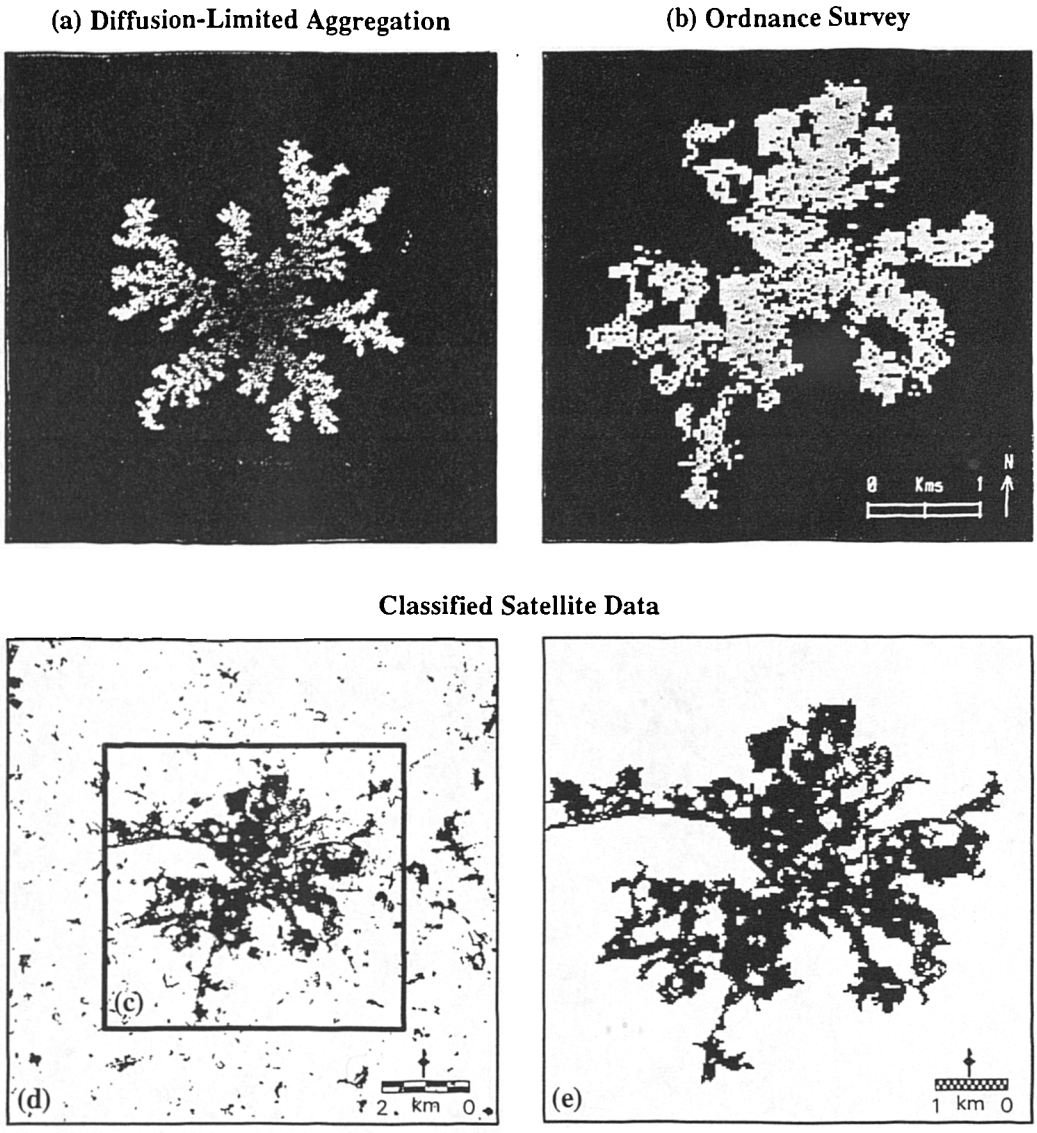

(c) RS - Reduced
(d) RS - Full

(e) RS - Town

Figure 4.2 Spatial Representations of Taunton

4.3.3 The Case of Taunton, Somerset

Comparisons between the idealized DLA model and an empirical analysis of the town of Taunton in south-west England were documented by Batty *et al.* (1989). Taunton was selected because its development was not severely affected by either underlying geomorphology or by large-scale man-made constraints, and as such, it satisfied the ideal isotropic assumptions of the DLA model. Furthermore, the relatively small size of Taunton, containing a population of approximately 49,000 in 1981, also complied with manageable digitising and storage limitations at that time. The empirical data set was composed of 50m grid cells created by the manual vector digitising of 1981 topographic Ordnance Survey maps at a scale of 1:10,000. There were 22,500 cells in total with 3,179 coded as developed, and the rest as undeveloped urban land.

Comparisons made by Batty *et al.* (1989) are re-examined in light of three further empirical data sets of Taunton created from classified satellite imagery. Unlike methodologies outlined in Chapters Two and Three, the classification technique used here followed simple principles of image density slicing with the surface model only acting in a very minor enabling role. A single Landsat TM-5 image, composed of bands 1, 2, 3, and 4 (visible blue-green, green, red, and near infrared), taken on April 26, 1984, was the only one available that was temporally close to the 1981 data set from the Ordnance Survey. From this image, an unsupervised spectral classification produced a binary distinction between built-up land cover and non built-up land cover. Unfortunately, areas such as quarries and bare fields frequently exhibited very similar spectral values to built-form and were subsequently mis-classified as such. In order to overcome this problem, the classified image and surface model were exposed to a simple Boolean overlay function that allowed the recognition of dubious classified areas. A brief inspection on the field by a ground survey was then all that was needed to determine the class membership of these areas. From the completed classification, three data sets were derived at a spatial resolution of 30m. The first, termed RS_{FULL}, was the most comparable with the DLA model, and represented the entire classified image that included not only Taunton but also a great deal of the rural hinterland comprised of many outlying villages and farmsteads. The other two were constrained to the geographical limits of the Ordnance Survey (OS) data set. $RS_{REDUCED}$ was a subset of RS_{FULL} and included rural built-form, while RS_{TOWN} represented only the town of Taunton, and as such is the most comparable with the OS data.

All five data sets, three from classified imagery, one from digitised OS maps, and one generated by DLA process are illustrated in Figure 4.2, with a summary of their spatial properties presented in Table 4.3.

The parameters for the DLA and OS data sets were extracted from the work of Batty *et al.* (1989), but those for the three classified satellite data sets were generated from a series of GIS functions performed by ERDAS (a proprietary image processing and GIS software). Techniques based on algorithms for vertical integration, proximity analysis, and neighbourhood operations (all discussed in Chapter Two) were routinely and systematically performed on all three satellite data sets.

Table 4.3 Spatial Properties of the Theoretical and Real Systems of Taunton

System Characteristics	*DLA**	*OS**	RS_{FULL}	$RS_{REDUCED}$	RS_{TOWN}
Dimension of Lattice	500 x 500	150 x 150	381 x 381	227 x 227	227 x 227
Lattice Points, P	250 000	22 500	145 161	51 529	51 529
Points Occupied, N	10 000	3 179	16 559	12 836	11 162
Maximum Radius, R_m	248.24	62.94	181.14	123.32	84.30
Total Effective Area, πR_m^2	193 601	12 444	103 081	47 776	22 326
Average Density, $N/\pi R_m^2$	0.052	0.256	0.161	0.269	0.500
Length of Boundary, B	19 855	3 994	23 675	14 204	9 482
Maximum Circumference, $2\pi R_m$	1 560.0	395.4	1 138.1	774.8	529.7
Tortuosity Index, $B/2\pi R_m$	12.73	10.10	20.80	18.33	17.90
Number of Boundary Points, N_b	10 000	2 709	13 997	7 543	4 281
Density of Boundary Points, N_b/N	1.000	0.852	0.845	0.588	0.384
Interior Points, N_i	0	470	2 562	5 293	6 881
Density of Interior Points, N_i/N	0	0.148	0.155	0.412	0.616
Dimension, D	1.66-1.71	1.77	1.55	1.60	1.69

*Extracted from Batty *et al.* (1989)

An initial survey of the parameters in Table 4.3 reveals that all three of the empirical RS data sets reveal a more compact form, as measured by the values from average density and boundary density, than in the DLA simulation. This is simply a result of the formulation parameters behind the development of the DLA model which assume no point can be completely surrounded by other points. The most striking dissimilarity between the OS data and those generated from satellite imagery is measured by the tortuosity index. Compared to the DLA clusters, the index is lower for the OS data but markedly higher for the satellite data. This is difference is due

largely to the finer resolution of satellite data which, in turn, greatly increases the length of their boundaries. Finer resolution may also be responsible for the lower fractal dimensions generated from classified satellite imagery. Unlike the result based on OS data, the dimension D of 1.69 from RS_{TOWN} falls right in the middle of the expected range ($1.66 < D < 1.71$) which is widely accepted as representative of DLA model assumptions. However, D values obtained from all the empirical data sets are close to this range, from a low of 1.55 to a high of 1.77, and as such approach the idealised concept of a fractal settlement.

Given that urban areas, represented by empirical data, exhibit spatial patterns that can be deemed fractal, tentative support can now be given to the notion that urban density functions may more appropriately be formulated using concepts from fractal geometry. If these assumptions hold, what the Taunton example should establish is a role for satellite data in empirical urban fractal estimation, leading to applications of urban density functions. This role can further be justified by an extensive review of conventional data sources in urban density functions, which is presented at the end of the chapter. However, there first needs to be a precise documentation of the fractal estimation procedures that will subsequently be used on classified satellite data.

4.4 Estimating Fractal Dimensions

This section outlines continued support for the contention that fractal geometry provides a much deeper insight into urban density functions than has so far been recognised. In particular, emphasis will be given to the ways in which the form of urban development can be linked to its spread and extent. Measurement is restricted to the manner and rate at which space is filled with respect to distance from the CBD (Mesev *et al.*, 1995).

4.4.1 Development of power function

The suggestion here is that the inverse power function (equation 4.2),

$$p(R) = K\ R^{-\alpha} \tag{4.2}$$

is able to accommodate scale independence observed in urban systems through the

notions of fractal geometry (Batty and Kim, 1992). It can now be shown that, given limits on the range of equation (4.2), that the cumulative population $N(R)$ associated with the density of $p(R)$ can be modelled as,

$$N(R) = G\ R^{2-\alpha} \tag{4.3}$$

from which the area $A(R)$ over which density is defined with respect to distance R from the centre is given as,

$$A(R) = Z\ R^2 \tag{4.4}$$

where a perfect circle of area would have $Z = \pi$. Applying the principle of self-similarity evident in fractal geometry, it is possible to show that the density parameter α is related to the fractal dimension D, such that $D = (2 - \alpha)$, and that the cumulative population relation can now be rewritten as,

$$N(R) = G\ R^D \tag{4.5}$$

where D is the fractal dimension measuring both the extent and the rate at which space is filled by population with increasing distance from the centre. Two sets of techniques have been developed for estimating the fractal dimension. The first set emphasises space-filling, the second set focuses on density attenuation.

4.4.2 Idealised Lattice

Space-filling involves perhaps the simplest, and most robust method of estimating fractal dimensions. The procedure uses idealized square lattices to generalise and model urban systems (Batty and Xie, 1994b). These lattices can be visualised as two-dimensional arrays with equal number of rows and columns (see Figure 4.3 extracted from Batty and Xie, 1994b).

The space-filling process assumes the binary decision of occupancy or vacancy, so that each cell of the lattice is allocated a label of occupied (developed) or vacant (undeveloped). Occupation can be population, buildings, building-type, or any other measurable urban feature.

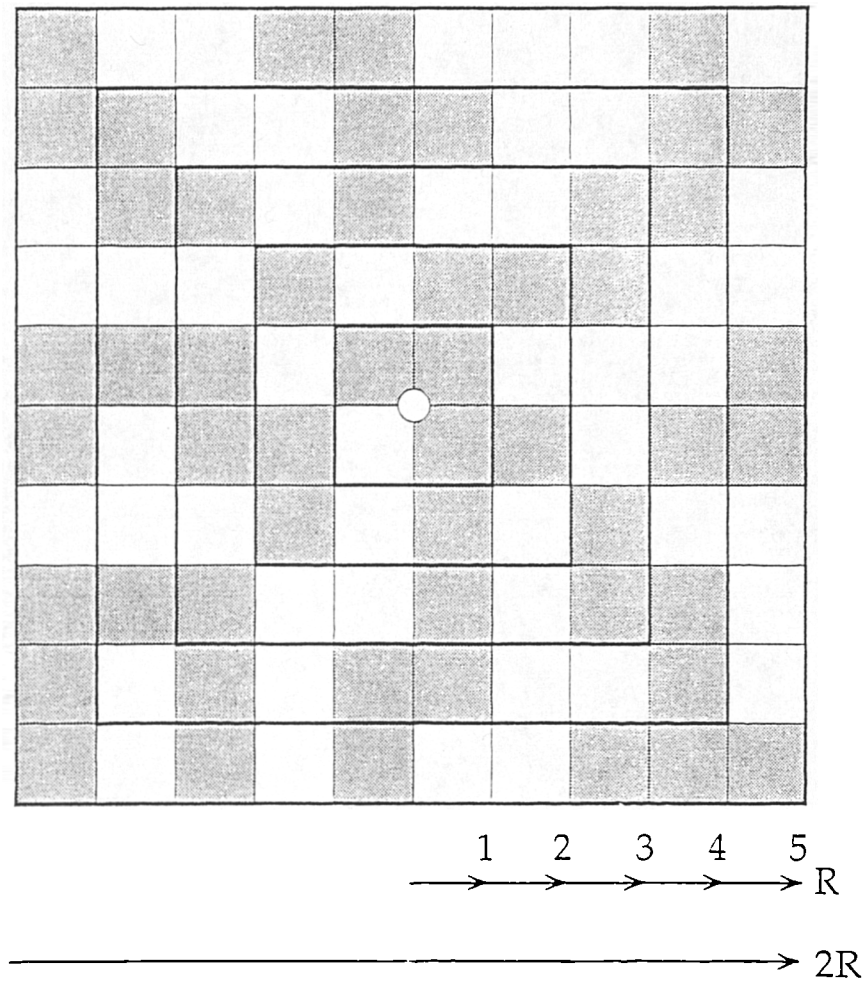

Figure 4.3 Idealised Grid Space (after Batty and Xie, 1994b)

Density is modelled by concentric zones radiating from the central point in the following sequence. The first concentric zone represents the 4 cells immediately surrounding the central point. The second zone contains a total of 16 cells (4 in zone one plus 12 surrounding zone one). The third zone contains 36 cells (4 in zone one, 12 in zone two, and 20 in zone three), and so on. The reason for a square lattice is that each concentric zone is identical in shape and width providing a consistent framework for estimating density from the centre to the most outer zone. Formally this zone relation can be summarised as,

$$N(R) = 4R^2 = (2R)^2 \tag{4.6}$$

The notion of an idealised lattice as the basic frame of measurement can now be applied to the mechanics of estimating fractal dimensions from space-filling sequences.

4.4.3 Space-Filling Dimensions

The approximation of a lattice grid which is less than completely occupied (as for most settlements) describes cumulative population as,

$$N(R) = 4R^D \tag{4.7}$$

This means that for any distance R, a value for D or α may be calculated. Extensive research reveals that the most appropriate and most representative value for D is associated with mean distance, R' (Batty and Kim, 1992; Batty and Longley, 1994). For a discrete distribution of populations n_i, where i indicates the grid location of the lattice, R' would be calculated as,

$$R' = \frac{\Sigma_i n_i R_i}{\Sigma_i n_i} \tag{4.8}$$

where R_i is the distance from the central point to i. The fractal dimension associated with R_i can now be estimated from cumulative population as,

$$D = \frac{\ln \{N(R')/4\}}{\ln R'} \tag{4.9}$$

A fundamental problem with equation (4.9) is the presence of a known constant, 4, which should be replaced with 2^D in discrete space, or π in a continuous system. The development of a fractal dimension based on density rather than cumulative population removes this restriction. Density $p(R)$ can simply be calculated as cumulative population $N(R)$ divided by the area of the grid proportional to its full occupation. This is simply equation (4.5) divided by equation (4.4), written as,

$$p(R) = \frac{G\ R^D}{Z\ R^2}$$

$$= R^{D-2} = R^{-\alpha} \qquad (4.10)$$

assuming $G \sim Z$. If equation (4.9) is rearranged, a second estimate of a fractal dimension for R' can then be expressed as,

$$D = 2 + \frac{\ln p(R')}{\ln R'} \qquad (4.11)$$

Any value of R can be calculated from equations (4.9) and (4.11), but all subsequent analysis here will be based on mean distance. This decision on only using mean values is based on the recommendation of Batty and Kim (1992) who found that values in the region of the origin were too volatile to represent the entire profile.

4.4.4 Dimensions from Linear Regression

The methods for estimating the fractal dimensions D from space-filling properties do not consider variance within the distributions, other than measures of the mean. A well known method which can take into account variance is to first, linearise the power laws in both equations (4.2) and (4.3), and then perform regression to calculate values for K and α, G and D respectively (Batty and Xie, 1994b; Mesev *et al.*, 1995). Linearised forms can be expressed for both discrete densities p_i and cumulative populations N_i, in this way,

$$p_i = \ln K - \alpha \ln R_i \qquad (4.12)$$

$$N_i = \ln G - D \ln R_i \qquad (4.13)$$

The slope parameters for both equations measure the rate at which density attenuates and population increases, each with respect to distance, respectively. These equations also allow the whole range of performance measures associated with linear regression to be meaningfully calculated, including the square of the correlation coefficient, r^2, as a goodness of fit indicator. Fractal dimensions are generated by the intercept parameters, K and G which are, in turn, affected by the slope parameters, α and $2 - D$, in equations (4.12) and (4.13) respectively. However, slope parameters may become volatile when confronted with abnormal data sets, leading to fractal dimensions that could lie beyond the logical limits associated with space-filling, i.e., $1 < D < 2$. These are considered abnormal, in the sense that data do not conform to established linear relationships in both cumulative population and discrete density with respect to distance. An example of abnormal data would result if physical constraints restrict development near the CBD, and in this case, fractal dimensions of over 2 may be calculated. Similarly, values of less than 1 are possible if "reversals in the norm" are encountered. This is when discrete density actually increases with distance from the urban centre.

4.4.5 Dimensions from Constrained Linear Regression

Comparisons between fractal dimensions generated from space-filling and linear regression are possible when the linear regression equations are constrained. This involves constraining the intercept parameters in equations (4.12) and (4.13) to values which reflect idealised space-filling limits. Operationally, this is simply replacing the constant K in equation (4.12) with a value of 1 as,

$$p_i = \ln 1 - \alpha \ln R_i \tag{4.14}$$

and G in equation (4.13) with a value of 4 or π,

$$N_i = \ln \pi - D \ln R_i \tag{4.15}$$

Constrained regression will allow for monitoring of the changes in variance in the distribution of both cumulative population and discrete density.

4.4.6 Dimensions from Partial Data Sets

A second method of refining dimensions involves reducing that set of observations which constitute the population density and count profiles. An examination of the theory of the fractal city (Batty and Longley, 1994) suggest that cities are generated according to some diffusion from a central core site (seed) in the industrial and pre-industrial ages and exhibit marked departures from inverse distance relations in the vicinity of the core and the periphery. Residential population at the core has been displaced by commercial activity, while on the periphery the city is constantly expanding, which tends to distort the inverse relation. Previous work has clearly demonstrated substantial improvements in dimension estimation and regression fitting from the elimination these extreme values at the core and periphery (Batty *et al.*, 1989; Batty and Kim, 1992).

4.5 Data Sources

Whatever approach to urban density modelling is taken, estimation procedures and empirical results are ultimately affected, and in many respects dictated, by the type, quality, consistency and cartographical representation of data and their sources. Of course, the cartographic representation of features and processes on the earth's surface is at the heart of many geographical analyses. The advent of GIS, furthermore, has brought a new technological framework within which geographical data are now routinely and rapidly manipulated and evaluated. The development of GIS has also sparked further research into the assessment of accuracy and error in data and data sources, with emphasis on the effects of scale and line generalisation. This section will examine some of the available sources of data used for estimating urban density profiles, both by conventional methods and those based on fractal concepts. A case for using classified satellite data will subsequently be developed in order to produce more accurate and detailed estimations of urban density functions.

As a precursor to the following discussion, the field of urban density functions boasts a vast literature pool that embraces research in subjects as diverse as econometrics, urban geography, city and regional planning, and civil engineering. However, many papers written on this topic frequently end with concerned comments over the practical relevance of function results.

(a) Zonal Data (Enumeration Districts)

(b) Disaggregate Data (Surface Model)

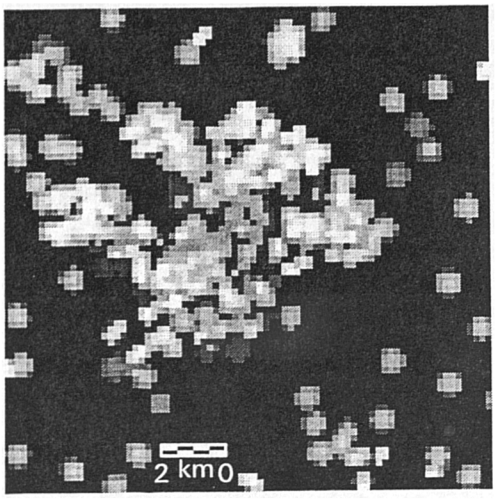

(c) Digital Urban Boundary Data

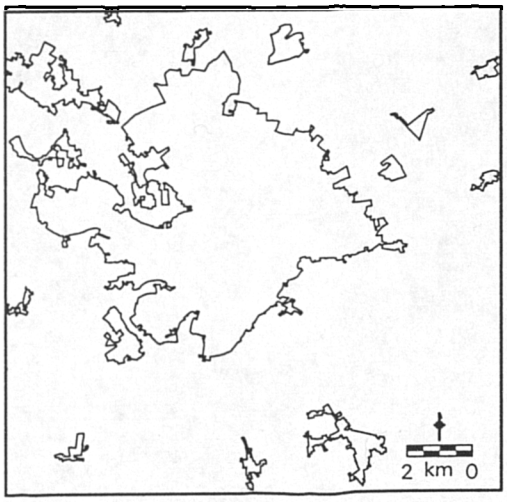

(d) Classified Satellite Data

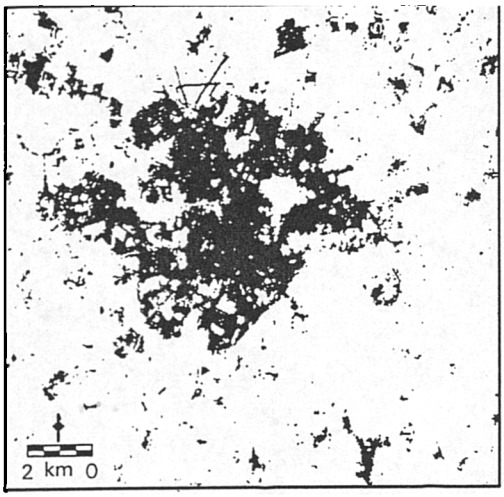

Figure 4.4 Spatial Representations of Norwich

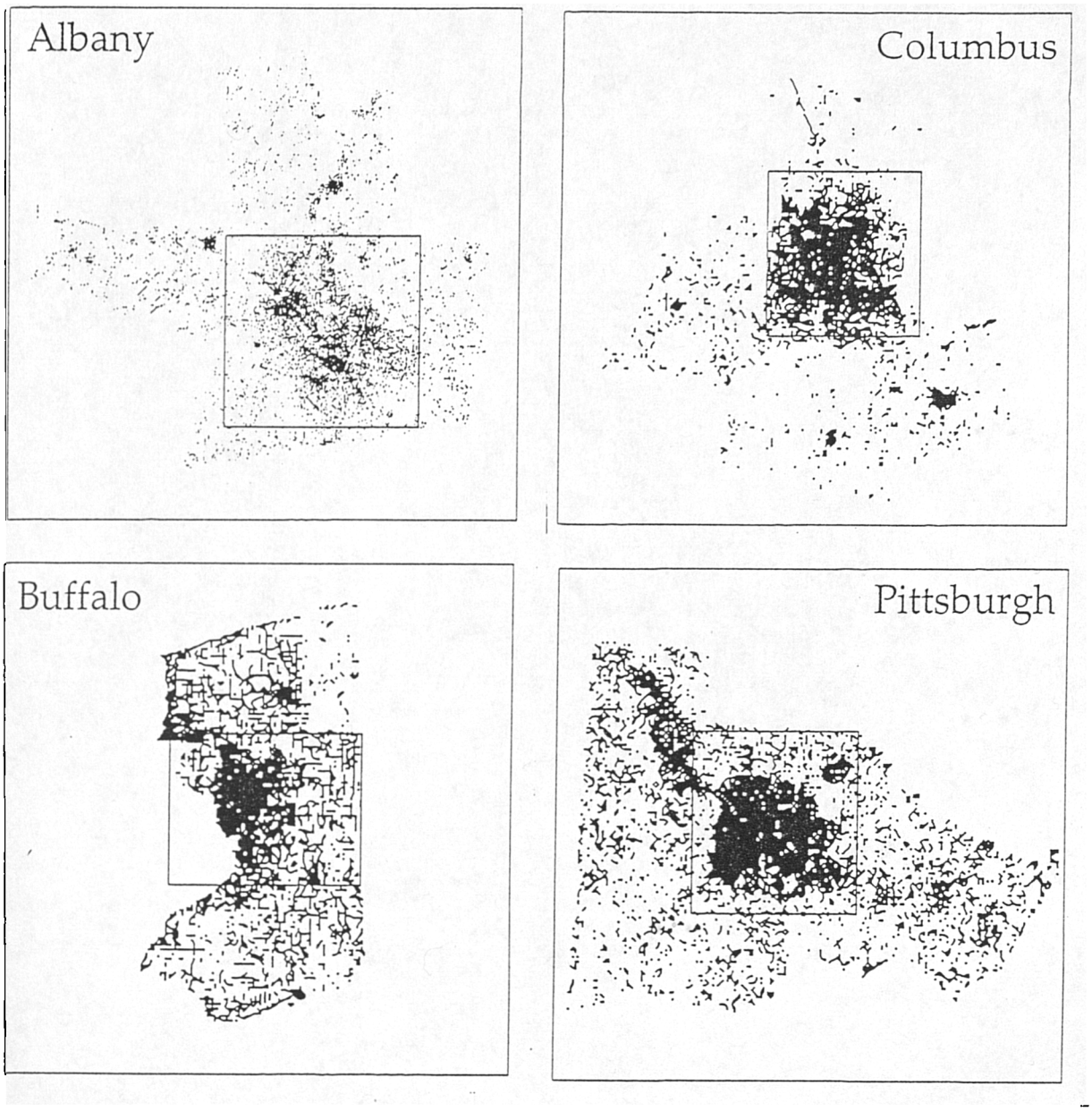

Figure 4.5 Digital Line Data (TIGER Files)

Their concern is further compounded by the lack of detailed and temporally consistent empirical data sets on which their functions are based.

The final section of this chapter will now evaluate some of the main urban data sets and data sources that have been, and may be used for applying urban density functions. In Figure 4.4, four of these data- representing zonal, disaggregate, digitised urban boundaries, and classified satellite imagery, have been used to represent the city of Norwich, England. Another data set, that of digital line graphs using the US TIGER files, is illustrated for four settlements in the United States in Figure 4.5. Each of these data will now be examined separately.

4.5.1 Data Based on Zonal Representations

Much of the earlier work on the empirical fitting of density functions was based on deriving gross population density measures directly from the spatial limits of conventional census tracts. In this approach, ordinal, interval and ratio census data are directly related to areal or volumetric data which are represented by simple choroplethic surfaces (Robinson *et al.*, 1984). The work of Clark (1951) on many large cities in Europe, the USA, and Australia, provides examples of some of the earliest estimates of population density functions based on simple census tract data. For each city, a series of consecutive concentric zones, spaced at intervals of one mile, and originating from the city centre, were drawn. Then, using census tracts, but excluding the central business district, the average density of residential population at each concentric zone was calculated and the natural log regressed on distance from the city centre. Density was then shown to decay exponentially in all cities, with gradients becoming flatter through time. This reduction in density gradients, incidentally, is argued to be attributable to the declining real cost of transportation through time. Although a more sophisticated statistical estimation of urban density functions, developed by Muth (1969), produced slightly higher significance values when fitted to empirical data, his source data were still nevertheless based on coarse census tracts. The only variations were that this work excluded cities with two or more centres, and selected sample census tracts by a random process. However, even these two examples were considered to be based on elaborate, large-scale data sets.

Some researchers estimated functions from only two observations of population and area, one at the central city, and the other from an adjacent region.

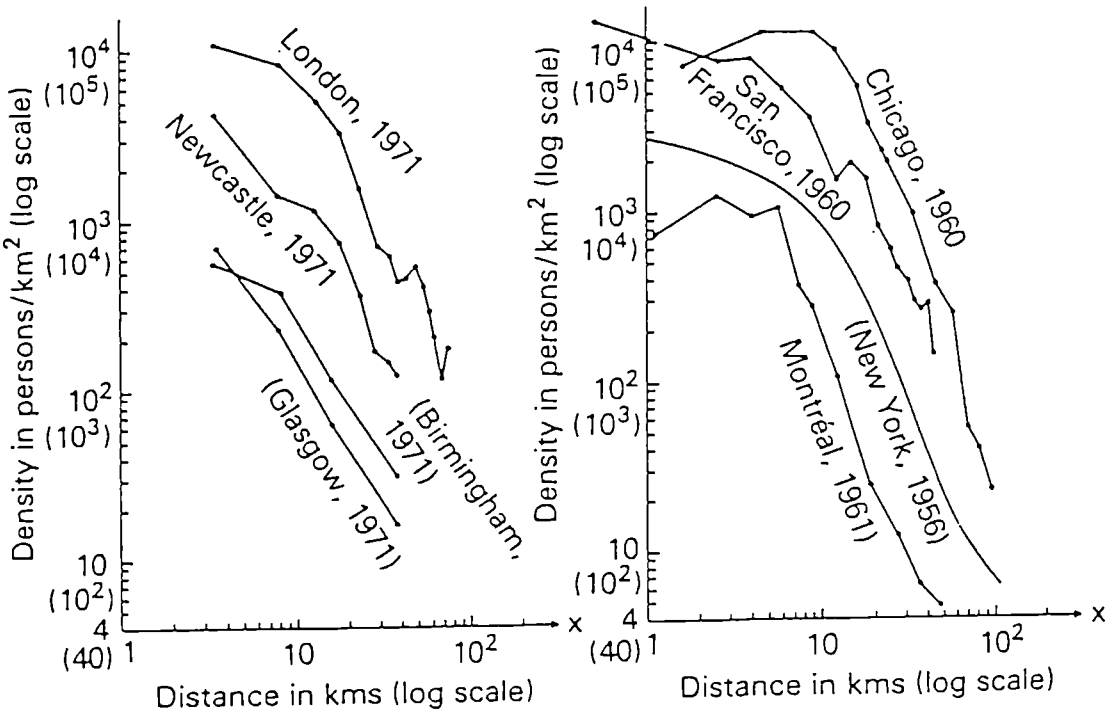

Figure 4.6 Density Gradients Based on Zonal Data Representation

Although this invariably produces rapid estimations, it also oversimplifies urban densities between the city's core and periphery. One such comparatively recent example by Edmonston *et al.* (1985) compared residential densities at *Standard Metropolitan Statistical Areas* (SMSAs) in the US and *Census Metropolitan Areas* (CMAs) in Canada, with those in adjacent counties in both cases. Assuming residential density at the urban perimeter is zero, an iterative solution of two simultaneous equations of the actual residential density at the boundary would then estimate the negative exponential function for the whole city.

Any variant of the estimation of density functions which is based on the zonal representations of urban populations will have the problems associated with aggregation and gross density. For census collection purposes, the populations of census tracts in urban areas are generally held constant. This means that populations determine the size of the tract, which usually follows a pattern of increasing size with increasing distance from the city centre. Unfortunately, this type of standardisation means that densities from census populations cannot be defined without measurement of the areas of the census tracts. Apart from recent introductions of digital databases, national censuses historically did not report areas of census tracts or other small zones. As a result, highly error-prone methods of estimating area include the use of,

> "...planimeters; placing a transparent paper with grids marked on it over a map and counting grids that cover the tract; and tracing the small area on transparent paper placed over a map of the area, cutting out the small area and inserting it in a machine that measures area by shining a light where the paper has been placed and recording the area that is in shadow." (Mills and Tan, 1980:314).

Furthermore, distances between the city centre and the census tract are measured between points. Here, both the precise point location of the city centre within the CBD, and the centre point of the tract are highly subjective decisions. Zonal data also frequently conceal unpopulated areas of the city, which are due to physical or bureaucratic impediments, such as water bodies, relief, or planning restrictions. Choropleth representations conceal these small-scale non-residential land uses in the production of gross densities (Figure 4.4a). As a consequence, zonal data provide only a small number of sample points that are usually well-spaced apart. When density functions are fitted to these data the usual results are gradients that are highly generalised and linear, concealing any localised density variations (Figure 4.6).

4.5.2 Data Based on Disaggregated Zonal Representations

The problems associated with choropleth population representations can be alleviated, to a certain degree, by basing surface on disaggregated zonal census data, as noted in Chapter Two. Here, techniques may be used which recognise unpopulated or other land use types within census tracts, or which base smoothing processes on statistical point interpolation. Latham and Yeates (1970) established one of the earliest examples of the former by fitting a hexagonal grid to a topographical map of Toronto to delineate the filtered out non-residential land, and then used census tract readings to estimate densities. In similar studies, other land use and land cover data were obtained from topographic maps and represented on one kilometre squares for a series of settlements in the UK (Zielinski, 1980). The other technique for disaggregation is based on the spatial interpolation of point data representing each census tract. The Bracken-Martin algorithm notes that census data can be interpolated from population-weighted tract centroids and hence produces a much more smoothed population surface (Figure 4.4b).

To anticipate the discussion on satellite data, a number of techniques have directly merged census data with satellite imagery to derive population densities that reflect the physical landscape. Work by Langford *et al.* (1991) determined population densities by fitting a classified image with census ward boundaries, and then estimated density by counting the number of residential pixels that lie within each ward. Chapter Two contains a review of this and other techniques.

The influx of digital representations of urban data has only begun relatively recently. Data from both remote sensing and digital survey-based databases can now be more rapidly and objectively handled by image processing and GIS functions. This invariably means that the empirical testing of urban density functions and fractal assumptions can now proceed along more automated lines, with the proviso that the analyst is clear about what is being measured! However, from the wealth of existing research it seems that all but remote sensing have been employed in urban modelling. Before the potential of remote sensing is examined there now follows a description of other digital databases that have been used in urban density functions and fractal measurements.

4.5.3 Digital Urban Boundary Data

The extensive work on the role of fractal relations in the development of urban functions by Longley *et al.* (1989), and Batty and Longley (1994), was primarily based on a digitised vector-based urban boundary database created by the Department of Environment (DoE) (Figure 4.4c). The database, for both 1981 and 1991, contains simple urban/non-urban boundaries based on DoE/OPCS definitions of what constitutes urban land, and captured from 1:50,000 and 1:10,000 Ordnance Survey maps in conjunction with Population Census Enumeration District (ED) base maps. Land deemed as urban within four or more EDs constituted urban areas, with population totals based on figures from EDs which had 50 per cent or more of their population within the designated urban area. As noted earlier, the rather vague and highly subjective definition of urban land, tied with the problems associated with the digital capture of what is essentially secondary data, has led the DoE database to be viewed only as a means for crude approximations to urban land use (Longley *et al.*, 1991). Furthermore, urban land use is far more complicated than a simple urban/non-urban dichotomy suggests, and what exactly constitutes land that is intrinsically urban is a matter of much debate. However, urban areas are incontrovertibly composed of many different physical coverages and human activities. A clearer understanding of urban growth and density must therefore be based not only on a general definition of "urban" but also on the many different land uses which together make up the urban mosaic.

4.5.4 Digital Line Data

A recognition of more appropriate data sets was the impetus behind the density modelling and fractal estimation procedures based on exclusively residential land use from work by Batty and Xie (1994b; 1994c). Patterns of residential development were identified from *TIGER* (Topologically Integrated Geographic Encoding and Referencing System) line files, a digital database combining information from the US Bureau of the Census with *digital line graphs* (DLG) from the US Geological Survey. TIGER files containing digitised streets that are labelled predominantly residential, were then converted to a grid matrix of 100m by 100m cells, with a cell deemed occupied or developed if it contained a residential street (Figure 4.5). This work shows how more pragmatic definitions of urban (residential) land use could rapidly generate a data set and thereby facilitate consistent comparisons. The method is an

attempt at distiling the all-embracing definition of urban into the essential subcategory, residential, which is more objectively interpreted and implemented. Indeed, the application of density modelling and fractal estimation to these urban sub-categories may reveal patterns not yet observed from data that is vaguely urban. Moreover, fractal dimensions and density decay parameters generated from the analysis of urban sub-categories may allow valuable insights into their juxtaposition, with particular practical applications for urban management policies. However, digitised data delineating urban boundaries although enabling rapid calculations of density indices, suffer from relatively high costs and errors associated with the digitisation process. Costs relate to the retrieval and digital capture of analogue source documents, while errors inherent in source documents are frequently compounded both by human subjectivity in digitisation, and by computer preprocessing in matters such as scale and generalisation modifications. Costs and availability issues have also further rendered digital databases temporally inflexible, and as such reduce the possibilities for frequent consistent comparisons both within and between urban areas.

4.5.5 Classified Satellite Data

The rest of this section will attempt to redress some of the problems of the previous data sources by assessing the potential of classified satellite imagery. First, it is important to reiterate the limitations of remotely-sensed data. The classification of images can only highlight spectral variabilities which represent the physical landscape, producing land cover categories (Figure 4.4d represents an image classified as "built-up"). The actual use to which land is exposed can only be indirectly inferred either by decision rules within the image or with external supplementary information. Chapters One and Two provided detailed assessments of the ways in which classified satellite data have been used in urban monitoring and inventory creation. They reviewed the possibility of inferring population and population densities either directly from the image (Iisaka and Hegedus, 1982), or by dasymetric methods using census data (Langford *et al.*, 1990b). However the focus here is on the classification of urban *land use* morphologies which is statistically more amenable to the spectral limitations of satellite imagery. Although land use classifications do not reveal population densities directly, population can be inferred from various sub-sets of the residential land use category, such as housing type, and housing density. The precise details of the land use classification strategy as used in

this thesis was outlined in Chapter Three and will form the basis of empirical testing in Chapter Five.

All that remains is a justification of the use of classified satellite data in empirical urban density function applications. The advantages may be summarised in terms of data accuracy, data representation, temporal flexibility, spatial coverage, and appropriateness. Accuracy refers as much to the amount of detail available in the data as to spatial precision. In both cases, satellite data have traditionally been considered to lag behind data from topographic maps or aerial photographs. This is because data extraction methods have not fully harnessed the large amounts of information on the land surface that are held by multivariate satellite data sets. However, improved information extraction techniques, including the one developed in this thesis, may eventually make satellite data as accurate, if not more, than survey-based maps. The recent improvements in the spatial resolutions of satellite data, moreover, mean that spatial precision is now approaching that of survey-based methods. Finer spatial resolutions invariably mean that more spatial variation in land use can be inferred from remotely-sensed data than those based on zonal representations. Many urban density models measure densities from concentric rings successively radiating out from the urban core. Data based on census tracts unfortunately produce rather coarse concentric rings, frequently between 1 km and 50 km in radius (Parr, 1985a). Commonly used satellite data from Landsat and SPOT are now capable of 30m and 10m spatial resolutions, respectively. As a result, concentric zones can now be as narrow as these spatial resolutions, and hence pick up greater spatial variability in land use. The ability to measure finer spatial variabilities is also a function of data representation. Here, methods that produce net density are understandably more appropriate than those that produce gross density measures from aggregated zonal representations. Furthermore, zonal data are highly dependent on zonal boundaries, which may make temporal comparisons difficult if boundaries change between censuses, as is often the case.

It is worth noting that studies as early as 1955 pointed out that the basic model for population densities, the negative exponential function, fits data represented by net density better than it fits gross density patterns (McDonald, 1989). Despite this, gross density measurements still became the dominant type of source data used in urban functions. Another important aspect of data representation concerns data type and data capture. Data represented digitally are seen as more convenient than analogue

maps, particularly when subjected to numerical analysis. In contrast with other digital data, satellite sensors are primary data acquisition devices, and as such are relatively free from those potential errors associated with the digitisation process. With respect to temporal flexibility, remotely-sensed data are the only source that can constantly, with relatively consistent accuracy, and allowing for atmospheric conditions, produce data over the same area as frequently as 16 days from Landsat, and 26 days from SPOT. Data based on the census are unfortunately constrained to the usual ten-year cycle. In addition, the wide areal coverages associated with satellite data allow both large cities and urban regions to be modelled from a convenient single data set, thus, keeping computer processing time within acceptable ranges, and eliminating possible errors from data merging. The last advantage of using classified satellite data in density function testing, that of appropriateness, is directly related to the manner in which functions are formulated here. First, evidence throughout this chapter indicates that the spatial form of urban areas closely resemble the dendritic, self-similarity patterns associated with fractal simulations. It is argued here and by the work of De Cola (1989; 1993) that the spatial patterns exhibited by classified satellite imagery capture this fractal nature, and in this way are the most appropriate data set for testing urban density functions based on fractal concepts.

Taking into account all these advantages, it is clear that satellite data are the best available source of accurate, detailed, consistent, digital, small-scale, and appropriate data for urban modelling using fractal geometry.

4.6 Summary & Conclusions

This chapter made a call for higher precision in two areas of research in quantitative urban analysis. First, in the formulation of conventional population density functions, and secondly, in the application of fractal geometry to both the measurement of urban form and the development of more appropriate density functions. Particular emphasis was given to the lack of interest in the generation of data on which conventional models of density were based. Furthermore, specific problems associated with the modifiable areal unit problem and ecological fallacy in the measurement of density were at the heart of many of the shortcomings of existing urban density analyses. Only recently has concern drifted towards the development of more appropriate, accurate and consistent data sources, especially those generated by the classification

of satellite imagery, argued here as the most suitable data sets of all. High spatial resolution and the ability to adapt to variable scale were both seen as essential in the role of satellite imagery in the formulation of density functions based on fractal concepts.

The Taunton case study illustrated the contribution of classified satellite data to developing the concept of the fractal city. However, only a simple spectral classification was carried out which produced a basic built-up category. The next chapter will be committed to the development of more extensive urban inventories from the classification of satellite imagery as outlined in Chapter Three. Comparisons can then be made, in Chapter Six, between density profiles and fractal dimensions derived from conventional data sources and those from classified satellite imagery. These comparisons should further reveal the abilities of image classification and fractal modelling to detect, and then model more detailed changes in the form and density of urban land use.

Chapter Five
URBAN LAND USE CLASSIFICATION

5.1 Introduction

The image classification strategy, employing training sample selection, the Bayesian decision rule, and postclassification sorting, was theoretically developed in Chapter Three and will be empirically applied to a number of settlements in the United Kingdom in this chapter. The main objectives of the strategy are two-fold. First, to demonstrate the potential of linking disaggregate representations of census data with image classification in order to produce more accurate urban land use inventories. Second, to establish the appropriateness of classified urban inventories for testing urban density functions that are built on fractal geometry.

All image classifications generated and discussed in this chapter are derived from the satellite imagery enhanced by socioeconomic surface models corresponding to the 1981 and 1991 Censuses. A number of settlements, representing various levels of the urban hierarchy, were accessible at both time points, and the study sites chosen were Bristol, Norwich, Swindon, and Peterborough. The actual land use categories produced by the classification strategy were urban (as defined by the OPCS), built-up, residential, non-residential, and four dwelling types (detached, semi-detached, terraced and purpose-built apartments). These categories provided both a feasible goal within the spectral limitations of image classification, as well as a means for demonstrating the potential of the classification strategy. Before the exact implementation procedures and results of the strategy are presented, the following two sections will outline first the specific physical, social and economic characteristics of each study area, and second, the retrieval, analysis, and limitations of each data set.

5.2 Study Areas

As mentioned earlier, the heavily restricted availability of satellite imagery primarily determined the number and location of study areas. Eventually four settlements, Bristol, Norwich, Swindon, and Peterborough were selected, each represented by imagery corresponding as closely as possible with the 1981 and 1991 Censuses.

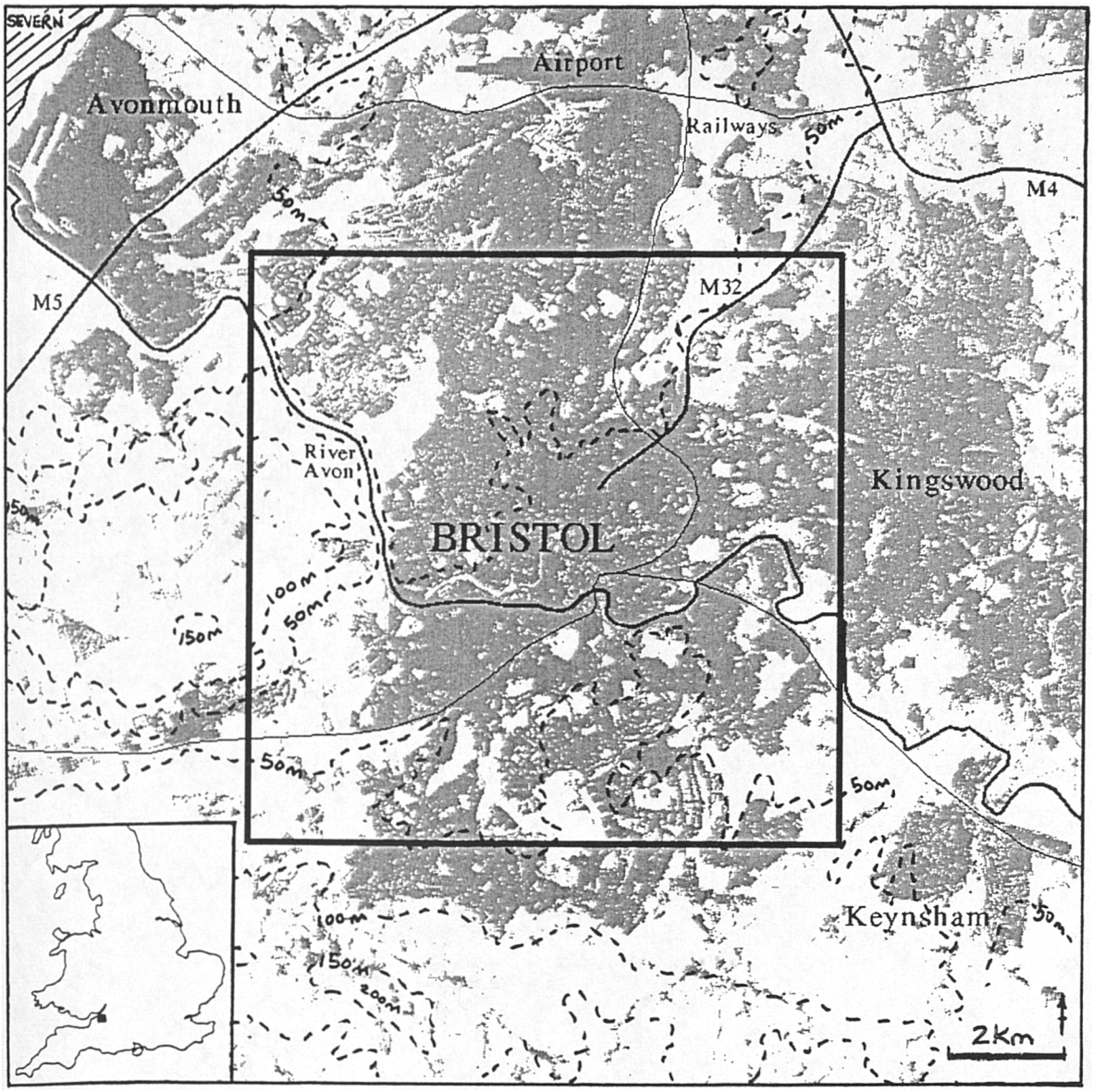

Figure 5.1 Bristol Study Area

The city of Bristol is the local study site, as well as an example of a settlement heavily influenced by its near-coastal location and the presence of strong physical constraints upon development. This is in contrast to the other three settlements which conform much more closely to the isotropic and free-standing characteristics of the idealized fractal city. However, this dissimilarity is not a hindrance but an opportunity to assess the effects of physiographical constraints on urban development and density gradients. Two of the settlements, Norwich and Swindon, have been the subjects of previous work employing similar methods of urban modelling. Norwich was part of a study on scaling relationships of size between population and area (Longley *et al.*, 1991), while Swindon was exposed to a series of fractal analyses of each of its constituent land uses (Batty and Longley, 1988). In both of these previous works, empirical data were derived from the DoE 1981 digital vector boundary database. As such, there exists the possibility of eventually comparing their results against those generated from the fractal modelling of classified satellite imagery.

5.2 1 Bristol, Avon

Bristol in the 1980s was regarded as a thriving city even within the economically active M4 corridor west of London (Bassett, 1991). Along with an expanding journey-to-work hinterland, Bristol had the highest car ownership rate of any city of comparable size in Britain at the 1991 Census. Today, population and employment distribution patterns in Bristol mirror trends in other major cities, with a marked process of decentralisation occurring, modified by recent inner-city revival and gentrification, and the continuing growth of the CBD as a major office centre (Barton, 1992).

Transport and land use policies in Avon and Bristol are presently undergoing a comprehensive review. Councillors are setting new priorities, including the goal of greater energy-efficiency, the opening of the Bristol spine road linking the M32 with the A4, and a renewed determination to restrict over-development within the statutory greenbelt. The results of the district-wide *Local Plan for Bristol*, which started in 1993, and a new version of the *Structure Plan*, have both been responsible for converting these priorities into policy (Bristol City Council, 1988).

As regards observed density patterns, Bristol still retains density variations reflecting linear development along the original tramlines and subsequent backland

development. In the city of Bristol, average density is around 45 dwellings per hectare (dph), although many urban renewal developments in the central areas are above 100 dph. Density decline with distance from the centre is still evident, with about 50% lower dph rates in the outer parts of Bristol, although greenfield sites in other parts of the county of Avon frequently exceed 30 dph. These densities are set to increase in the foreseeable future, if forecasts of a 53% increase in dwellings over the next 45 years made by Bristol City Council and Avon County Council prove to be correct (Bristol City Council, 1988). Given the severe physical constraints on development by the river Avon gorge in the south-west of Bristol and the statutory green belt, relief from this projected growth in density may involve expansion of major peripheral settlements (Bristol Development Corporation, 1993).

Located near the industrial Severn estuary in south-west England, the city of Bristol can no longer be regarded as a free-standing settlement. Figure 5.1 illustrates the sprawl of urban development into surrounding towns such as Kingswood, Keynsham and Avonmouth. Image restrictions have truncated the actual spatial limits of the study area in this figure to only include the majority of the city of Bristol. Because of this, Bristol is the only data set that is based entirely on the central area of a major city. Figure 5.1 also illustrates the effects of severe physical constraints (by the river Avon gorge) on urban development in the western part of the city.

5.2.2 Norwich, Norfolk

In contrast to Bristol, the other three study sites are very much more consistent with some of the assumptions of the fractal model of urban form. Norwich, Swindon, and Peterborough are good empirical examples of free-standing settlements located on land that is relatively unaffected by serious impediments to urban development (Cherry, 1974).

Of these three settlements, Norwich is the only one that can compare with both the spatial size and population of Bristol. However, in contrast to Bristol, the data sets associated with Norwich are able to include the entire spatial extent of the city, as well as representing a more isotropic physical landscape to urban development (Figure 5.2).

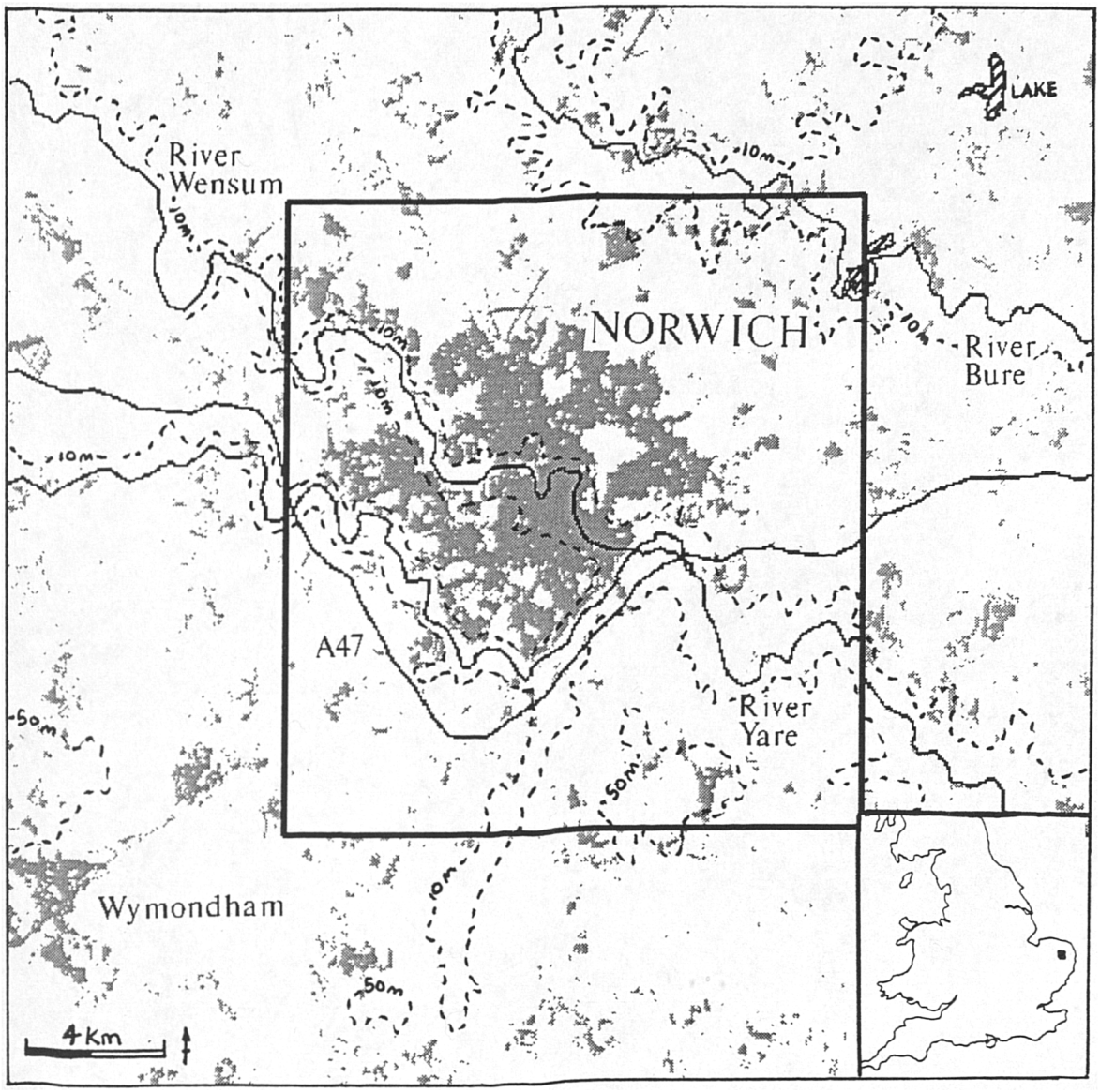

Figure 5.2 Norwich Study Area

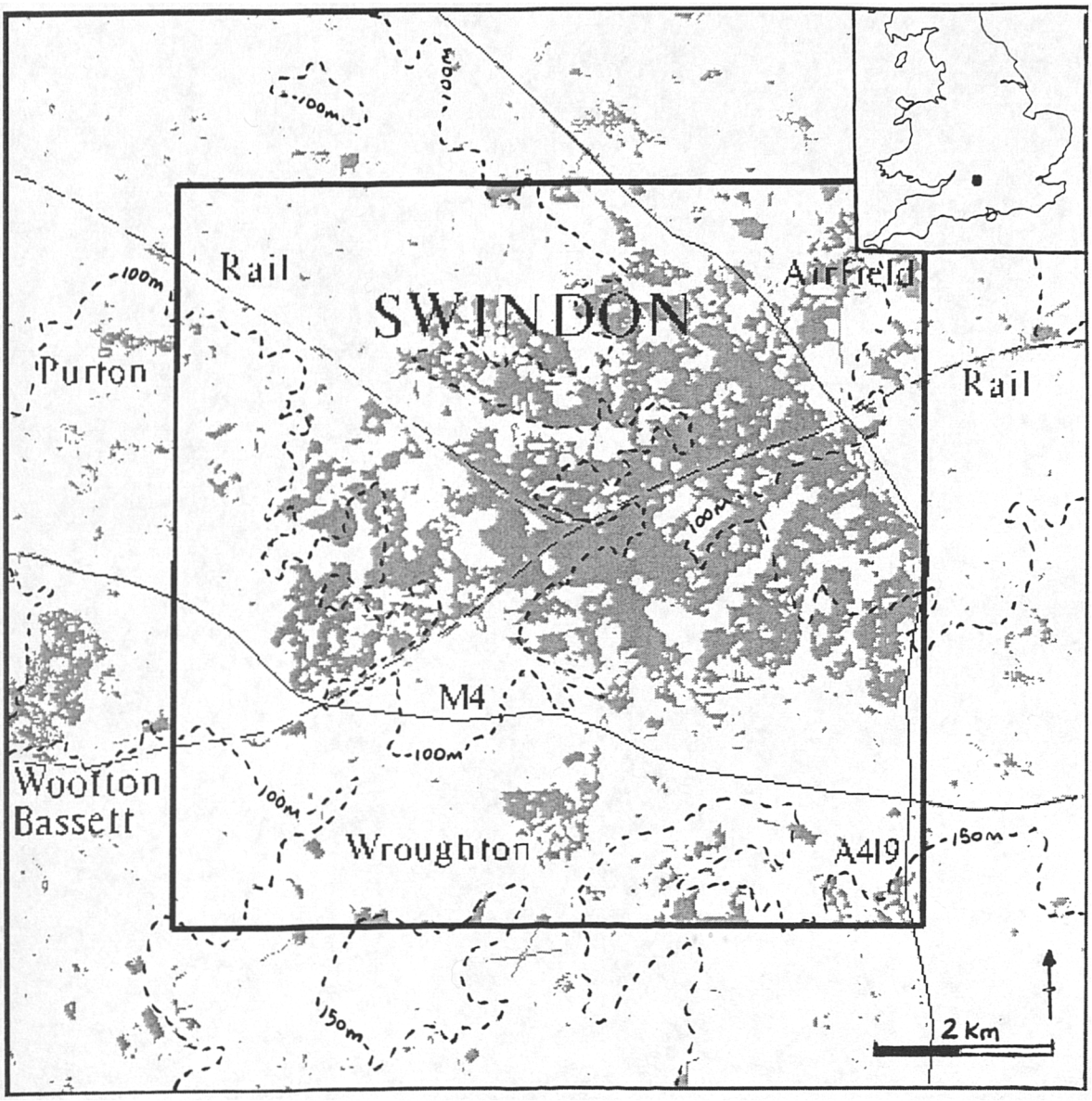

Figure 5.3 Swindon Study Area

5.2.3 Swindon, Wiltshire

Swindon is located in south central England about 70 miles west of London. The town is quite compact and is not affected in its form by the presence of any rapidly growing nearby towns (Figure 5.3). It has a reasonably buoyant economy which in the 1960s arose from its designation as an expanded town, taking overspill population from Greater London (Barton, 1992).

More recently, its favoured location in the expanding so-called M4-corridor of southern England has led to the creation of new service and high-technology industries in and around the town itself (Bassett, 1991). This rapid urban growth in the 1980s has also been associated with the assimilation of nearby villages on its periphery.

5.2.4 Peterborough, Cambridgeshire

The development of Peterborough can be traced back to the surge in national population growth from the mid-1950s, leading to the subsequent wave of new towns in the 1960s, mainly to take pressure off the South-East region of England. The *Greater Peterborough* proposed scheme by Tom Hancock in 1967 envisaged a number of townships as linked settlements in an expansion programme designed to increase the size of Peterborough to 185,000 people by mid-1980s (Cherry, 1974). However, the growth of Peterborough's population between the 1981 and 1991 Censuses (115,000 and 123,000 respectively) did not fulfil this target but was, to a certain extent, a vindication of the expansion programme. The growth of Peterborough in the 1980s can also be viewed as an example of the role of small and medium-sized settlements in accounting for the majority of counter-urbanisation (or population turnaround) processes observed in the 1970s (Shepherd and Congdon, 1990) and 1980s (OPCS, 1991).

The location of Peterborough on the flat Fen land of north Cambridgeshire (Figure 5.4) means this settlement most nearly fulfils the isotropic assumptions of the DLA model. As such, particular attention will be given to the range and magnitude of fractal dimensions generated from the satellite images representing Peterborough.

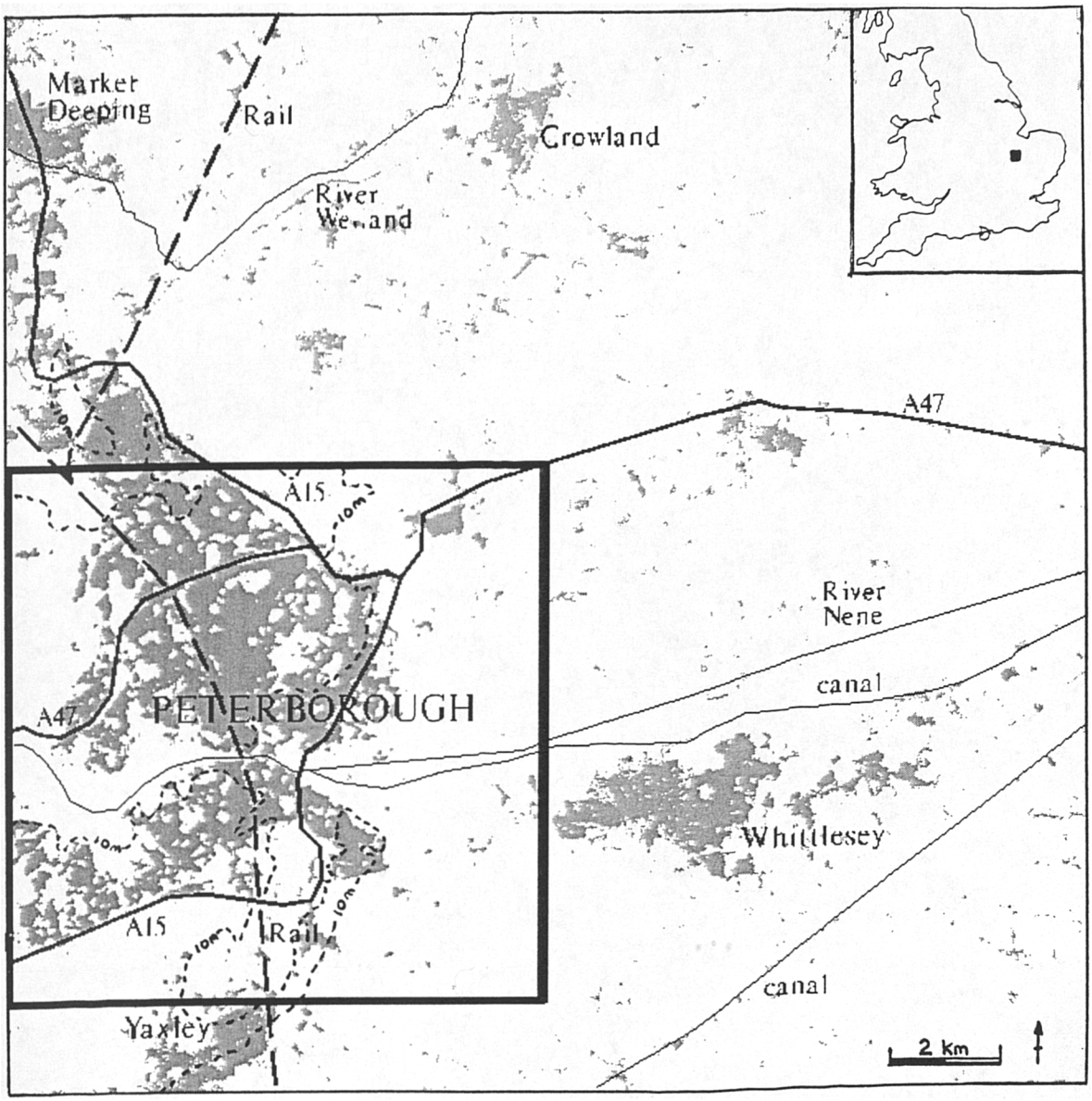

Figure 5.4 Peterborough Study Area

Table 5.1 Satellite Imagery

Data Set	Satellite	Sensor	Scene	Date	Bands*†
Bristol 81	Landsat 5	TM	203-024	26-04-84	1,2,3,4
Bristol 91	SPOT 1	HRV-XS	027-246	17-05-88	1,2,3
Norwich 81	Landsat 4	TM	201-023	27-12-82	3,4,5,7
Norwich 91	Landsat 5	TM	201-023	15-07-89	1,2,3,4,5,6,7
Swindon 81	Landsat 5	TM	203-024	26-04-84	1,2,3,4
Swindon 91	Landsat 5	TM	203-024	30-10-88	1,2,3
Peterborough 81	Landsat 4	TM	201-023	27-12-82	3,4,5,7
Peterborough 91	Landsat 5	TM	201-023	15-07-89	1,2,3,4,5,6,7
Taunton 81	Landsat 5	TM	203-025	26-04-84	1,2,3,4

*LANDSAT TM BANDS:

Band #	Band Name	Wavelength (μm)
1	Visible Blue-Green	0.45-0.52
2	Visible Green	0.52-0.60
3	Visible Red	0.63-0.69
4	Near Infrared	0.76-0.90
5	Middle Infrared	1.55-1.75
6	Thermal	10.40-12.50
7	Middle Infrared	2.08-2.35

IFOV: 30m x 30m (120m x 120m for Band 6)
Data Rate: 85 Mb/s
Quantization Levels: 8 bits, 256 levels
Earth Coverage: 16 days
Altitude: 705 km
Swath Width: 185 km
Orbit: Circular, Sun-Synchronous

†SPOT HRV-XS BANDS:

Band #	Band Name	Wavelength (μm)
1	Visible Green	0.50-0.59
2	Visible Red	0.61-0.68
3	Near Infrared	0.79-0.89

IFOV: 20m x 20m
Data Rate: 25 Mb/s
Quantization Levels: 8 bits, 256 levels
Earth Coverage: 26 days
Altitude: 832 km
Swath Width: 60 km
Orbit: Circular, Sun-Synchronous

5.3 Data Sets

For each of the four study areas, two sets of data, satellite imagery and socioeconomic surfaces, are required for subsequent land use classifications. This section will examine the retrieval and all necessary processing of both of these data sets into forms that are amenable to the classification strategy.

5.3.1 Satellite Imagery

After examining all possible sources of remotely-sensed data, it was decided, given availability, that satellite imagery from either SPOT HRV-XS or Landsat TM sensors came the closest to the objectives of this thesis. What was required was a data source that could provide consistent, multitemporal data at a spatial resolution that would facilitate small-scale urban classifications, and would also be amenable to rapid computer processing.

5.3.1.1 Image Retrieval

The availability of satellite imagery inevitably affected the number and location of study areas. Furthermore, to satisfy the temporal requirements for empirical testing, study areas had to be represented by one image at each of the 1981 and 1991 Census collection dates. Unfortunately, the cost limitations of a thesis and the lack of consistent and comparable imagery for 1981, resulted in a sub-optimal collection of satellite data. Even so, the tape archives of the Department of Geography at Bristol included enough satellite imagery to allow an adequate selection and areal coverage of five settlements. Table 5.1 lists all satellite sensors, scenes, and associated available bands for the four main study areas, as well as the scene of Taunton that was used in Chapter Four. The dates show the most available imagery for both 1981 and 1991. Although the dates do not strictly coincide with the exact collection of the 1981 and 1991 Censuses, the images were judged to be sufficiently representative, given availability, to demonstrate the classification strategy. Hereafter, all images are referred to as either 1981 or 1991 data sets, although the usual caveats apply where data are being synthesized from sets at different points in time.

The majority of the images listed in Table 5.1 are from US *Landsat Thematic Mapper* (TM) sensors on board Landsat 4 and 5. The exception is the 1991 Bristol scene which is derived from the French commissioned *SPOT 1* satellite using the *Very High Resolution* (HRV), False-Colour (XS) sensor.

Figure 5.5 shows true-colour examples of both Landsat TM and SPOT data for Bristol 1981 and 1991 respectively.

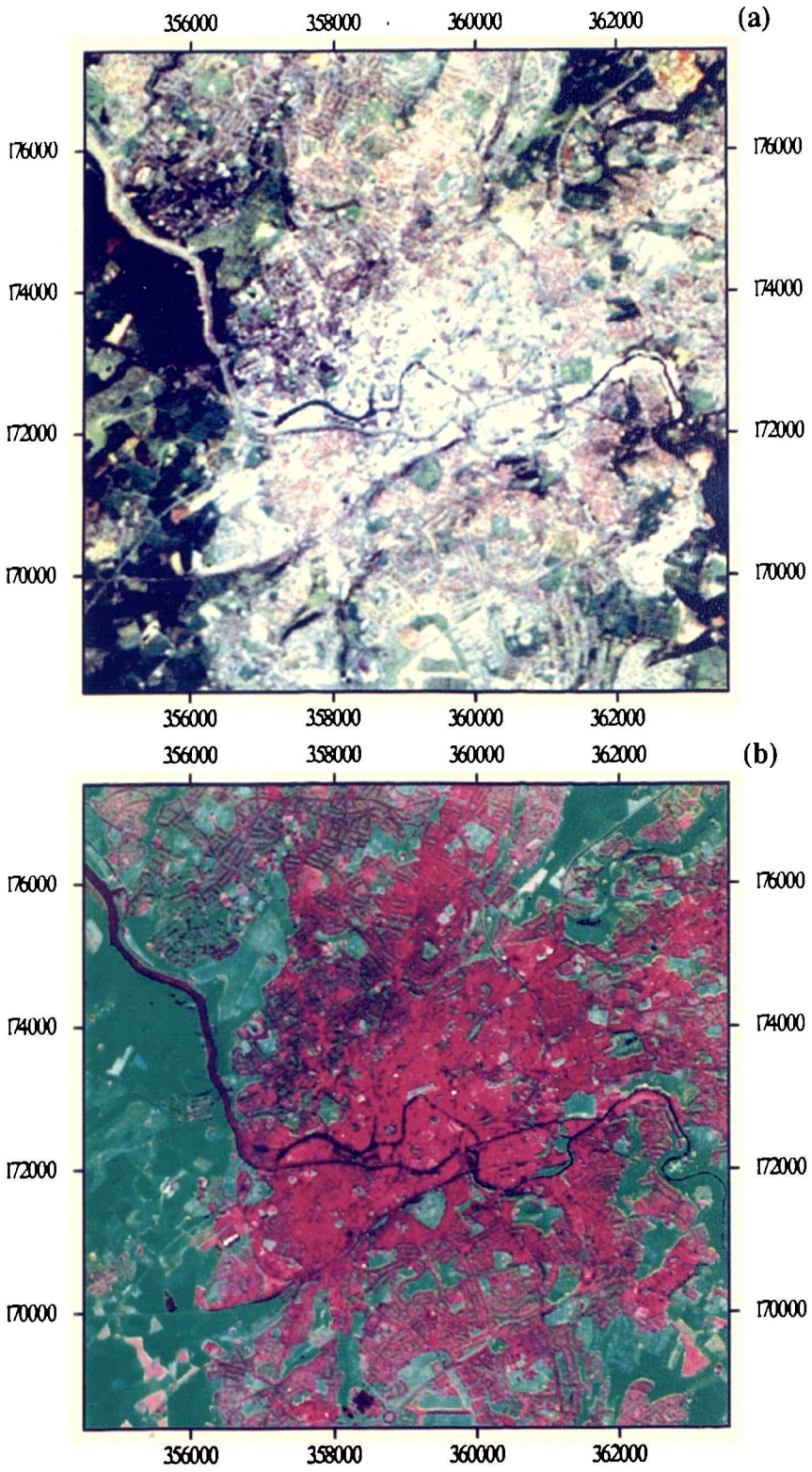

Figure 5.5 Satellite Images for the Bristol Study Area
(a) Landsat 5 (Green-Band 2, Blue-Band 1, Red-Band 4)
(b) SPOT 1 (Green-Band 1, Blue-Band 2, Red-Band 3)

The images listed in Table 5.1 represent data sets that satisfy both the requirements of image classification *and* subsequent urban modelling. First, although the spatial resolutions of 30m for Landsat, and 20m for SPOT may not be ideal for precision land use mapping, they are at a scale that would allow adequate classifications for many Level II and some III categories (Anderson *et al.*, 1972), given the strategy outlined earlier. Moreover, these spatial resolutions of 30m and 20m also allow the full extent of each settlement to be captured within one scene. From a computational stand-point, this would allow rapid and consistent fractal estimations of urban form and density to be calculated from one convenient data set.

5.3.1.2 Image Pre-Processing

Initial processing of each image included geometric registration to the UTM coordinate system and image enhancement, to reveal maximum radiometric contrast. Both of these methods were discussed in detail in Chapter Two. Here, geometric registration was operationalized by ERDAS functions using as many ground control points (GCPs) as possible from topographic maps. Root-mean-square (RMS) errors for pixels in both x and y directions fell between the ranges, $0.46 < x < 1.3$, and $0.48 < y < 1.5$, with total RMS error between 0.65 and 1.5. All images were then resampled to the UTM system at spatial resolutions of 20m for SPOT and 30m for Landsat TM using a cubic convolution algorithm. The reason for this is that cubic convolution resampling avoids the disjointed appearance of the nearest neighbour method and provides slightly sharper images than the bilinear method (Jensen, 1986).

Image enhancements were based on the equalization of spectral histograms in all bands. This had the effect of levelling out radiometric histograms in all bands so that they become nearly flat in appearance. Histogram equalization increases image contrast for data values that are frequent (the peaks of the histogram) and decreases contrast for values that are not frequent (the tails). As subsequent image classification is primarily based on urban areas, scenes will be dominated by frequent similar values associated with urban spectral responses. As such, histogram equalization will be necessary to improve the radiometric contrast of these similar urban values, and hence aid in the selection of separable training samples.

Pre-classification processing techniques involved in data reduction, such as principal components analysis or band ratioing, were not deemed necessary. Instead, the

maximum amount of radiometric information from all bands was used in subsequent image classifications. One other pre-classification technique, however, did reduce the amount of data in each image.

Table 5.2 Image Resampling

Data Set	Pixel Dimensions	Pixel Size (m)	Coverage (km^2)	Upper Left Coordinate	Lower Right Coordinate
Bristol 81, 91	453 x 453	20	82.08	354508, 177411	363568, 168351
Norwich 81, 91	511 x 511	30	235.01	615880, 316250	631210, 300920
Swindon 81, 91	353 x 353	30	112.15	409024, 190016	419614, 179426
Peterborough 81, 91	339 x 339	30	103.43	514339, 303705	524509, 293535
Taunton 81 (Full)	381 x 381	30	130.64	316886, 130423	328316, 118993
Taunton 81 (Reduced)	227 x 227	30	46.38	319196, 128113	323696, 121303
For all data sets: Cubic Convolution Resampling Algorithm UTM (Clarke, 1866) Coordinate System					

In response to urban modelling algorithms based on idealised grid spaces, each image had to replicate a square grid of equal number of rows and columns of pixels. Furthermore, the centre of each square image had to be focussed on the historical core of each settlement. These and other parameters are listed in Table 5.2. Subsequent urban modelling is heavily reliant on the ability to compare parameter estimations between 1981 and 1991 data sets. As such, it is important to standardise the number of pixels and the amount of area coverage between 1981 and 1991 images for each settlement. In all but Bristol, images are derived from Landsat TM scenes with equal spatial resolutions, and therefore do not present a problem. In the Bristol case, however, the 1981 data set is from Landsat, but the 1991 data set is derived from the 20m resolution sensor of the SPOT 1 satellite. Instead of losing detail, it was decided that a more pragmatic approach would be to convert the 30m resolution of Landsat to the finer resolution of SPOT (Figure 5.5). However, this does not mean that finer information was introduced into the 1981 data set. The process of resampling at higher resolution is simply an interpolation procedure that spatially disaggregates the inherent information in the image.

The differing sizes of data sets (represented by pixel dimensions) between each settlement is both a reflection of available imagery and the actual spatial size of

settlements. In the Bristol and Peterborough cases, each settlement was close to the edge of its respective satellite scene, and therefore the images do not represent the entire urban area. However, in the Norwich and Swindon cases, sufficient imagery was available to accommodate the whole built-up area, and in this respect, the larger data sets associated with Norwich are a reflection of its wider spatial limits.

5.3.2 Census Data

As discussed in Chapter Two, the Bracken-Martin surface model is generated from point data associated with the centroids of the ED level of census aggregation. Census data from both 1981 and 1991 are retrieved at the ED level from the Small Area Statistics (SAS) database (UMRCC, 1989; MCC, 1992). The software specifically commissioned, designed and written for handling SAS data is known as *SASPAC*. SASPAC allows full facilities for editing and file manipulation, and on-line compilation and execution of programs designed purely for the full interrogation of census data. Both the SASPAC program and SAS data are now accessed through the *National Datasets Service* on the Cray Superserver CS6400 at Manchester Computing Centre (MCC), which started in February 1994. The operating system is a version of Unix called *Solaris*, the Sun implementation of Unix System V Release 4 (SVR4), with extensions from Cray.

Table 5.3 1981 and 1991 Census Variables

1981 Census	
Reference	*Variable*
S010043	Total Population (1981 base)
S121170	Total Households
1991 Census	
Reference	*Variable*
S010057	Total Population (1981 base)
S610001	Total Households
S610003	Total Detached Dwellings
S610004	Total Semi-Detached Dwellings
S610005	Total Terraced Dwellings
S610006	Total Purpose-built Flats (Residential buildings)
S610007	Total Purpose-built Flats (Commercial buildings)

The SAS database for 1991 consists of some 9,000 counts or variables (measures of socioeconomic and housing attributes) arranged as 83 tables for all 110,000 EDs in England. Each variable is labelled by a unique six figure reference code, where the first two digits refer to the table, and the last four refer to the unique variable within that table. This is slightly different for the 1981 data sets, where each count or variable is a unique number regardless of the table. Table 5.3 lists all the variables used in this thesis.

The imbalance in the number and type of census variables between 1981 and 1991 is both a reflection of available census data, and the quality of satellite imagery. The measures of dwelling type are simply not available from the 1981 database and other counts, such as number of rooms per household, would not be comparable surrogates. Furthermore, the reduced quality of the satellite scenes, in particular for Norwich 1981 and Peterborough 1981, in terms of radiometric contrast and atmospheric disturbance, heavily limit their abilities to differentiate between dwelling types. As a result, only four categories (urban, built-up, residential and non-residential) were deemed acceptable goals for classification from 1981 data sets, but a further four (detached, semi-detached, terraced and purpose-built apartments) are discernible from 1991 data sets. The exact figures for each census variable listed in Table 5.3 are found in Table 5.4, for all data sets.

Table 5.4 Census Figures for All Settlements

Data Set	*EDs*	*Population*	*Households*	*Detached*	*Semi-Det.*	*Terraced*	*Apartments*
Bristol 1981	696	278,130	109,841	-	-	-	-
Bristol 1991	673	261,309	122,001	5,714	28,621	51,893	19,377
Norwich 1981	445	199,410	76,305	-	-	-	-
Norwich 1991	449	201,659	90,056	21,286	22,795	27,030	17,013
Swindon 1981	270	139,704	49,573	-	-	-	-
Swindon 1991	331	146,642	64,962	10,969	19,841	25,576	7,763
Peterbro 1981	256	117,055	41,968	-	-	-	-
Peterbro 1991	257	125,603	52,901	11,211	16,233	18,424	7,033

The figures in Table 5.4 are the basic data that will be used in each of the three components of the classification strategy. For training sample selection and postclassification sorting, the data will be spatially represented by census probability surfaces using the Bracken-Martin model.

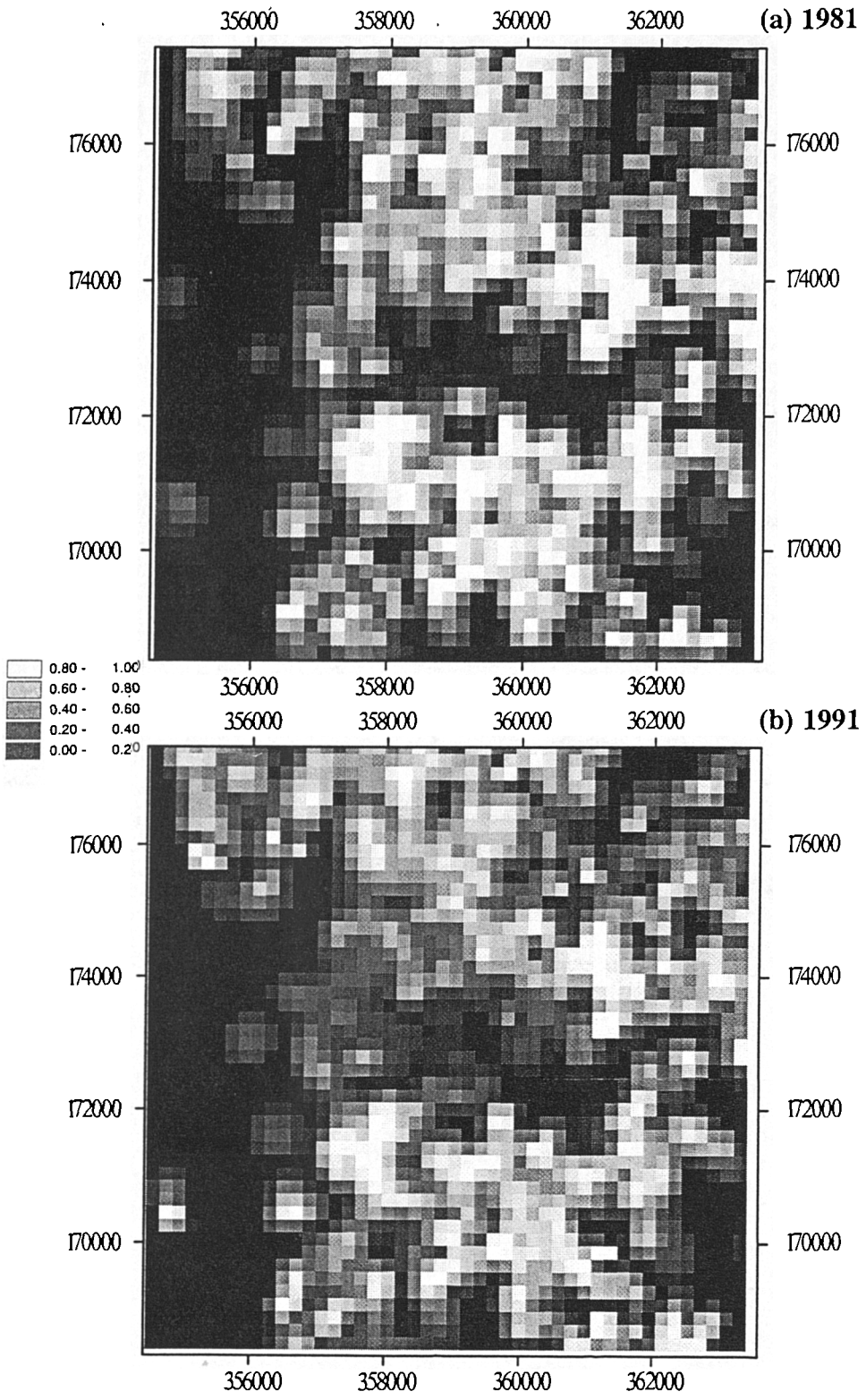

Figure 5.6 Probability Surfaces of the "Number of Household" Census Variable for the Bristol Study Area (a) 1981, (b) 1991

But, for the Bayesian decision rule, the same data will be transformed to represent relative areal proportions, used as prior probabilities in the maximum likelihood classifier.

5.3.2.1 Census Probability Surfaces

Census probability surfaces are the spatial representation of census frequencies by the surface model. Instead of spatially interpolating *absolute* values at each ED centroid, the surface model is called upon to disaggregate *probability* values. In section 5.4.4, these census probability surfaces will be used to inform the selection of training samples for the classification of residential land use and the classification of the four dwelling types. Further, in section 5.4.5 the same probability surface used for residential classification will be employed to aid in postclassification sorting.

The probability surface used for residential classification is based on a single census variable, "Total Number of Households". The surface is generated by first calculating the objective probability distribution of the number of households for the whole study site, and then assigning a probability value to each centroid. From there it is then a matter of employing the Bracken-Martin model to systematically disaggregate the probability values associated with these centroids into a smoother surface of residential patterns (Figure 5.6). The effect is to allocate a proportion of the total number of households in the study area to each cell of the surface model.

In the matter of dwelling type classifications, two census variables are used, again "Total Number of Households", as well as the appropriate dwelling type count: "Total Detached Dwellings", "Total Semi-Detached Dwellings", "Total Terraced Dwellings", and "Total Purpose-built Flats (in commercial and residential buildings)". This time, however, probability values assigned to each ED centroid are the joint probabilities of the two census variables, derived by assuming independence, and calculating their product. Again, surfaces are generated by assigning probability values to ED centroids, and then implementing the Bracken-Martin model. The reason for using the "Total Number of Households" variable is so that the dwelling type probabilities in each surface cell are weighted according to the proportion of dwellings that they represent. Figure 5.7 illustrates the joint probability values of the dwelling types categories, detached, semi-detached, and terraced, based on "Number of Households".

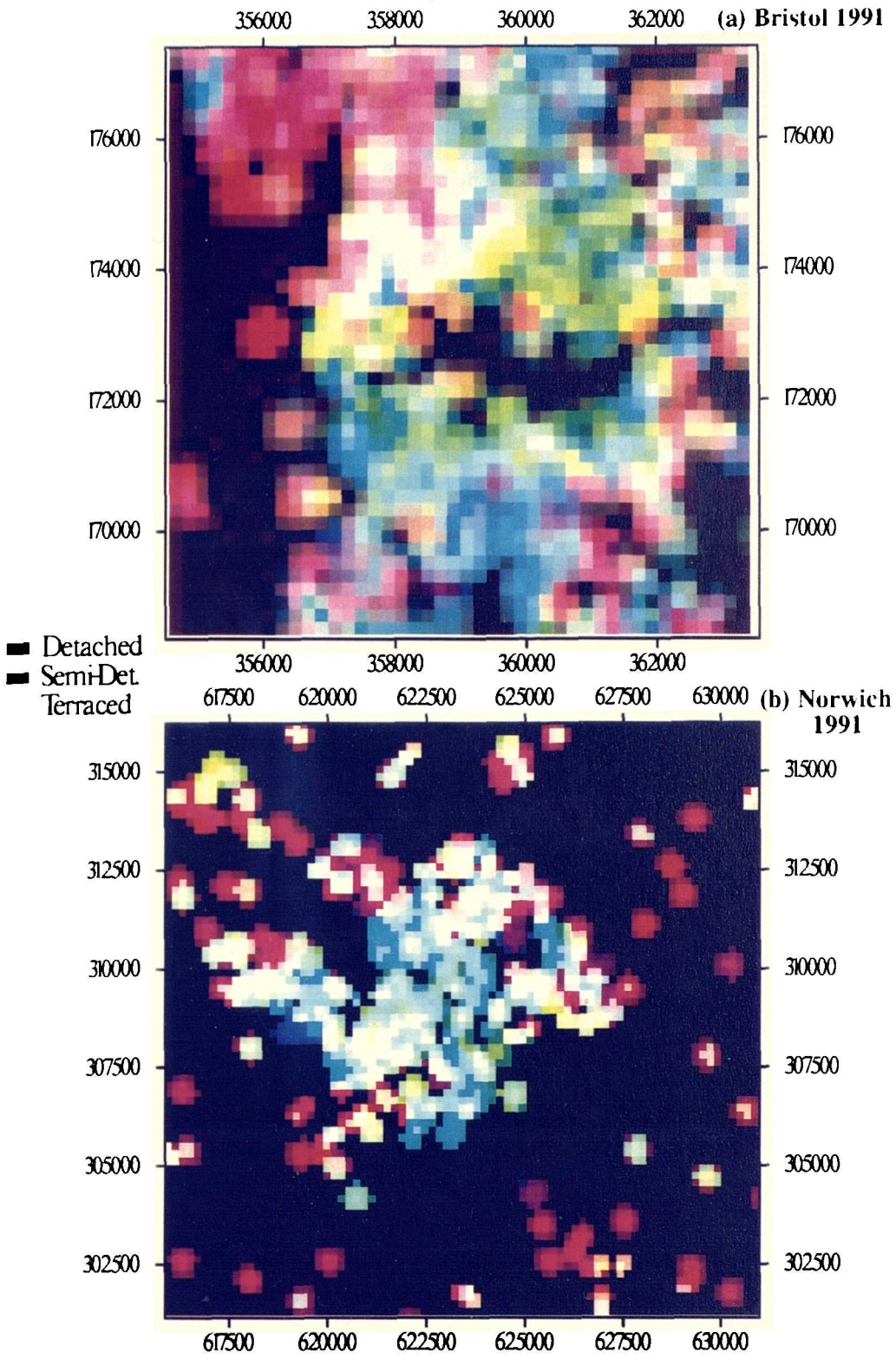

Figure 5.7 Probability Surfaces of the Dwelling Type Census Variables (excluding Apartments) for (a) Bristol, and (b) Norwich

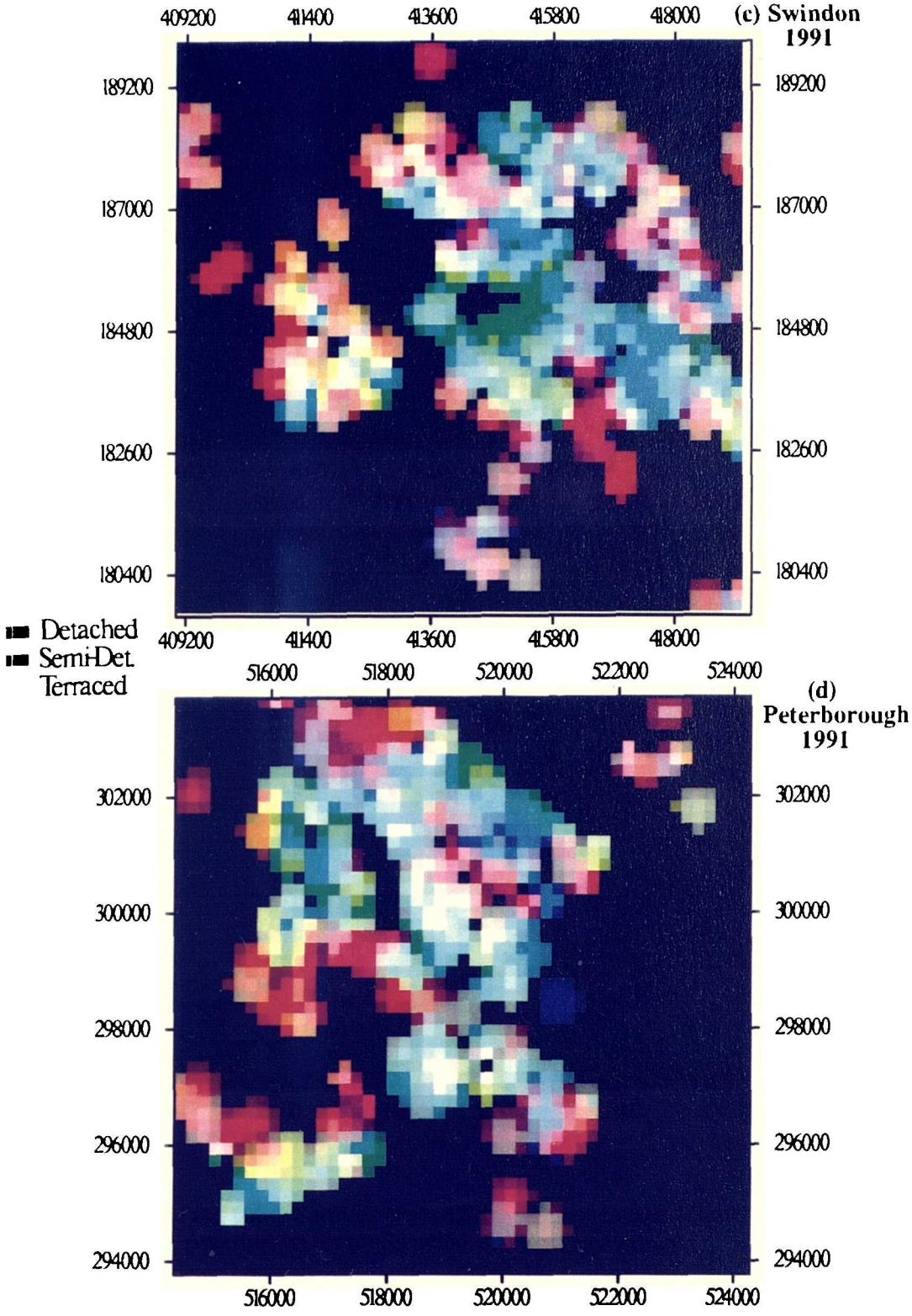

Figure 5.7 (cont.) Probability Surfaces of the Dwelling Type Census Variables (excluding Apartments) for (c) Swindon, and (d) Peterborough

Using GIS functions, these values are shown by modifying the intensities of three colours: red for detached, blue for semi-detached, and green for terraced dwellings. As only three colours are available, the figures omit the apartments/flats category.

For both classification scenarios, residential and dwelling types, the probability values redistributed by the surface model are subjected to one further transformation before being employed in the classification strategy. This transformation involves the conversion of probability values from real to byte, and is a necessary requirement for direct integration with raster image data. Usually, image data are represented by 8-bit words of 256 integers (DNs). As a result, probability values from the surface model are rescaled to fit within this 256 range. Although this transformation invariably reduces the amount of information and precision in the surface values, there is still enough scope for the recognition of cells with high occurrence of residential or dwelling types for use in training sample selection and postclassification sorting.

5.3.2.2 Prior Probabilities

The other role of census data is as prior probabilities in the implementation of the Bayesian decision rule for the classification of dwelling types. The procedure begins with the selection of representative training samples for each dwelling type using probability surfaces, as outlined in the previous section. Next, these samples are entered into the maximum likelihood classifier and weighted by their prior probability of occurrence (Chapter Three). In this case, the prior probabilities of occurrence are the relative areal proportions of each dwelling type within the exclusively residential segments of the image. These relative areal proportions can be calculated from the Population Census, and indeed the total number of dwellings in each housing type were documented in Table 5.3. After the satellite image is segmented into exclusively residential areas, these areal proportions can then be converted into objective probabilities and directly entered into the Bayesian decision rule.

However, there is still the concern of variable size of buildings within and between dwelling types. In other words, the simple calculation of areal proportions from absolute numbers does not take into account the actual spatial extent of each building. For instance, detached houses will often be much larger than terraced dwellings, and similarly, one detached house may be much larger than another detached house. This means that areal proportions from simple absolute frequencies will tend to

underestimate the actual spatial coverage of detached housing, and also heavily overestimate the coverage of terraced housing. Semi-detached housing should generally fall in between these extremes. In the case of purpose-built apartments, gross overestimation is foreseeable because single buildings may contain up to as many as 20 individual households. What is required is a means of estimating a general size relationship between each dwelling type. For example, the determination of a size-ratio between detached and semi-detached housing, detached and terraced, and semi-detached and terraced. Also needed is a calculation of the average number of apartments per building.

For each of these size ratios, it was decided that the most rapid and accurate method of calculation would involve measurements from sample aerial photographs. In each of the four settlements, two pairs of aerial photographs were acquired for stereoscopic interpretation, one pair near the central parts of the urban area, the other on the periphery. Using standard interpretative skills, 20 samples of the areal sizes of each dwelling type were measured. Eventually, average size ratios began to emerge which were in the range of around 1 detached dwelling to 1.5 semi-detached dwelling, 1 detached to 2.25 terraced, and 1 semi-detached to 1.5 terraced. Although these figures are approximate averages which disregard anomalies, they are still an intuitive improvement over the original assumption of identical sizes for each dwelling type. Again using aerial photographs, an average number of apartments for a building was also determined.

Table 5.5 Dwelling Type Prior Probabilities

Data Set	*Households*	*Detached*	*Semi-Detached*	*Terraced*	*Apartments*
Bristol 1991	1.0	0.1145	0.3779	0.4686	0.0390
Norwich 1991	1.0	0.4240	0.3027	0.2393	0.0339
Swindon 1991	1.0	0.3014	0.3642	0.3138	0.0210
Peterbro 1991	1.0	0.3625	0.3500	0.2648	0.0227

Using these more representative size ratios, the raw absolute values listed in Table 5.4 were then converted into objective probabilities of occurrence. These are documented in Table 5.5 and represent the actual prior probabilities to be used in the Bayesian decision rule in section 5.4.7. The prior probabilities in Table 5.5 are of sufficient inequality to assure representation and adequate modification of the maximum likelihood classifier (Mather, 1985). However, the exceptionally small probabilities

associated with the apartments category may significantly diminish their presence in the classification, and this will need to be closely observed.

5.4 Implementation of the Classification Strategy

The classification strategy will now be operationalized for all empirical data sets to produce the eight land use categories. However, it is important to first develop the classification scheme within which the strategy will function. With regard to the specific partitioning assumptions behind the Bayesian decision rule, a *hierarchical classification* approach and scheme was regarded as the most appropriate strategy framework. Incidentally, a discussion about the hierarchical needs of the Bayesian decision rule will follow in section 5.4.7.

5.4.1 Hierarchical Classification

A classification based on a hierarchical approach (sometimes known as *decision-tree* classification) is essentially a process that allows a series of decision rules to select and successively partition spatial elements or features of an image. The procedure permits ancillary information to define breaks in the image by thresholding pixels that do not conform to decision criteria. The layered classification approach was outlined in Chapter Two, as part of the use of census data in image classification.

Census data, modified by the surface model, will be used to assemble a series of decision rules that will form the basis of hierarchical layered classification strategies for all empirical applications. Each decision rule is designed to spatially partition satellite images into hierarchical segments or categories determined either by purely-spectral data, or by the classification strategy (training sample selection, the Bayesian decision rule, and postclassification sorting), in the following manner:

Decision 1: Urban/rural distinction by spectral contrast only.

Decision 2: Built-up/Non-Built-up by spectral contrast only.

Decision 3: Residential/Non-residential by training sample selection, and postclassification sorting.

Decision 4: Dwelling type differentiation (detached, semi-detached, terraced, purpose-built apartments) by training sample selection, and the Bayesian-type classifier.

Each decision produces a category upon which the next decision is based. For example, decision 2 generates built-up land cover on which the residential/non-residential contrast from decision 3 is based (Figure 5.8). The application of a hierarchical layered classification is reflected in the development of the classification scheme.

5.4.2 Development of a Classification Scheme

A discussion of urban classification schemes in Chapter One compared those used in human geography to those used in remote sensing.

Table 5.6 Land use Categories

Land use Category	*Description*
1. Urban land use	Land on which permanent structures are situated; transport corridors (roads, railways and canals) which have built-up sites which are less than 50 m apart; transport features such as railway yards, motorway service areas, car parks as well as operational airfields and airports; mineral workings and quarries, and any area completely surrounded by built-up sites (OPCS, 1984)
2. Built-up land cover	All human structures, including vegetation as part of residential gardens; and transport routes (excluding transport routes through predominantly rural landscapes)
3. Residential land use	Built-up land associated with all residential property types
4. Non-Residential land use	Built-up land associated with all non-residential property types
5. Detached Dwellings	Residential land associated with low-rise buildings predominantly each single-family dwelling units
6. Semi-Detached Dwellings	Residential land associated with low-rise buildings partitioned into two single-family dwelling units
7. Terraced Dwellings	Residential land associated with low-rise buildings partitioned into more than two single-family dwelling units
8. Apartments/Flats	Residential land associated with high-rise buildings partitioned into multiple-family dwelling units

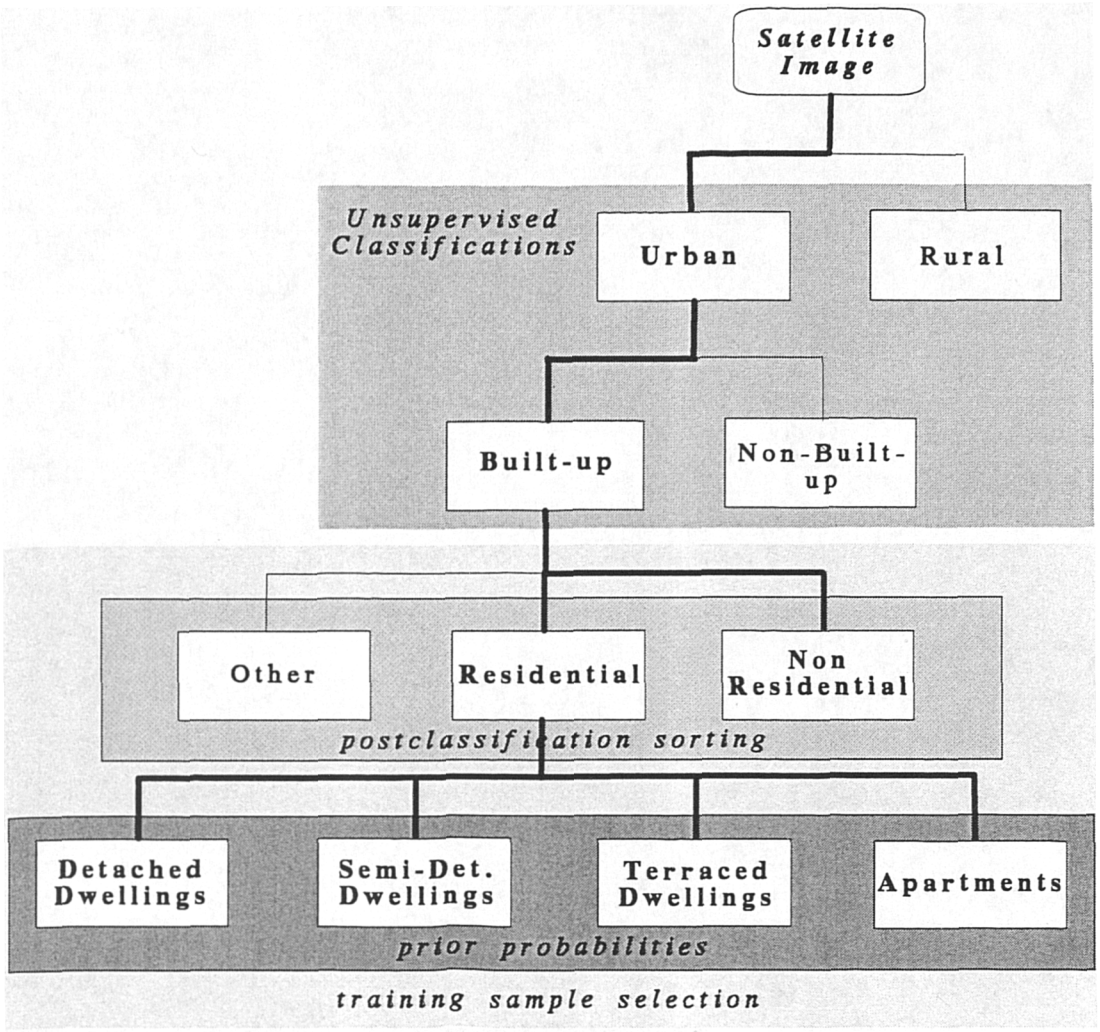

Figure 5.8 Hierarchical Classification Scheme

It was clearly apparent that classification schemes based on remotely-sensed data, are heavily influenced by image resolutions, interpretation procedures, and available ancillary information. All three factors act together in limiting both the number of classification categories and the amount of detail in each category. It must also be emphasised that classification schemes are designed for specific purposes, ranging from resource management to identification of land use activities. The classification system proposed in this thesis is primarily urban activity oriented, that is, it attempts to construct as many measures and definitions of *urban land* as are realistically feasible from spectral data, and are within the abilities of the classification strategy. The classification scheme endeavours to strike a balance between the vast array of census data available, and the confines of the spatial and spectral limitations of satellite data. Census data are collected at the household level, and as such are limited mainly to residential activity. In other words, the Census can only be used in the classification of residential land use, and the classification of various sub-categories of residential land use, but not non-residential land uses. The proposed urban land use categories with descriptions are listed in Table 5.6.

Table 5.7 Urban Land use Hierarchy

Full Scene	-------	Rural						
	-------	*Urban*	-------	Non Built-up				
			-------	*Built-up*	-------	Other		
					-------	*Non-Residential*		
					-------	*Residential*	-------	*Detached*
							-------	*Semi-Detached*
							-------	*Terraced*
							-------	*Apartments*

N.B. Only categories in *italics* will form the classification scheme

As mentioned earlier, these categories are inherently hierarchical in structure (Table 5.7).

Of the eight categories, only "built-up" is a land cover criterion; the others are land uses. Built-up is the most objective class and is defined as predominantly composed of man-made structures. The most vague class, "urban", derived from OPCS definitions, is a composition of various land covers, and is exemplified by the inclusion of large stretches of vegetated land as long as they are within predominantly built-up areas (DoE, 1991). Unfortunately, the generality and subjectivity in the

urban class is expected to produce lower classification accuracies simply because spectral data are not able to accommodate subjective bureaucratic decisions.

The "residential"/"non-residential" distinction is primarily based on the type, orientation, size and spacing of building materials. The distinction will produce adequate classification accuracies only if buildings are significantly different in some or all of these criteria (Forster, 1993). Buildings used for manufacturing, storage, transport (eg. airfields, railway stations, etc) and most large commercial complexes should be relatively distinguishable from residential dwellings. These non-residential uses are commonly larger in size than residential housing and usually have larger driveways and parking areas. Furthermore, many are constructed with flat roofs producing a more specular reflectance resulting in higher radiometric values (Lo *et al.*, 1984). However, problems in residential/non-residential classifications are expected from certain retail and commercial activities which occur in buildings that are either converted or identical to dwelling types or occur in parts of urban areas characterised by mixed land uses. Other difficulties that are envisaged include residential dwellings that are as large, or composed of similar building materials, as non-residential types giving rise to similar spectral variations.

The residential land use category is sub-divided into four dwelling types: "detached", "semi-detached", "terraced", and "purpose-built apartments". These sub-categories represent as much detail as is possible from a satellite image given its resolution parameters. The spectral distinction between dwelling types is based on pixels with reflectance values that represent the ratio of building structures (composing the dwellings) to non-building structures (gardens, roads, footpaths, driveways, etc). As such, spectral classes of dwelling type can be viewed as measures of the density of building structures per pixel. In this way, these spectral classes can be converted into information classes by generally assuming that detached dwellings have the lowest density measures, with semi-detached the next lowest, followed by terraced dwellings, and high-rise purpose-built apartments having the highest. The identification of breaks within this density continuum is of course the prime objective of all image classifications, including the strategy outlined here. However, as stressed repeatedly, urban areas are highly spectrally heterogeneous. This is ever more apparent when subtle differences, such as defining breaks in the spectral representation of residential land use, is attempted. Here, possible spectral confusion is likely to be present between all dwelling types. For example, the difference

between detached and semi-detached dwellings may only be a matter of a slightly higher proportion of vegetation associated with detached dwellings. Confusion is also envisaged between apartments and non-residential buildings, where the main identifier is based upon spatial context. The distinction between all residential dwelling types is nonetheless very marginal when the classification is based solely on spectral data.

Census data will now be examined as a means for reducing some of the problems outlined above in three ways: assistance in the selection of separable training samples, as criteria for postclassification sorting, and in the generation of class prior probabilities. Before each of these techniques is applied to the empirical data sets, there now follows a brief mention of the software used for operationalization.

5.4.3 Software

The main computer processing software employed in all image classifications are versions 7.5 and 8.1 (*Imagine*) of the *Earth Resources Data Analysis System* (ERDAS). This is a proprietary image processing and GIS package, designed and developed by ERDAS Inc., Atlanta GA., USA (ERDAS, 1994) This software package is mounted on Sun Workstations driven by a Unix-based operating system. Support software includes *Unimap*, a proprietary raster mapping package from *Uniras*, used here to graphically display population surface models from the Bracken-Martin program. Also used are *Minitab* (release 8.0), a statistics package for analysing census attributes, and *Arc/Info* version 6.0 (ESRI, 1990) for handling digitised DoE vector urban boundary data. A suite of purpose-written programs in the FORTRAN 77 and C languages were also required to allow data conversions, probability estimations, and modifications to the Bracken-Martin FORTRAN algorithm.

Figure 5.9 is a diagrammatic representation of the flow of operations that will systematically be applied to each data set to produce land use categories for all four settlements at both points in time. The exact details of each operation required to fulfil every stage will now be discussed, beginning with standard unsupervised clustering, followed by the three techniques of the classification strategy: training sample selection, postclassification sorting, and the Bayesian decision rule, in that order.

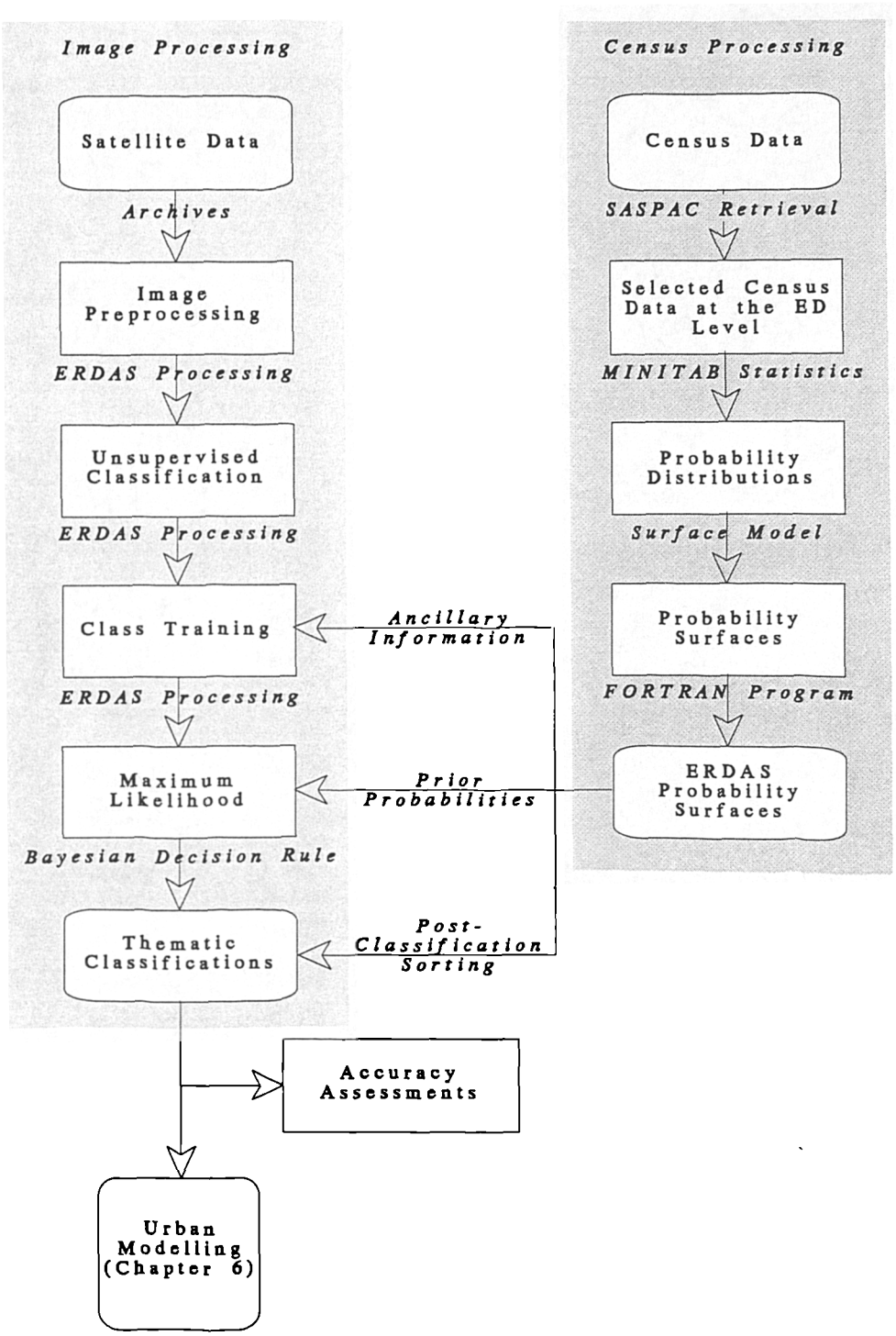

Figure 5.9 Flow of Operations for the Land Use Classification Strategy

5.4.4 Unsupervised Classification

Once all images are geometrically rectified and enhanced (see again section 5.3.1.2), the initial classifications are based on an unsupervised clustering algorithm designed to spectrally slice urban built-form from the rural landscape. The *ISODATA* program in ERDAS uses the maximum spectral distance formulae to produce spectrally distinct clusters, similarly to the *K*-means classifier outlined in Chapter One. The analyst controls only the number of spectral classes produced, the maximum number of iterations to be performed, and the class convergence threshold level (ERDAS, 1991).

ISODATA accounts for two of the land use categories, urban and built-up. Built-up is the more objective category and represents more standard and routine procedures in contemporary image classification. In general, urban built surfaces can be spectrally separated from predominantly rural areas by the way urban structures reflect energy. The more solid and geometrically angular physical characteristics of urban structures, combined with lower moisture content, invariably lead to different spectral response patterns, compared to those associated with rural surfaces. However, as will be discussed later, this simple building/non-building spectral contrast is neither perfect nor routine. Spectral confusion is frequently caused by rural surfaces (such as bare soil or certain agricultural fields) which can exhibit spectral response patterns that are very similar to those produced by built surfaces. In response to this type of spectral confusion, the surface model will later be assessed as a means for postclassification sorting of misclassified built pixels.

As regards the urban category, this involves a more subjective process of matching spectral classes that fit within the rather broad criteria of the OPCS definitions (OPCS, 1994). For instance, the criterion, "*...any area completely surrounded by built-up sites.*" allows for open spaces, such as parks, derelict land, and woodland. As a result, spectral classes representing vegetation are very difficult to separate between those completely surrounded by built-up sites and those outside the urban limits. However, an attempt was made to classify land according to the OPCS definitions. The process first involves a spectral separation of built and non-built classes, and then a GIS scanning function effectively removes all non-built pockets from within the spatial limits of the settlements.

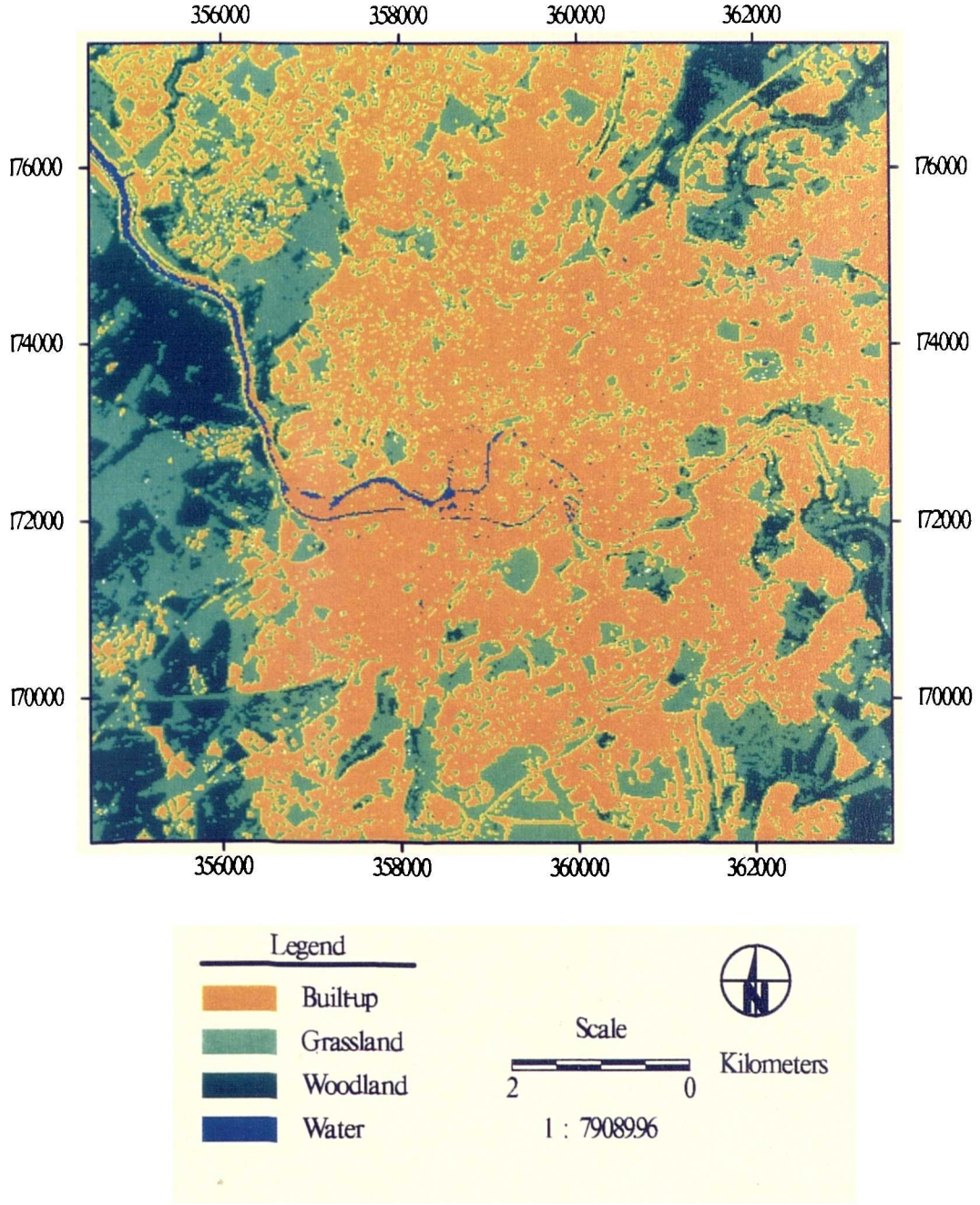

Figure 5.10 Unsupervised Land Use/Land Cover Classification of the Bristol 1991 Data Set

The scanning function is a neighbourhood operation where a roaming window systematically scans the whole image, converting pixels that are a minority within the window to the majority class. Unfortunately, apart from an inherent smoothing effect, the process also tends to remove minority pixels classified as built from the majority non-built pixels in the urban hinterland.

Figure 5.10 shows the results of the unsupervised method where "built-up" is defined as a single category but "urban" will need to be derived from a combination of "built-up" and intra-urban vegetated areas which are similar to rural "grassland".

5.4.5 Training Sample Selection

Chapter Three not only examined the detailed development of the Bayesian decision rule, but also the role of high probability surface cells in the selection of representative training samples. As a summary, the disaggregate nature of the surface model is able to generate a more continuous plane of residential patterns. Each cell of the surface model is assigned the value of a census variable. These values are expressed as a proportion, and have been smoothed by the model. Cell values are then further converted to probability values based on frequency distributions (see also section 5.3.2.2). High probability values, commonly over 0.9, are used as support data for the process of selecting and labelling inherently homogeneous spectral training areas in an image. These samples are then used by the Bayesian-type classifier (section 5.4.7).

Figure 5.11 illustrates a typical transect of 40 surface cells derived from the Bristol 1991 data set. Each cell has been assigned a probability value representing the joint occurrence of the number of households and a particular dwelling type. The threshold level of 0.9 is an arbitrary probability value used to reflect the ability of a cell to represent only one dwelling type category. These high probability cells are employed in two main areas of the classification strategy, the development within the residential/non-residential dichotomy, and the differentiation of the residential category. Sets of training samples for both groups of categories are generated by relating surface cells possessing high probabilities of one class to homogeneous areas of the image deemed to represent the same class. The enabling device is a basic Boolean image/surface overlay applied using standard GIS functions.

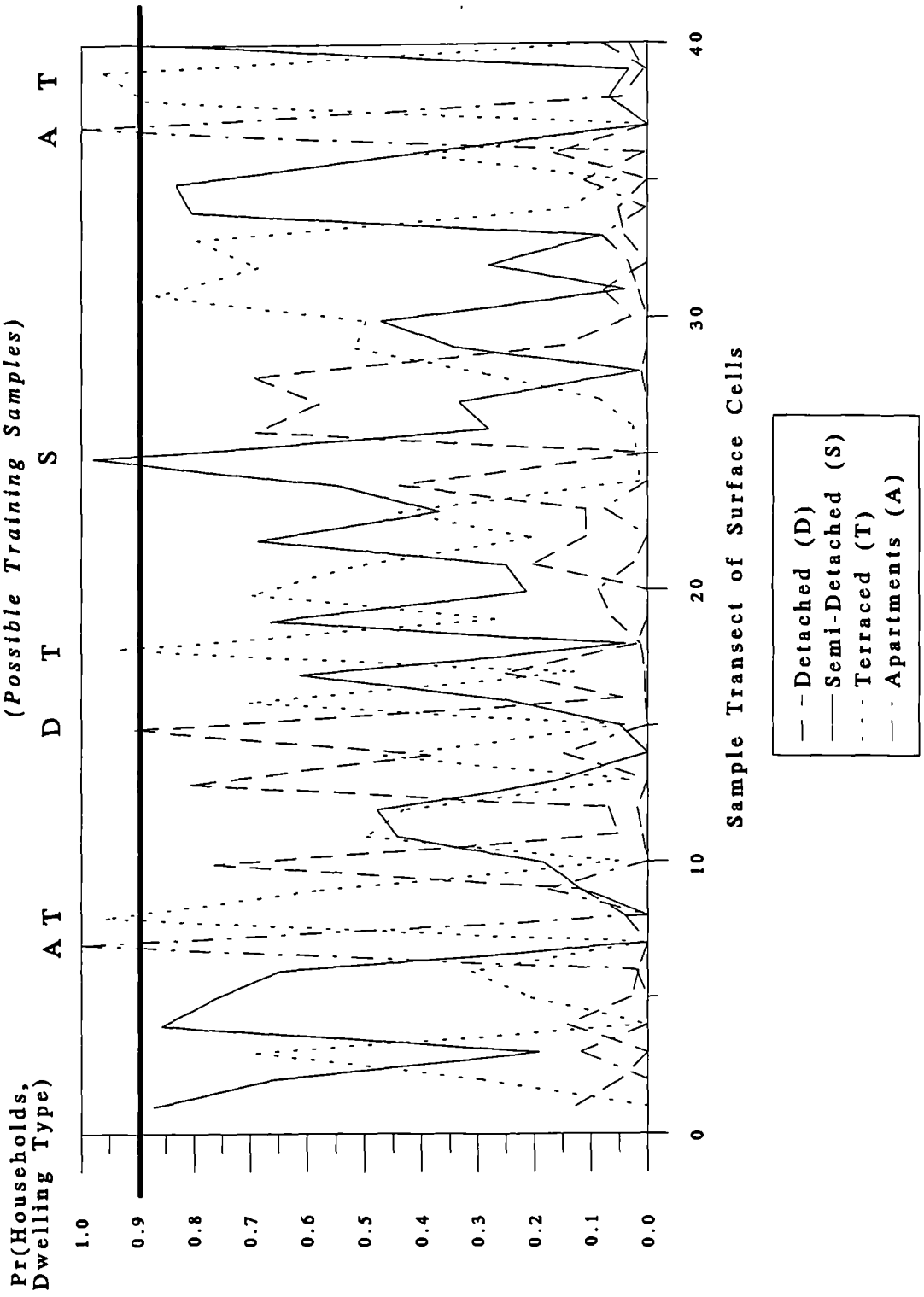

Figure 5.11 Transect of the Probability Surface for the Bristol Study Area

The resulting combined coverage is then used to highlight possible locations for the selection of training samples. Referring back to Figure 5.11, although only 40 surface cells are illustrated, as many as 7 of these were above the 0.9 probability threshold. Many samples will be generated for each class to ensure maximum representation, with enough of these samples exhibiting a Gaussian distribution for further use in the maximum likelihood parametric classifier.

The first area where training samples are informed by cells from the surface model is in the classification and distinction between the residential and non-residential land use categories. In this situation, the census variable, *number of households*, is used by the surface model to represent the occurrence of residential households.

Output from the surface model is then overlayed on to an image that only displays the built-up extent of the corresponding settlement (Figure 5.12: red denotes low probability of being residential, blue denotes high probability). Recall that the built-up extent is derived from the spatial segmentation (or masking) of the original satellite image by the classified built-up category (section 5.4.4 again). In Figure 5.12, the overlay of the 1991 surface model and image data sets clearly reveals general spatial similarity, despite the coarse resolution and approximate smoothing assumptions of the surface model. Also, the areas of the image that are ignored by the surface model (shown in red) generally correspond to the non-residential regions of Bristol. These non-residential sections are the CBD (labelled *1*), central manufacturing and harbour areas (labelled *2* and *7*, respectively), outlying commercial, industrial (labelled *5* and *6*), retail, storage, and institutional facilities (labelled *3* and *4*). The circled areas, labelled A and B are also areas of the image that are not covered by the surface model. However, in these cases subsequent ground and collateral information have determined them not as non-residential built-up areas, but as a quarry (*A*) and an agricultural field (*B*). More discussion on the use of such areas will be provided in section 5.4.6. One other aspect of Figure 5.12 reveals an example of how the image based on the "built-up" category is seriously unable to accommodate the surface model. The area labelled *Z* has surface representation but considerably less image representation. An investigation into this case found that the area under *Z* is characterised by highly dispersed housing within a forested habitat. This resulted in vegetation being the most observable land cover by a satellite and would explain why the unsupervised classification failed to locate many of the individual buildings.

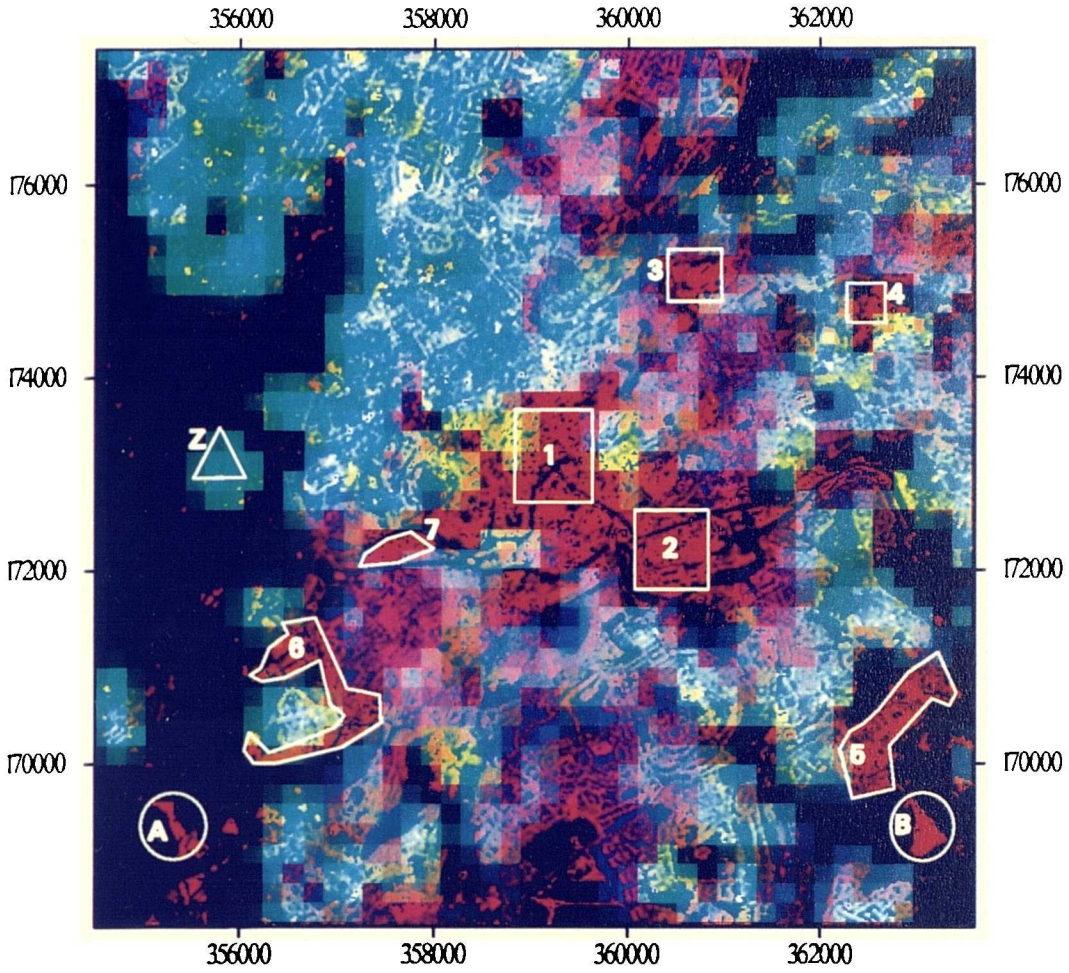

Figure 5.12 Overlay of Surface Model on Top of Satellite Image for Bristol 1991

Only those parts of the image where the surface model is in general agreement with either residential or non-residential land uses will inform the selection of training samples of both categories.

Differentiation within the residential category is the second, and most important, area where high probability surface cells are used in conjunction with spectral training samples. Again, the enabling process is a simple Boolean overlay between an image, segmented into residential land use (derived from previous classification), and a surface model representing dwelling types. The generation of homogeneous training samples for each dwelling type is then assisted by surface cells representing high probabilities of corresponding dwelling types (refer back to Figure 5.11). Once again, all training samples are collected and statistically evaluated, and directly entered into the Bayesian-type classifer. The process of selecting homogeneous training samples for each dwelling type category has now become a less subjective exercise if the selection is informed by high probability surface cells. Each training sample is selected within a framework of general agreement between high probability surface cells and homogeneous groups of pixels. If the classified dwelling types are directly compared with their surface model representation there is an immediate visual similarity in the spatial patterns of each dwelling type. Figure 5.13 shows this general similarity for the Norwich 1991 data set. Except for the apartments category, inspection points to close agreement, and hence a limited vindication of the technique outlined in this section. Furthermore, in both the residential and dwelling type classifications, the standard assumptions regarding the minimum number of pixels per training sample and the ability to produce covariance matrices are always upheld (see Chapter Three).

5.4.6 Postclassification Sorting

The method of postclassification sorting is applied solely to those problem pixels associated with the extraction of the residential category from the built-up class. As noted earlier during the discussion on unsupervised classification, the built-up class is derived by a simple partitioning of radiometric values that best represent the reflectance of built structures. Within a hierarchical classification scheme the residential class is a subsection of the built-up class. Unfortunately, as was also noted, some pixels classified as built-up may, in actual fact, be derived from similar spectral values associated with non built-up features.

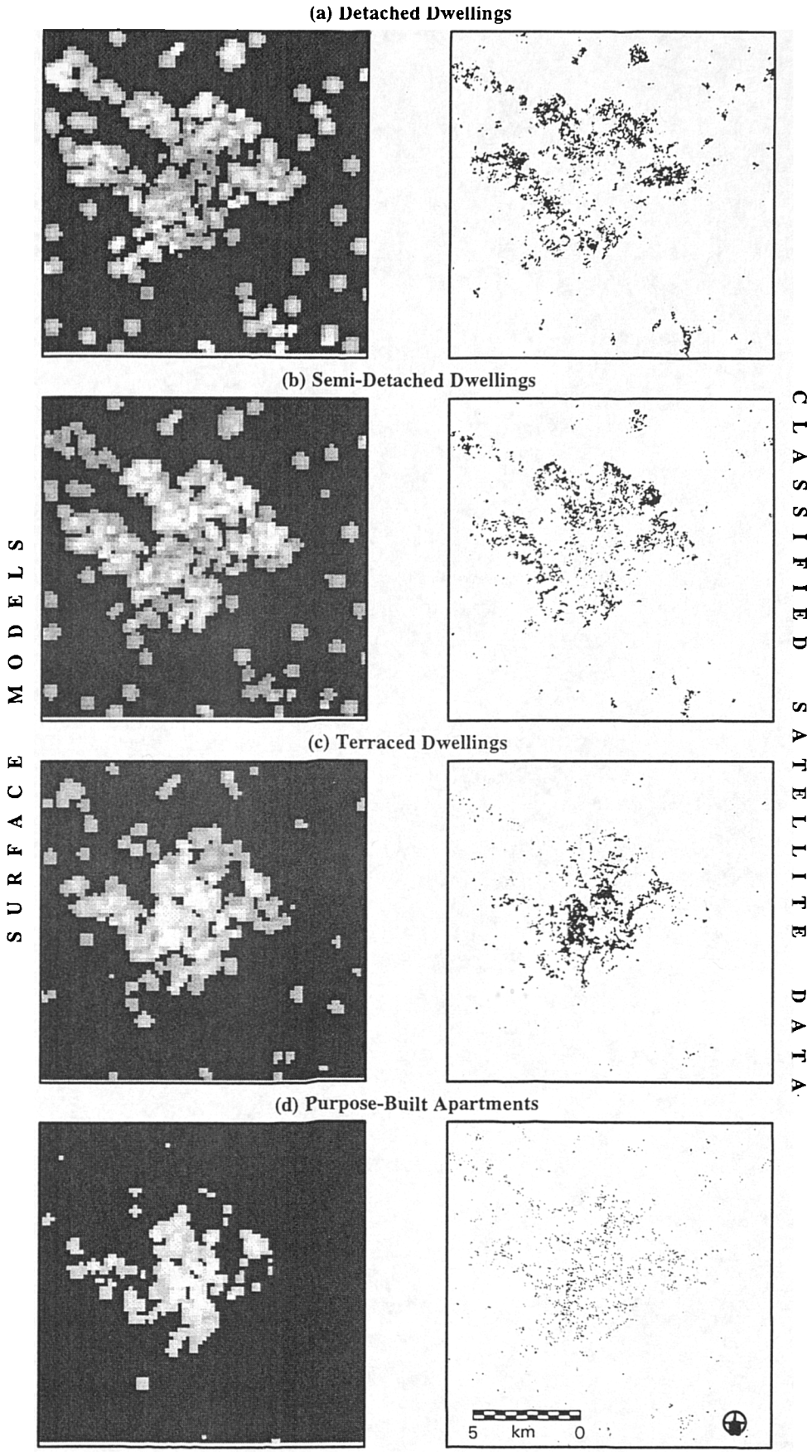

Figure 5.13 Dwelling Type Comparisons between Surface Model Representation and Classified Satellite Data

The surface model representing information pertaining to spatial patterns of residential land use will here be employed to "weed out" such misclassified pixels and reduce spectral ambiguity during the transition from built-up to residential. Using the image classified as built-up, training samples are then extracted for both residential and non-residential categories, following the procedures outlined in the previous section. Next, the classification of these two categories proceeds using a conventional maximum likelihood algorithm. From here, the surface model applies as segmentation criteria for the potential elimination of pixels classified as residential, but which clearly do not conform to residential patterns exhibited by the surface model. The procedure involves a simple GIS overlay function, where the classified image and surface model are registered to common coordinates (see again Figure 5.12). Areas spectrally classified as residential are then cross-checked against corresponding surface cells. Anomalous pixels that visually do not fit the spatial patterns of the surface model are then labelled as potentially misclassified and are excluded. Most of these eliminated pixels are expected to be outside the main settlements, representing quarries and other exposed soil features. In this respect, the segmentation qualities of the surface model may go some way towards resolving the frequent spectral confusion between bare soil and residential land use (Sadler and Barnsley, 1990).

However, it must be recognised that as the surface model is residential-oriented, potential misclassification between non-residential and non built-up categories remains unaffected. As such, postclassification sorting plays a small, yet interesting, role in the overall classification strategy presented in this thesis. More importantly, the Bayesian decision rule, which follows next, is responsible for the classification of four sub-categories of residential land use, namely detached, semi-detached, terraced, and purpose-built apartments.

5.4.7 Bayesian Decision Rule

The primary reason for employing a layered classification strategy concerns the optimal implementation and statistical performance of the Bayesian decision rule classifier. All modified prior probabilities are drawn from census data, and these in turn are a reflection of the spatial characteristics of residential patterns. A Bayesian decision rule, with prior probabilities based on residential criteria, must only be implemented using satellite data representing residential land use.

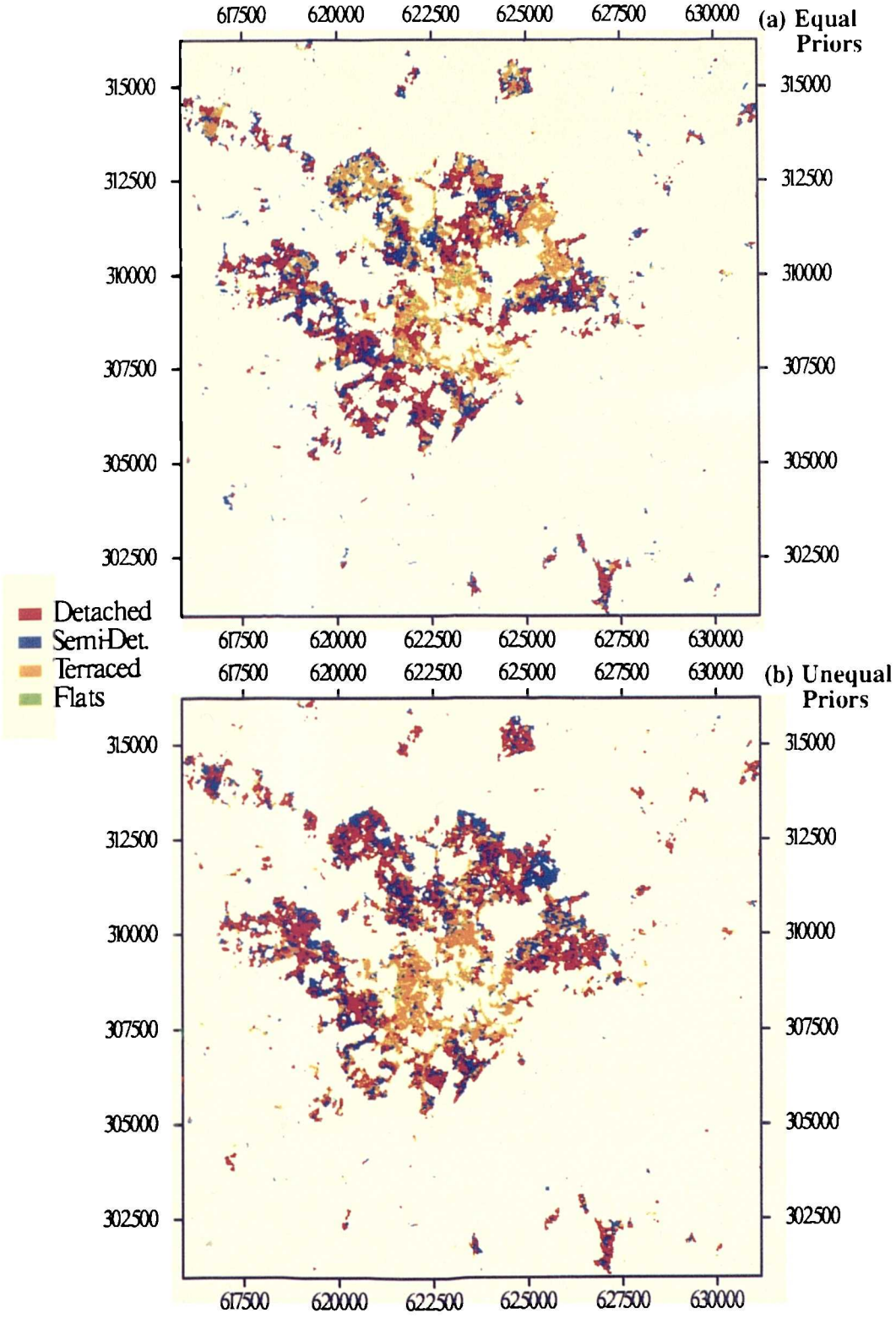

Figure 5.14 Bayesian-Type Classification of the Norwich Study Area Under (a) Equal Priors, and (b) Unequal Priors

For example, prior probabilities generated by dwelling type information can only be used to classify residential land into dwelling types, and no other categories. Logically, the denominator of the Bayesian decision rule assumes all prior probabilities are normalised (summed to 1.0), and as such decision space can only be partitioned into dwelling types. The strict assumptions employed by the Bayesian classifier must be met for the results to be coherent.

The Bayesian decision rule is executed by modifying the prior probabilities of the conventional maximum likelihood classifier. Numerical examples of the statistical mechanisms of the Bayesian decision rule can be found in Chapter Three. Briefly, the first step follows the segmentation procedures of unsupervised classification and postclassification sorting in defining areas of a satellite image that represent exclusively residential land use. Next, prior probabilities of the occurrence of each dwelling type for the whole study area are directly generated from frequencies derived from the UK Population Census. This also involves establishing associations between spectral training samples for each dwelling type and corresponding census variable using the surface model and the process of training sample selection, outlined in section 5.4.5. Finally, the Bayesian decision rule is employed by modifying the maximum likelihood classifier with these prior probabilities of dwelling type occurrence. Again, the reader may wish to refer to Chapter Three for a full discussion and examples of the statistical operations of the decision rule.

Figure 5.14 shows the results of Bayesian-type classifications under equal and unequal prior probabilities of the Norwich 1991 image. These prior probabilities are derived from Table 5.5 in section 5.3.2.2. What is clearly apparent, is the considerable differences in the spatial patterns of dwelling types between the two scenarios. A visual comparison suggests that the classification with unequal priors (Figure 5.14b) shows, for example, greater coverage of detached dwellings than the one with equal priors. A more objective comparative assessment involves the calculation of areal proportions.

5.4.7.1 Areal Proportions

The final stage of analysis for all image classifications is testing for accuracy and precision. Before attention is switched towards standard classification accuracy assessments, results from the Bayesian decision rule can be quickly evaluated by

observing class areal proportions. These are expressed as the number of pixels of the image classified into different categories. Areal proportions are calculated by simply multiplying the number of pixels for each category by the area of a single pixel, for example $400m^2$ (20m x 20m pixels) for SPOT XS, and $900m^2$ (30m x 30m pixels) for Landsat TM. A performance measure can then be built around comparisons between known areal distributions and those generated by image classification. In other words, it is possible to determine the degree to which known areal proportions of land use categories, as relative proportions of a study site, are replicated by the classification of satellite imagery. Of course, similar areal proportions between known and classified data do not necessarily mean that the classification is completely accurate. Further tests are required on how well each land use category is represented by the classified image at specific locations on the ground, and indeed this will be comprehensively examined in the next section. However, for the time being, an evaluation of area estimates provides valuable insights into the discriminatory power of the Bayesian decision rule. Recall that the decision rule is based on prior probabilities of class occurrence, which means that known areal proportions are accommodated *a priori* to classification. This allows spectral classification to proceed within constrained parameters where each class is weighted according to its prior probability value. As a result, the relative areal proportions of each classified category should reflect these prior probabilities.

In Table 5.8 the results of the Bayesian-type classification of the four dwelling types for the four settlements are assessed using known areal proportions from the Population Census, as well as results generated under conditions of equal prior probabilities. Known areal proportions from the Census are calculated by determining the relative number of dwellings for each type (adjusted by the size ratio scale) in all EDs within each study area. When compared to areal proportions generated by equal priors (conventional maximum likelihood), and unequal priors (Bayesian-type), an error term is derived which simply measures whether the classified image underestimated the areal coverage (negative error percentage points), or overestimated (positive percentage points). The total error is then expressed as an absolute term.

The main conclusion that can be drawn from Table 5.8 is that the Bayesian-type method consistently out-performs the conventional maximum likelihood classifier.

Table 5.8 Accuracy Assessment of Areal Coverage by Dwelling Type

a. Bristol, 1991

Dwelling Type	Census		Equal Priors			Unequal Priors		
	n	%	n*	%	ε†	n*	%	ε†
Detached	11827	11.45	10416	11.63	0.18	10377	11.54	0.09
Semi-Detached	39033	37.79	33326	37.21	-0.58	33066	37.10	-0.69
Terraced	48402	46.86	40813	45.57	-1.29	41722	46.39	-0.47
Apartments	4028	3.90	5006	5.59	1.69	4480	4.98	1.08
Total	103290	100.00	89561	100.00	**3.74**‡	89645	100.00	**2.33**‡

b. Norwich, 1991

Dwelling Type	Census		Equal Priors			Unequal Priors		
	n	%	n*	%	ε†	n*	%	ε†
Detached	37364	42.40	12486	38.75	-3.65	13910	43.17	0.77
Semi-Detached	26675	30.27	10311	32.00	1.75	9161	28.43	-1.84
Terraced	21088	23.93	8030	24.92	0.99	7440	23.09	-0.84
Apartments	2987	3.39	1395	4.33	0.94	1712	5.31	1.92
Total	88114	100.00	32222	100.00	**7.33**‡	32223	100.00	**5.37**‡

c. Swindon, 1991

Dwelling Type	Census		Equal Priors			Unequal Priors		
	n	%	n*	%	ε†	n*	%	ε†
Detached	19580	30.14	8316	31.19	1.05	8462	30.54	1.54
Semi-Detached	23659	36.42	10608	39.79	3.37	9834	36.82	0.40
Terraced	20385	31.38	7254	27.21	-4.17	8034	30.08	-1.30
Apartments	1364	2.10	483	1.81	-0.29	381	1.43	-0.67
Total	64962	100.00	26661	100.00	**8.88**‡	26711	100.00	**3.99**‡

d. Peterborough, 1991

Dwelling Type	Census		Equal Priors			Unequal Priors		
	n	%	n*	%	ε†	n*	%	ε†
Detached	19177	36.25	67345	36.46	0.21	7171	37.30	1.05
Semi-Detached	18515	35.00	10311	38.75	3.91	6990	36.36	1.36
Terraced	14008	26.48	8030	23.09	-2.69	4756	24.74	-1.74
Apartments	1201	2.27	1395	1.70	-0.57	308	1.60	-0.67
Total	52901	100.00	18471	100.00	**7.92**‡	19225	100.00	**4.82**‡

*number of pixels. †error of % coverage between census and classified map using equal or unequal priors ‡total error in absolute terms

Individual dwelling type and total errors for settlements are generally lower using unequal prior probabilities adopted by the Bayesian decision rule. In most cases, the terraced category seems to be underestimated, and the semi-detached category overestimated, by both equal and unequal prior scenarios. These trends may be a result of size scaling relations, or problems in the actual detection of dwelling types from the image. Assuming the former is constant, the latter will be more fully evaluated in the next section. One other striking feature from Table 5.8 suggests that the classifications of the Bristol study area are far superior, in terms of lowest errors, to those for the other three sites. The reasons for this may include the use of a higher spatial resolution image (SPOT XS compared to Landsat TM for the others), or, because it is the local site, extra local knowledge in the selection of training samples.

5.5 Accuracy Assessment of Bristol, 1991

One of the prime objectives of developing a new classification strategy is to improve upon existing classification strategies. The standard practice in remote sensing, concerning classified images, involves some measures of spatial accuracy Typically this is defined as the degree to which the classified images match the reference data. In thematic image classification, accuracy assessment is usually reserved for comparisons of the spatial locations of nominal classes between the classified image and the reference data, or ground truth. Accuracy is reported in the form of confusion matrices, overall percentages, and measures of agreement beyond chance agreements. All of these measurements of classification accuracy were examined in Chapter Three.

For convenience, the Bristol study area was selected to demonstrate the accuracy assessment techniques. Classification assessments were based primarily on a ground survey collected by the author between April 28 and May 3, 1994. Assessment of the other areas would follow a similar format.

5.5.1 Test Sample Strategy

According to Fitzpatrick-Lins (1980) the ideal number of sample points to be tested can be determined from formulae from the binomial probability theory. In Chapter Three, this was calculated at 204 points if the Anderson *et al.* (1972) guidelines of

85% expected accuracy with a 5% allowable error were assumed. With this in mind, 250 sample points for each set of land use categories were deemed both statistically sufficing as well as realistically feasible, within time constraints. The sets of land use categories refer to the logical assessments of urban as opposed to non-urban, built-up against non-built, residential against non-residential, along with dwelling types classified both with equal and unequal prior probabilities. As these sets of categories are hierarchical, where for instance residential is a subset of built-up, not all of the 250 sample points fell within the classified regions of each set of categories. Therefore, in practice, an additional 112 points were needed to guarantee each set had at least the required 204 points.

The next step involved the computer generation of 250 points for each set of categories within a stratified random sampling frame. Stratification was based on class percentages where the proportion of points extracted for each land use category was based on their proportion of the classified scene. However, individual pixels are not necessarily the most appropriate representations of sample points. This is because classified images over highly heterogeneous urban areas are frequently associated with 'salt and pepper' pixels where categories contain a degree of extraneous foreign pixels. As a result, it was decided to employ a 3 by 3 window which was centred on each randomly generated pixel. From there, the class of the random pixel was determined by a clear majority of pixels with the same class within the window.

5.5.2 Field Survey

Once the location of each test point was determined by x and y coordinates, the next stage involved the actual collection of reference data to be used in subsequent classification assessments. In the field, the visual recognition of each land use category did not present major problems. The only concern was determining the precise geographical locations of the test points in the field. Preliminary inquiries into the acquisition of GPS equipment proved unreliable and inconvenient within time limits. Nevertheless, the use of OS maps at 1:25,000 was regarded as an acceptable alternative given the highly accessible and well-surveyed nature of urban areas. Once the approximate location of each test point was determined in the field, a number of decisions were made on the type of land use that were visually assessed to dominate the landscape. Determining whether land contained built structures did not present a problem. However, the rather subjective definition of urban land use by the OPCS,

and the categorisation of building types required more careful considerations. On the issue of the OPCS urban definition, a certain degree of subjectivity forms part of the decision as to whether open space can be considered urban. Overall, the distinction between residential and non-residential was reasonably unambiguous, apart from buildings used for retail activity on the ground floor and residence on the first floor. In this instance, the type of neighbouring buildings were taken into account, and if the distinction is still unresolved, the building is assumed to be non-residential. With regard to dwelling type, this was again fairly straightforward as long as the assumption of purpose-built high-rise apartments containing five or more storeys was met. Information from the ground survey was then cross-checked with the results of all classifications to produce a series of assessments based on accuracy criteria outlined in Chapter Three.

5.5.3 Accuracy Results

The format of the assessments for each set of categories follows standard practice in remote sensing, namely an ordinary error matrix, proceeded by commission and omission errors, and individual category errors (Jensen, 1986). The two most important global measures of accuracy are the simple overall percentage and the more refined Kappa coefficient, which approaches 1.0 with higher accuracy. With respect to significance, the time-honoured criterion of 85% advocated by Anderson *et al.* (1972) was employed (referred to simply as the Anderson criterion). This level was adopted for one-tailed and two-tailed 95% confidence limits in overall accuracy and individual category accuracy respectively.

The problems associated with the classification of urban land use according to the OPCS definitions are clearly apparent in the first of the accuracy assessments in Table 5.9. Although overall accuracy is 85.6%, this was merely a reflection of the predominantly urban dominated scene of central Bristol. More revealing figures of 49.1% accuracy pertaining in the rural category and a low Kappa coefficient is indicative of the difficulty in annexing spectral classes representing non-structure classes based on bureaucratic decisions. As a result, significance tests for both the rural category and overall accuracy fell below the 85% threshold. With these problems in mind, it can be assumed that the urban category does not yield a reliable and consistent classification, and as such, subsequent modelling of this category should be treated with a degree of caution.

Table 5.9 Accuracy Assessments of Urban Land Use

a. Error Matrix

Classified Data	Reference Data		
	Rural	Urban	Row Total
Rural	**28**	7	35
Urban	29	**186**	215
Column Total	57	193	250
Overall Accuracy: (214/250) = **85.6%** (95% One-tailed Lower Confidence Limit = **81.7**) Kappa Coefficient = **0.526**			

b. Commission and Omission Errors

	Commission Errors		Omission Errors		Correct	
Classified	Total	%	Total	%	Total	%
Rural	7/57	12.3	29/57	50.9	28/57	49.1
Urban	29/193	15.0	7/193	3.6	186/193	96.4
Average Accuracy: [(49.1 + 96.4) / 2] = **72.8%**						

c. Individual Category Error Evaluation

		Commission			Omission		
Classified	Points Correct	n	% Correct	95% Conf limits	n	% Correct	95% Conf limits
Rural	28	35	80.0	65.3 - 94.7	57	49.1	35.2 - 63.0
Urban	186	215	86.5	81.7 - 91.3	193	96.4	93.5 - 99.3

The main reason for including the urban category is to allow direct comparison with the OPCS-defined urban category from the DoE digital boundary database. However, the lack of significant accuracy in the classified urban category may not allow this comparison to be particularly reliable. Instead, the built-up category, founded on physical structures, will provide a more accurate and consistent basis for comparison.

Table 5.10 Accuracy Assessments of Built-up Land Cover

a. Error Matrix

Classified Data	Reference Data		
	Rural	Built-up	Row Total
Rural	**86**	0	86
Built-up	7	**157**	164
Column Total	93	157	250

Overall Accuracy: (243/250) = **97.2%** (95% One-tailed Lower Confidence Limit = **95.3**)
Kappa Coefficient = **0.939**

b. Commission and Omission Errors

	Commission Errors		Omission Errors		Correct	
Classified	Total	%	Total	%	Total	%
Rural	0/93	0.0	7/93	7.5	86/93	92.5
Built-up	7/157	4.5	0/157	0.0	157/157	100.0

Average Accuracy: [(92.5 + 100.0) / 2] = **96.3%**

c. Individual Category Error Evaluation

		Commission			Omission		
Classified	Points Correct	n	% Correct	95% Conf limits	n	% Correct	95% Conf limits
Rural	86	86	100.0	99.4 - 100.0	93	92.5	86.6 - 98.4
Built-up	157	164	95.7	92.3 - 99.1	157	100.0	99.7 - 100.0

Table 5.10 illustrates the potential of satellite classification if the end classes are based exclusively on physical land cover. An overall accuracy level of 97.2% and a Kappa coefficient of 0.939 are as high as can be expected from satellite-based data. It also follows that all significance tests are above the Anderson criterion. What margin of improvement there is in the classification of built-up can be attributed to land surfaces (such as bare soil) that exhibit similar spectral reflectance to the built-form.

Table 5.11 Accuracy Assessments of Residential/Non-Residential Land Uses

a. Error Matrix

Classified Data	Reference Data			
	Outside	Residential	Non-Residential	Row Total
Outside	0	0	0	0
Residential	6	**187**	14	207
Non-Residential	1	3	**39**	43
Column Total	7	190	53	250

Overall Accuracy: (226/250) = **90.4%** (95% One-tailed Lower Confidence Limit = **87.1**)
Kappa Coefficient = **0.713**

b. Commission and Omission Errors

	Commission Errors		Omission Errors		Correct	
Classified	Total	%	Total	%	Total	%
Outside	0/7	0.0	7/7	100.0	0/93	0.0
Residential	20/190	10.5	4/190	1.6	187/190	98.4
Non-Residential	4/53	7.5	14/53	26.4	39/53	73.6

Average Accuracy: [(0.0 + 98.4 + 90.7) / 3] = **63.0%**

c. Individual Category Error Evaluation

		Commission			Omission		
Classified	Points Correct	n	% Correct	95% Conf limits	n	% Correct	95% Conf limits
Outside	0	0	-	-	7	100.0	92.9 - 100.0
Residential	187	207	90.3	86.0 - 94.6	190	98.4	96.4 - 100.0
Non-Residential	39	43	90.7	80.9 - 100.0	53	73.6	60.8 - 86.4

As illustrated earlier, the discriminatory effects of scene segmentation based on population surface cells can, to a certain extent, reduce these problem areas.

The distinction between residential and non-residential land uses was based on numerous and representative training samples, selected with the aid of the surface model. In Table 5.11 an overall accuracy of 90.4% along with a Kappa coefficient of 0.713 means that this distinction was defined reasonably well enough to exceed the Anderson criterion. However, the anticipated problems with the residential/non-residential differentiation from buildings that are very similar in structure are very much apparent. This is illustrated by the fact that 14 of the 53 sample points for non-residential were classified as residential. This deficiency is a reminder of the dangers of attempting to define categories that are spectrally inseparable. Incidentally, the category "outside" was necessary in order to capture the 7 erroneous points that were perpetuated from the built-up category.

The final three tables document the effects of the Bayesian decision rule on the classification of dwelling types. The first of these, Table 5.12 is the control where the effects of the decision rule are nullified by setting prior probabilities equal for all categories. Even so, accuracy parameters seem fairly high (overall 73.6%, Kappa coefficient 0.607) given the level of categorisation. One explanation could be the effects of numerous and representative training samples, along with the high spatial resolution capabilities (20m) of the SPOT scene. Nevertheless, all significance tests are well below the Anderson criterion, and as such follow most previous work in the image classification of intra-residential land use.

Next, Table 5.13 applies the Bayesian decision rule by modifying prior probabilities for each category based on areal proportions from the 1991 Census. Although the 95% one-tailed lower confidence limit is still below the Anderson criterion, the use of unequal prior probabilities have substantially increased all measures of accuracy well above those generated from equal prior probabilities. Indeed one category, semi-detached, in fact slightly exceeds the 85% criterion in accuracy associated with omission errors. More detailed comparisons between the two tables (5.12 and 5.13) reveals that the pattern of individual category accuracies and the distribution of errors are very much consistent, although different in magnitudes. This observation is in line with the assumptions of the Bayesian decision rule which does not produce drastically different classifications, but only modifies the magnitudes of class area proportions. Furthermore, both tables represent classifications that utilised the same training samples.

Table 5.12 Accuracy Assessments of Dwelling Type (Equal Prior Probabilities)

a. Error Matrix

Classified Data	Reference Data					
	Non-Resid	Detached	Semi-Det	Terraced	Apartments	Row Total
Non-Residential	**0**	0	0	0	0	0
Detached	0	**22**	3	2	0	27
Semi-Detached	2	2	**72**	13	3	92
Terraced	14	3	12	**81**	5	115
Apartments	1	2	1	3	**9**	16
Column Total	17	29	88	99	17	250

Overall Accuracy: (184/250) = **73.6%** (95% One-tailed Lower Confidence Limit = **68.8**)
Kappa Coefficient = **0.607**

b. Commission and Omission Errors

	Commission Errors		Omission Errors		Correct	
Classified	Total	%	Total	%	Total	%
Non-Residential	0/0	-	17/17	100.0	0/17	0.0
Detached	5/29	17.2	7/29	24.1	22/29	75.9
Semi-Detached	20/88	22.7	16/88	18.2	72/88	81.8
Terraced	34/99	34.3	18/99	18.2	81/99	81.8
Apartments	7/17	41.2	8/17	47.1	9/17	52.9

Average Accuracy: [(0.0 + 75.9 + 81.8 + 81.8 + 52.9) / 5] = **58.5%**

c. Individual Category Error Evaluation

		Commission			Omission		
Classified	Points Correct	n	% Correct	95% Conf limits	n	% Correct	95% Conf limits
Non-Residential	0	0	-	-	17	0.0	0.0 - 2.9
Detached	22	27	81.5	65.0 - 98.0	29	75.9	58.6 - 93.2
Semi-Detached	72	92	72.7	63.1 - 82.3	88	81.8	73.2 - 90.4
Terraced	81	115	70.4	61.6 - 79.2	99	81.8	73.7 - 89.9
Apartments	9	16	56.3	28.9 - 83.7	17	52.9	26.2 - 79.6

Table 5.13 Accuracy Assessments of Dwelling Type (Unequal Prior Probabilities)

a. Error Matrix

Classified Data	Reference Data					
	Non-Resid	Detached	Semi-Det	Terraced	Apartments	Row Total
Non-Residential	**0**	0	0	0	0	0
Detached	0	**25**	2	1	0	28
Semi-Detached	2	1	**81**	7	2	93
Terraced	14	2	5	**90**	5	116
Apartments	1	1	0	1	**10**	13
Column Total	17	29	88	99	17	250

Overall Accuracy: (206/25)0 = **82.4%** (95% One-tailed Lower Confidence Limit = **78.2**)
Kappa Coefficient = **0.737**

b. Commission and Omission Errors

	Commission Errors		Omission Errors		Correct	
Classified	Total	%	Total	%	Total	%
Non-Residential	0/0	-	17/17	100.0	0/17	0.0
Detached	3/29	10.3	4/29	13.8	25/29	86.2
Semi-Detached	12/88	13.6	7/88	8.0	81/88	92.0
Terraced	26/99	26.3	9/99	9.1	90/99	90.9
Apartments	3/17	17.6	7/17	41.2	10/17	58.8

Average Accuracy = [(0.0 + 86.2 + 92.0 + 90.9 + 58.8) / 5] = **65.6%**

c. Individual Category Error Evaluation

		Commission			Omission		
Classified	Points Correct	n	% Correct	95% Conf limits	n	% Correct	95% Conf limits
Non-Residential	0	0	-	-	17	0.0	0.0 - 2.9
Detached	25	28	89.3	76.1 - 100.0	29	86.2	71.9 - 100.0
Semi-Detached	81	93	87.1	79.8 - 94.5	88	92.0	85.8 - 98.2
Terraced	90	116	77.6	69.6 - 85.6	99	90.9	84.7 - 97.1
Apartments	10	13	76.9	50.1 - 100.0	17	58.8	32.5 - 85.1

The semi-detached and terraced categories are the most accurate in both tables, closely followed by detached, with the apartments category showing the lowest and least significant levels of accuracy.

Although confidence in the classification of apartments is slightly higher by using unequal prior probabilities, an accuracy of 58.8% means subsequent modelling results should be treated with great caution. Problems with the apartments category could be linked to the small number of test points, as well as the difficulty in differentiating apartment blocks from other types of buildings. Classification confusion is also evident between terraced and non-residential buildings with 14 non-residential test points classified as terraced. Again this can be attributed to spectral inseparability in central parts of Bristol where both land uses frequently intermix. Incidentally, the non-residential category was included into the assessments to represent inaccuracies perpetuated from the residential/non-residential classification.

The use of unequal prior probabilities has shown that substantial increases in classification accuracy can be realised even from a limited number of categories. However, although unequal prior probabilities are more applicable to spectrally heterogeneous urban landscapes (Mather, 1985), the apartments example illustrates that some classes will always remain spectrally inseparable no matter how rigorous the probability of estimation.

The last assessment table (5.14) attempts to further support the concept of unequal prior probabilities by evaluating all mis-classified test points. The evaluation determines whether the correct class represented the second most frequent number of pixels within mis-classified 9-pixel windows. In the event of the correct class being the first alternative, the error matrix is updated to include that mis-classified point as a correct point. In this way, the effects of the Bayesian decision rule can be assessed in terms of the degree of mis-classification.

Using the modified error matrices in Table 5.14 accuracy measures have increased by approximately the same magnitudes under both equal and unequal prior probability assumptions. However, the exceptionally high overall accuracy of 93.2%, along with a Kappa coefficient of 0.901, have further validated the effectiveness of the Bayesian decision rule.

Table 5.14 Modified Error Matrices to Include 2nd Choice Classes as Correct Points

a. Dwelling Type (Equal Prior Probabilities)

Classified Data	Reference Data					
Non-Resid	Detached	Semi-Det	Terraced	Apartments	Row Total	
Non-Residential	**8**	0	0	0	0	8
Detached	0	**24**	2	1	0	27
Semi-Detached	1	2	**79**	4	3	89
Terraced	7	3	7	**92**	5	114
Apartments	1	0	0	2	**9**	12
Column Total	17	29	88	99	17	250

Overall Accuracy: (184/250) = **84.8%** (95% One-tailed Lower Confidence Limit = **80.9%**)
Kappa Coefficient = **0.778**

b. Dwelling Type (Unequal Prior Probabilities)

Classified Data	Reference Data					
	Non-Resid	Detached	Semi-Det	Terraced	Apartments	Row Total
Non-Residential	**11**	0	0	0	0	11
Detached	0	**27**	1	1	0	29
Semi-Detached	0	1	**85**	0	1	87
Terraced	6	1	2	**97**	4	110
Apartments	0	0	0	1	**12**	13
Column Total	17	29	88	99	17	250

Overall Accuracy: (206/25) = **93.2%** (95% One-tailed Lower Confidence Limit = **90.4%**)
Kappa Coefficient = **0.901**

5.6 Summary & Conclusions

This chapter illustrated an exercise in the generation of spatial representations of urban land use from the more conventional means of per-pixel classifications from satellite imagery. Here, image classification was significantly aided by the employment of a strategy based on disaggregate surfaces of socioeconomic data

extracted from the UK Population Census. The strategy was composed of simple scene segmentation, training sample selection, as well as the application of a Bayesian modification to the conventional maximum likelihood discriminant function. Developed theoretically in Chapter Three, the strategy was applied in this chapter to a series of empirical data sets drawn from four settlements in the United Kingdom. The goal was to produce various categories of urban land cover/land use that would form the measurement base to develop subsequent urban models.

Per-pixel image classification is an established part of remote sensing methodology. However, the inherent spatial heterogeneity of built surfaces has tended to restrict detailed image classifications of urban areas. Attempts to untangle the complex spectral pattern associated with urban areas have often resorted to the use of ancillary data from non-spectral sources. Unfortunately, this type of supervised image classification has relied on localised ancillary data, which invariably tend to produce highly scene-specific classifications.

Considering these limitations, and those discussed in Chapter Four, this chapter has attempted to establish the empirical basis for the two main objectives of the classification strategy adopted in this thesis. These are the generation of more accurate inventories of classified urban categories, and the establishment of these inventories as reliable and consistent measurements for subsequent urban modelling techniques. On the first objective, accuracy assessments on areal proportions for all settlements, and on individual categories for Bristol 1991, together demonstrate the validity of the empirical application of the classification strategy. Furthermore, the use of a national database of disaggregate socioeconomic variables as ancillary data has allowed classification to proceed within a more routine and consistent framework. This ability to standardise the classification procedure for any urban area is the basis for objective urban modelling. The next chapter will apply the urban modelling techniques developed in Chapter Four to the results of the empirical land use classifications outlined in this chapter.

Chapter Six
URBAN LAND USE MODELLING

6.1 Introduction

The theoretical foundations of the relationship between urban density functions and fractal concepts were examined in Chapter Four. That chapter ended with an assessment of the conventional data sets upon which most analyses of urban population density gradients have been based, and a discussion of the proposed role of classified satellite data. Chapter Five reported a series of classified satellite images of the urban morphology of four settlements in the United Kingdom at two time periods. This chapter will now apply the theoretical estimations of urban density gradients and fractal dimensions from Chapter Four to the empirical data sets generated in Chapter Five.

To briefly reiterate the essential concepts in Chapter Four, urban analysis may be cast as fractal notions in which densities of urban development, or occupancy, at different distances from fixed points are modelled using power functions. The process first involves the definition of squared arrays, or matrices of grid cells, such as pixels, where urban development, or occupancy, is represented by an integer of 1, and absence of development is represented by 0. Next, the matrices of cells are partitioned into a series of concentric zones, which radiate from the central cell, or pixel. From here, the cumulative and incremental frequencies of occupation are calculated, along with the corresponding mean radius from the centre. The cumulative measure is simply the running total number of cells in each successive zone, which is subsequently referred by as the "count" values, N_i (where i refers to the individual zone). When normalised by the area of each zone, these counts form the individual densities p_i (refer to Chapter Four for clarification). Both methods of space-filling, counts and frequencies, are then used to both derive fractal dimensions as well as to generate profiles of cumulative population and incremental density that are comparable with conventional notions of urban gradients.

This chapter will continue with a review of the precise means of converting classified images into a form amenable to model estimation parameters based on fractal notions of spatial growth, as outlined in Chapter Four. These model assumptions are then operationalized by a series of purpose-written computer programs, many based on the

initial work by Batty and Kim (1992) and Batty and Xie (1994a; 1994b), but specially adapted for this thesis.

The largest part of the chapter will be devoted to a comprehensive evaluation and discussion of results generated from the empirical modelling of classified land use categories derived from the four test sites, Bristol, Norwich, Swindon, and Peterborough. Three sets of comparative analyses are performed and discussed with particular reference to their social, economic and planning implications. The first involves a look at the way in which the various land use categories of each urban area inter-relate and contribute to morphology and density patterns. In the second set of analyses, these morphology and density patterns are then compared between settlements, with the third set introducing the temporal component by comparing land use patterns between the 1981 and 1991 Population Censuses.

The chapter further assesses the contention that satellite imagery are an ideal data source for such extensive comparative analysis of urban morphologies. This is done by conducting a brief comparison with a close alternative, that of vectorized urban boundary data from the Department of Environment (DoE), which is now held alongside the Census by the *National Datasets Service* on the Cray Superserver CS6400 at Manchester Computing Centre. Fractal dimensions from both classified imagery and urban boundary data are examined with respect to the levels of accuracy, spatial resolutions, and temporal consistencies of each data set, as outlined in Chapter Four. It is anticipated that this comparison will add further support to the use of satellite technology as a supplier of superior raw data for the empirical testing of fractal-led density functions, both in terms of providing more detailed urban land use inventories, and establishing temporal consistency between repeated measurements.

6.2 Implementation

The classification strategy in Chapter Five demonstrated the conversion of satellite images from multivariate continuous data sets into discrete thematic coverages, where each pixel is assigned a single urban land use or land cover category. This means that each pixel is deemed either a member of a category (coded 1-black) or not (coded 0-white) (Figure 6.1). These binary surfaces of urban land use categories were the end result of Chapter Five, and they will now form the initial data input for this chapter.

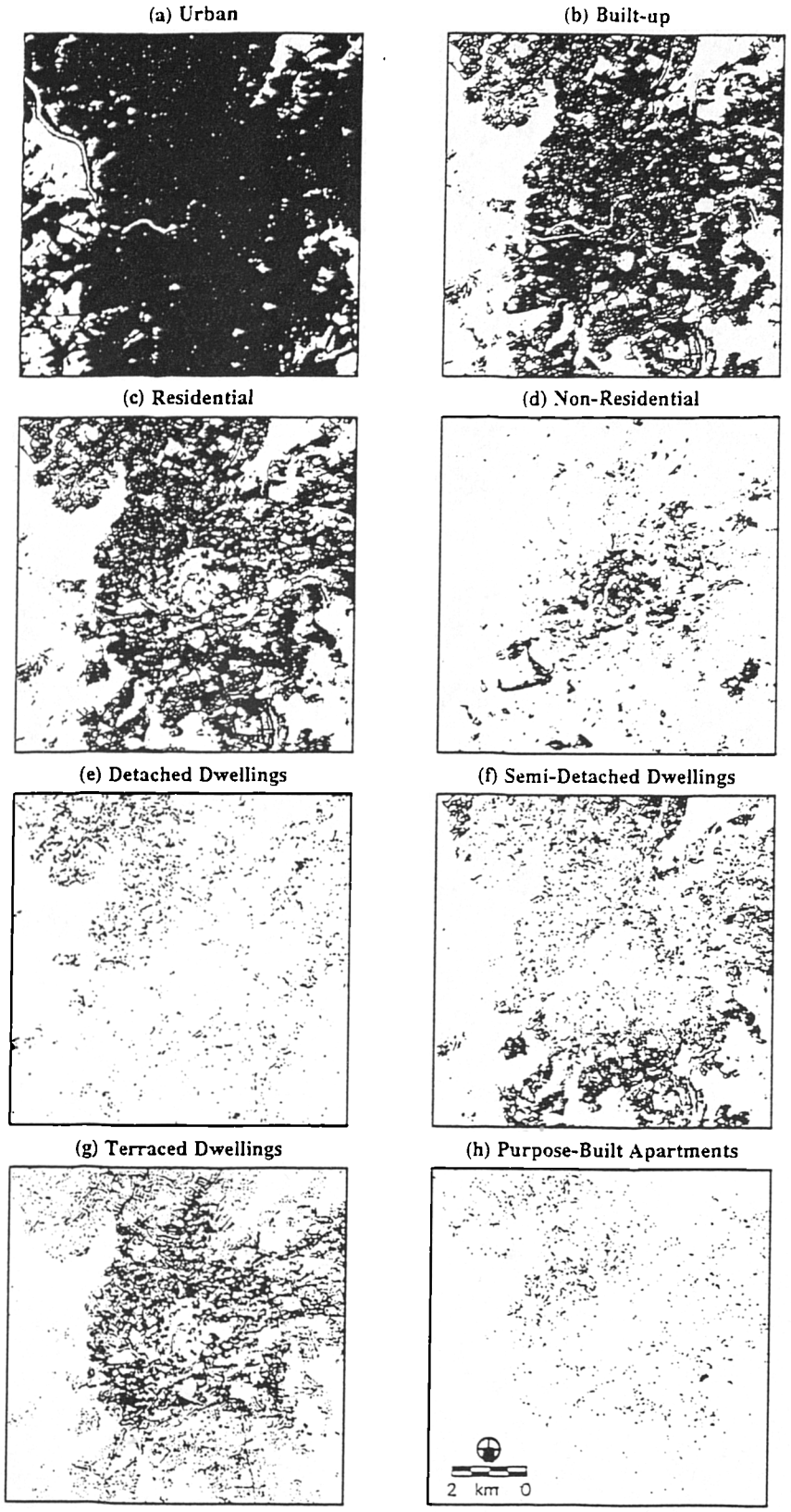

Figure 6.1 Binary Land Use Categories for Bristol 1991

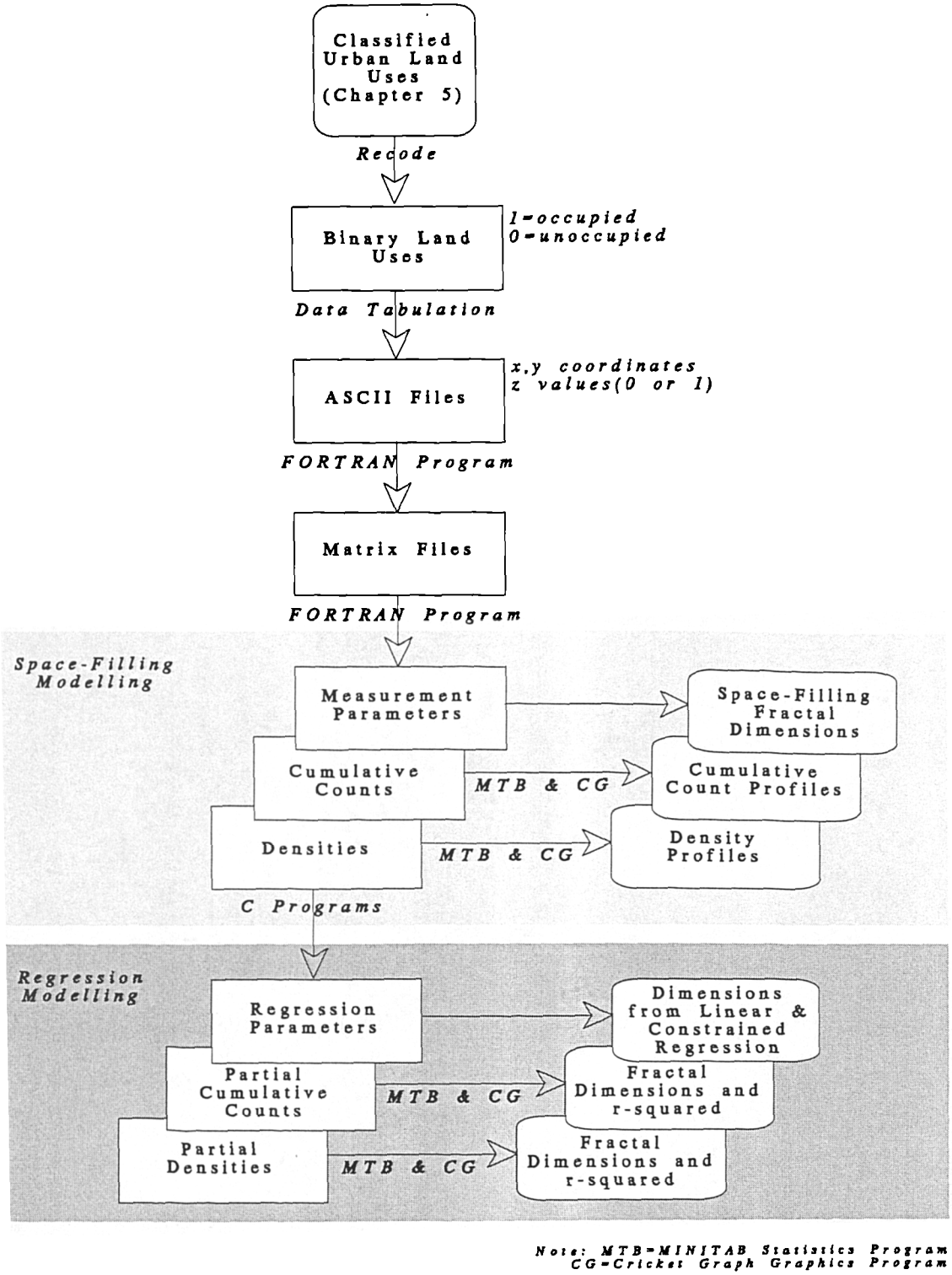

Figure 6.2 Flow of Operations for Urban Modelling Techniques

6.2.1 Software

Figure 6.2 is a diagrammatic representation of the flow of data analysis needed to convert binary urban land surfaces into measures of fractal dimensions and urban density profiles for all empirical data sets. The procedure begins with the conversion of classified satellite coverages into ordinary ASCII files containing three columns of integers. The first column contains values of either 1 or 0, representing each classified pixel, and the other two columns indicate the location of the pixel in the coverage in rows and columns. The data are then in a state which complies with input requirements of the main program that generates fractal dimensions based on space-filling properties, as well as fractal signatures, cumulative population counts, and density measures for each concentric zone radiating from the centre. This main program is a FORTRAN algorithm developed by Batty and Xie (1994b), with minor modifications to the coding made by the author to allow successful operations on Unix-based software. Graphic output of urban count and density profiles is produced by a combination of subroutines by the MINITAB statistics package and the CRICKET GRAPH drawing software. Finally, a series of regression programs written in the C language are applied to both the cumulative count and density profiles. This enables other fractal dimensions based on linear and constrained regression functions to be generated for both entire and partial data sets.

6.2.2 Data Set Parameters

As mentioned, all fractal estimations are based on squared lattices representing land use surfaces. This means that all classified urban surfaces are required to have the same number of pixels in both the x and the y directions, and to be centred on the historical core of the settlement. The maximum extent of each data set is determined by the maximum radius of the settlement in all except the Bristol case, where image availability problems confined data to the central parts of the city only. With these assumptions, Table 6.1 lists the results of the land use/cover classifications from Chapter Five, in terms of the number of developed points (pixels), along with the number of concentric zones radially generated from the central point for each data set.

A brief assessment of Table 6.1a can reveal coarse measures of urban growth by observing the increase in the number of points (classified pixels), and the increase in the number of concentric zones between 1981 and 1991.

Table 6.1 Data Set Parameters (Occupied Points and Concentric Zones)

a. Urban Definitions, 1981 and 1991

	Urban		Built-up		Residential		Non-Residential	
Data Set	Points	Zones	Points	Zones	Points	Zones	Points	Zones
Bristol 1981	171392	355	109718	321	92686	321	17131	258
Bristol 1991	176401	350	113594	321	95052	321	18542	268
Norwich 1981	70535	352	34739	316	28630	316	6109	246
Norwich 1991	86538	358	48673	319	41083	319	7688	247
Swindon 1981	79000	277	26663	237	20028	237	2658	146
Swindon 1991	87028	279	33701	239	25426	239	6258	218
Peterborough 1981	75820	243	20243	204	16361	204	3529	135
Peterborough 1991	81460	247	30100	218	23096	217	4367	144

b. Dwelling Type, 1991

	Detached		Semi-Detached		Terraced		Apartments	
Data Set	Points	Zones	Points	Zones	Points	Zones	Points	Zones
Bristol 1991	10377	320	33066	309	41722	286	4480	298
Norwich 1991	13910	316	9161	316	7440	243	1712	262
Swindon 1991	6570	214	8831	227	5731	221	381	184
Peterborough 1991	7010	204	7449	213	4438	205	327	122

All settlements exhibit some form of growth during this time period. As regards dwelling type in Table 6.1b, the number of points is a reflection of area estimates of relative proportions within each settlement, and the number of zones represent the maximum spatial extent of each dwelling type. Here, apart from Norwich, semi-detached is the most prevalent category, with terraced housing the most centralized. Although these measures are somewhat simplistic, they do indicate general patterns of land use change that are consistent with contemporary observed patterns in urban systems. However, this chapter is more concerned with relating urban growth to specific changes in urban form and density from the city centre. For this, models

based on fractal geometry assuming basic space-filling properties will be applied to all empirical examples.

The next four sections will document each of the various models of fractal estimations and urban profiles from empirical data sets classified from satellite imagery. Again, these data sets are categorised as urban, built-up, residential and non-residential for four settlements (Bristol, Norwich, Swindon, and Peterborough), at two time points (1981 and 1991). The 1991 data sets also include a further four land uses: detached, semi-detached, terraced, and purpose-built apartments.

6.3 Space-Filling Models

The first estimations of density and dimension are those based on the idea of measuring the occupancy, or space-filling properties, of urban development. The fractal dimensions D, which are generated should fall between the established range of 1 and 2, where each land use fills more than a line across space (D = 1) but less than the complete plane (D = 2). Table 6.2 lists the fractal dimensions for all classified remotely-sensed data sets. The COUNT measures refer to the estimation process generated by,

$$D_{\text{count}} = \frac{\ln \{N(R')/4\}}{\ln R'} \qquad (4.9)$$

where $N(R')$ is the total number of occupied cells at mean distance R' from the central point of the settlement; and DENSITY refers,

$$D_{\text{density}} = 2 + \frac{\ln p(R')}{\ln R'} \qquad (4.11).$$

where $p(R')$ is the proportion of occupied cells, again at mean distance R'. Both of the above equations, and indeed all others in this chapter were fully developed and explained in Chapter Four.

Table 6.2 Space-Filling Dimensions Based on Occupancy

a. Urban Definitions, 1981 and 1991 (**Count**)

	Land Use							
	Urban		Built-up		Residential		Non-Residential	
Settlement	1981	1991	1981	1991	1981	1991	1981	1991
Bristol	1.804	1.817	1.776	1.781	1.745	1.750	1.566	1.555
Norwich	1.757	1.780	1.723	1.766	1.688	1.735	1.541	1.554
Swindon	1.750	1.759	1.628	1.702	1.572	1.610	1.446	1.440
Peterborough	1.845	1.852	1.685	1.731	1.633	1.678	1.565	1.534

b. Urban Definitions, 1981 and 1991 (**Density**)

	Land Use							
	Urban		Built-up		Residential		Non-Residential	
Settlement	1981	1991	1981	1991	1981	1991	1981	1991
Bristol	1.823	1.837	1.790	1.797	1.756	1.761	1.551	1.540
Norwich	1.770	1.796	1.731	1.780	1.692	1.743	1.522	1.535
Swindon	1.761	1.771	1.625	1.709	1.558	1.603	1.412	1.409
Peterborough	1.869	1.876	1.685	1.742	1.630	1.679	1.542	1.509

c. Dwelling Type, 1991 (**Count** and **Density**)

	Land Use							
	Detached		Semi-Detached		Terraced		Apartments	
Settlement	Count	Density	Count	Density	Count	Density	Count	Density
Bristol	1.424	1.394	1.563	1.551	1.680	1.682	1.297	1.250
Norwich	1.538	1.521	1.459	1.431	1.526	1.504	1.232	1.171
Swindon	1.498	1.471	1.401	1.365	1.379	1.338	0.925	0.819
Peterborough	1.501	1.476	1.419	1.384	1.429	1.392	0.909	0.796

An initial survey of the results in Table 6,2 shows that all fractal dimensions, apart from those generated from the apartments category, fall between the range $1.338 < D < 1.837$, with a mean value over all land uses, the two time points, and the two equations as $D = 1.620$. These estimates are very much in line with theories of the fractal city that suggest settlements have fractal dimensions between 1.60 and 1.71, and are exemplified by randomly constrained diffusion processes such as Diffusion Limited Aggregation (see Chapter Four; Vicsek, 1989; Batty and Longley, 1994). This seems to suggest that fractal dimensions generated from remotely-sensed data may be regarded with a high degree of reliability which is consistent with urban fractal theory. The rather low dimensions associated with the apartments category, especially for Swindon and Peterborough may be largely due to the sparseness and highly dispersed locations of this land use within the urban areas.

Another consistent pattern to emerge from Table 6.2 is the highly stable order in the fractal dimensions derived from the four main urban land use categories, both for 1981 and 1991. All settlements exhibit descending values in the order of urban > built-up > residential > non-residential. The logic behind this pattern undoubtedly reflects the hierarchical nature of the classification strategy used to generate these surfaces, where residential and non-residential are subsets of built-up which is, in turn, a subset of urban. This hierarchical structure implies that there should be an obvious relation between complementary categories. However, although it may be possible to derive one fractal dimension from the other, it is not clear how this might be done in terms of mean distances R'. This is undoubtedly a matter for further research.

The most striking temporal comparisons between 1981 and 1991 reveal that urban, built-up and residential dimensions from both count and density increase, while those associated with non-residential (except Norwich's density measure) decrease. These patterns are consistent with observed growth in population of settlements over the 1980s particularly in the southern half of England. At the same time, manufacturing and commercial activities have either rationalised, disappeared, or decentralised to the periphery. The Norwich exception to this pattern seems to suggest that either growth in non-residential activities actually took place in this city in the 1980s or that some non-residential activities such as manufacturing were never a major land use. However, it must be stressed that very little further information on spatial growth or contraction can be inferred from such a broad category as non-residential or indeed

from the rather restrictive time period over which these profiles are compared.

In terms of dwelling types, there does not seem to be a clear pattern of rank order, apart from the apartments category which exhibits the lowest dimensions in both types of fractal estimates for all settlements. This variability between land uses is most likely a reflection of the different built forms of each of the settlements. Built forms can be contrasted between those of an expanded town (Peterborough), a railway town (Swindon), and a Georgian city (Bristol). Notwithstanding this variability in dwelling type densities, the space-filling analysis suggests that all are now subject to the same trends in urban growth, whether by peripheral expansion or by infill. This urban growth in all four settlements seems to defy the UK national trend. The reasons for this variation may stem from their southerly location in England, and their increase in service-based activities throughout the 1980s.

Furthermore, the three main dwelling type categories appear to fluctuate in relative magnitudes between settlements, seemingly according to size. Although Bristol is by far the largest of the settlements analysed here, its data sets are restricted to the central parts of the city where urban development is at its densest. As a result, fractal dimensions are highest for each land use. The dwelling type with the highest fractal dimension in Bristol is therefore not surprisingly the terraced housing category, reflecting its established central clustering location. However, in the Norwich case, the detached housing category exhibits the highest fractal dimensions, supported both by a high number of occupied pixels and also a high degree of irregularity in its spatial form. The other two settlements are very similar in population size, and Peterborough's dimensions are consistently slightly higher than Swindon's in all land coverages except apartments.

6.4 Linear Regression Modelling

The two types of fractal estimates, COUNT and DENSITY, previously presented in the space-filling models, do not account for the variance in each land use pattern. As such, it is impossible to speculate upon the shapes of these patterns with respect to density gradients or profiles.

Table 6.3 Dimensions From Regression

a. Urban Definitions, 1981 and 1991 (**Count** and **Density**)

Urban						
	1981			1991		
Settlement	D	r^2_{count}	$r^2_{density}$	D	r^2_{count}	$r^2_{density}$
Bristol	1.966	0.990	0.030	1.861	0.989	0.335
Norwich	1.681	0.996	0.508	1.660	0.969	0.570
Swindon	1.833	0.993	0.545	1.953	0.984	0.034
Peterborough	1.725	0.979	0.539	1.754	0.973	0.419
Built-up						
	1981			1991		
Settlement	D	r^2_{count}	$r^2_{density}$	D	r^2_{count}	$r^2_{density}$
Bristol	2.496	0.971	0.573	2.262	0.966	0.274
Norwich	1.492	0.952	0.697	1.508	0.953	0.682
Swindon	1.845	0.988	0.370	1.520	0.984	0.861
Peterborough	1.744	0.971	0.419	1.713	0.976	0.536
Residential						
	1981			1991		
Settlement	D	r^2_{count}	$r^2_{density}$	D	r^2_{count}	$r^2_{density}$
Bristol	2.438	0.975	0.561	2.199	0.969	0.204
Norwich	1.429	0.952	0.759	1.456	0.953	0.737
Swindon	1.784	0.992	0.637	1.528	0.994	0.941
Peterborough	1.660	0.976	0.631	1.625	0.981	0.732
Non-Residential						
	1981			1991		
Settlement	D	r^2_{count}	$r^2_{density}$	D	r^2_{count}	$r^2_{density}$
Bristol	1.799	0.968	0.274	2.098	0.955	0.044
Norwich	1.112	0.862	0.798	1.188	0.889	0.790
Swindon	1.283	0.950	0.856	1.401	0.976	0.879
Peterborough	1.156	0.947	0.905	1.159	0.937	0.886

Table 6.3 Dimensions From Regression (cont.)

b. Dwelling Type, 1991 (**Count** and **Density**)

	Detached			Semi-Detached		
Settlement	D	r^2_{count}	$r^2_{density}$	D	r^2_{count}	$r^2_{density}$
Bristol	1.712	0.971	0.483	2.468	0.967	0.515
Norwich	1.423	0.953	0.770	1.408	0.954	0.787
Swindon	1.800	0.967	0.266	1.502	0.991	0.926
Peterborough	1.498	0.968	0.774	1.558	0.989	0.883
	Terraced			Apartments		
Settlement	D	r^2_{count}	$r^2_{density}$	D	r^2_{count}	$r^2_{density}$
Bristol	1.658	0.988	0.779	1.919	0.961	0.042
Norwich	1.661	0.919	0.320	1.176	0.950	0.903
Swindon	1.326	0.991	0.967	1.261	0.989	0.970
Peterborough	1.891	0.884	0.025	1.311	0.936	0.802

To circumvent the problem of variance, the main line of analysis will now be focussed on fitting regression lines to the profiles generated from each surface in terms of counting land use cells in each concentric zone from the urban centre, given as N_i, along with their normalisation to densities expressed as p_i. These data are then used to estimate the parameters in equations,

$$N(R) = G\ R^D \tag{4.5}$$

$$p(R) = K\ R^{-\alpha} \tag{4.2}$$

respectively from their natural logarithmic transforms in equations,

$$N_i = \ln G - D \ln R_i \tag{4.13}$$

$$p_i = \ln K - \alpha \ln R_i \tag{4.12}$$

from Chapter Four.

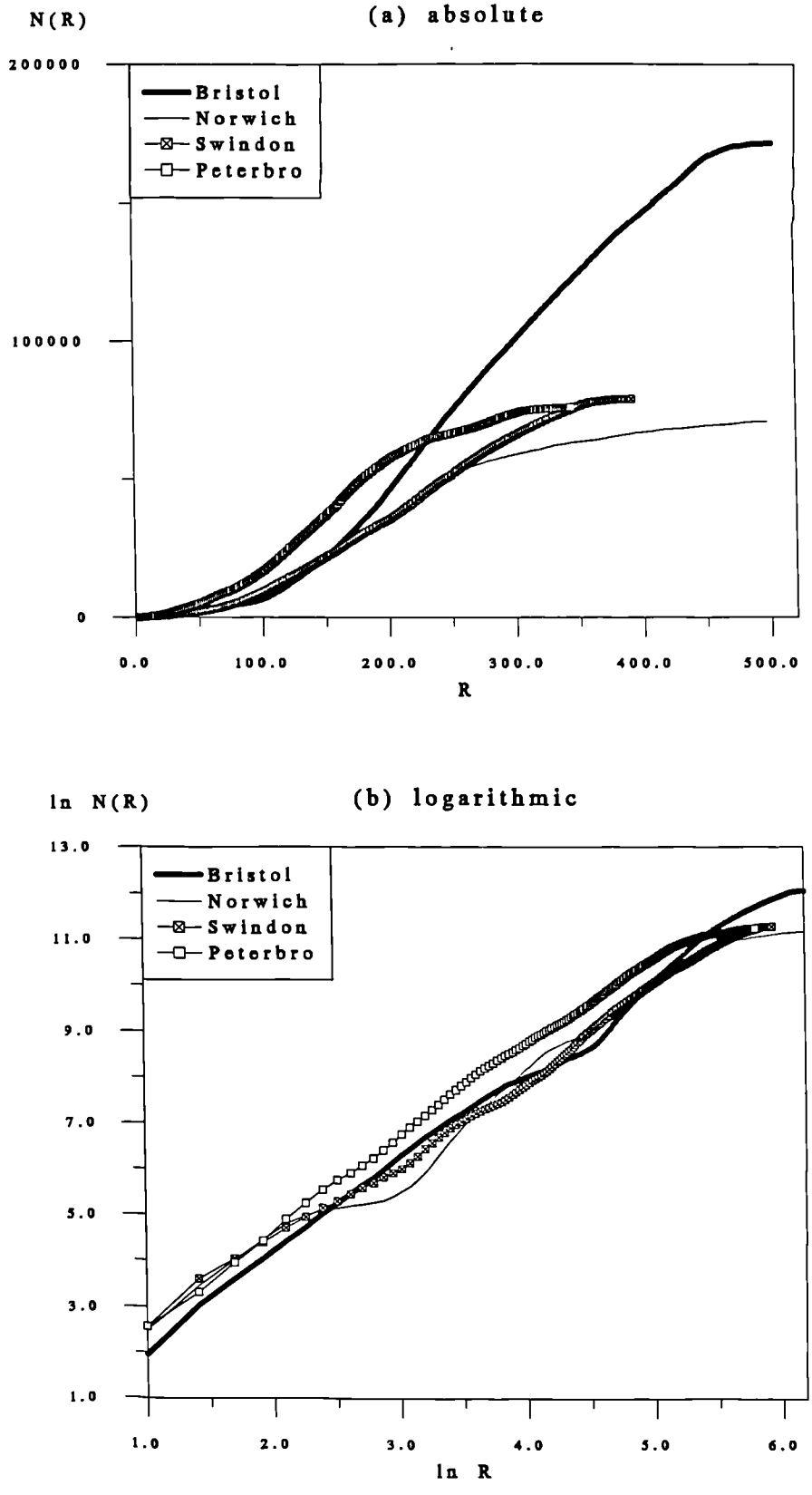

Figure 6.3 The 1981 Cumulative Count Profiles of the Urban Category

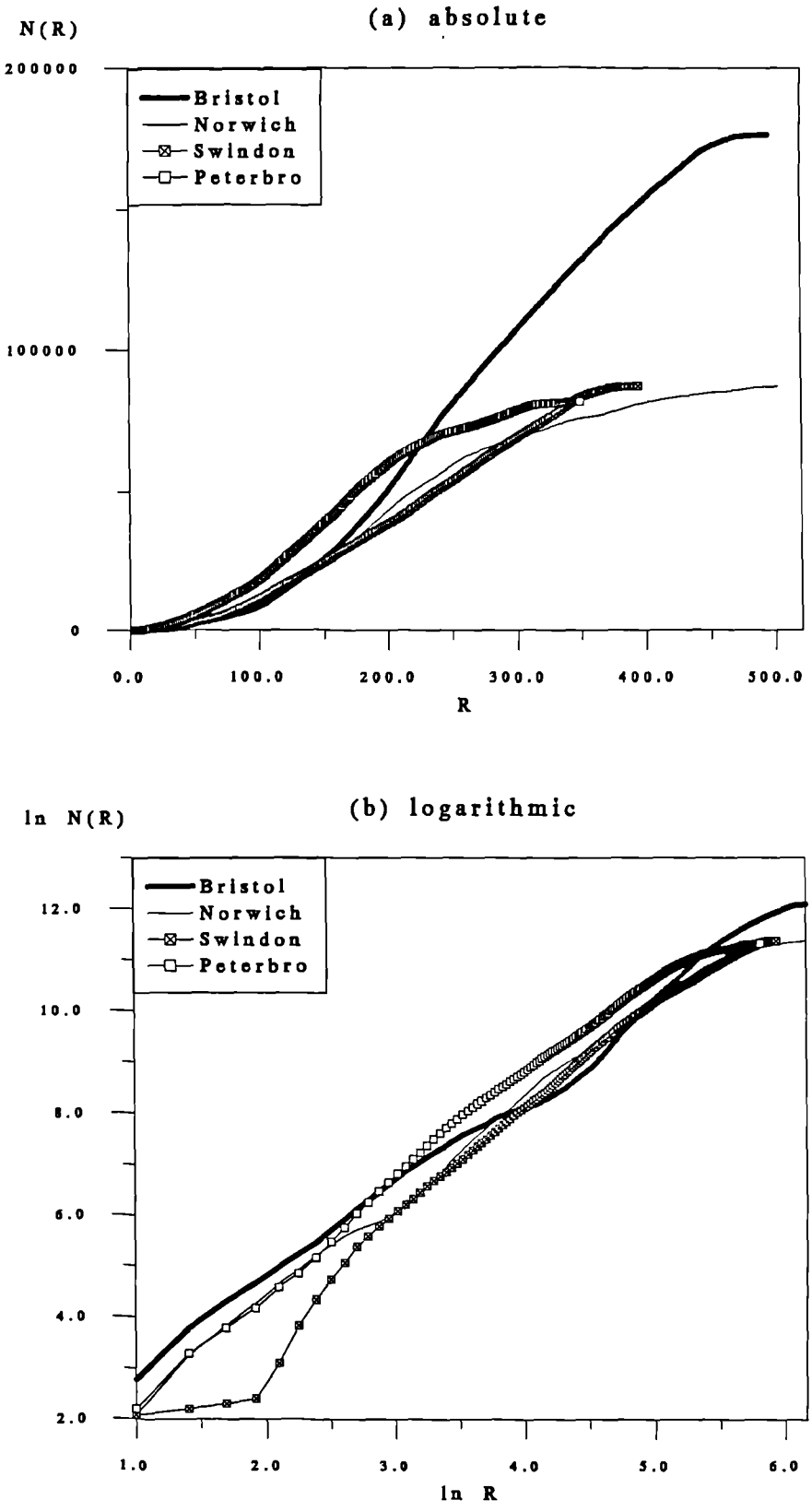

Figure 6.4 The 1991 Cumulative Count Profiles of the Urban Category

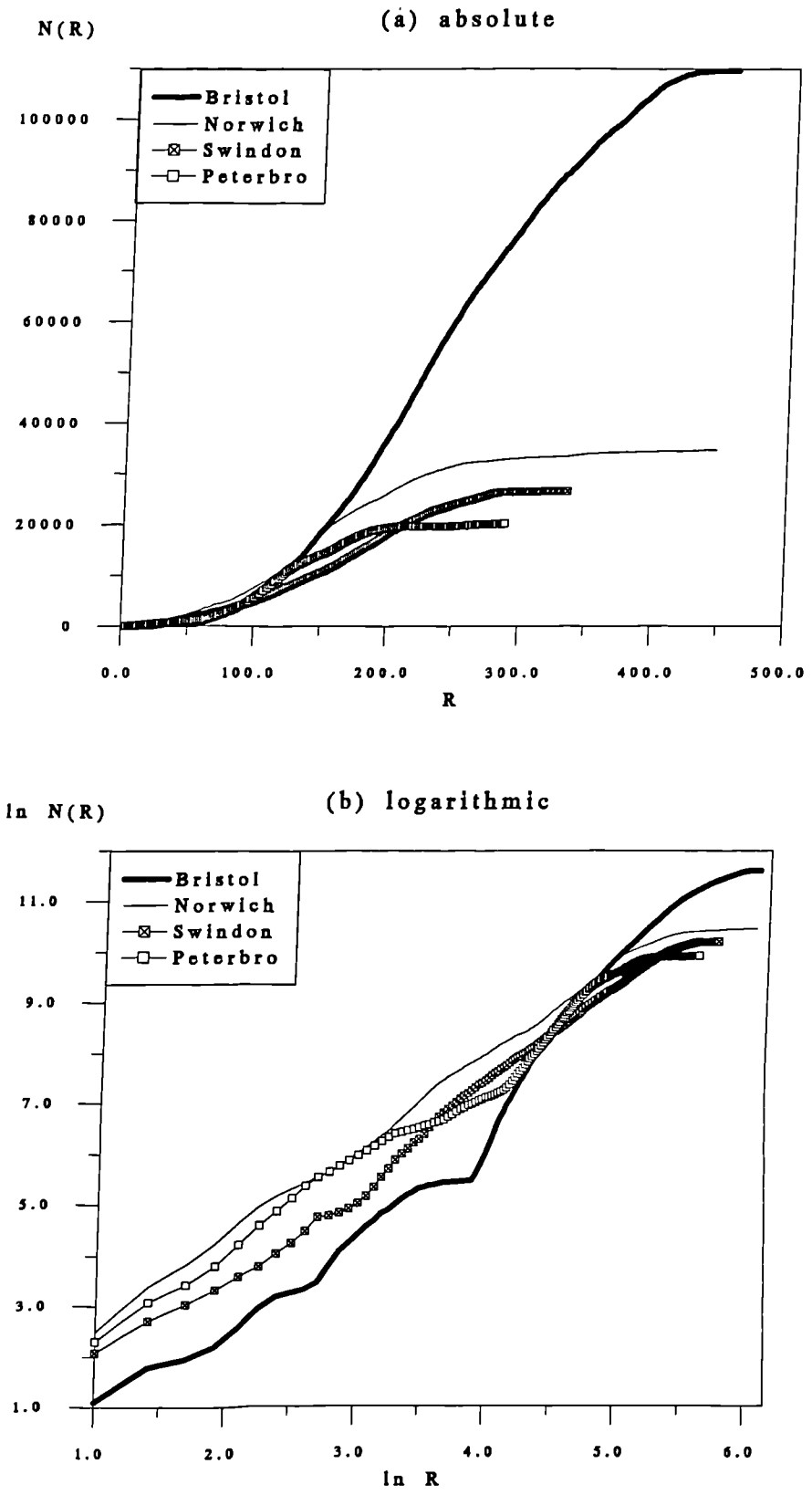

Figure 6.5 The 1981 Cumulative Count Profiles of the Built-up Category

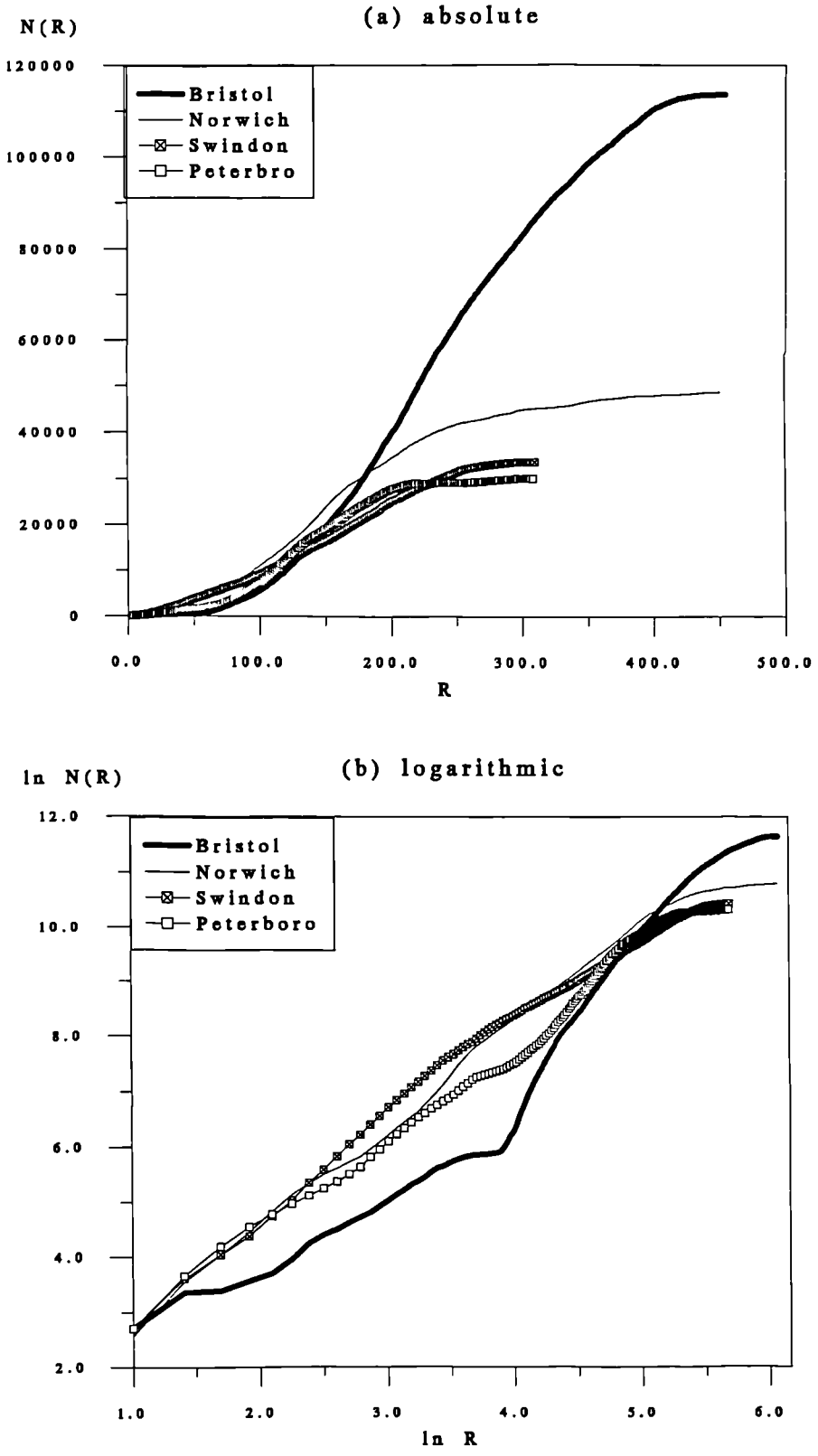

Figure 6.6 The 1991 Cumulative Count Profiles of the Built-up Category

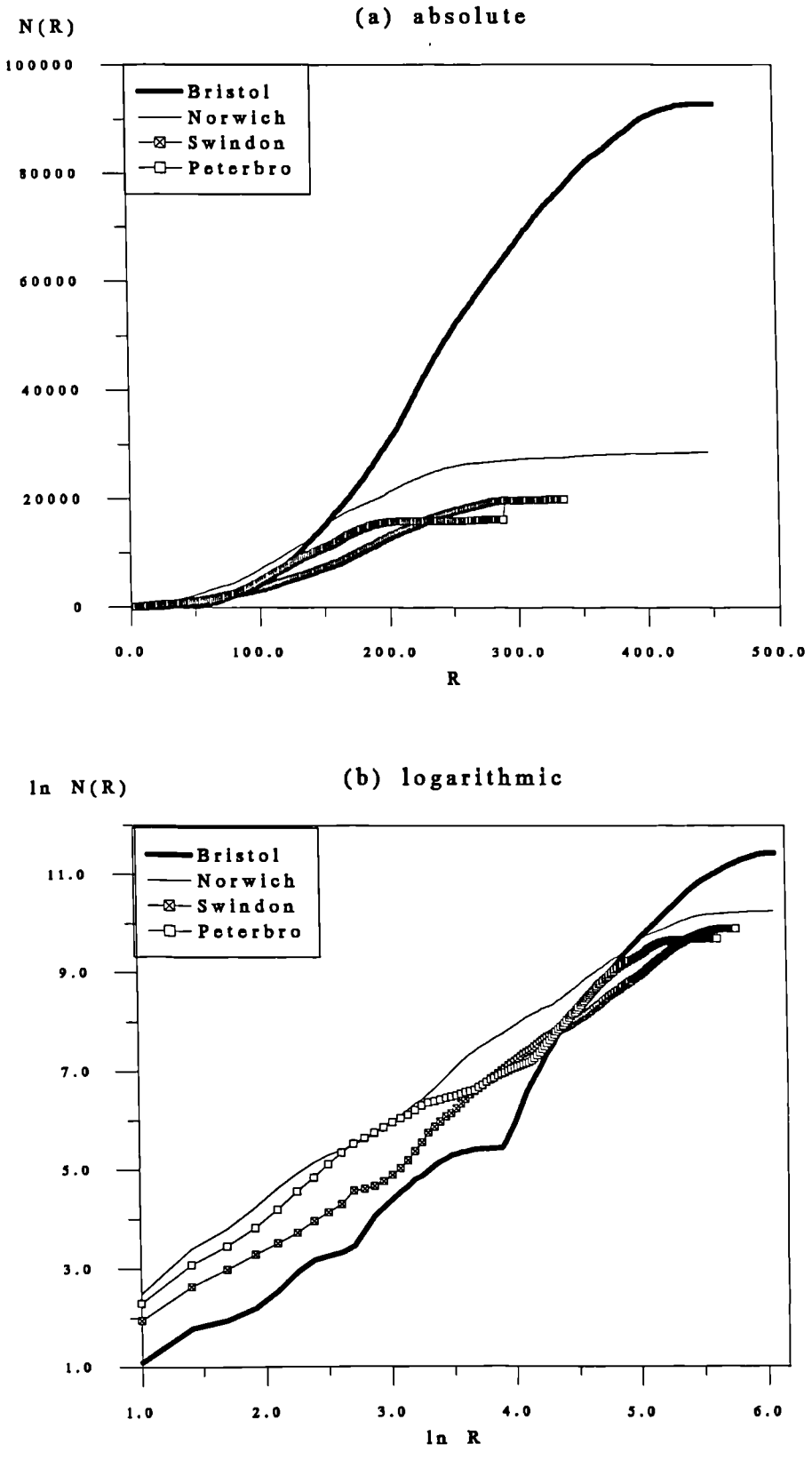

Figure 6.7 The 1981 Cumulative Count Profiles of the Residential Category

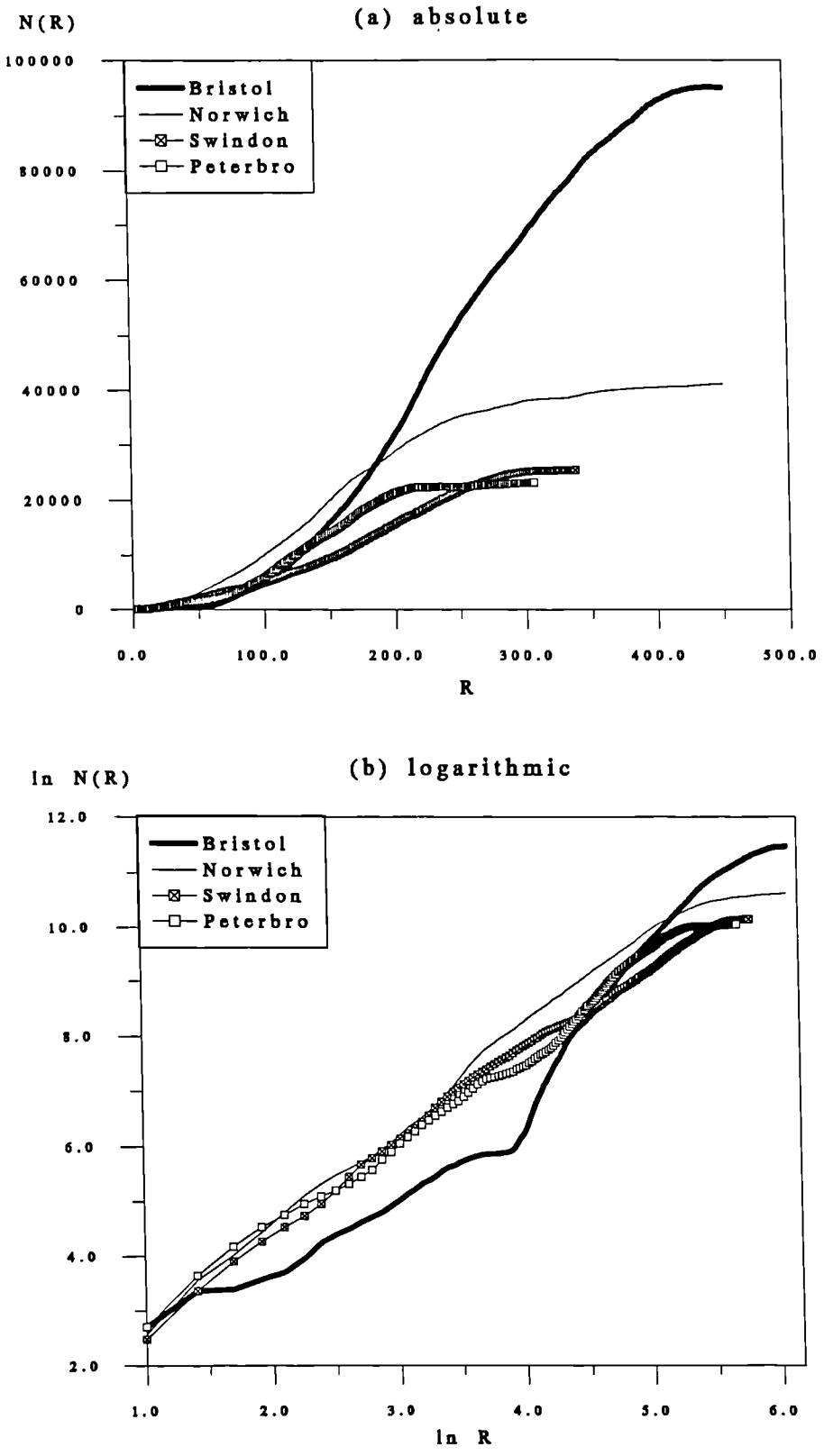

Figure 6.8 The 1991 Cumulative Count Profiles of the Residential Category

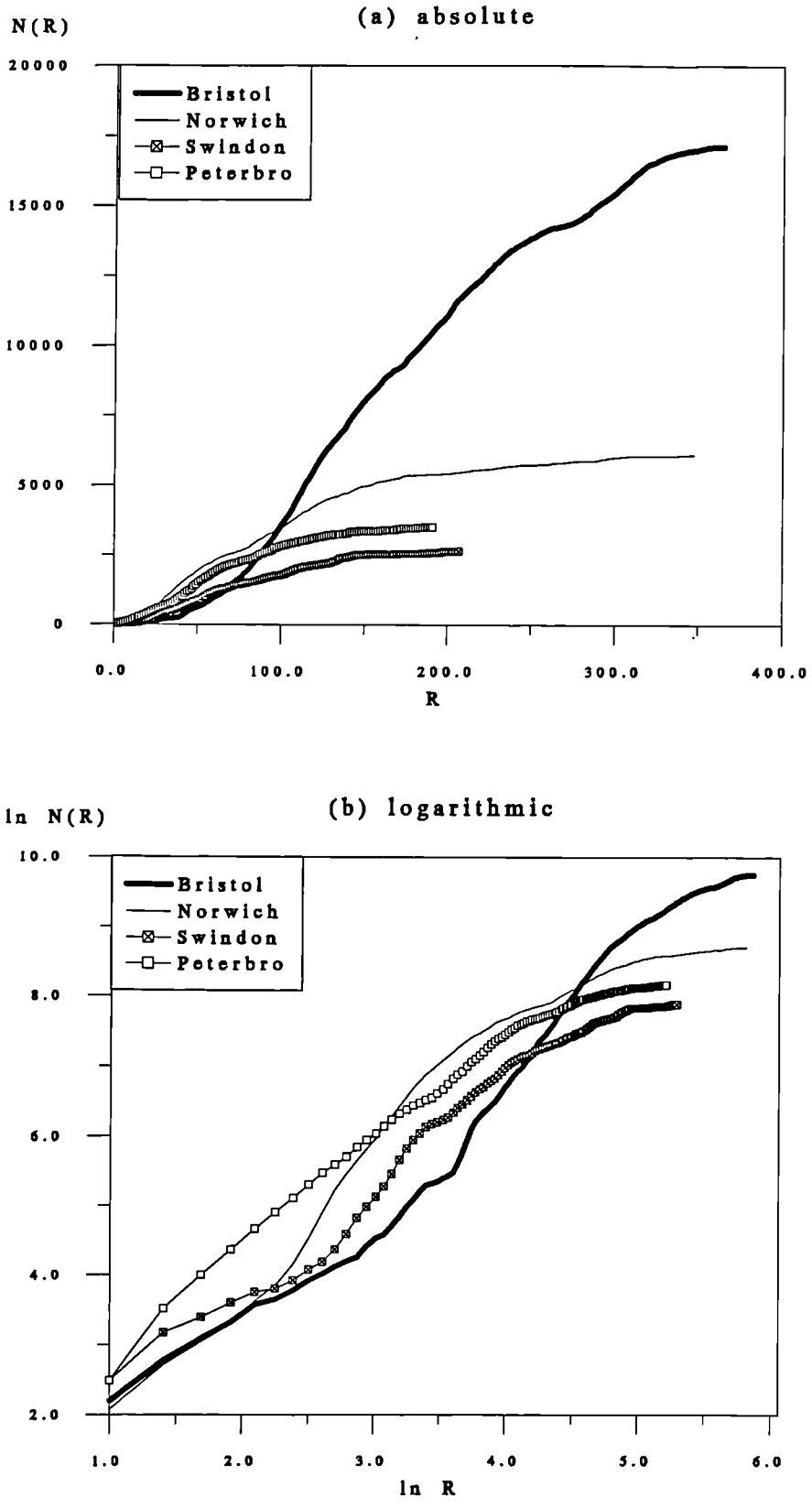

Figure 6.9 The 1981 Cumulative Count Profiles of the Non-Residential Category

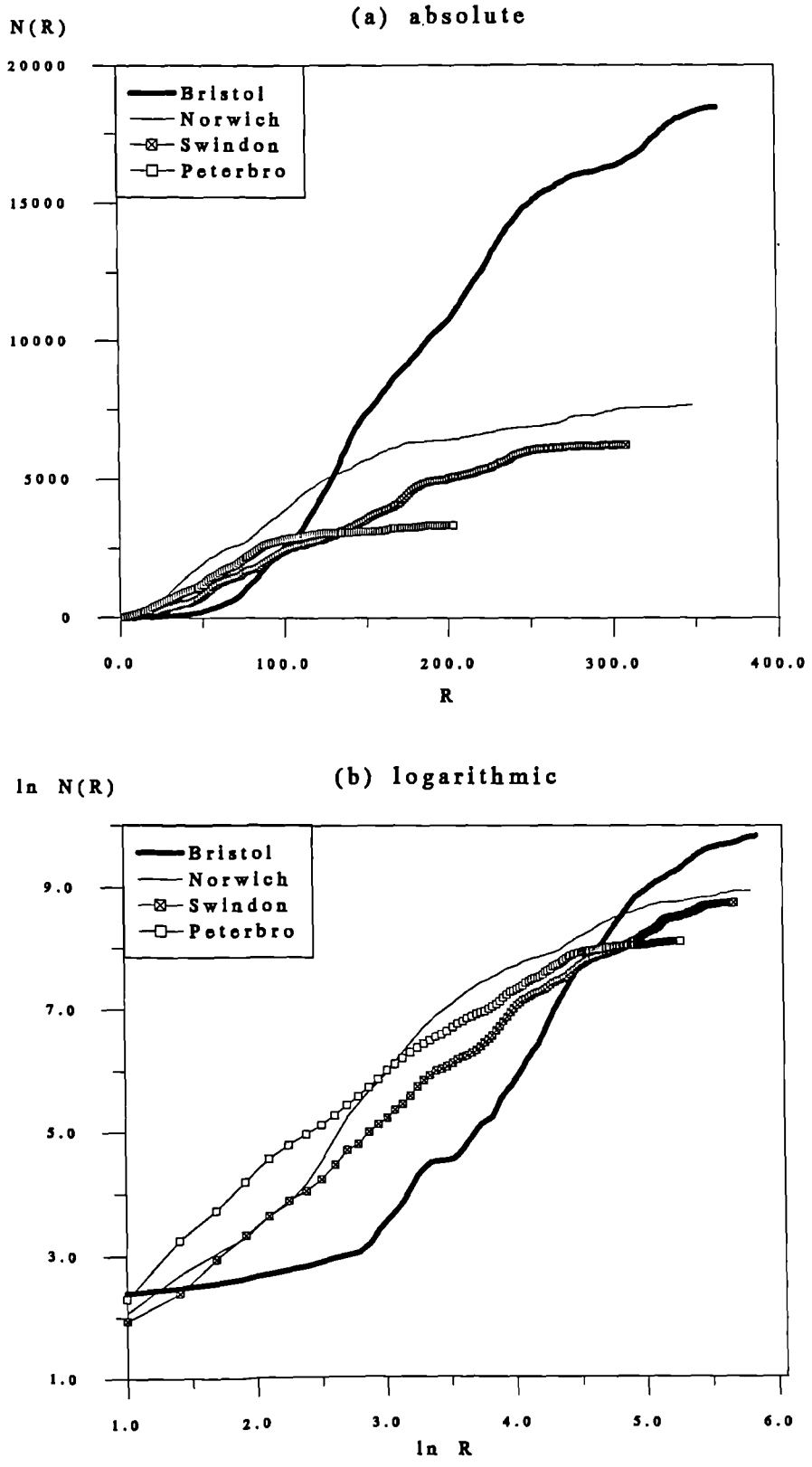

Figure 6.10 The 1991 Cumulative Count Profiles of the Non-Residential Category

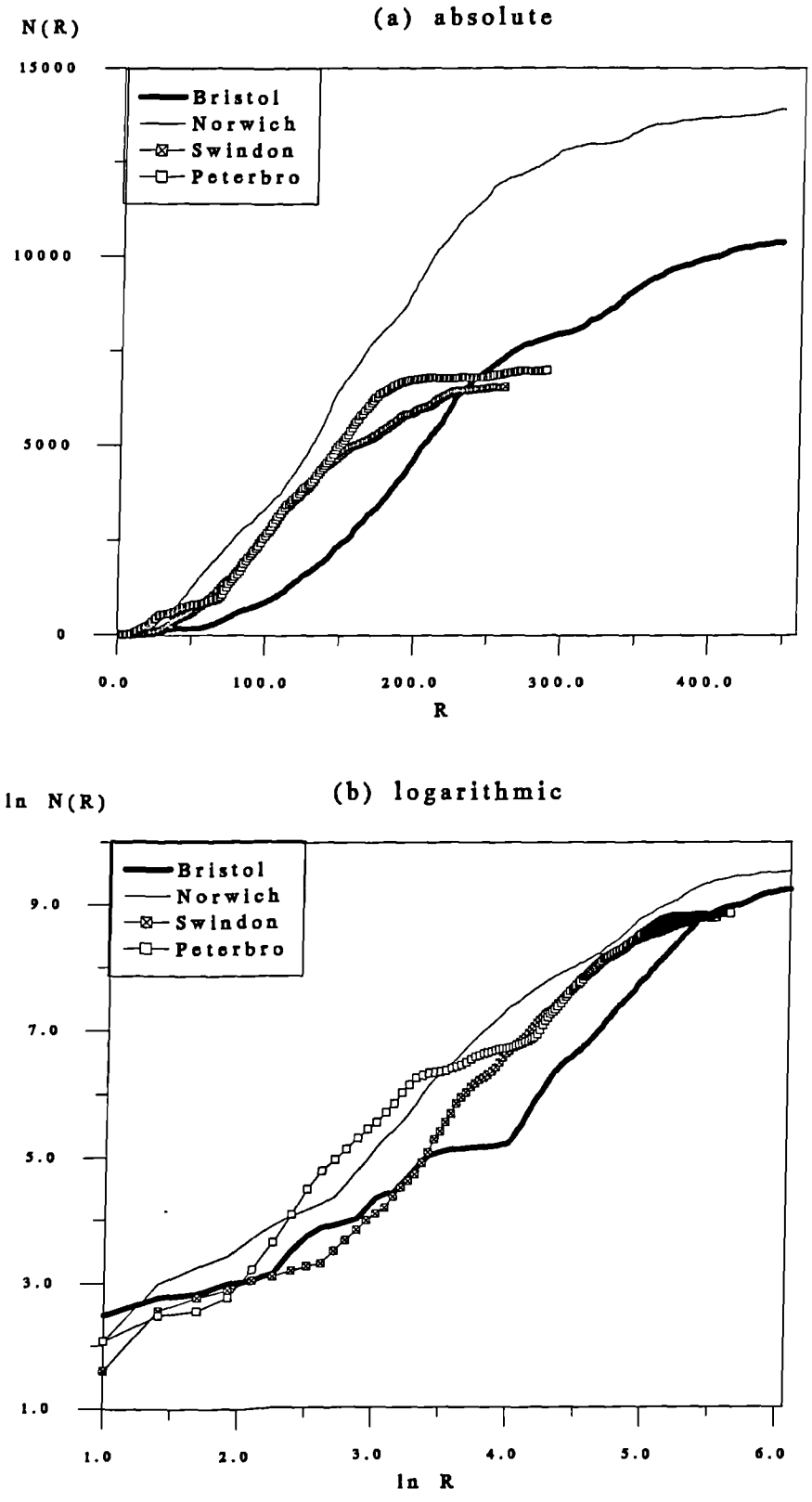

Figure 6.11 The 1991 Cumulative Count Profiles of the Detached Category

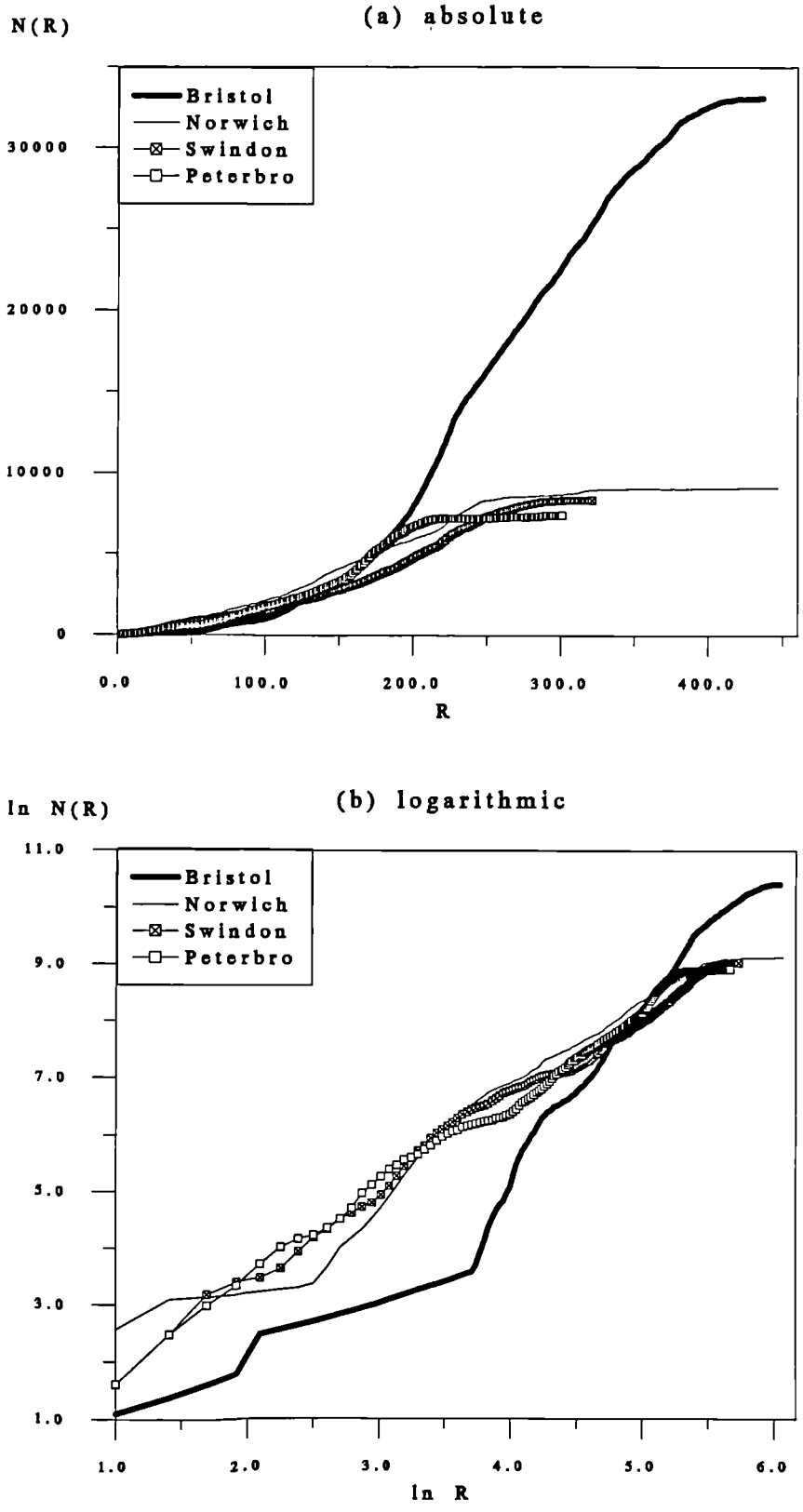

Figure 6.12 The 1991 Cumulative Count Profiles of the Semi-Detached Category

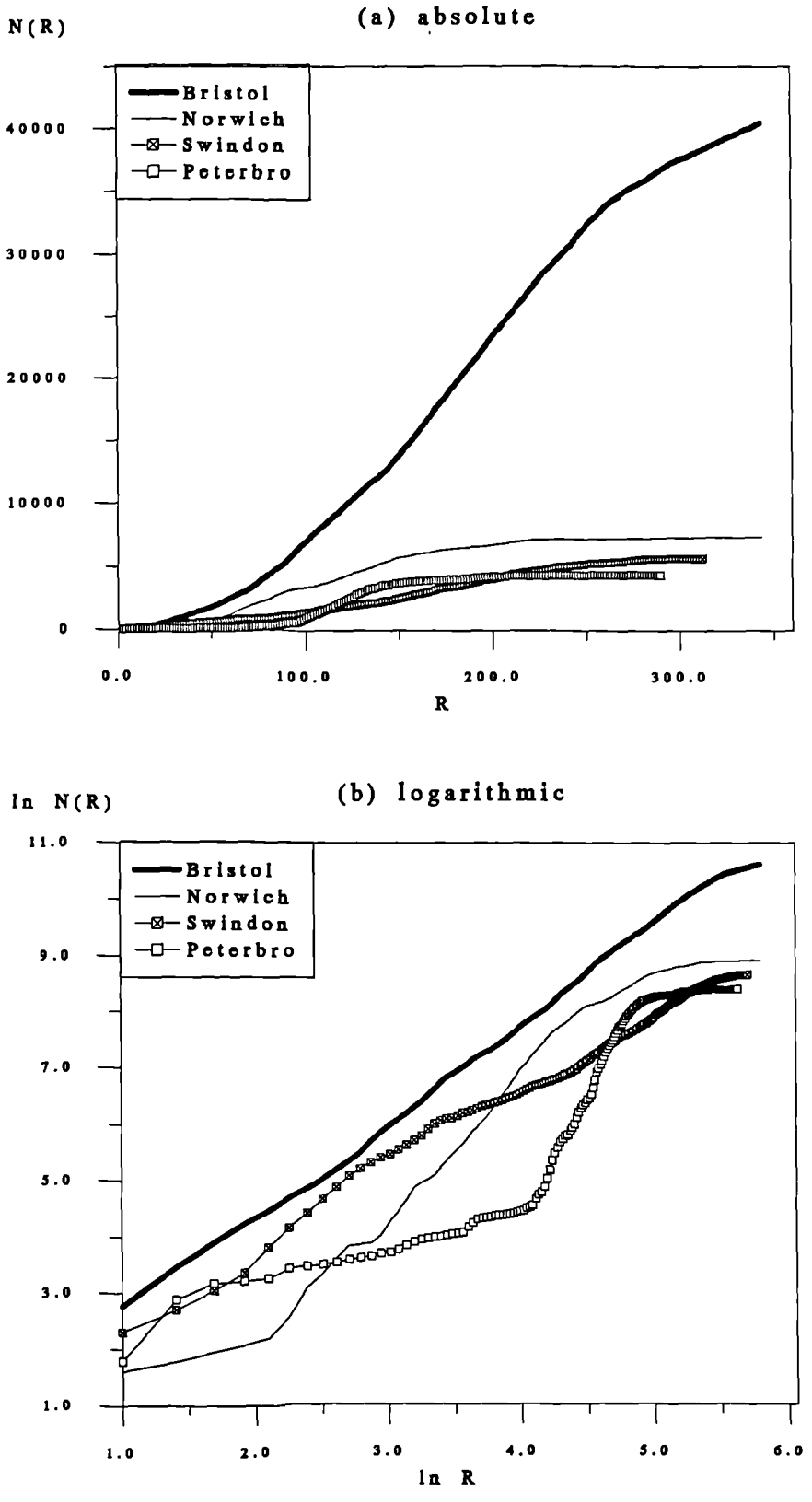

Figure 6.13 The 1991 Cumulative Count Profiles of the Terraced Category

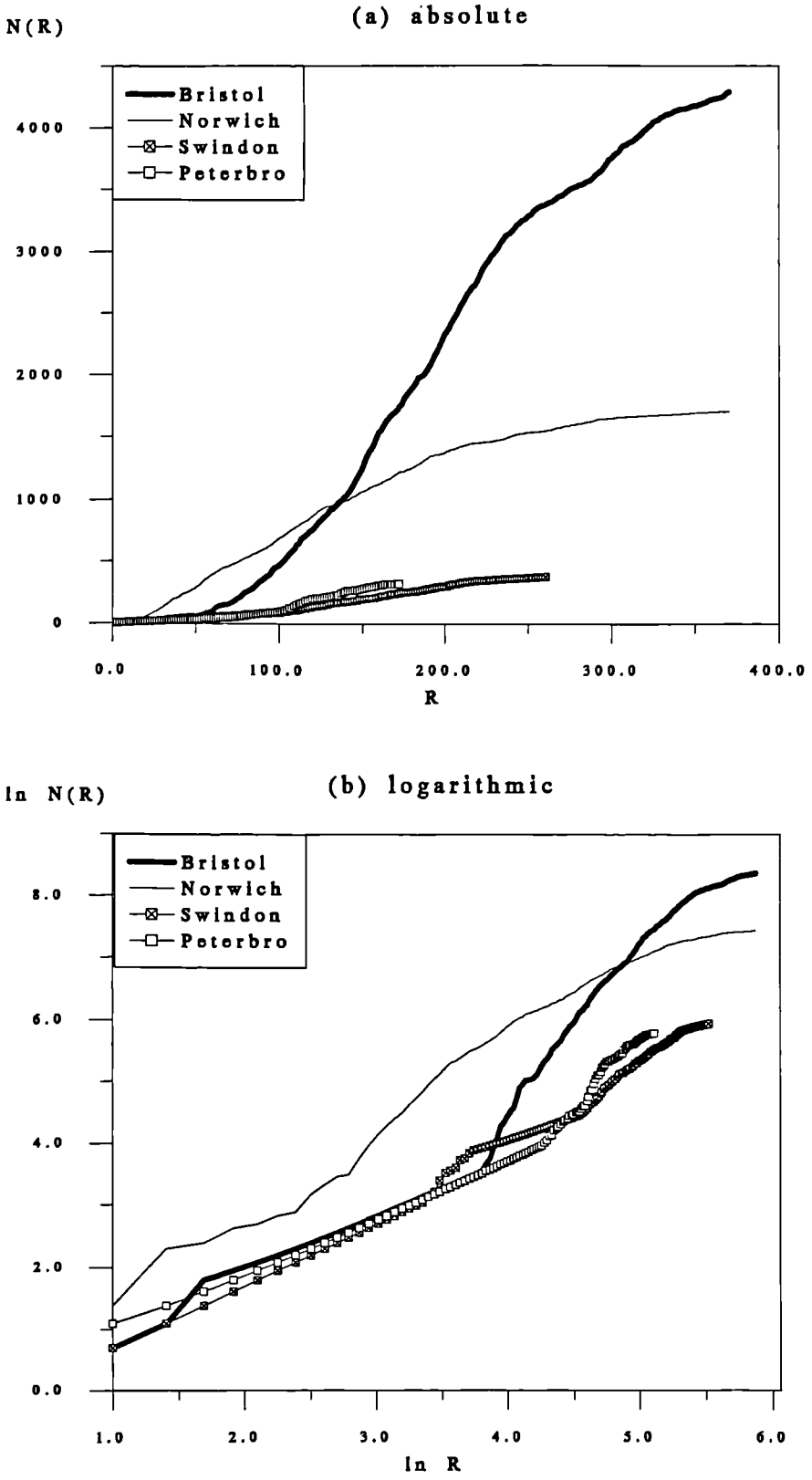

Figure 6.14 The 1991 Cumulative Count Profiles of the Apartments Category

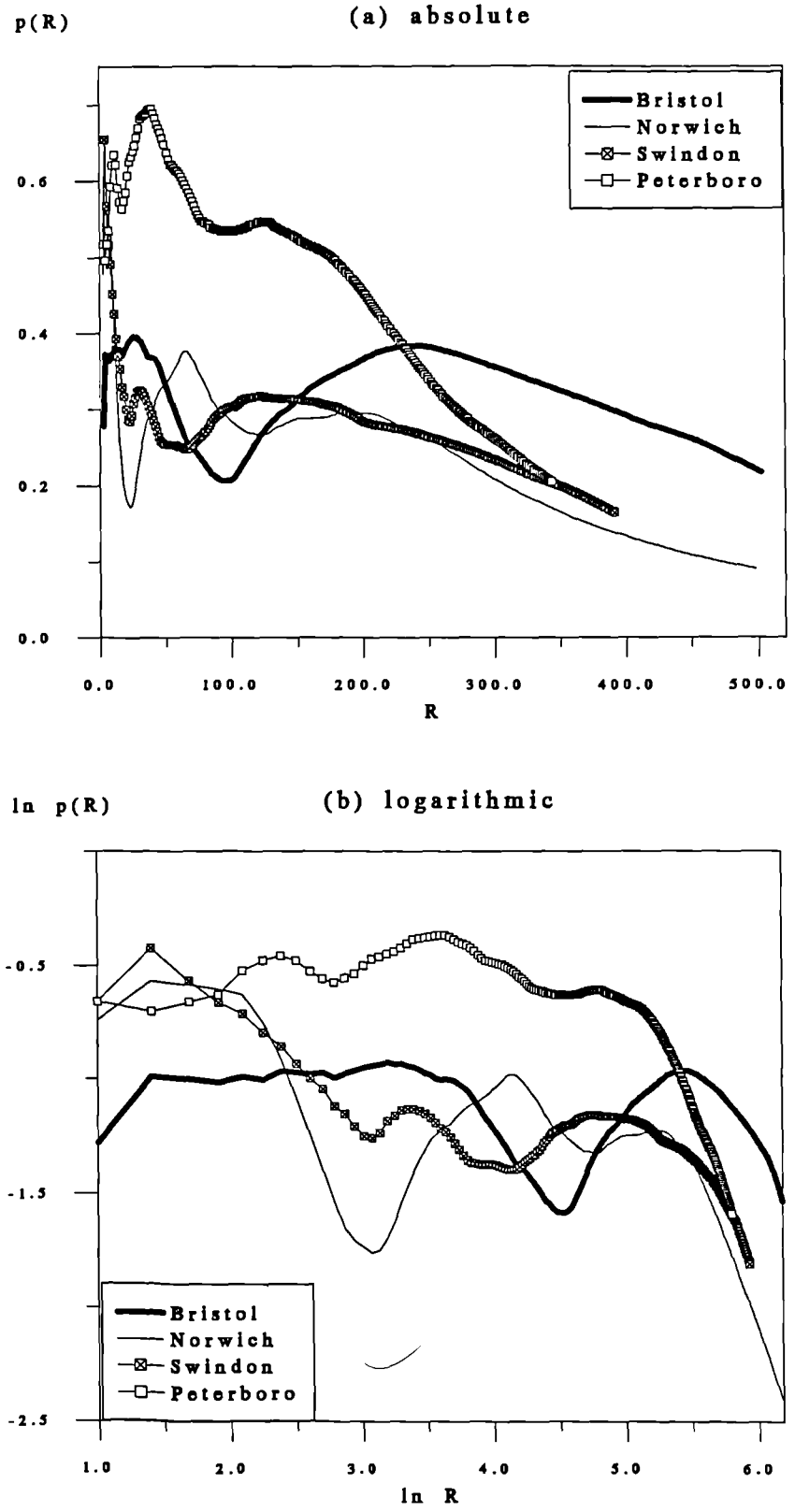

Figure 6.15 The 1981 Density Profiles of the Urban Category

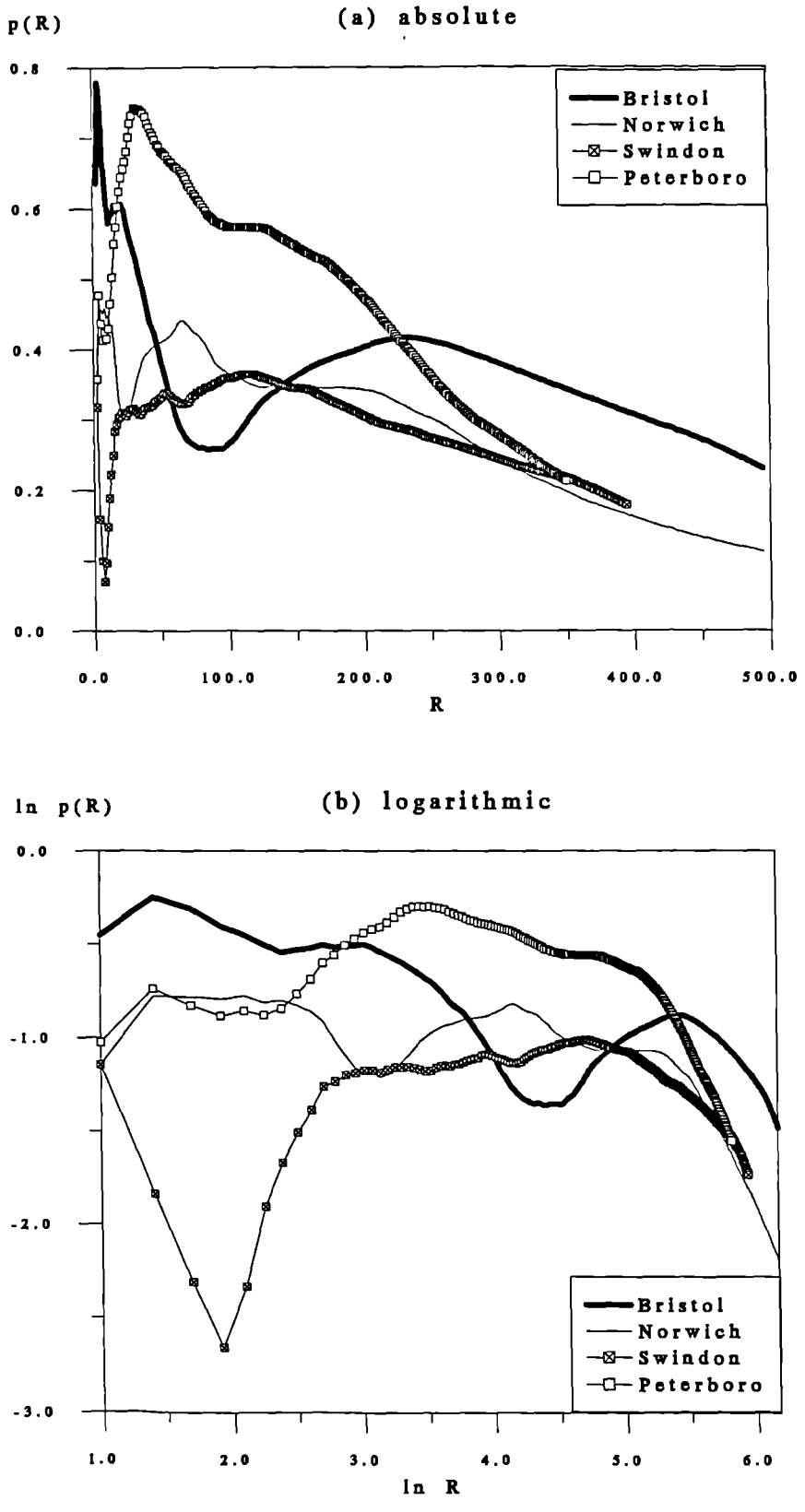

Figure 6.16 The 1991 Density Profiles of the Urban Category

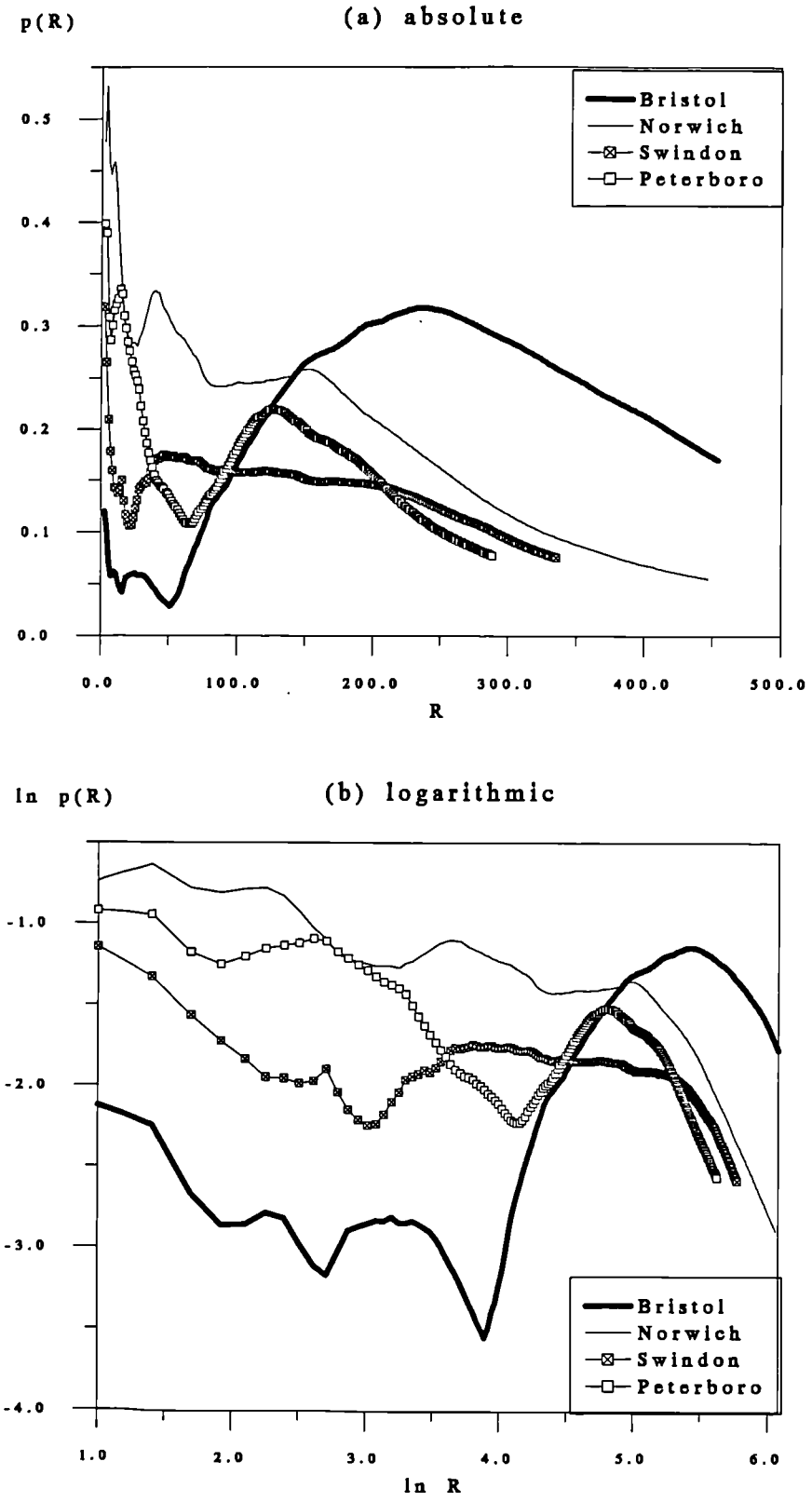

Figure 6.17 The 1981 Density Profiles of the Built-up Category

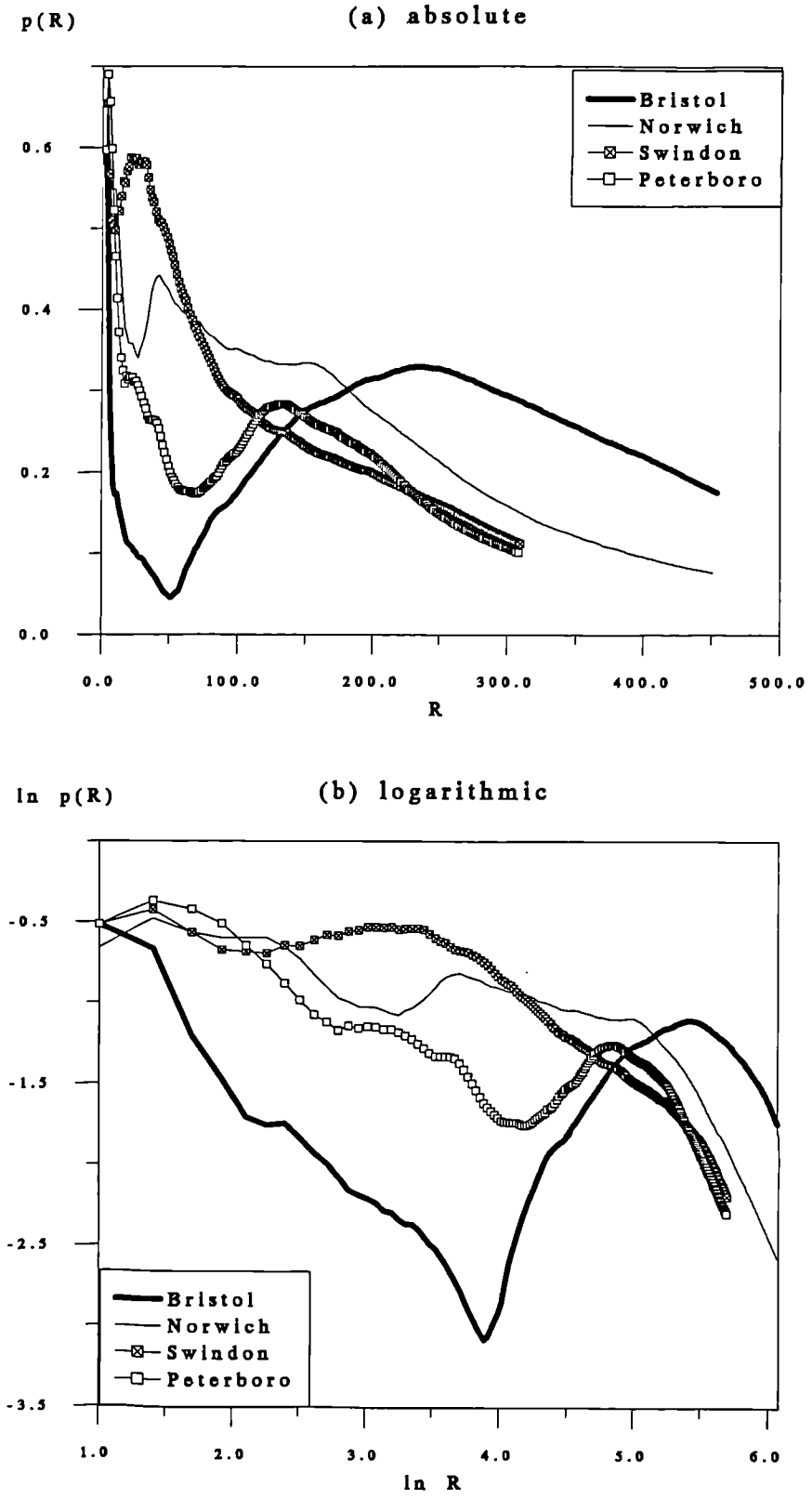

Figure 6.18 The 1991 Density Profiles of the Built-up Category

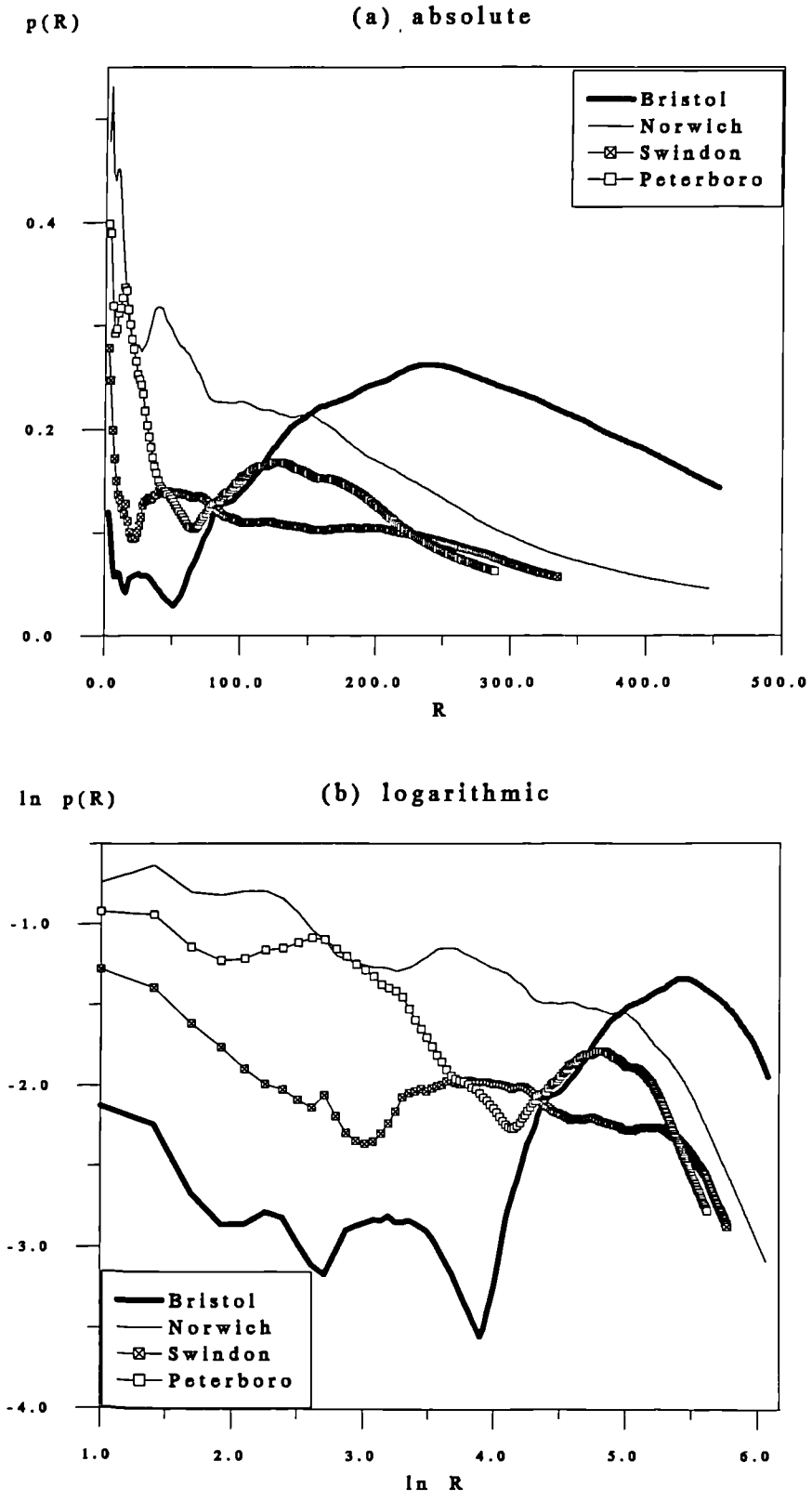

Figure 6.19 The 1981 Density Profiles of the Residential Category

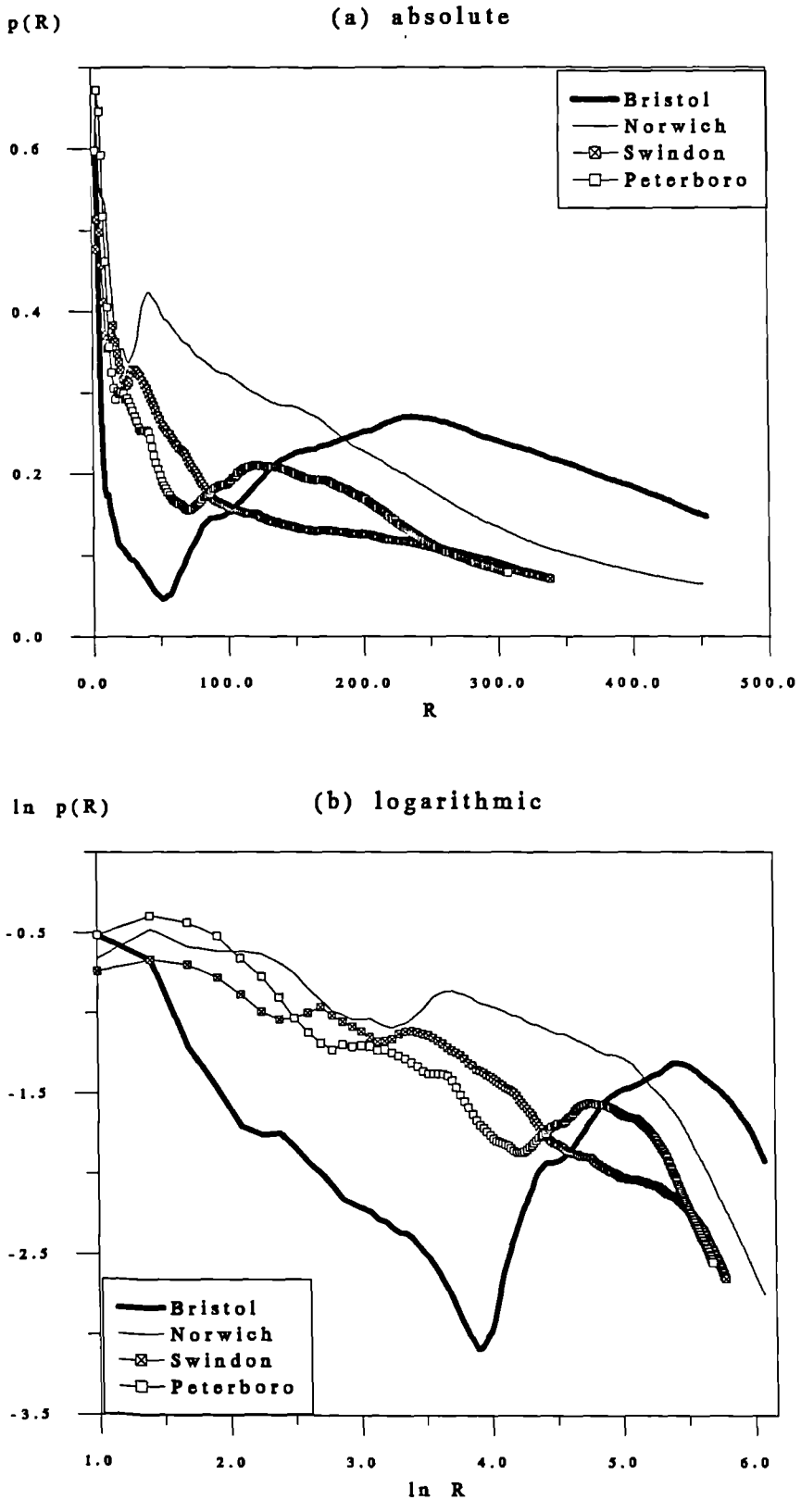

Figure 6.20 The 1991 Density Profiles of the Residential Category

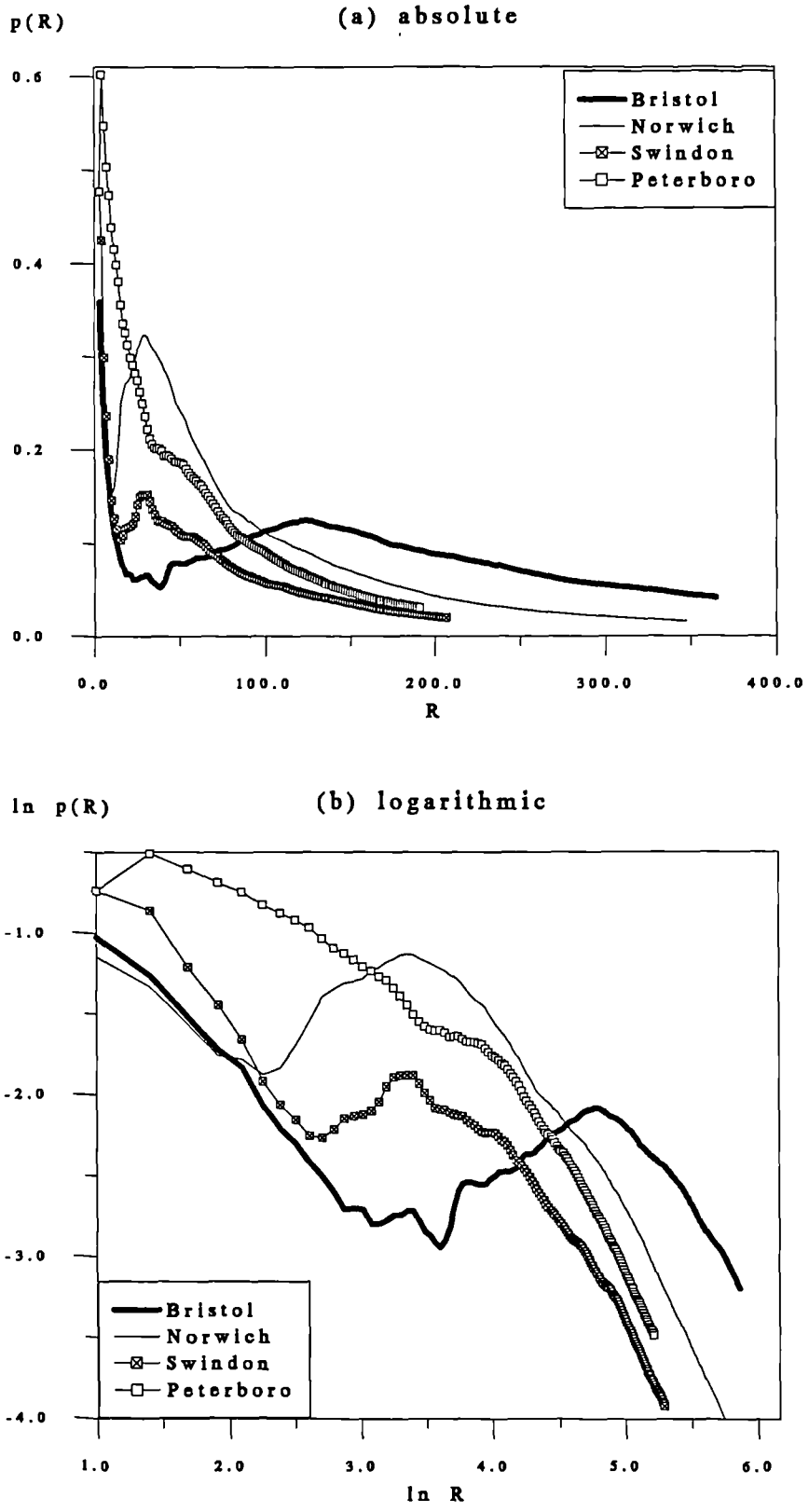

Figure 6.21 The 1981 Density Profiles of the Non-Residential Category

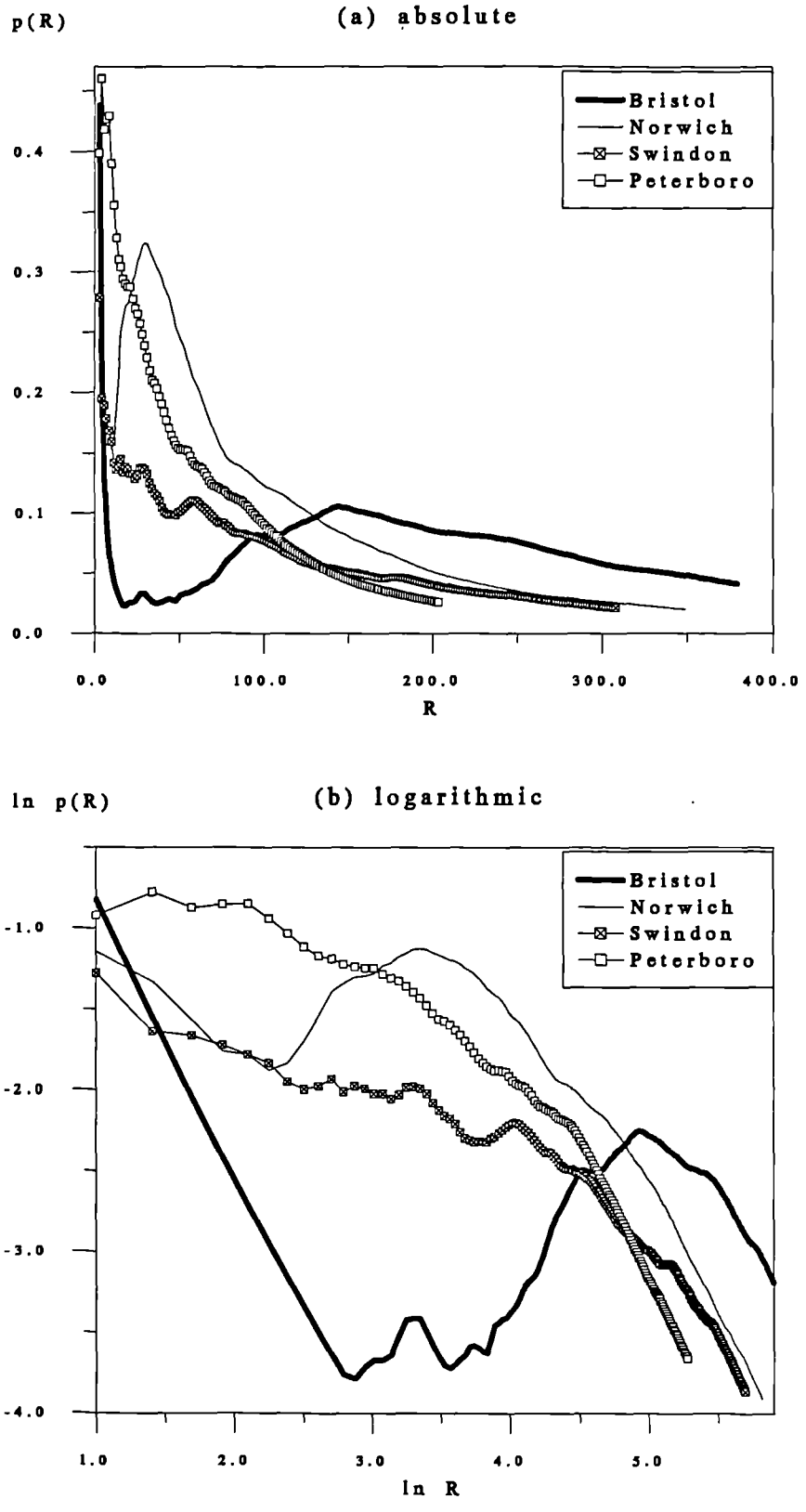

Figure 6.22 The 1991 Density Profiles of the Non-Residential Category

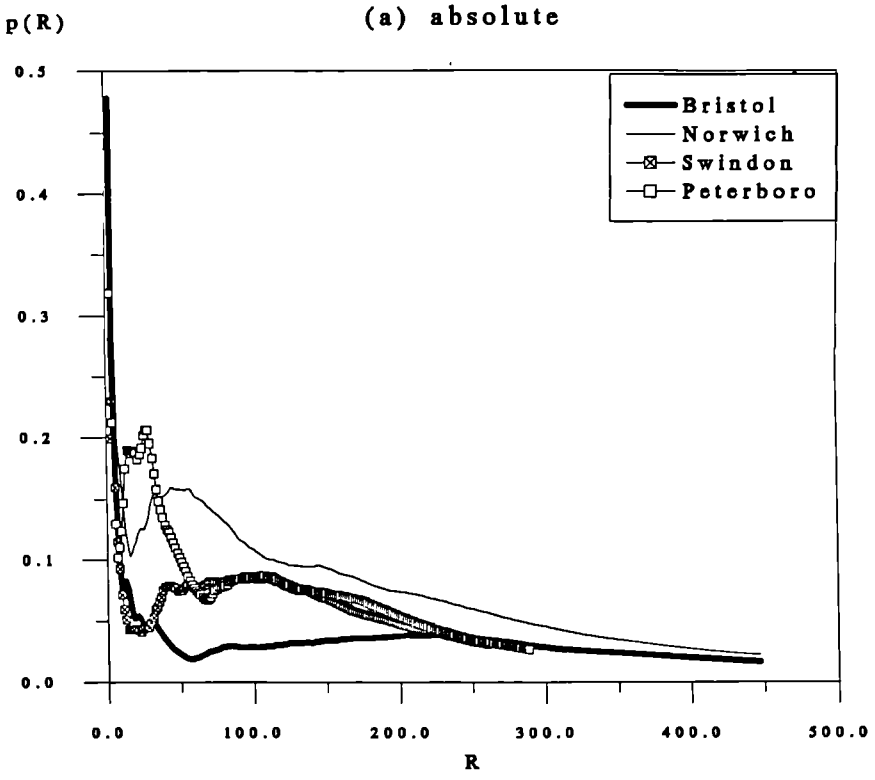

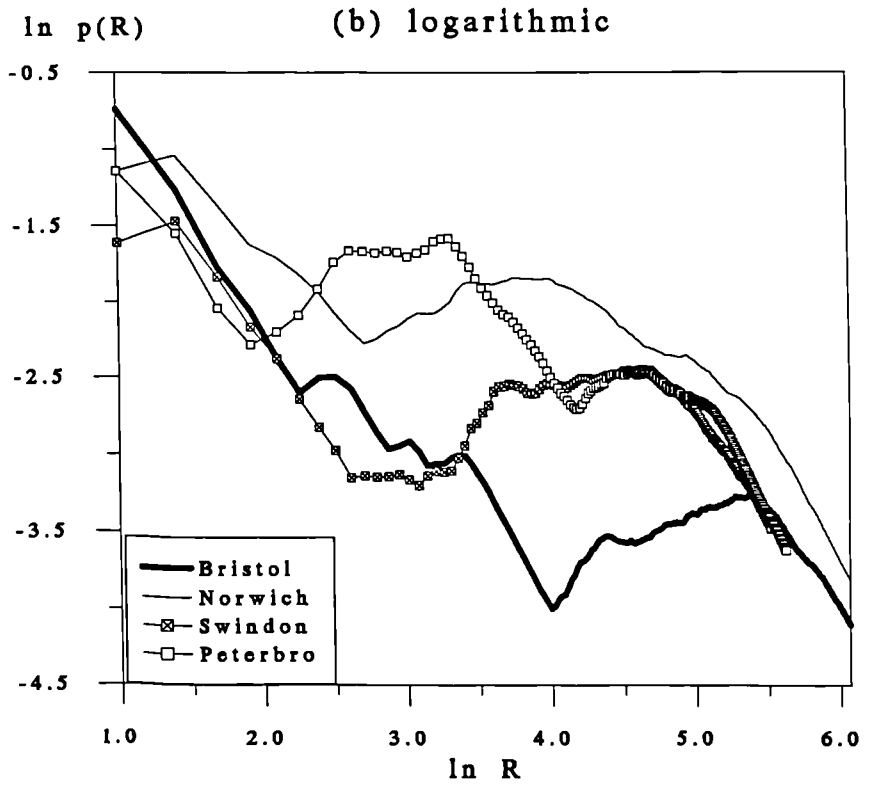

Figure 6.23 The 1991 Density Profiles of the Detached Category

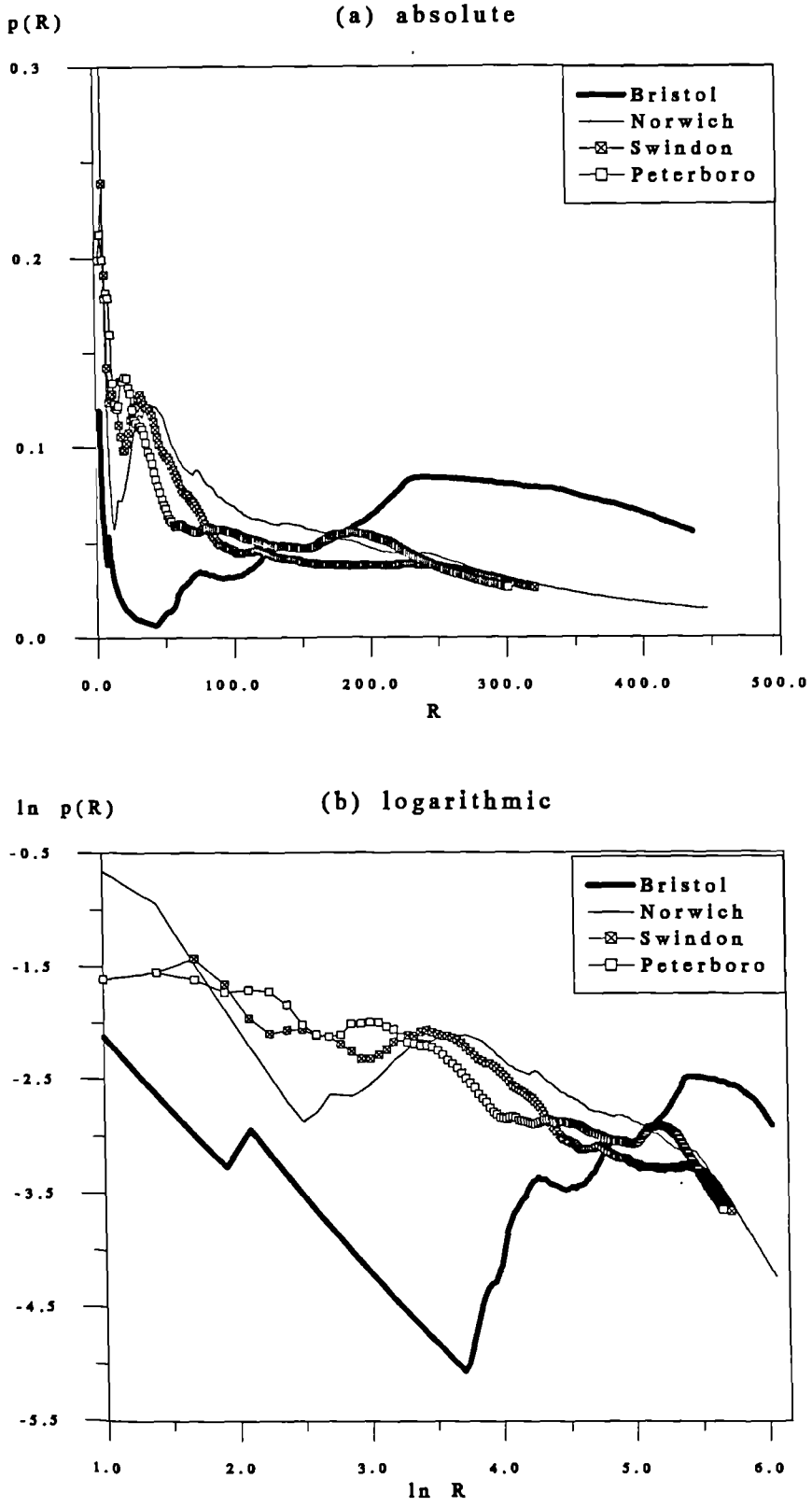

Figure 6.24 The 1991 Density Profiles of the Semi-Detached Category

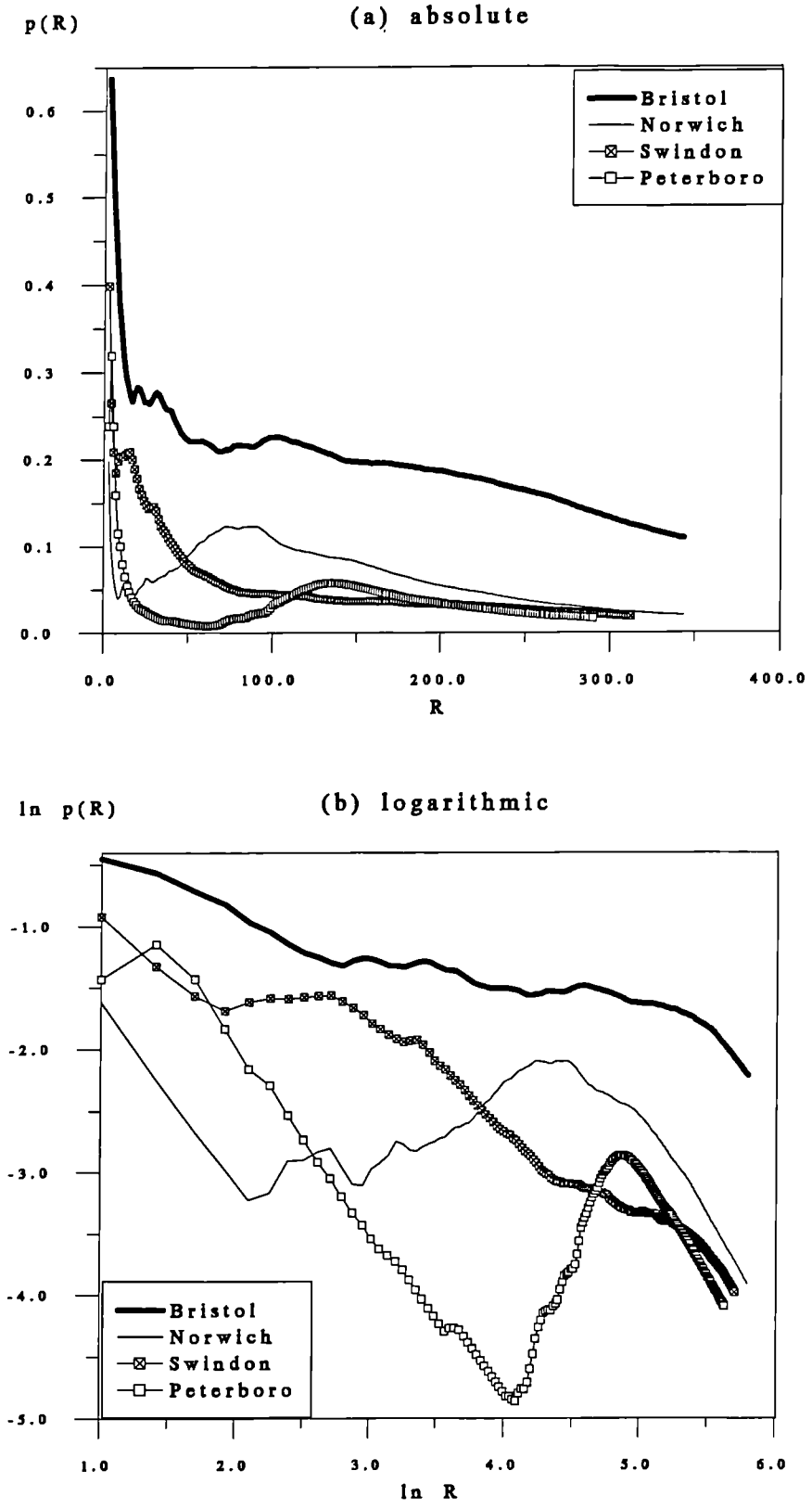

Figure 6.25 The 1991 Density Profiles of the Terraced Category

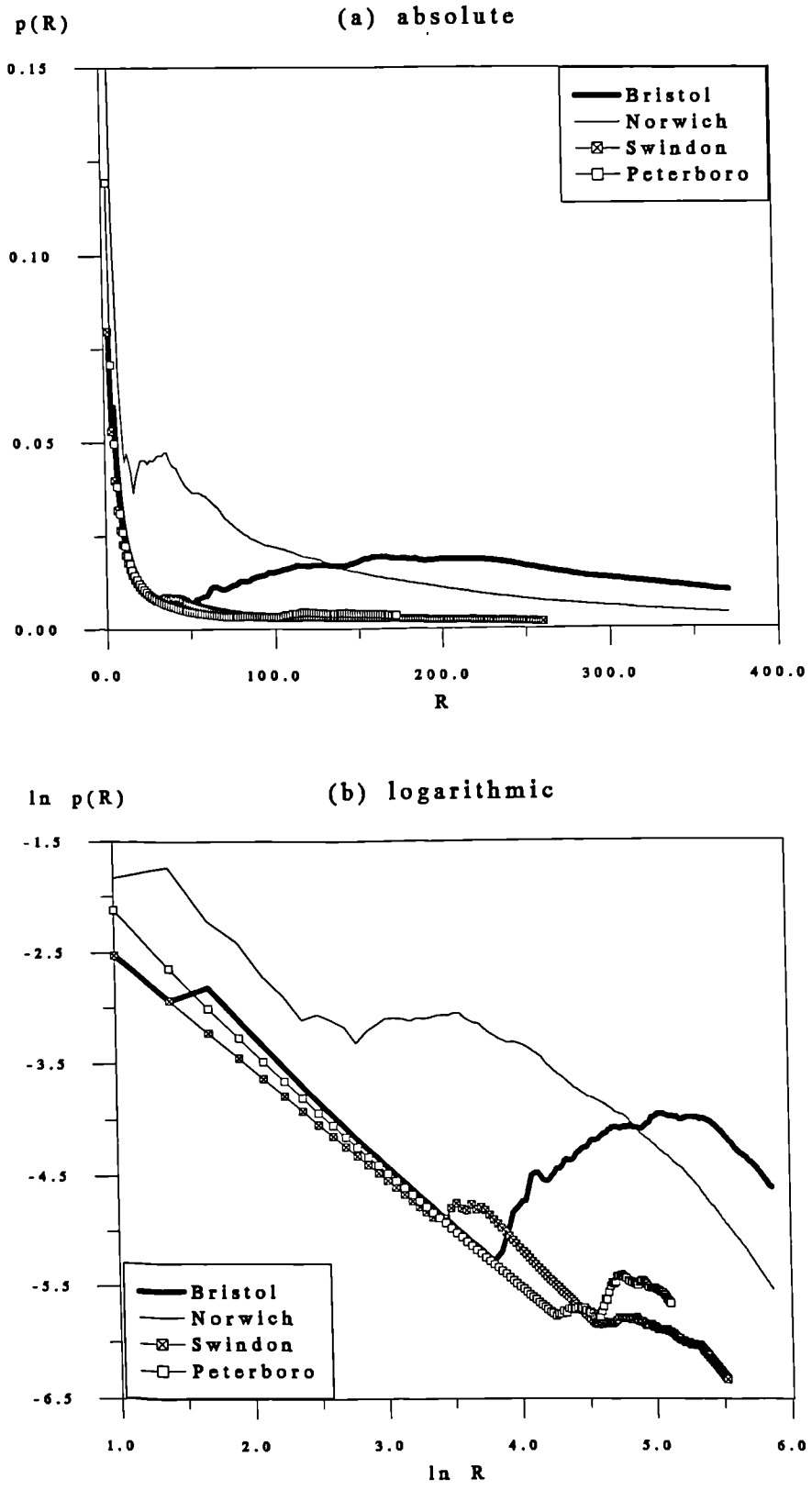

Figure 6.26 The 1991 Density Profiles of the Apartments Category

The results of all land use profiles from all settlements, at both time points, using both count and density estimations are graphically presented by Figures 6.3 to 6.48. For clarity these figures have been partitioned into three logical groups of count and density profiles, which are designed to further illustrate the abilities of classified satellite data for extensive comparative analyses. The first, and largest group (Figures 6.3 to 6.26) compares each individual land use for each of the four settlements on both an absolute and logarithmic scale in order to get a complete picture of the way counts and densities vary over distance from the urban centre. The second group (Figures 6.27 to 6.32) assesses the relationships of land use profiles in terms of the four main categories (urban, built-up, residential and non-residential), and the four sub-categories of residential (detached, semi-detached, terraced and apartments). The third, and final group (Figures 6.33 to 6.48), is a temporal comparison of the profiles for each settlement and the four main land uses between the 1981 and 1991 data sets. Recall that the sub-categories of residential are only available for 1991. Reference to the figures in each of these three groups will be made frequently and extensively throughout the remainder of the chapter.

To begin with, a brief visual examination of each of the profiles in the first group, quickly reveals how classified satellite imagery have been able to draw out the detailed characteristics of the four urban morphologies. This ability is most evident in Figures 6.15 to 6.26, where the combination of higher accuracy and precision over conventional data sources has allowed the satellite images to reveal distinct irregularities in the density of urban development. The most significant features pertaining to these irregularities expose the existence of clear physical constraints on development in all cases, but are most apparent in Bristol. The presence of the Avon river gorge (as well as other central open space) in Bristol causes density profiles for all land use categories in both time periods to behave in a highly erratic manner (see also Figures 6.30 to 6.32). These densities first fall in the way anticipated as distance increases away from the core. For the dwelling type categories (Figure 6.32), this decline is steepest at a distance of about 3-4 kilometres from the core, where the city is cut by the river gorge. Once these and other constraints (e.g. public open space) are passed, land uses increase in density quite rapidly, soon peaking again in the manner expected.

These effects of physical and zoning constraints to urban development can be further illustrated when the count profiles for Bristol are directly compared with those for the

other three settlements (Figures 6.3 to 6.14). In most of these plots, the cumulative count for Bristol is the lowest from the city centre to the break in slope, which is between R=100 to R=150 (2 km to 3 km). After that, the count for Bristol is consistently higher than the other settlements, reflecting the increase in development once the physical constraints are passed, as well as the actual larger size of the urban area. The count profiles for Norwich, Swindon and Peterborough on the other hand, are much more linear than Bristol as the absolute profiles in Figures 6.3a to 6.14a demonstrate. It can be assumed that urban development from the centre in each of these three settlements is of a much more uniform pattern. The only real exceptions to this are the count profiles for the detached dwelling category (Figure 6.11). Here, not only is the count profile for Norwich much higher than the one for Bristol, but also the profile for Peterborough appears to level off at R=180 (Figure 6.11a). In the Norwich case, detached housing is simply the most extensive residential land use, while for Peterborough, it is terraced housing that is the most abundant dwelling type, as represented by a rapid increase from R=120 to the periphery (Figure 6.13).

The third group of profiles (Figures 6.33 to 6.36 for count, and 6.41 to 6.44 for density) attempt to harness the temporal perspective. Generally speaking, there are strong similarities between graphs from the two time points for the same land use. This might have been expected from actual satellite data which are only, in the Bristol and Swindon cases, 4 years different. However, this similarity also provides some check on the confidence in the classification strategy that generated these land uses. This claim, of course, allows for inevitable discrepancies between different satellite images of the same area. These discrepancies are very much dependent on factors such as local atmospheric conditions, vegetation cover at various times of the year, and possible specific technical errors in image capture and pre-processing. Nevertheless, this group of profiles does provide an invaluable indication of some of the urban processes that may have been at work during the 1980s. Despite high levels of suburbanisation experienced by many large urban areas in recent times, each of the four sample settlements demonstrates small but marked increases in the built-up (Figure 6.34 and 6.42) and residential (Figures 6.35 and 6.43) land uses. Of these, only Norwich provides any clear evidence of increased development towards the periphery. Although the urban category has a lower classification accuracy (Chapter Five) and may not be as reliable as built-up or residential, the profiles associated with it indicate all but the truncated Bristol data set, with a more expected pattern of reduced development near the centre and expansion at the periphery.

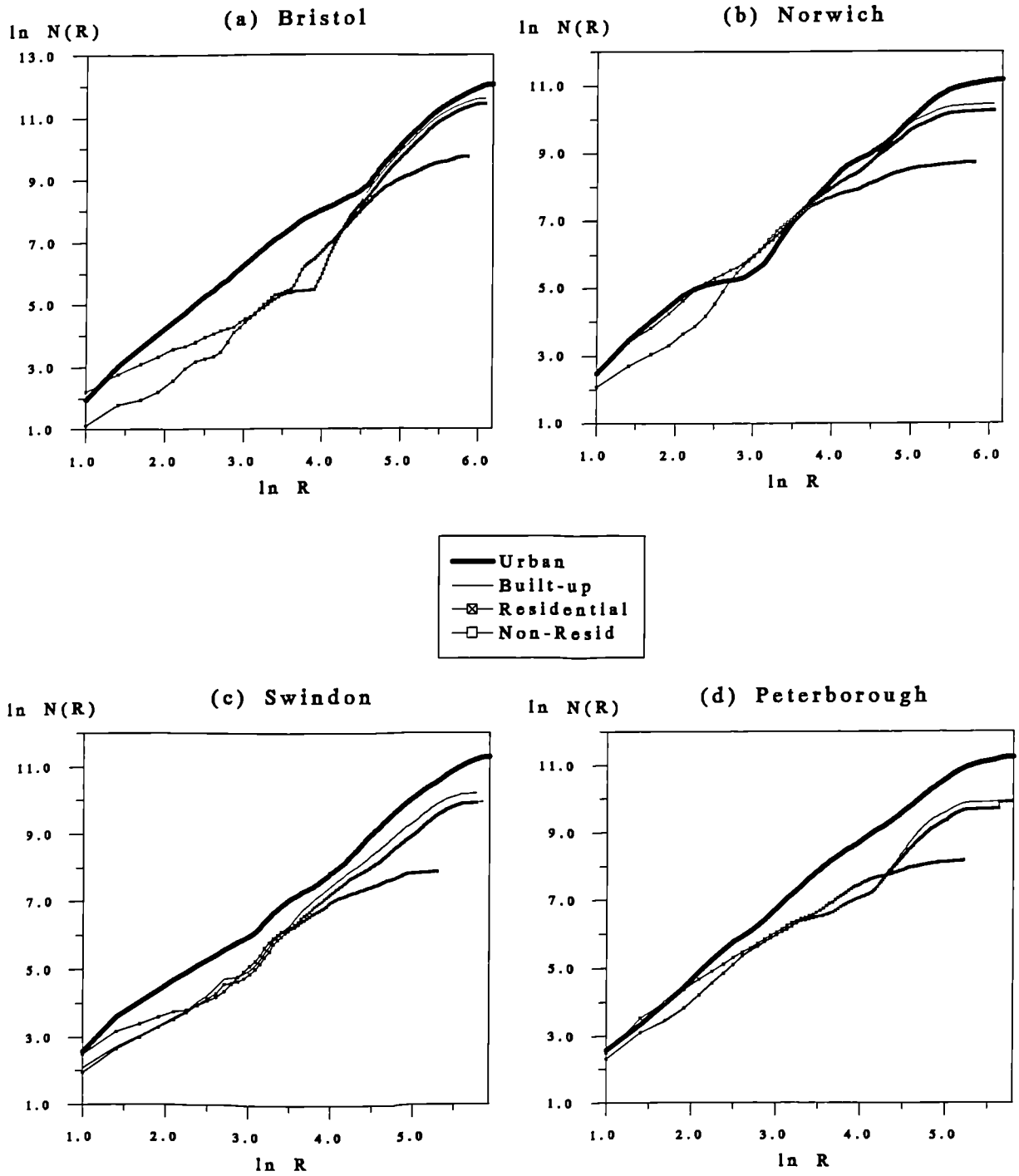

Figure 6.27 The 1981 Cumulative Count Profiles of All Urban Definitions

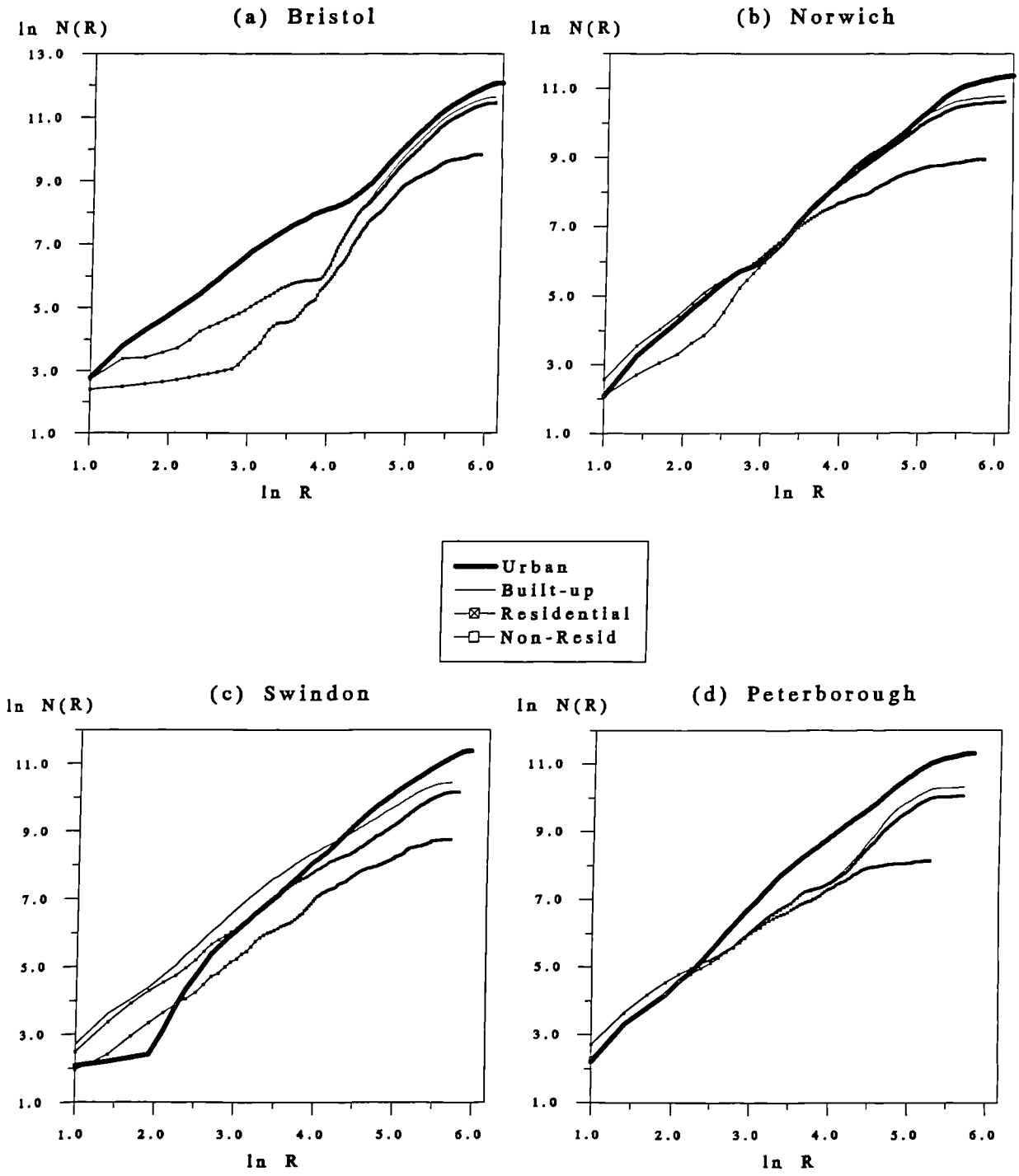

Figure 6.28 The 1991 Cumulative Count Profiles of All Urban Definitions

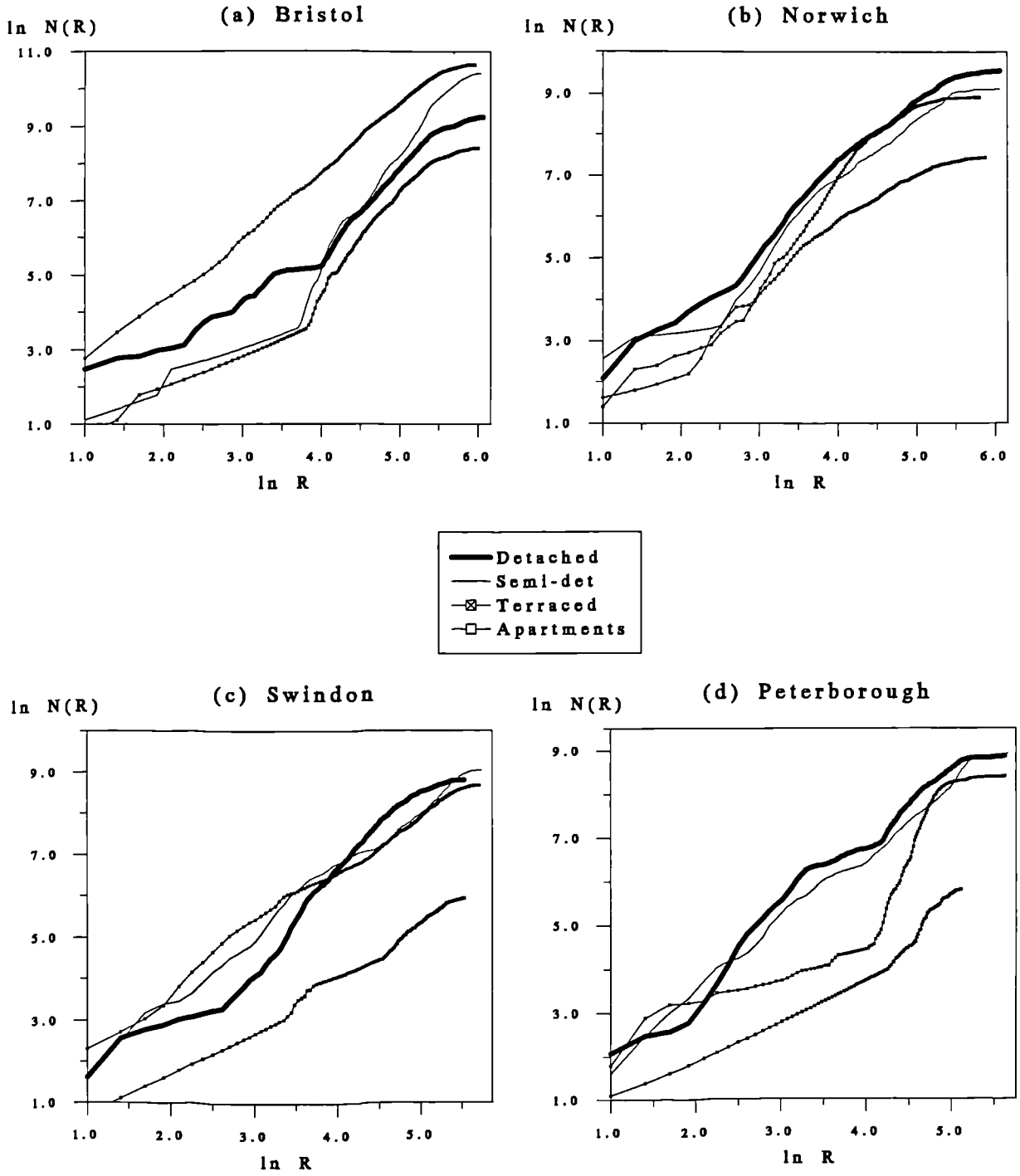

Figure 6.29 The 1991 Cumulative Count Profiles of All Dwelling Type Categories

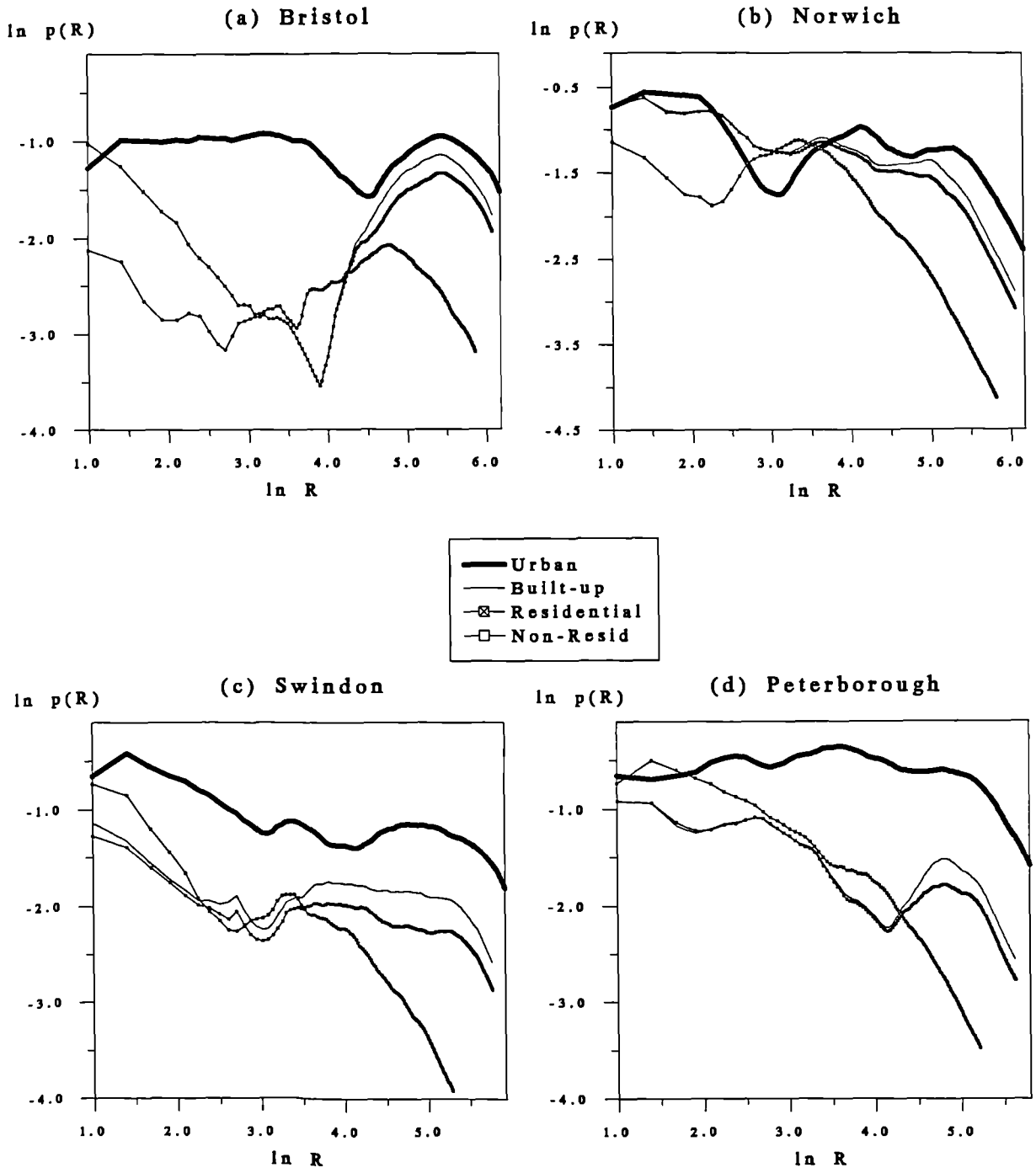

Figure 6.30 The 1981 Density Profiles of All Urban Definitions

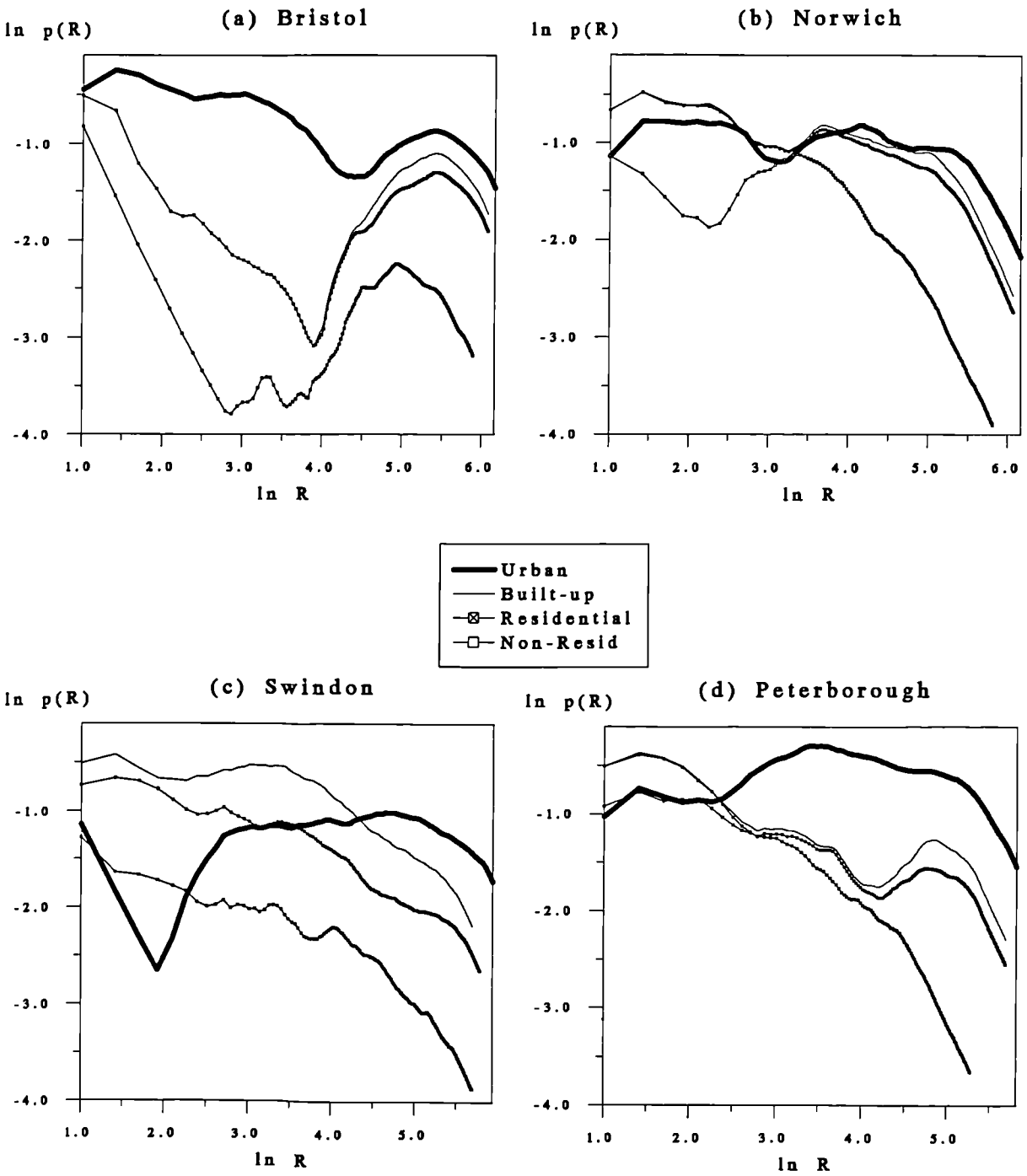

Figure 6.31 The 1991 Density Profiles of All Urban Definitions

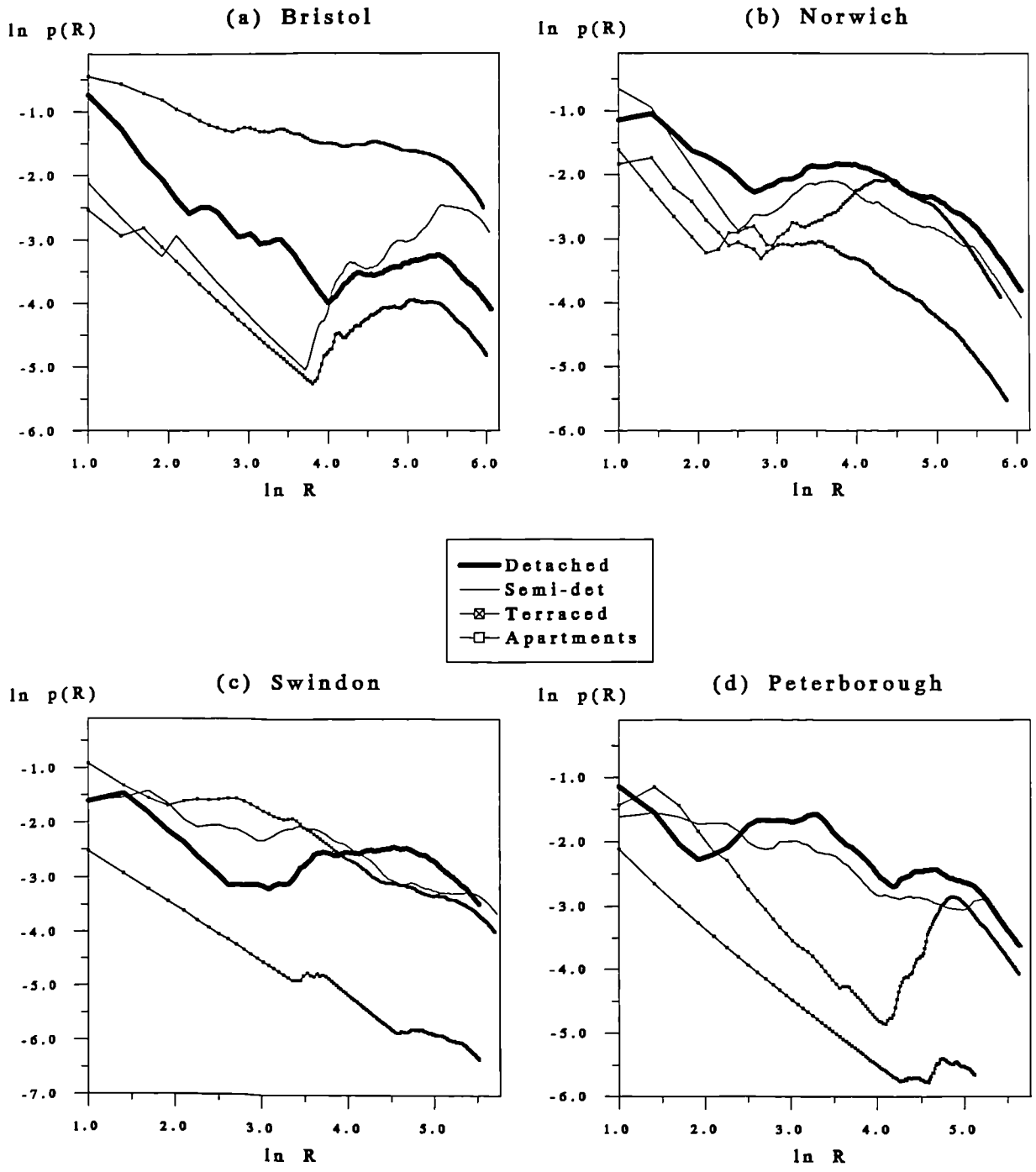

Figure 6.32 The 1991 Density Profiles of All Dwelling Type Categories

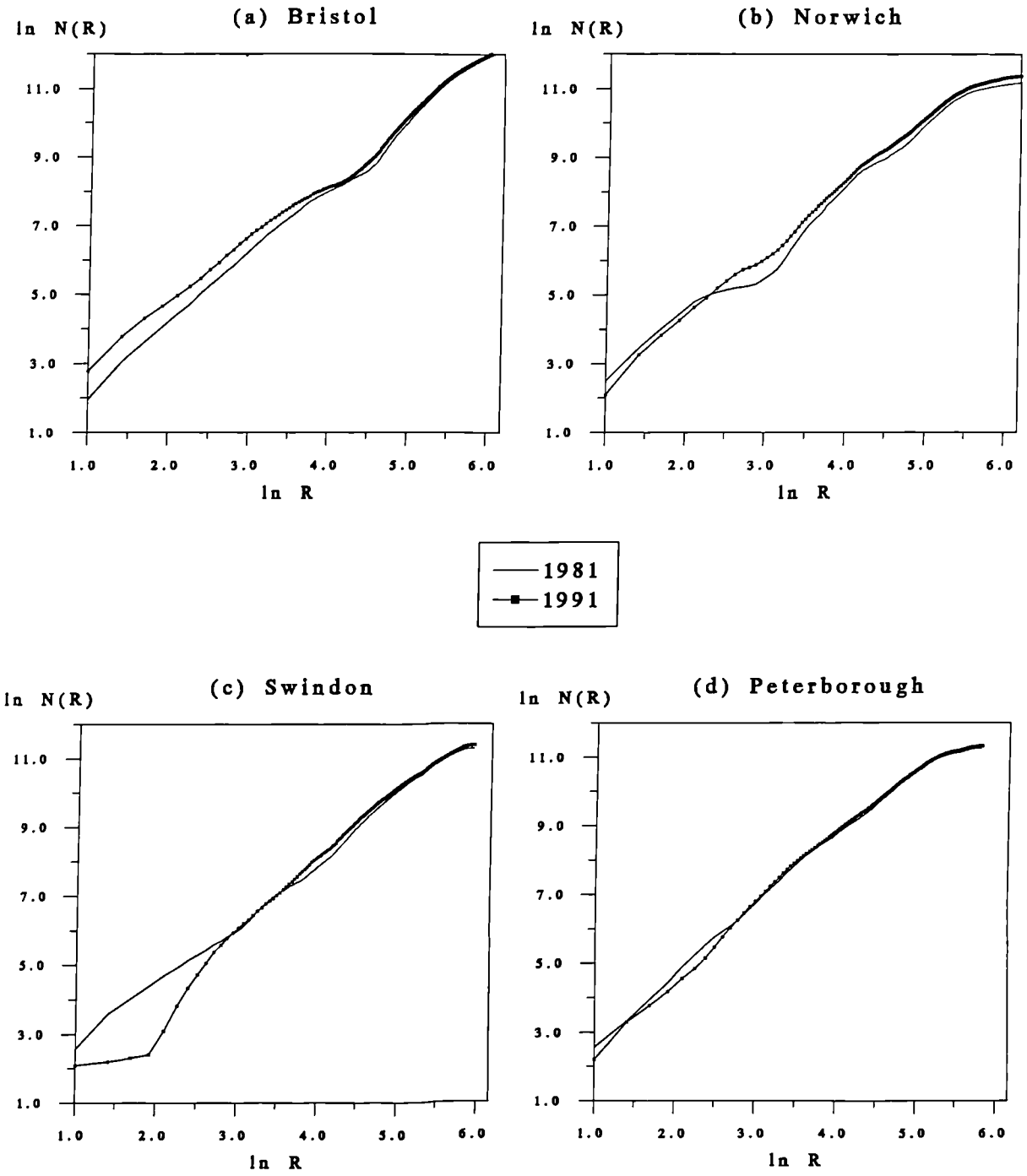

Figure 6.33 The 1981/1991 Cumulative Count Profiles of the Urban Category

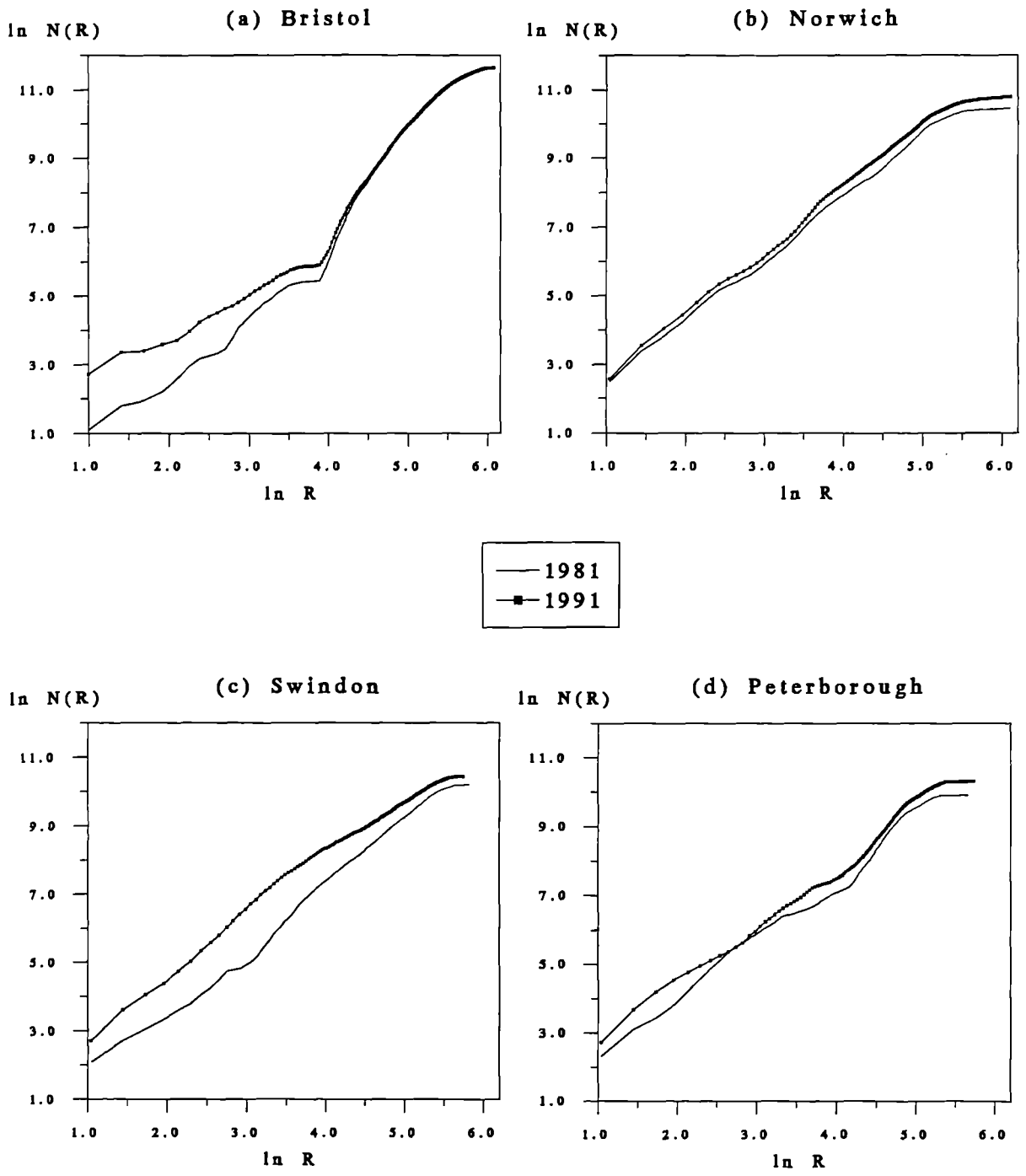

Figure 6.34 The 1981/1991 Cumulative Count Profiles of the Built-up Category

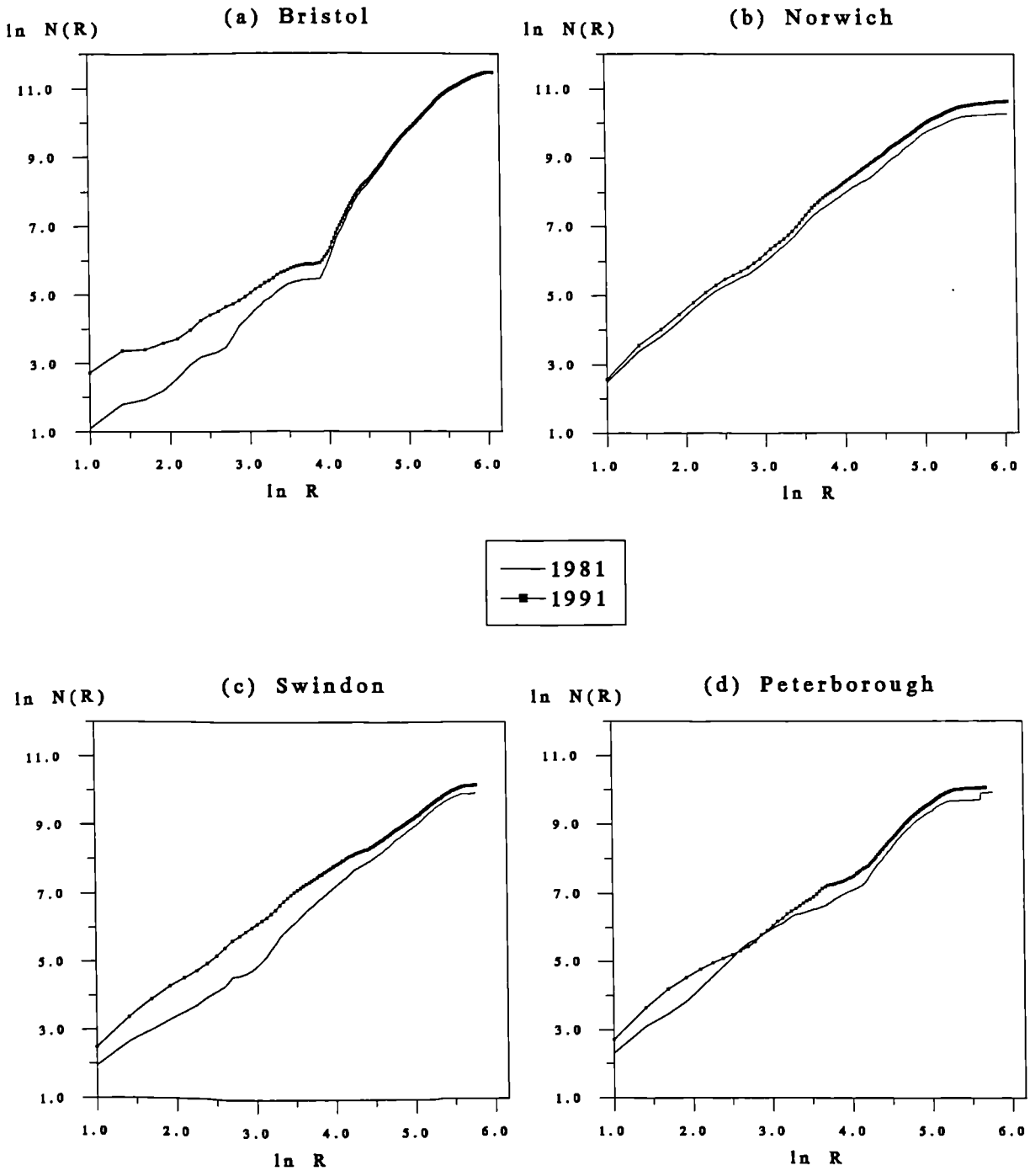

Figure 6.35 The 1981/1991 Cumulative Count Profiles of the Residential Category

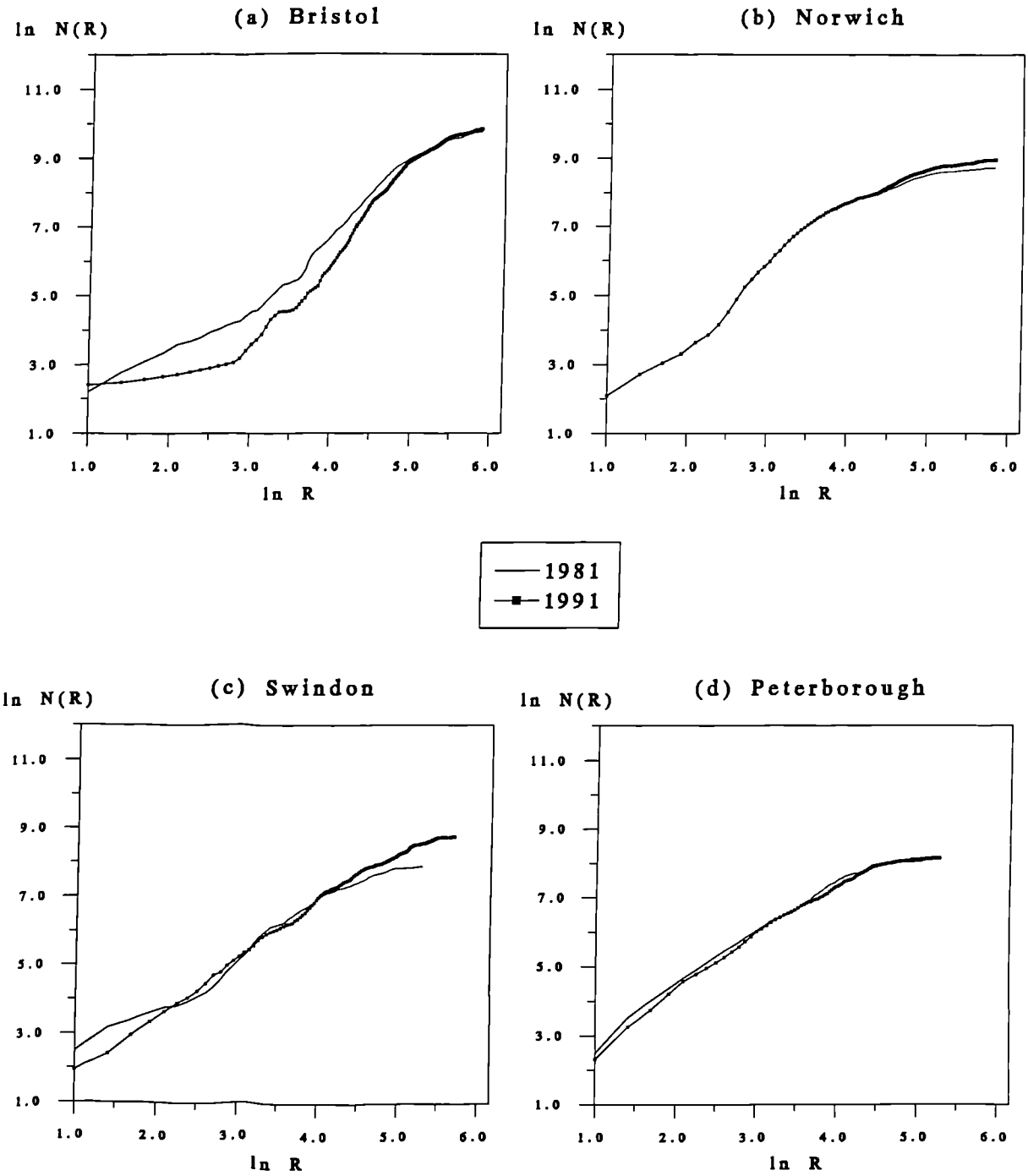

Figure 6.36 The 1981/1991 Cumulative Count Profiles of the Non-Residential Category

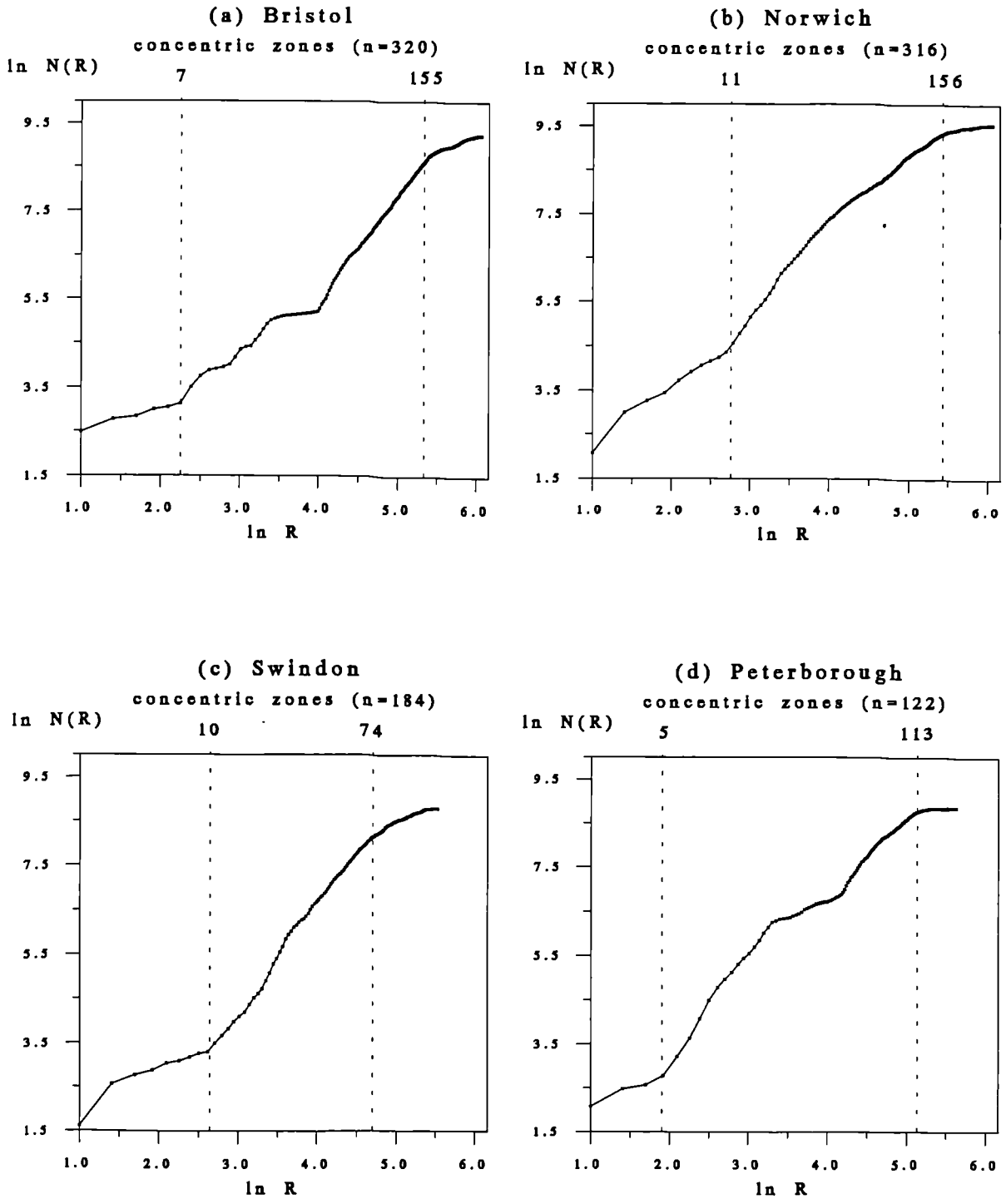

Figure 6.37 The 1991 Cumulative Count Profiles of the Detached Category (with cut-off zones)

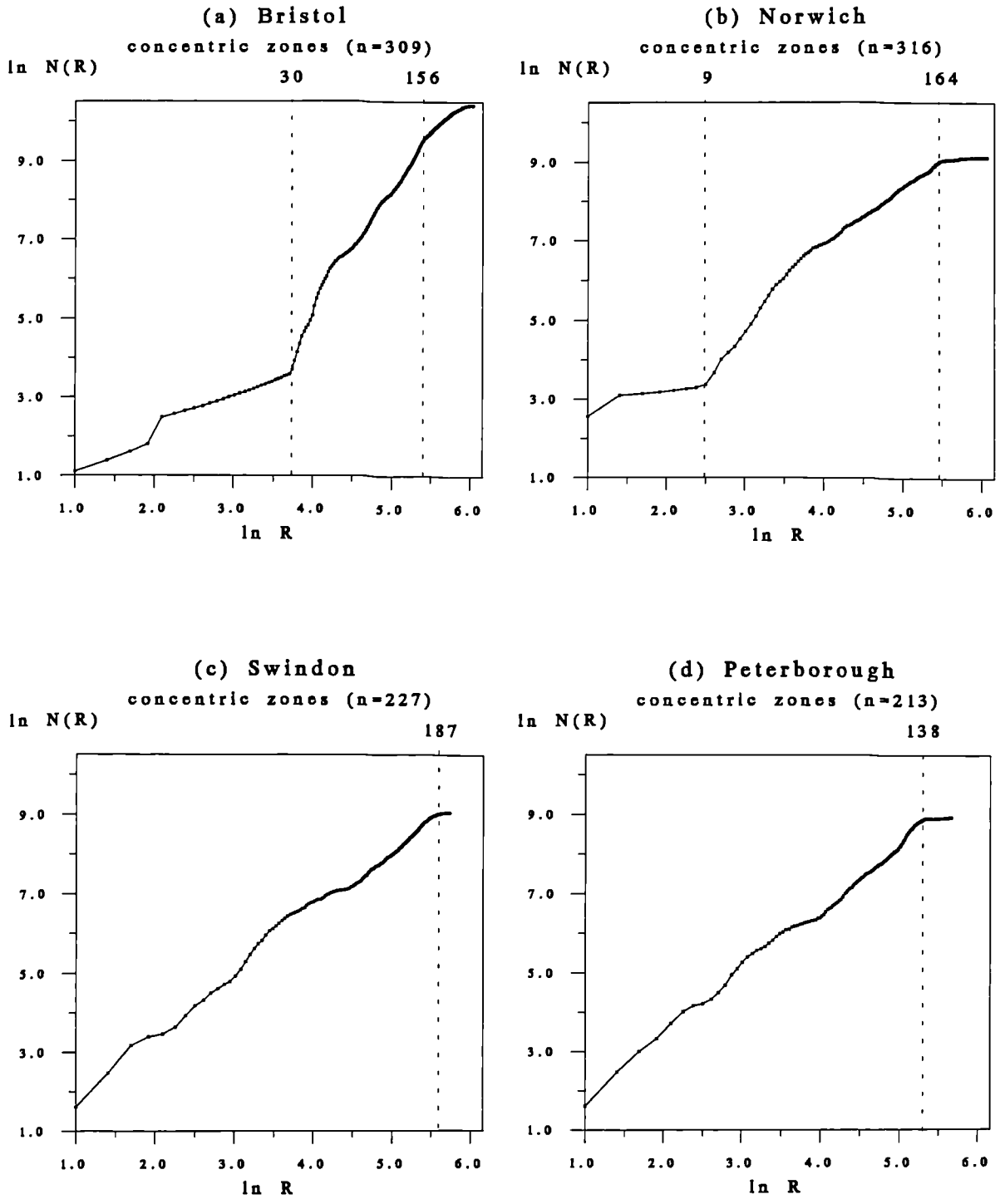

Figure 6.38 The 1991 Cumulative Count Profiles of the Semi-Detached Category (with cut-off zones)

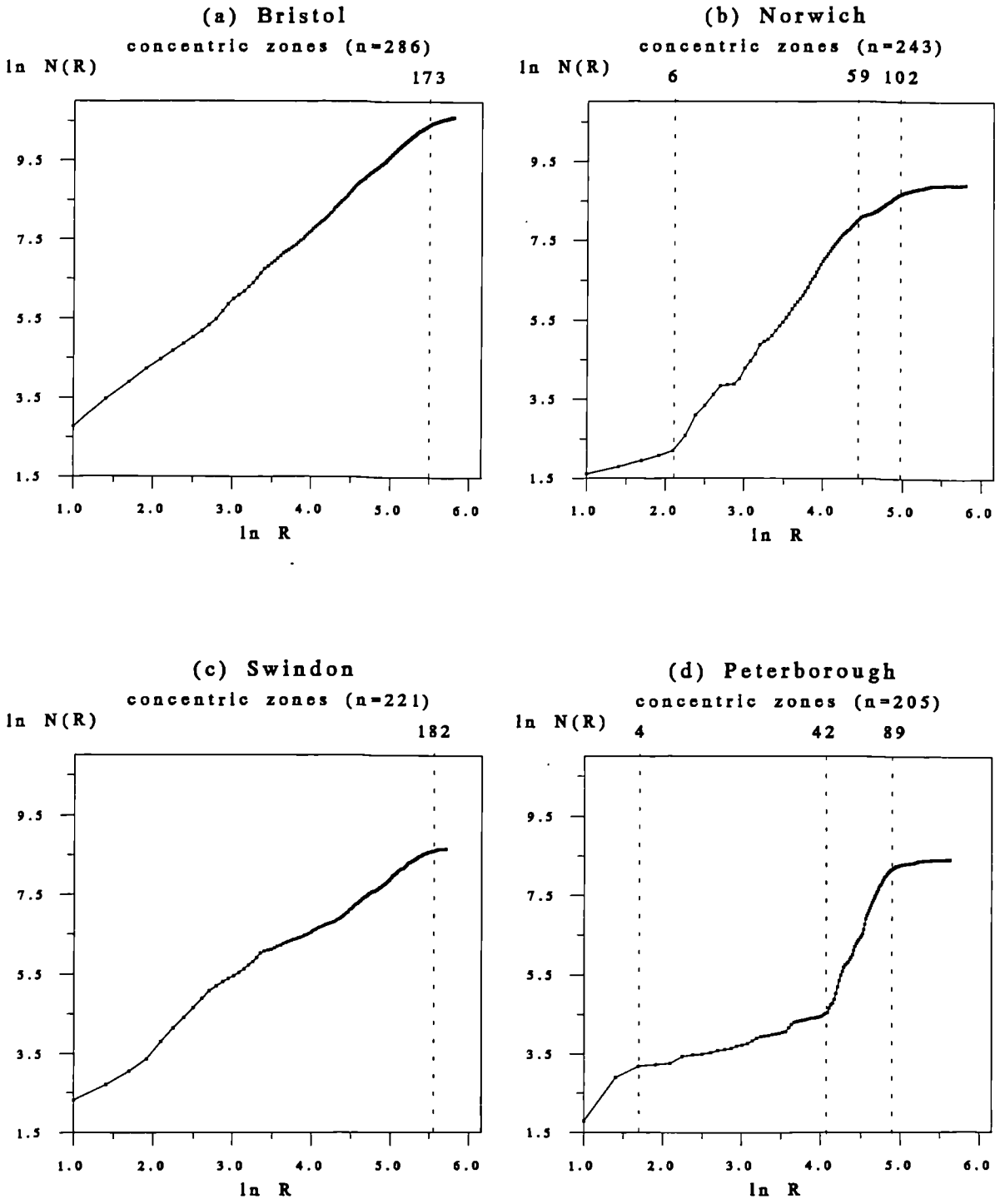

Figure 6.39 The 1991 Cumulative Count Profiles of the Terraced Category (with cut-off zones)

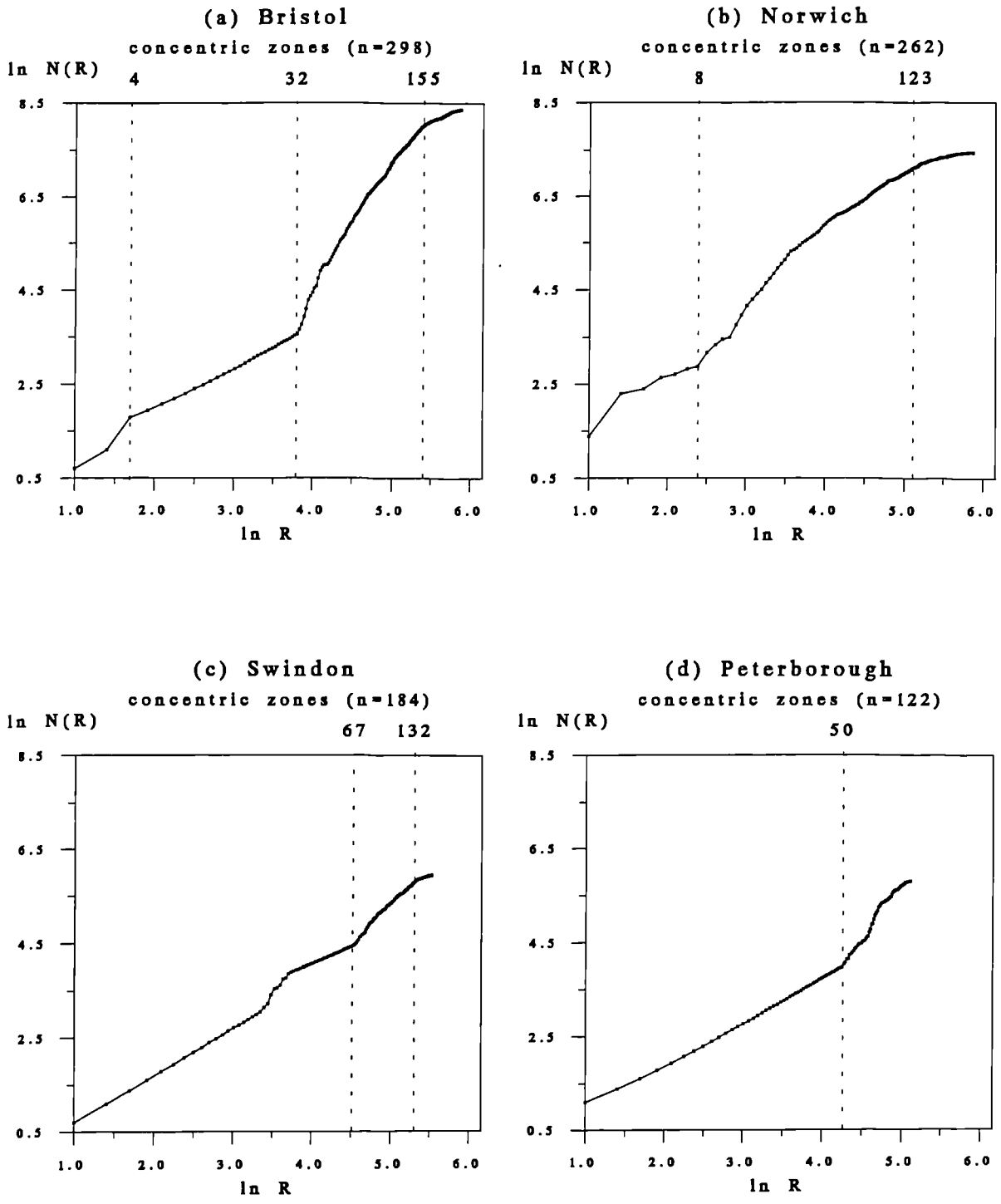

Figure 6.40 The 1991 Cumulative Count Profiles of the Apartments Category (with cut-off zones)

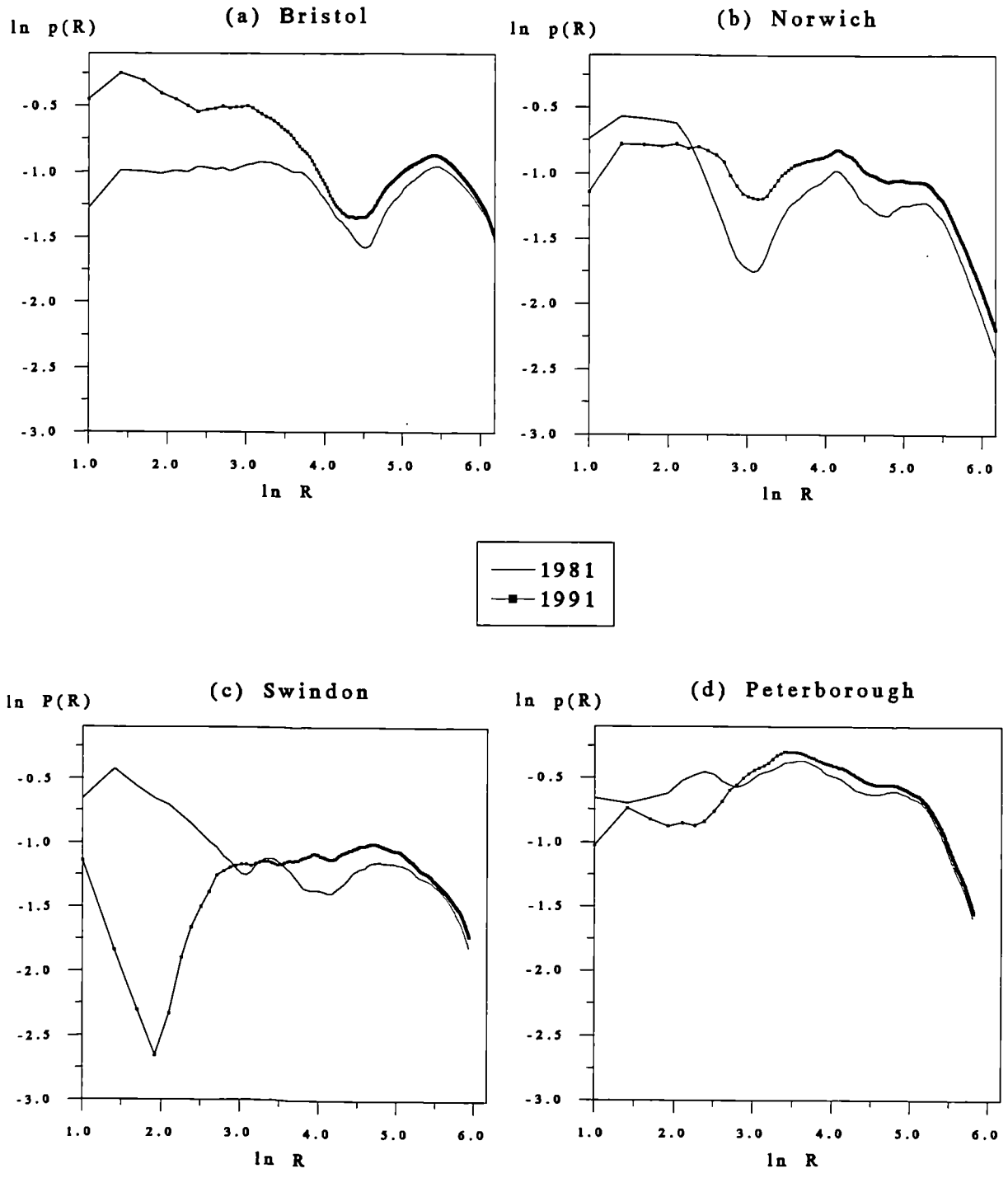

Figure 6.41 The 1981/1991 Density Profiles of the Urban Category

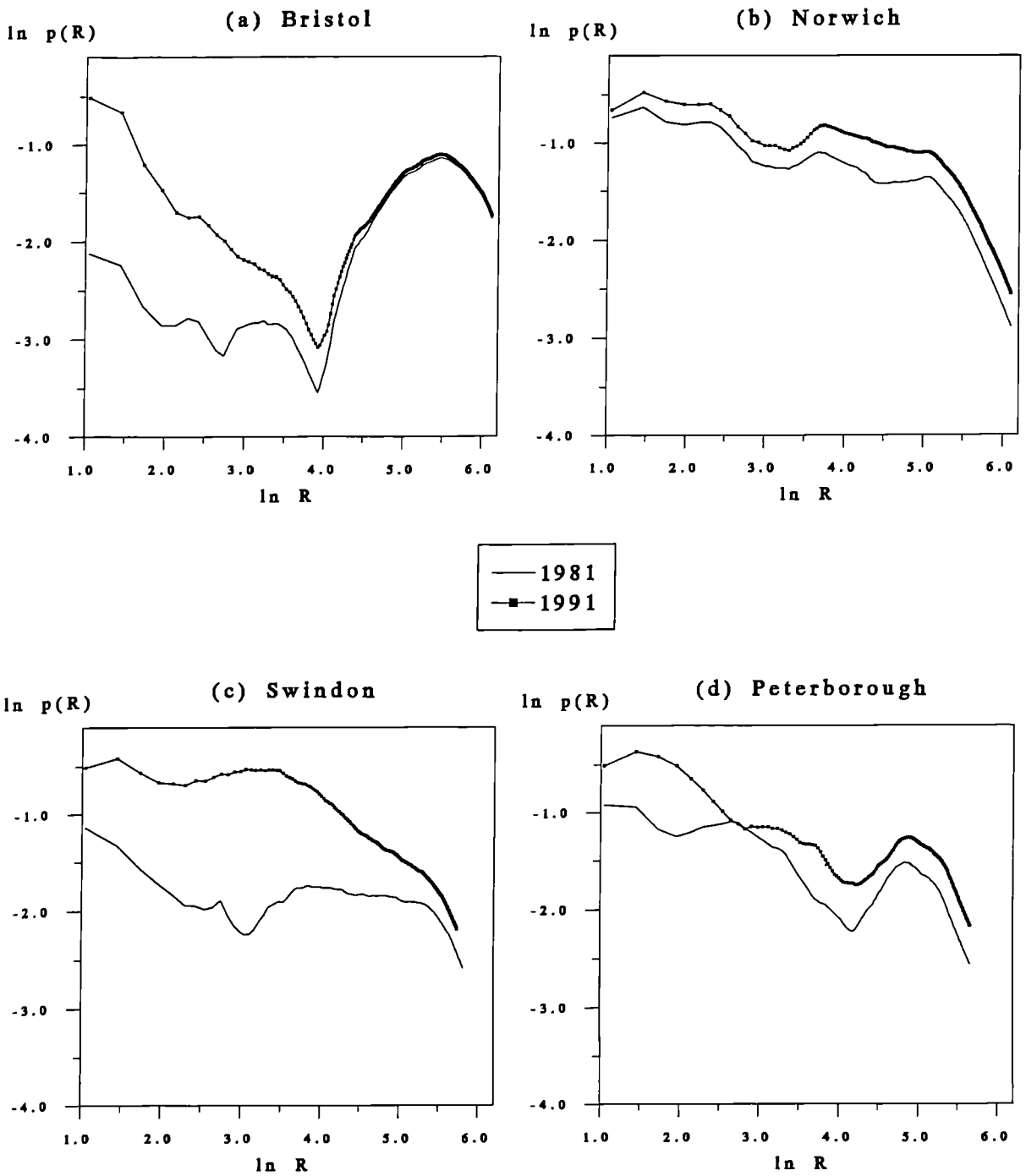

Figure 6.42 The 1981/1991 Density Profiles of the Built-up Category

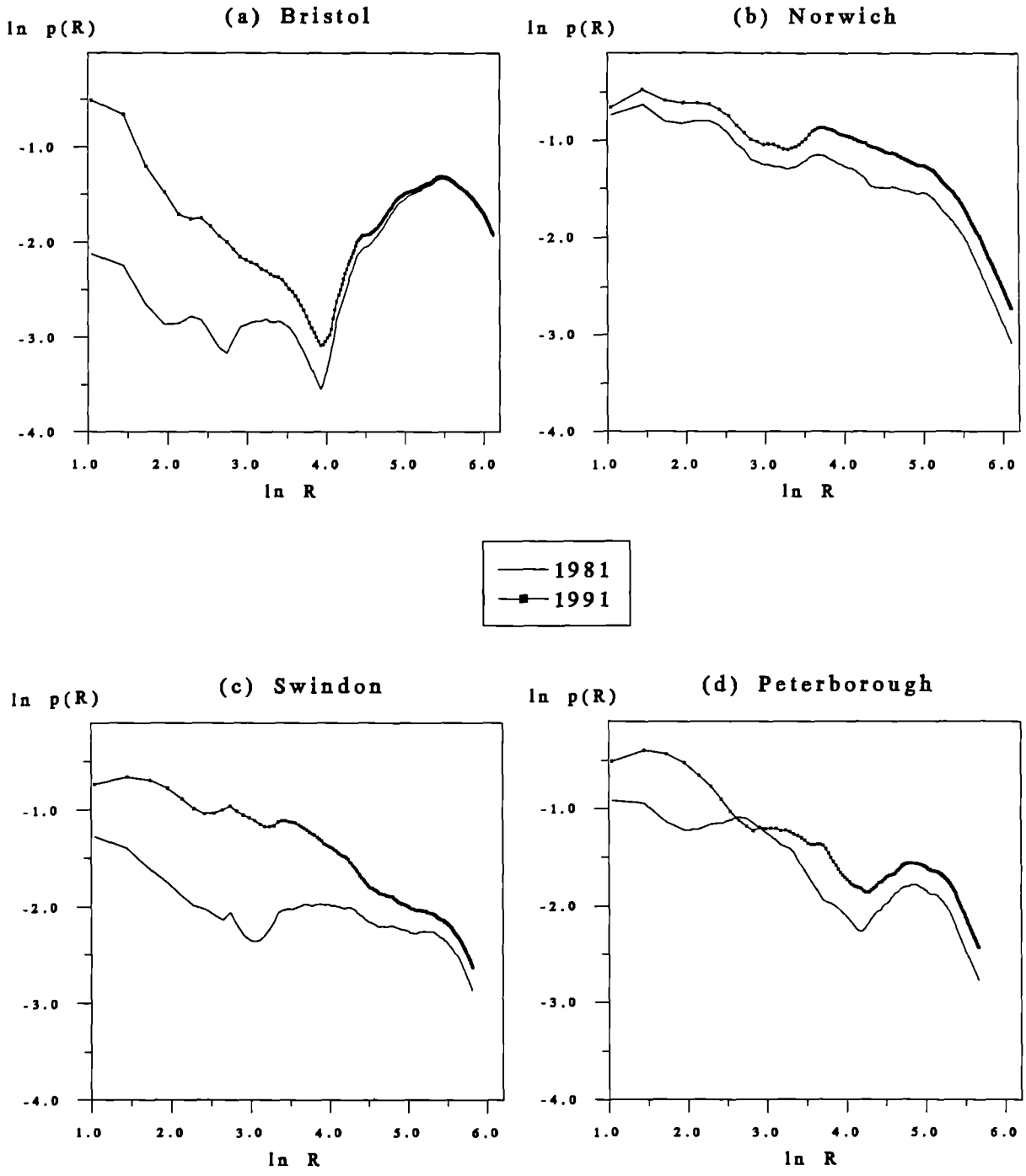

Figure 6.43 The 1981/1991 Density Profiles of the Residential Category

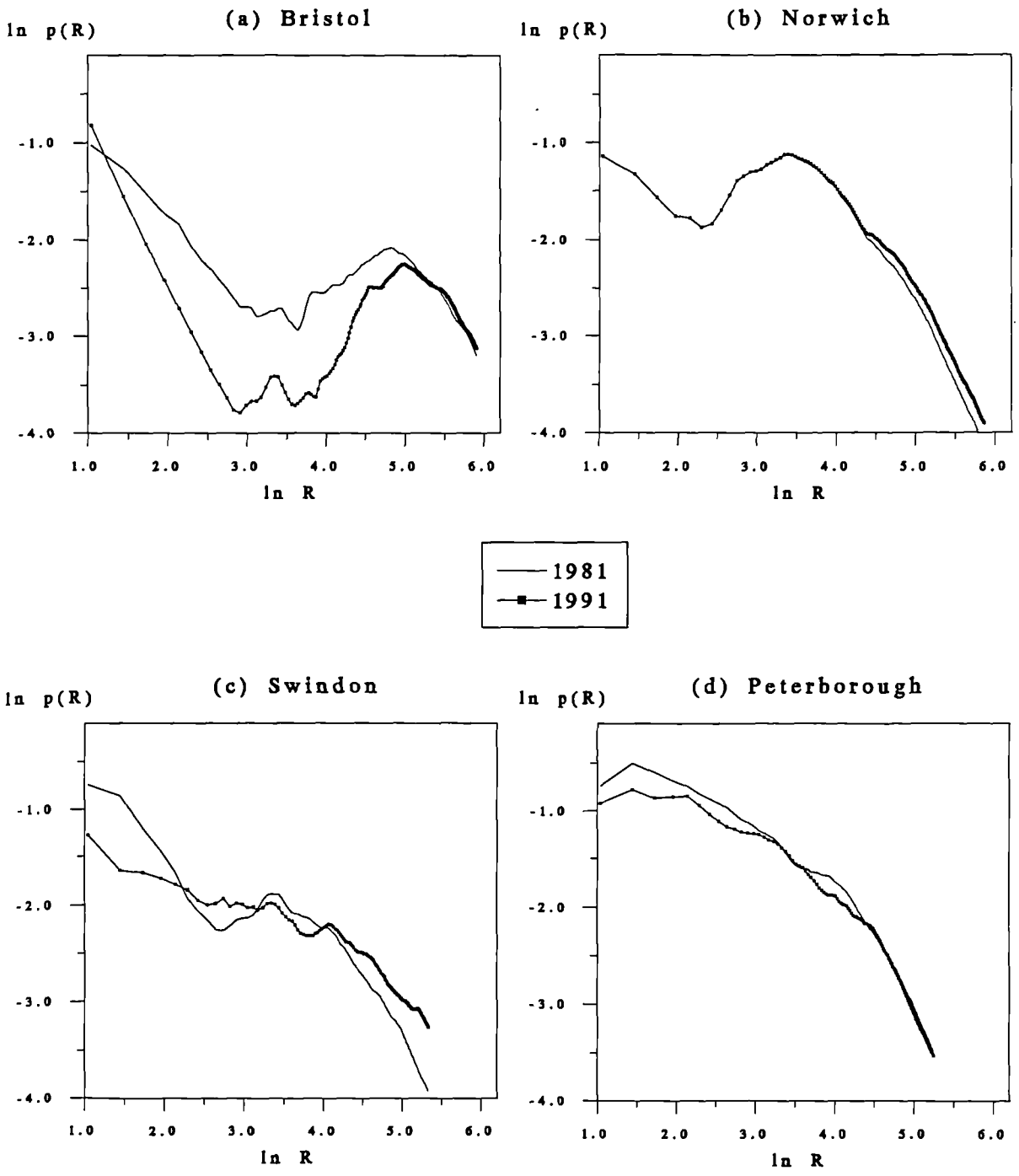

Figure 6.44 The 1981/1991 Density Profiles of the Non-Residential Category

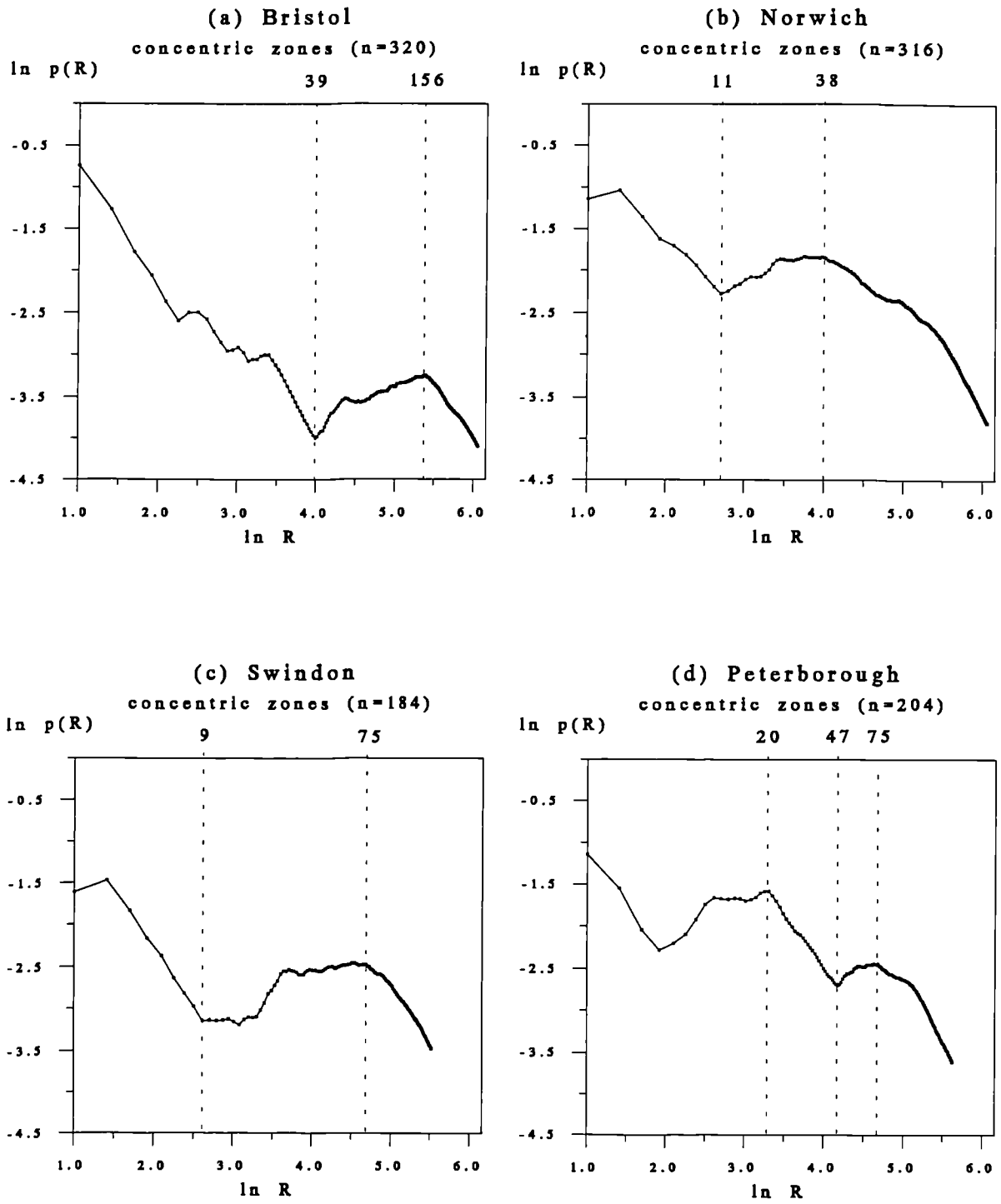

Figure 6.45 The 1991 Density Profiles of the Detached Category (with cut-off zones)

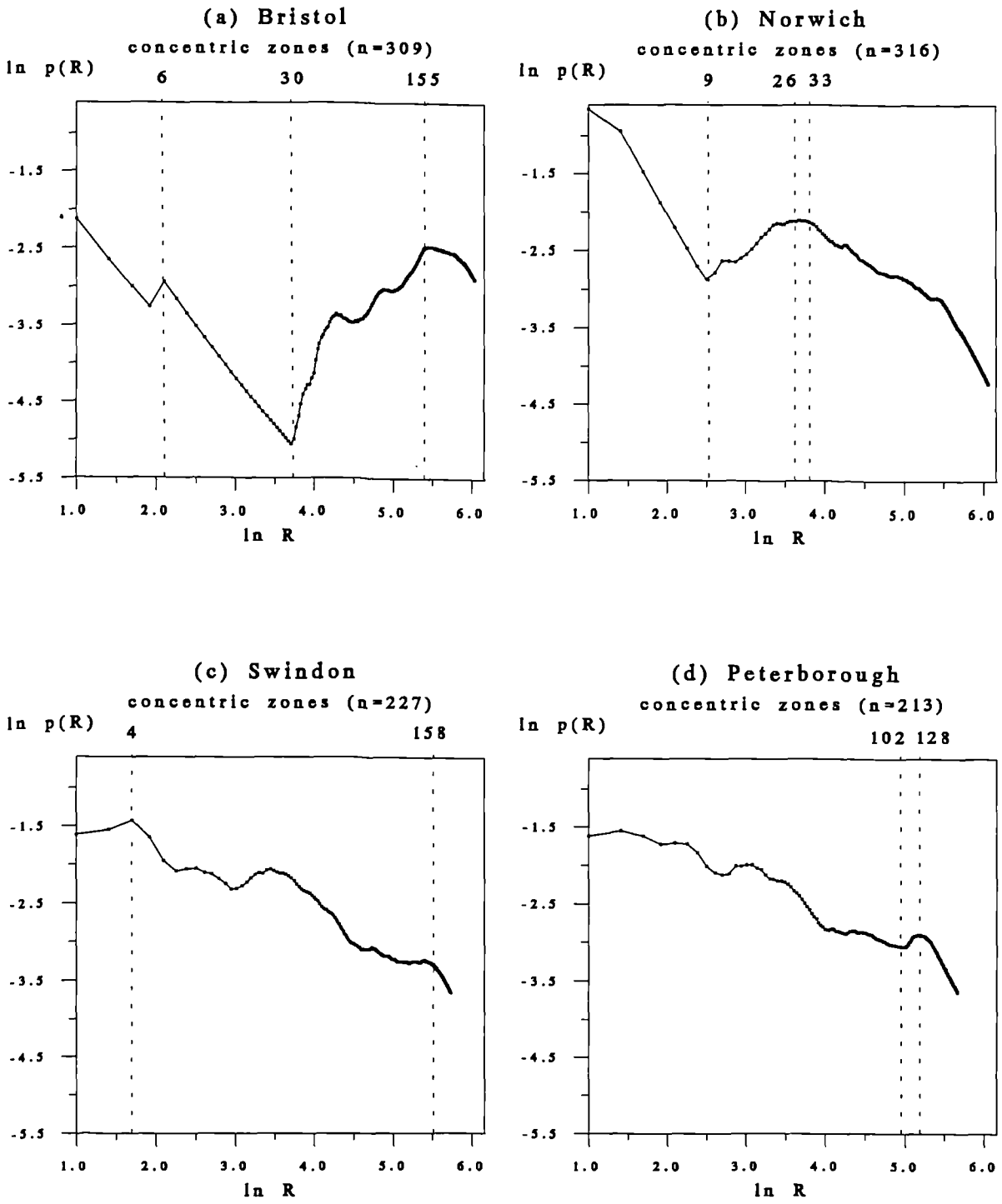

Figure 6.46 The 1991 Density Profiles of the Semi-Detached Category (with cut-off zones)

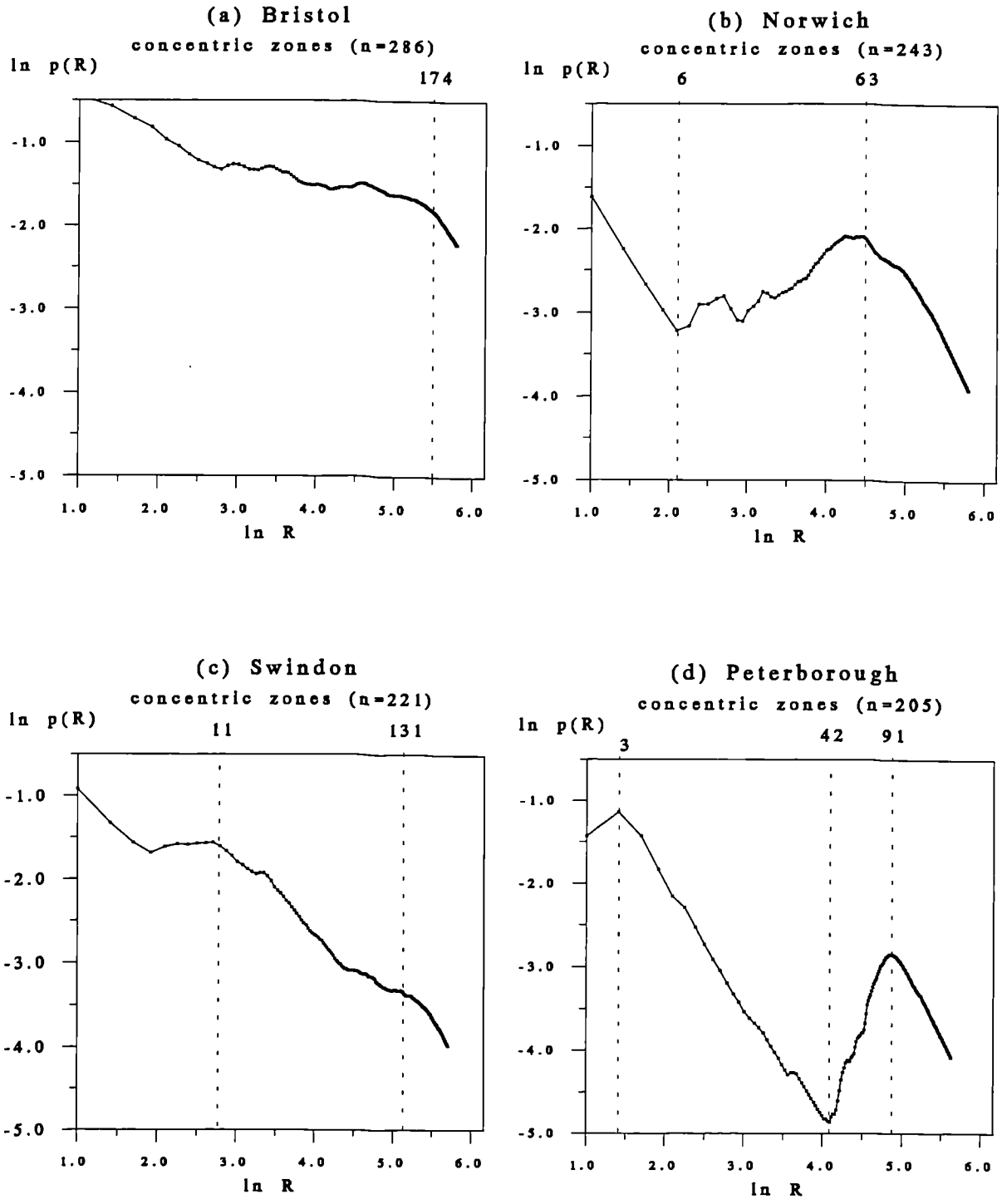

Figure 6.47 The 1991 Density Profiles of the Terraced Category (with cut-off zones)

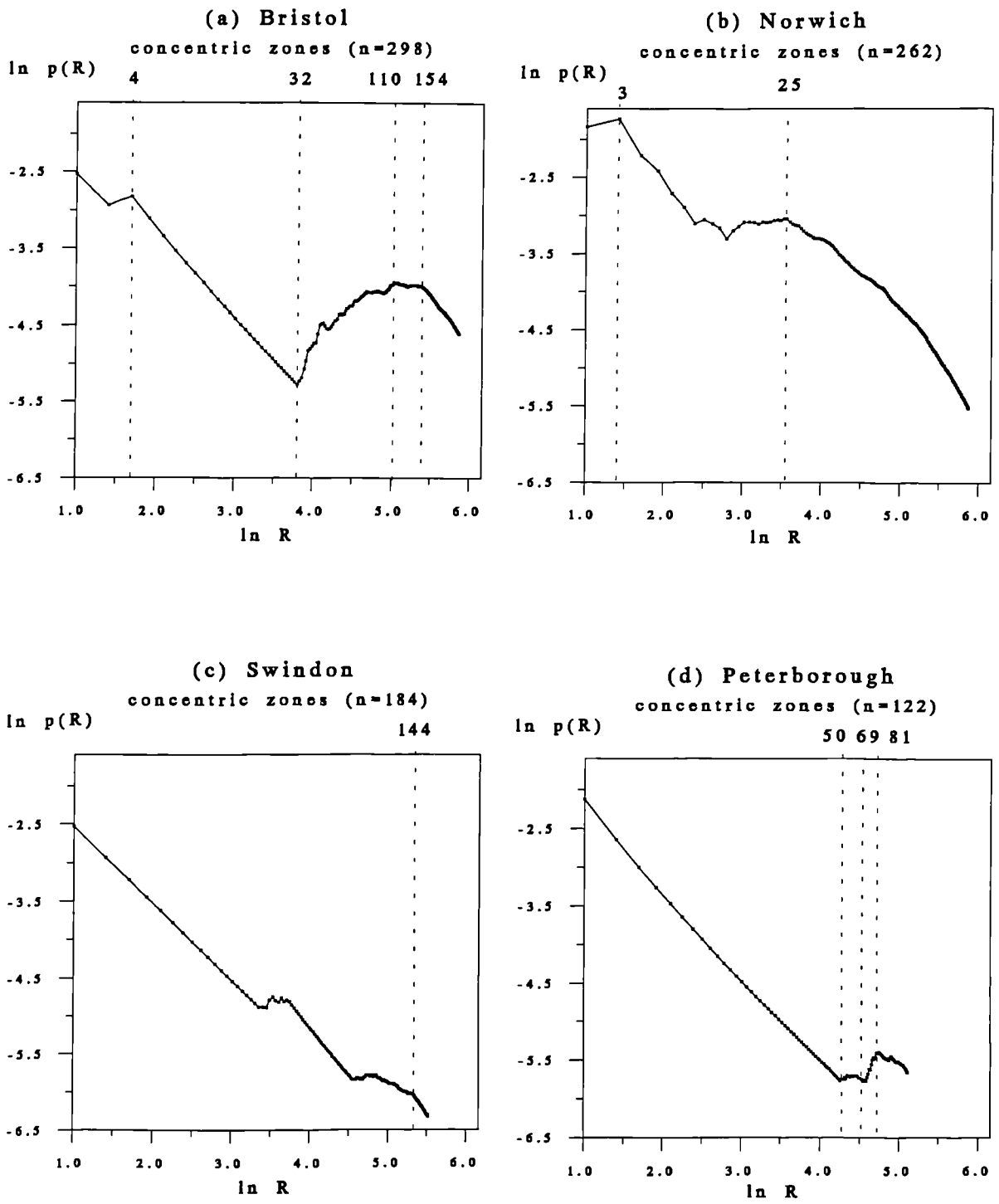

Figure 6.48 The 1991 Density Profiles of the Apartments Category (with cut-off zones)

With respect to the non-residential land use, there are strong indications of decentralisation, characterised by marked decreases in development close to the centre and growth on the periphery, in all but the Norwich data sets (Figures 6.36 and 6.44).

The results of calibrating fractal dimensions from linear regression equations (4.12) and (4.13) for all land uses from both time slices are shown in Table 6.3. The fractal parameter estimates D, from each of these equations are identical (see Chapter Four), but the performance measures based on the coefficient of determination (r^2) differ substantially. The order in land uses is a direct reflection of the changes in slope in the gradients due to physical constraints. Again, the effects of the Avon gorge in Bristol are apparent by fractal dimensions frequently exceeding 2, although there is an overall reduction from 1981 to 1991 as urban infilling diminishes these effects. The consequences of physical barriers to urban development are most evident in density estimates where the r^2 values are exceptionally poor, for example, 0.030 for the Bristol 1981 urban category. This is in contrast to the performance of the count distributions, which are always high in terms of r^2 values for cumulative profiles.

It should have become clear that most density profiles are far from linear, which leads to poor estimates in terms of fitting these profiles using equation (4.12). For the cumulative counts (Figures 6.23 to 6.25) these reversals in gradients simply manifest themselves in terms of breaks in slope, but the implications of fitting equation (4.13) to these graphs is that fractal dimensions are likely to exceed 2 in several cases.

6.5 Constrained Linear Regression Modelling

An examination of most of the profiles between Figures 6.3 to 6.48 reveals immediately the problems of attempting to fit linear assumptions to curvilinear plots. The results of these problems were further reflected in Table 6.3 by exceptionally low $r^2_{density}$ values. Short of fitting a completely different functional form of the regression relation, there are two ways in which more "acceptable" fractal dimensions may be generated from the empirical data. First, regression can be constrained by fixing the intercept values in advance, which will ensure that fractal dimensions fall within the range $1 < D < 2$ (subject to a normal error range).

Table 6.4 Dimensions From Constrained Regression

a. Urban Definitions, 1981 and 1991 (**Count** and **Density**)

Urban								
	1981				1991			
	Count		Density		Count		Density	
Settlement	D	r^2	D	r^2	D	r^2	D	r^2
Bristol	1.993	0.996	1.781	0.194	2.012	0.935	1.800	0.483
Norwich	1.913	0.909	1.701	0.476	1.946	0.880	1.734	0.445
Swindon	1.959	0.943	1.737	0.859	1.973	0.994	1.751	0.180
Peterborough	2.050	0.860	1.823	0.347	2.058	0.875	1.832	0.286
Built-up								
	1981				1991			
	Count		Density		Count		Density	
Settlement	D	r^2	D	r^2	D	r^2	D	r^2
Bristol	1.919	0.747	1.703	0.343	1.936	0.826	1.720	0.292
Norwich	1.853	0.846	1.637	0.498	1.908	0.830	1.692	0.429
Swindon	1.824	0.977	1.596	0.968	1.931	0.800	1.699	0.540
Peterborough	1.853	0.975	1.608	0.641	1.903	0.922	1.672	0.614
Residential								
	1981				1991			
	Count		Density		Count		Density	
Settlement	D	r^2	D	r^2	D	r^2	D	r^2
Bristol	1.888	0.755	1.673	0.418	1.904	0.839	1.688	0.319
Norwich	1.821	0.824	1.605	0.525	1.880	0.813	1.664	0.445
Swindon	1.764	0.981	1.536	0.731	1.600	0.844	1.599	0.797
Peterborough	1.807	0.941	1.572	0.794	1.859	0.891	1.627	0.728
Non-Residential								
	1981				1991			
	Count		Density		Count		Density	
Settlement	D	r^2	D	r^2	D	r^2	D	r^2
Bristol	1.720	0.925	1.495	0.689	1.688	0.769	1.465	0.243
Norwich	1.643	0.786	1.417	0.525	1.672	0.799	1.446	0.539
Swindon	1.630	0.844	1.399	0.777	1.620	0.887	1.388	0.898
Peterborough	1.708	0.860	1.453	0.587	1.682	0.736	1.430	0.601

Table 6.4 Dimensions From Constrained Regression (cont.)

b. Dwelling Type, 1991 (**Count** and **Density**)

	Detached				Semi-Detached			
	Count		Density		Count		Density	
Settlement	D	r^2	D	r^2	D	r^2	D	r^2
Bristol	1.544	0.875	1.328	0.889	1.664	0.652	1.447	0.609
Norwich	1.678	0.890	1.462	0.718	1.601	0.952	1.385	0.818
Swindon	1.645	0.884	1.406	0.790	1.604	0.945	1.374	0.860
Peterborough	1.664	0.929	1.430	0.878	1.622	0.971	1.971	0.819
	Terraced				Apartments			
	Count		Density		Count		Density	
Settlement	D	r^2	D	r^2	D	r^2	D	r^2
Bristol	1.868	0.899	1.648	0.802	1.395	0.698	1.176	0.424
Norwich	1.642	0.908	1.415	0.553	1.348	0.919	1.124	0.960
Swindon	1.571	0.852	1.340	0.948	1.041	0.817	0.802	0.636
Peterborough	1.499	0.701	1.265	0.167	1.032	0.737	0.771	0.699

Second, the range of the plots over which these regressions are made may be reduced, therefore cutting off, or eliminating extreme segments and omitting outliers. The first of these, that of constrained regressions, will now be applied to each empirical data set, with results of fitting equations (4.12) and (4.13) in this manner presented in Table 6.4. With this method, the fractal dimensions generated for the count and densities now greatly differ. In general, the performance of the estimates (r^2) improves for the density profiles and worsens slightly for the counts.

As expected and designed, most fractal dimensions generated now fall within the range $1 < D < 2$. The exceptions are the urban count profiles for Bristol 1981 (2.012), and Peterborough 1981 (2.050) and 1991 (2.058). These are due to the fact that the intercept values, which have to be fixed in advance, are always approximations to an unknown value which would ensure that the constraints were met. In fact, it is likely that the intercept values used should be higher and thus this would lower the dimensions a little in all cases, enough to keep all values within the desired range.

The order of fractal dimensions between land uses in this way now corresponds much more closely to those calculated from space-filling equations (4.9) and (4.11) and presented in Table 6.2. The order for the 1981 and 1991 data for both count and density land uses categories in terms of D is urban > built-up > residential > non-residential. With respect to changes over time, dimensions for urban, built-up and residential again increase, while dimensions for non-residential in all, except Norwich, decrease. As regards dwelling type, the rank order is consistent between the time periods but variable between settlements.

It must be stressed that although these changes in density gradients over time in Table 6.4 are remarkably consistent, the r^2 measures do not always approach 1.00, and therefore significance may not always be over the 95% confidence limits. However, this is precisely why it makes sense to model relationships using only sub-sets of the data. The fractal modelling of partial data sets will be the subject of the next section.

6.6 Modelling Partial Data Sets

The second method of refining the fractal dimensions involves cutting down the set of empirical observations which constitute the population density and count profiles. In terms of a theory of the fractal city (Frankhauser, 1994; Batty and Longley, 1994), if such cities are generated according to some diffusion about a seed or core site (as historic cities in the industrial and pre-industrial ages clearly were), then it is likely that the profiles observed show departures from inverse distance relations in the vicinity of the core and periphery. Around the core, population has been displaced while on the periphery the city is still growing and thus the inverse relation will be distorted. Since the urban structure is not here "complete", it is standard practice to exclude observations in both of these areas and in previous work (Batty *et al.*, 1989; Batty and Kim, 1992), dimensions have been considerably refined by such exclusions. The problems of measuring density around the urban core can be illustrated by the profiles for each of the four dwelling type categories in Figures 6.45 to 6.48. In these graphs, density of land use is at its highest in the first 5 or 6 concentric zones. Apart from maybe terraced housing, this is intuitively incorrect. Unfortunately due to the use of mutually-exclusive land uses for discrete pixels, along with the modelling parameters of the inverse power function, this is unavoidable, but can be controlled if these first zones around the central seed are eliminated. In the case of Bristol, this

issue is further complicated by physical barriers to urban development due primarily to the river gorge that cuts through the city. Accordingly, count and density relations are fitted to their various linear segments of these convoluted density profiles. Figures 6.37 to 6.40 for count and Figures 6.45 to 6.48 for density, illustrate the way profiles have been partitioned for all dwelling types.

Taking a particular case may clarify the effects of using partial data sets. The count estimates for Bristol 1981 and 1991 (Figures 6.33a to 6.40a) have characteristic profiles for each of the land uses, and reveal a single break in slope. The basic pattern is that most categories accumulate slowly up to the gorge area of the city and then suddenly increase, thereby producing fractal dimensions greater than those generated by the simpler occupancy equations (4.9) and (4.11). For some land uses, particularly non-residential, this pattern is reversed in that the break in slope is from steep to less steep when the gorge is encountered (Figure 6.36a).

Tables 6.5 (count) and 6.6 (density) present the results of applying equations (4.12) and (4.13) to individual segments of each data set, where these segments are identified by a range of concentric zones. Many of the regressions emphasize the steepest parts of the profiles and yield dimensions greater than 2 (eg. counts for Bristol 1981 urban between zone 2 and 238, and Swindon detached between zone 10 and 74; and also densities for Swindon 1881 urban between zone 11 and 83, and Peterborough 1981 residential between zone 46 and 88). These dimensions over 2 illustrate yet again the effects of physical constraints on urban development on most notably, Bristol. In most of the partial counts and densities, the fractal dimensions of outer zone ranges are substantially lower than those closer to the urban core. For example in the Norwich 1981 built-up category (Table 6.5a), the fractal dimension of the inner zone range is 1.792, but only 0.152 for the outer range. The reasons for this, illustrated by all the plots showing absolute values (Figures 6.3a to 6.26a), is that most counts and densities assume much flatter profiles on the urban periphery. Constrained regressions are less meaningful in this context although these can still be considered relevant for the portion of the curves considered. However, these are not included.

Table 6.5 Dimensions Associated with Partial Population Counts

a. Urban Definitions, 1981 and 1991

Urban						
	1981			1991		
Settlement	Zone Range		D	r^2	Zone Range	D	r^2
Bristol	2 - 238		2.032	0.990	2 - 238	1.912	0.988
	239 - 350		1.016	0.979	239 - 350	0.935	0.971
Norwich	2 - 178		1.941	0.991	2 - 178	1.933	0.997
	179 - 352		0.426	0.970	179 - 358	0.518	0.975
Swindon	2 - 223		1.888	0.996	13 - 223	1.895	0.994
	234 - 277		0.616	0.925	13 - 279	1.807	0.989
Peterborough	2 - 131		1.940	0.998	2 - 131	2.000	0.994
	132 - 243		0.577	0.970	132 - 247	0.609	0.965
Built-up							
	1981				1991		
Settlement	Zone Range		D	r^2	Zone Range	D	r^2
Bristol	2 - 35		1.702	0.980	2 - 35	1.203	0.987
	36 - 215		2.999	0.972	36 - 215	2.870	0.980
	216 - 321		0.732	0.953	216 - 321	0.764	0.957
Norwich	2 - 170		1.792	0.997	2 - 170	1.814	0.996
	171 - 316		0.152	0.945	171 - 319	0.262	0.966
Swindon	2 - 163		1.959	0.996	2 - 163	1.599	0.989
	164 - 237		0.463	0.863	164 - 219	0.472	0.889
Peterborough	2 - 141		1.873	0.977	2 - 141	1.840	0.984
	142 - 204		0.087	0.885	142 - 218	0.142	0.887

Table 6.5 Dimensions Associated with Partial Population Counts (cont.)

a. Urban Definitions, 1981 and 1991 (cont.)

	Residential					
	1981			1991		
Settlement	Zone Range		D	r^2	Zone Range	D	r^2
Bristol	2 - 35		1.702	0.980	2 - 35	1.203	0.987
	36 - 215		2.907	0.977	36 - 215	2.768	0.982
	216 - 321		0.767	0.947	216 - 321	0.809	0.953
Norwich	2 - 170		1.717	0.997	2 - 170	1.750	0.995
	171 - 316		0.159	0.937	171 - 319	0.266	0.957
Swindon	2 - 163		1.866	0.996	2 - 163	1.574	0.996
	164 - 237		0.532	0.857	164 - 239	0.669	0.908
Peterborough	2 - 141		1.773	0.983	2 - 141	1.738	0.989
	142 - 204		0.076	0.830	142 - 217	0.146	0.893
	Non-Residential					
	1981			1991		
Settlement	Zone Range		D	r^2	Zone Range	D	r^2
Bristol	11 - 95		2.405	0.994	11 - 95	2.155	0.916
	96 - 258		0.899	0.976	96 - 268	1.064	0.956
Norwich	2 - 55		1.926	0.974	2 - 55	1.936	0.975
	56 - 246		0.454	0.878	56 - 247	0.558	0.911
Swindon	2 - 40		1.637	0.970	2 - 40	1.715	0.997
	41 - 146		0.688	0.955	41 - 218	1.024	0.982
Peterborough	2 - 63		1.448	0.991	2 - 63	1.488	0.992
	64 - 135		0.374	0.938	64 - 144	0.245	0.967

Table 6.5 Dimensions Associated with Partial Population Counts (cont.)

b. Dwelling Type, 1991

	Detached			Semi-Detached		
Settlement	Zone Range		D	r^2	Zone Range	D	r^2
Bristol	7 - 155		1.891	0.968	2 - 30	0.905	0.968
	156 - 320		0.747	0.978	30 - 156	3.030	0.984
					156 - 309	1.467	0.964
Norwich	11 - 156		1.676	0.983	9 - 164	1.651	0.977
	157 - 316		0.335	0.915	164 - 316	0.194	0.783
Swindon	10 - 74		2.410	0.994	2 - 187	1.509	0.990
	75 - 184		0.841	0.954	187 - 227	0.367	0.852
Peterborough	5 - 113		1.642	0.975	2 - 138	1.583	0.992
	114 - 204		0.237	0.720	138 - 213	0.193	0.694
	Terraced				Apartments		
Settlement	Zone Range		D	r^2	Zone Range	D	r^2
Bristol	2 - 173		1.786	0.998	4 - 32	0.854	0.998
	174 - 286		0.549	0.949	32 - 155	2.637	0.987
					156 - 298	0.694	0.975
Norwich	6 - 59		2.535	0.994	8 - 123	1.426	0.976
	60 - 102		1.231	0.987	124 - 262	0.398	0.949
	103 - 243		0.279	0.834			
Swindon	2 - 182		1.348	0.991	2 - 67	1.144	0.986
	183 - 221		0.385	0.875	68 - 132	1.766	0.990
					133 - 184	0.938	0.923
Peterborough	4 - 42		0.607	0.974	2 - 50	0.914	0.998
	43 - 89		4.808	0.996	51 - 122	2.297	0.976
	90 - 205		0.386	0.770			

Table 6.6 Dimensions Associated with Partial Population Densities

a. Urban Definitions, 1981 and 1991

Urban						
	1981			1991		
Settlement	Zone Range		D	r^2	Zone Range	D	r^2
Bristol	20 - 72		1.083	0.955	13 - 60	1.309	0.960
	73 - 177		2.816	0.964	162 - 350	1.234	0.952
	209 - 350		1.065	0.964			
Norwich	6 - 16		1.504	0.986	3 - 145	1.942	0.945
	18 - 49		2.624	0.922	146 - 358	0.646	0.987
	145 - 352		0.577	0.985			
Swindon	3 - 46		1.678	0.914	11 - 83	2.105	0.888
	127 - 208		1.562	0.978	84 - 245	1.501	0.974
Peterborough	9 - 92		1.898	0.472	25 - 92	1.774	0.964
	93 - 243		0.907	0.946	93 - 247	0.928	0.946
Built-up							
	1981			1991			
Settlement	Zone Range		D	r^2	Zone Range	D	r^2
Bristol	4 - 36		1.755	0.407	2 - 36	1.136	0.962
	37 - 165		2.816	0.883	62 - 153	2.908	0.820
	180 - 321		1.065	0.967	180 - 321	0.954	0.971
Norwich	3 - 110		1.695	0.798	3 - 108	1.867	0.670
	111 - 316		0.430	0.984	146 - 358	0.522	0.984
Swindon	2 - 16		1.493	0.951	17 - 139	1.411	0.990
	144 - 237		0.663	0.972	140 - 219	0.699	0.979
Peterborough	10 - 46		1.180	0.984	3 - 49	1.532	0.945
	47 - 88		3.200	0.992	50 - 92	2.891	0.992
	93 - 204		0.600	0.956	96 - 218	0.661	0.949

Table 6.6 Dimensions Associated with Partial Population Densities (cont.)

a. Urban Definitions, 1981 and 1991 (cont.)

Residential						
	1981			1991		
Settlement	Zone Range	D	r^2	Zone Range	D	r^2
Bristol	2 - 36	1.073	0.815	2 - 36	1.195	0.971
	37 - 167	1.645	0.882	37 - 161	2.998	0.891
	176 - 321	1.727	0.956	180 - 321	1.005	0.965
Norwich	3 - 103	1.760	0.990	3 - 103	1.820	0.771
	109 - 316	0.465	0.981	109 - 319	0.542	0.982
Swindon	2 - 15	1.452	0.979	4 - 144	1.550	0.946
	143 - 237	0.776	0.956	145 - 239	0.876	0.953
Peterborough	11 - 46	1.127	0.988	3 - 50	1.479	0.956
	47 - 88	2.771	0.977	83 - 94	2.617	0.992
	93 - 204	0.650	0.938	95 - 217	0.719	0.933
Non-Residential						
	1981			1991		
Settlement	Zone Range	D	r^2	Zone Range	D	r^2
Bristol	2 - 27	1.259	0.952	2 - 13	0.396	0.997
	28 - 87	2.602	0.955	14 - 102	2.892	0.888
	90 - 258	0.923	0.982	103 - 268	1.015	0.954
Norwich	2 - 8	1.442	0.955	2 - 8	1.442	0.955
	9 - 21	2.669	0.910	9 - 21	2.672	0.908
	22 - 246	0.642	0.980	22 - 247	0.750	0.977
Swindon	3 - 11	0.861	0.989	3 - 31	1.744	0.862
	12 - 18	2.535	0.918	41 - 218	1.020	0.981
	19 - 146	0.943	0.957			
Peterborough	3 - 35	1.464	0.982	6 - 60	1.389	0.980
	36 - 135	0.907	0.990	61 - 144	0.256	0.999

Table 6.6 Dimensions Associated with Partial Population Densities (cont.)

b. Dwelling Type, 1991 (cont.)

	Detached			Semi-Detached		
Settlement	Zone Range	D	r^2	Zone Range	D	r^2
Bristol	2 - 39	1.100	0.946	6 - 30	0.699	0.999
	40 - 156	2.428	0.916	31 - 155	3.039	0.872
	157 - 320	0.741	0.993	180 - 321	1.479	0.763
Norwich	11 - 38	2.356	0.898	9 - 26	2.738	0.968
	39 - 316	1.043	0.929	109 - 319	1.116	0.912
Swindon	9 - 75	2.409	0.838	4 - 158	1.467	0.909
	143 - 237	0.829	0.977	159 - 227	0.855	0.939
Peterborough	20 - 47	1.395	0.646	2 - 102	1.525	0.938
	48 - 75	2.537	0.882	128 - 213	0.362	0.976
	76 - 204	0.759	0.931			
	Terraced			Apartments		
Settlement	Zone Range	D	r^2	Zone Range	D	r^2
Bristol	2 - 174	1.786	0.901	4 - 32	0.853	0.999
	175 - 286	0.542	0.993	33 - 110	2.877	0.885
				154 - 298	0.700	0.992
Norwich	6 - 63	2.535	0.896	3 - 25	1.527	0.614
	64 - 243	0.603	0.967	8 - 21	0.889	0.971
Swindon	11 - 131	1.231	0.966	2 - 144	1.239	0.967
	132 - 221	0.841	0.968	41 - 218	0.654	0.987
Peterborough	3 - 42	0.602	0.996	2 - 50	0.914	0.999
	43 - 91	4.788	0.989	69 - 81	4.318	0.939
	92 - 205	0.354	0.988	82 - 122	1.494	0.866

Reducing the range of density profiles however, is likely to provide more significant and relevant results. This is most expected for the density profiles which are, in many cases, heavily distorted in a characteristic manner over all land uses (see especially Figures 6.30 to 6.32). Generally speaking, the more convoluted the density profiles, the more its gradient will be partitioned. For instance, the detached, semi-detached and apartments profiles of Bristol (Figures 6.45a, 6.46a, 6.48a, respectively, and Table 6.6b) have all been dismembered into three segments, as have the profiles for detached, terraced and apartments of Peterborough (Figures 6.45d, 6.47d, 6.48d, respectively, and Table 6.6b). The reasons for so many partitions again seem to be due to factors which either constrain development (the Avon Gorge in Bristol), or factors that promote specific patterns of development (transport routes in Peterborough). In all cases, density profiles are partitioned into linear segments at breaks in slope that are most visually apparent. Each of these segments can then be fitted, as in the linear regression models, using equation (4.12). Finally, in Tables 6.5 and 6.6, fractal dimensions are generally lower than expected, that is, nearer 1 than 1.7, while the positive, or increasing, density segments of the profiles produce dimensions greater than 2. However, the model fits are good, with most r^2 values greater than 0.8 and many over 0.95. The exceptionally low r^2 values are all for the density plots, including Bristol 1981 built-up (0.407), and Norwich apartments (0.614). These could be the result of either too few zones or a misjudgement of the breaks in slope. Nevertheless, all that this analysis of partial data sets serves to do is to demonstrate that where physical constraints have a major effect on urban development, it becomes exceptionally difficult to unravel the effect of distortions at the core and the periphery. These distortions still need to be excluded if the equilibrium fractal dimensions are to be measured reliably.

6.7 Comparisons with Urban Boundary Data

The potential for using classified satellite data in urban modelling can be further strengthened by a comparison with a digital data set that is widely used for representing urban areas. This alternative source is derived from the 1991 Urban Areas Database commissioned by the Department of Environment, which contains urban boundary information in digital vector-based data structures. The principal uses of these data have been targeted with mapping software in order to display results from the 1991 UK Population Census. They may, of course, be used to

display a wide variety of other information as thematic maps, and to support the use of geographical information systems. Both data sets, satellite and urban boundary, are easily available for all parts of England and Wales, and are in a digital form that facilitates rapid computer handling and statistical modelling. Also, both can be regarded as more precise and more accurate sources for handling and mapping urban information, and a move away from conventional analogue representations.

Using the OPCS/DoE definitions of "urban" (Chapter One), these urban boundaries were identified using 1991 1:10,000 Ordnance Survey Series maps in conjunction with 1991 Population Census ED base maps. For land to qualify as "urban", a minimum of four contiguous EDs were needed. The boundaries were then reduced to a scale of 1:50,000, and digitised to an accuracy of 0.5mm permitting inaccuracies of up to 25m on the ground. The digitising process was manually supervised in point mode with a weed tolerance of 2.54mm. However, three sources of error exist in the database, namely, errors inherent in the two base maps, error created by the transfer of the urban areas between the two map scales, and errors related to manual digitising. Although this data set corresponds to the 1991 Census, it has only now (1994) become available for general access. The delay has not been because of the difficulty of the task of digitising, nor because of the time needed for the development of interface software. Instead, it has been because of two factors dealing with the need for quality assurance and problems in negotiating the purchase of the data with suppliers on behalf of a large community of users. In particular, suppliers have been too reticent over guarantees that users in academia should only handle these data for non-profit applications.

For the purpose of direct comparisons with classified imagery, urban boundary data for each of the settlements are accessed and downloaded from the DBD91 (digital boundary data 1991) database held at Manchester Computing Centre via the 'gopher' on the CS6400 (see section on census retrieval in Chapter Five) as a single Arc/Info export coverage. This coverage is then partitioned into four subsections, where each subsection represents one of the four settlements within spatial coordinates that are consistent with those used for the classified satellite data. Next, each Arc/Info subsection coverage is rasterised to cell dimensions that reflect the degree of spatial precision at the time of digitising. In each case, this was 25m. This conversion from a vector-based data structure to a raster-based representation is essential to force the urban boundary data sets to conform to the input requirements of the cell-based

fractal models. It is duly noted that rasterisation causes a less precise representation as well as the possibility of a reduction in accuracy. However, these are the inevitable difficulties that must be faced when attempting to compare information directly between different data structures. Ideally, a fractal model should be created that accepts all spatial data regardless of format. This is a matter for future research.

Table 6.7 Area/Perimeter Relationships

	Classified Satellite Imagery			Urban Boundary Data		
Settlement	Points	Area(m^2)	Perimeter(m)	Points	Area(m^2)	Perimeter(m)
Norwich 1991	48,673	43,805,700	419,940	65,421	58,696,273	197,575
Swindon 1991	33,701	30,330,900	235,800	44,180	39,944,657	112,493
Peterborough 1991	30,100	27,090,000	213,780	42,730	38,666,757	103,497

Nevertheless, the comparisons between satellite imagery and the urban boundary database outlined in the rest of this section are certainly still valid, if only to demonstrate the differences in the way urban land is defined. Indeed, an initial comparison of simple area/perimeter relationships for three of the four settlements quickly suggests inherent dissimilarities in the way urban land is being detected and measured (Table 6.7). The comparison excludes the Bristol case, simply because the study area only examined part of the city and both data sets would be incomplete. For the other three settlements, the classified satellite imagery are being represented by the built-up category, which was demonstrated in Chapter Five to be the most accurate and representative classification of the spatial extent of urban development. Although, a specific urban land use category was classified in the image analysis, this was unable to replicate the entire OPCS/DoE criteria of "urban", and was shown to be less accurate by the ground survey.

The first comparison that can be made from Table 6.7 is in the identical ranking of settlements based on the number of points (cells), the area represented as urban, and the length of the perimeter of this area. This similarity gives qualified support to the consistency in the way satellite images have been classified. However, the most striking dissimilarities are in the ratios of area to perimeter. The areas of the settlements represented by the urban boundary data are consistently larger than those from the classified satellite imagery.

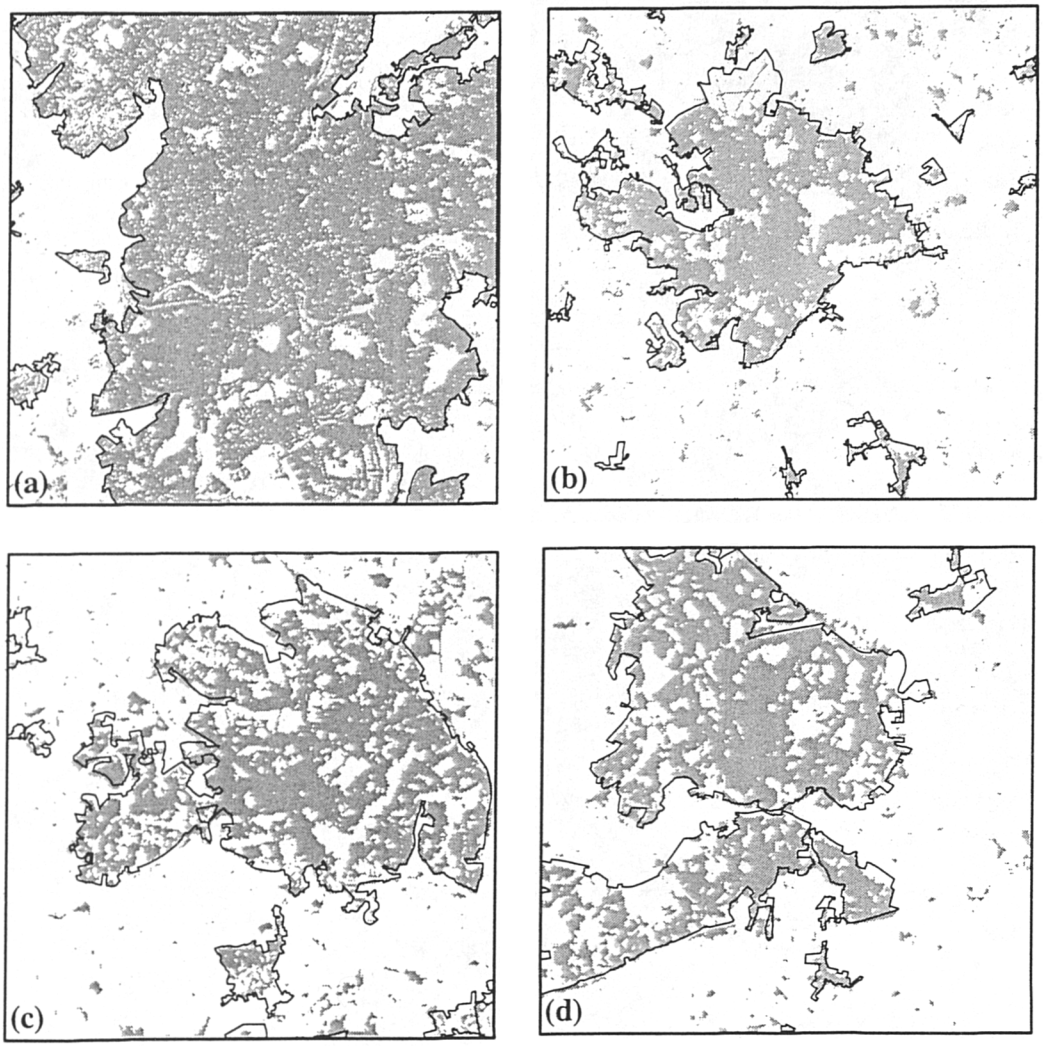

Figure 6.49 Comparisons between Urban Boundary Data and Classified Satellite Data
(a) Bristol, (b) Norwich, (c) Swindon, (d) Peterborough

Conversely, the length of perimeters are consistently shorter than ones measured from satellite data. Although the actual area/perimeter ratios are not shown in Table 6.7, these crude comparisons seem to suggest that settlements represented by classified satellite data are more stringently defined, with the ability to detect 'holes' in the urban fabric, rather than simply 'envelopes' from the boundary data. This fundamental difference between the two data sets can be illustrated by simple common-registration overlays for all four settlements in Figure 6.49. Here, 'holes' within the urban fabric are represented as intra-urban land that is unoccupied by human construction by classified imagery, while 'envelopes' are entire unbroken urban blocks and represented by boundary data. Whether urban holes should be considered as part of the urban landscape is obviously a matter of interpretation, but by using classified imagery interpretation certainly becomes much more flexible. The overlays further show many similarities between the two data sets in the way urban land is spatially delineated, especially for Bristol in Figure 6.49a. Conversely, disagreements in boundaries are also evident, not more so than in the south-west quadrant of the Norwich area (Figure 6.49b). Finally, it can be noticed that in the classified satellite data sets, there are many more clumps of urban pockets outside the main settlements. These pockets are isolated buildings and farms which are too small to constitute as urban land in the DoE database.

More objective comparisons can be determined by exposing the urban boundary data to the same fractal models that were used on the classified satellite data (Table 6.8). The fractal dimensions generated from the classified satellite imagery are consistently lower than those produced from the urban boundary data. This consistency seems to suggest that although each data set has a different definition for urban, this difference is maintained for all settlements. The lower fractal dimensions associated with satellite data are also an indication of its ability to generate more restrictive definitions of urban land, which, unlike urban boundary data, take into account pockets or holes (such as open space and difficult relief) in the urban fabric. Furthermore, and again unlike the urban boundary data, satellite imagery are amenable not only to the production of simple urban/rural contrasts but also to a disaggregation of the urban morphology into various other land uses. Also, the routine and rapid means of classifying satellite data, along with a greater temporal flexibility, allow satellite data to be used as a robust and dynamic model for detecting and measuring urban land morphologies and land use change.

Table 6.8 Comparisons Between Urban Boundary Data (UBD) and Classified Satellite Data in all Model Estimations

a. Space-Filling Dimensions Based on Occupancy

	Count		Density	
Settlement	Image	UBD	Image	UBD
Bristol 1991	1.781	1.788	1.797	1.804
Norwich 1991	1.766	1.803	1.780	1.822
Swindon 1991	1.702	1.765	1.709	1.780
Peterborough 1991	1.731	1.808	1.742	1.828

b. Dimensions From Regression

	Classified Satellite Imagery			Urban Boundary Data		
Settlement	D	r^2_{count}	$r^2_{density}$	D	r^2_{count}	$r^2_{density}$
Bristol 1991	2.262	0.966	0.274	2.271	0.970	0.314
Norwich 1991	1.508	0.953	0.682	1.578	0.950	0.577
Swindon 1991	1.520	0.984	0.861	1.557	0.976	0.768
Peterborough 1991	1.713	0.976	0.536	1.889	0.974	0.113

c. Dimensions From Constrained Regression

	Image (Count)		UBD (Count)		Image (Density)		UBD (Density)	
Settlement	D	r^2	D	r^2	D	r^2	D	r^2
Bristol 1991	1.936	0.826	1.977	0.845	1.720	0.292	1.720	0.325
Norwich 1991	1.908	0.830	1.961	0.847	1.692	0.429	1.745	0.348
Swindon 1991	1.931	0.800	1.995	0.800	1.699	0.540	1.763	0.411
Peterborough 1991	1.903	0.922	1.981	0.979	1.672	0.614	1.749	0.257

Given the potential of remotely-sensed data and their rapidly evolving classification techniques, claims made by the DoE that see vector data as the most sound and practical means of defining the extent of urban areas may be questioned.

6.8 Summary & Conclusions

The purpose of this chapter has been to demonstrate the power of integrating remote sensing and GIS in a practical urban application. Chapters One, Two, Three and Five all examined the way urban land use could more readily and consistently be detected by accessing the 'value-added' element from the integration of population surfaces with satellite imagery. This chapter has taken the results of this urban mapping methodology and, using the theoretical foundations of fractal-led density functions from Chapter Four, applied them to the empirical analysis of the spatial characteristics and profiles of four settlements in the United Kingdom.

From the results of these analyses a number of conclusions may be drawn. To begin, classified satellite data provide an invaluable means of detecting urban land use, which can become even more profitable when used as the basis for intensive modelling. All fractal dimensions and profiles documented in this chapter have been generated routinely by spatially extensive, multitemporal, digital remotely-sensed data. There is no other data set which has such properties of generality and allows the production of consistent land use classifications for various types of settlements to be explored through time. The closest 'state of the art' alternative is, perhaps, the vector-based urban boundary data set from the DoE. Although seemingly more precise, these data are only able to provide a measure of urban/rural contrast, which suffers from both a highly subjective definition of urban, and the problems associated with manual digitising. Furthermore, as these data are produced in association with the Population Census, they are only available every ten years.

Using both classified satellite imagery and the fractal dimensions subsequently produced, have enabled changes in the spatial form and density of the four test settlements to be described and explained within established fractal theories of growth dynamics (Vicsek, 1989). Furthermore, classified satellite imagery are also able to illustrate distinctive detailed characteristics in the profiles of urban areas. Many of these characteristics are as much a result of the fine resolution of the satellite data, as a symptom of local constraints in urban development arising from factors such as physical barriers and restrictive planning policies. The general pattern in these profiles seems to suggest that density in the four settlements is increasing throughout but becoming flatter, or tapering off, as a result of particular expansions in development on the periphery.

There are many policy implications stemming from this work, particularly involving accessibility and energy uses, as well as questions of social and economic segregation, and the effects of physical and planning constraints. The existence of remotely-sensed data and advances in their land use classifications will speed progress towards the goal of understanding how cities fill the space available to them, and how distortions to this process due to policy intervention might affect issues of spatial efficiency and equity. These implications, however, lie beyond the scope of this thesis. Moreover, it is important to stress that this thesis is primarily concerned with the issues of remote sensing/GIS integration for human geographers, and less of a discussion on the particular historical and contemporary features and processes in localised urban geography.

Chapter Seven
CONCLUSIONS

7.1 Summary

The development of geographical information systems (GIS) can be in part accredited to the field of remote sensing. From this beginning there was a quick realisation of the immense potential that could be gained from integrating remotely-sensed data with data and technology from GIS. Research has examined both the technical impediments to integration as well as various empirical applications. However, an assessment of these applications reveals a distinct lack of research in the area of urban spatial recognition and analysis. Indeed the development of the DoE Urban Database still maintains the view of GIS and remote sensing as separate technologies in the delineation of settlements, when in fact they can be highly complementary. There is considerable potential for a closer parallel and symbiotic development GIS and remote sensing in urban geography, particularly in terms of data formatting, positional integrity, statistical analyses and classification compatibility. With these issues in mind, this thesis has examined how spatial data handled by a GIS and remote sensing can be simultaneously developed to address problems in the way urban land is defined, measured, classified and analysed. In particular, it investigated how urban land use can be more effectively, frequently and consistently detected and measured using a classification strategy that integrates land observation satellite images with socioeconomic information. The strategy, outlined in Chapter Three, was the first to harness the potential of disaggregate surface models of socioeconomic data for improving the classification of remotely-sensed images of urban areas. This improvement focused on the selection of training samples for class signatures, postclassification sorting of erroneous pixels, and most importantly, the adoption of a Bayesian-type classifier where Census data are used to generate *a priori* probabilities of class membership.

Once the classification strategy was developed it was then used, in Chapter Five, to demonstrate the generation of a series of land use categories from eight satellite images representing four settlements taken around the 1981 and 1991 Censuses. The number and choice of settlements were determined by both image availability, as well as, for the sake of comparison, selections made by previous work in this field. The categories "urban", "built-up", "residential", and "non-residential" were classified for

both dates using a combination of conventional spectral density slicing along with training sample selection and postclassification sorting. These methods were again applied to generate a further four categories pertaining to the type of dwelling, for the higher quality 1991 images. The classification of these images also benefited from greater information on dwelling types from the 1991 Census which was fully exploited by the Bayesian-type classifier. The level of utility derived from the use of the Bayesian method was measured by an intensive accuracy assessment based on a detailed ground and areal photography survey.

The increase in land use accuracy from the deployment of the classification strategy was followed by a general assessment of the role of remotely-sensed information in fractal-led urban density functions in the second part of the thesis. This assessment began in Chapter Four where theoretical modifications to the inverse power function using fractal concepts were coupled with a discussion of the comparative merits of classified satellite imagery over other urban data sources. Initial empirical analyses suggested that the fractal dimensions of the English town of Taunton, represented by remotely-sensed data, were well within the range for the idealised 'fractal city' (Vicsek, 1989, Frankhauser, 1994, Batty and Longley, 1994). In other words, classified satellite data were able to capture those self-similarity properties of fractal patterns widely viewed as intrinsic characteristics of urban form. It was also recognised that the more detailed, reliable and consistent land use inventory derived from remote sensing was a more extensive and efficient means of measuring various land use patterns of urban morphologies. These claims were comprehensively assessed in Chapter Six, where the fractal modelling of classified satellite data for four settlements- Bristol, Norwich, Swindon, and Peterborough, produced a host of insightful results and comparative analyses. In particular, it highlighted the effects of urban growth and changes in the density of urban development as measured by land use types from a single settlement, from different settlements, and through time.

7.2 Results

The value of the thesis can perhaps be most comprehensively measured by two sets of empirical results. One set on the accuracy of the classification strategy, the other set on how well the fractal dimensions and profiles, generated from classified images, fit the established theories of the fractal city, giving a deeper insight into the spatial characteristics of urban morphologies.

The classification strategy adopted in the thesis produced an overall acceptable level of urban land use detection. Highly significant accuracies were accredited to the classification of the "built-up", and "residential" categories, and supported results from established work by Haack *et al.* (1987); Harrison and Richards (1987); and Barnsley *et al.* (1993). However, the low levels of accuracy associated with the "urban" and "non-residential" categories were attributable to the subjective definitions for classification and the lack of representative non-residential data, respectively. In the case of the "urban" land use, an attempt was made to conform to the strict bureaucratic definitions set by the DoE, which were proved to be beyond the capabilities of current spectral pattern recognition. The "non-residential" category was also poorly classified, but this was simply a result of the inability of the surface models to represent activities other than those based on 'night-time' or residential measures of human presence. However, the most insightful classification results were those that assessed the merits of a Bayesian approach against the conventional maximum likelihood discriminant function. In each of the four dwelling type categories, the Bayesian-type classifier consistently out-performed its equal prior probability alternative in both assessments of locational accuracy and class areal estimation.

The other set of empirical results involved the application of the fractal models outlined in Chapter Four to all the classified land uses for both time points. When compared to fractal dimensions generated from other data sources, those from remote sensing were generally lower, but still consistently fell within the expected boundaries of the theoretical 'fractal city' (Vicsek, 1989; Frankhauser, 1994; Batty and Longley, 1994). This propensity for lower dimensions was only discernible due to the finer resolution of satellite imagery over more conventional zonal based socioeconomic data representations. With this finer spatial resolution, greater detail and irregularity in urban morphologies were also captured by density profiles for all types of land uses. Graphical comparisons of these profiles highlighted the general flattening of density gradients, the existence of urban craters around the CBD, and the contortion effects of physical impediments to urban development.

7.3 Conclusions

The most fitting way to conclude this thesis is to evaluate of how well the research

objectives made right at the beginning were fulfilled. The first of these statements hoped to explore the potential of linking satellite data with surfaces of socioeconomic information. This objective culminated in the successful design, development and implementation of the three-point classification strategy. The strategy demonstrated the immense benefits to urban mapping that could be derived from the efficient integration of physical-based land cover data from remote sensing with aspatial socioeconomic attributes pertaining to land use held by a GIS. Although the whole issue of remote sensing/GIS integration has been a matter of intensive research over the last decade and a half, very few studies have specifically explored the role of disaggregate models of socioeconomic data in the classification of satellite imagery. Furthermore, fewer still have attempted to harness the intuitive and statistical benefits of the Bayesian modification to the parametric maximum likelihood discriminant function with non-parametric prior probabilities. What this thesis has shown is that by careful consideration of the objective prior probabilities of socioeconomic indicators, a more informed maximum likelihood classification can be implemented. This application of the Bayesian approach to urban mapping represented the second research goal. Its fulfilment demonstrated that, given reliable ancillary information, the per-pixel classification of urban areas has enough scope for improvement. Furthermore, although there is currently on-going research in the classification of urban areas at the sub-pixel level, a methodology which couples the vast amounts of socioeconomic information at this level of measurement has yet to be established. Proposals for further research in this particular area are outlined in the next section.

The third research direction was concerned with the subsequent application of satellite imagery, once classified by the strategy. In particular, it examined the role of satellite data in the empirical testing of fractal-led urban density functions for the monitoring of urban form, growth and morphological changes. In effect, two questions were posed. One on the relative merits of using classified satellite data over other sources, and the other on the contribution of satellite data to the empirical testing of the 'fractal city'. Although these questions will now be covered separately, they are obviously interrelated.

The first of these concerns the role of classified satellite imagery in the application of urban density functions. Throughout the thesis, this role was considerably emphasised given the state of available alternatives, with particular reference to extensive spatial coverage, multidimensionality, and temporal flexibility and

consistency. Furthermore, as a digital product, satellite imagery were seen as more conducive to intensive and routine modelling, a feature that perhaps could only be matched by data from the DoE digital Urban Areas Database. Indeed as a vector-based representation, boundary information from this database was seen as the closest alternative, and even a better source in terms of precision. Nonetheless, it distinctly lagged behind remote sensing technology in its ability to define sub-categories of urban, the errors introduced from digitising, and its restricted availability to the 10-year Census cycle.

A widely recognised focus within contemporary urban theory concerns the evolution of cities. Another aspect of the third research statement dealt with how remotely-sensed imagery can be seen as the database on which such dynamics of the city can be truly developed in fractal terms (Dendrinos, 1992; Longley and Batty, 1993). For changes in fractal dimension through time, fractal theory is well worked out in terms of growth dynamics (Vicsek, 1989) but there remains more work to be done on how the morphologies of individual land uses coalesce to produce more aggregate morphologies of urban development.

Furthermore, the theory of the fractal city still requires extensive empirical testing through the development of typologies based on different urban morphologies as well as different urban land uses. The empirical data for these typologies were generated by the classification of eight urban land use categories representing four settlements-Bristol, Norwich, Swindon, and Peterborough. By examining and comparing the results of the fractal properties and density profiles of each of these land uses for each settlement, valuable insights have been made into the measurement of urban form and structure. Furthermore, temporal perspectives allowed these results to help evaluate urban changes which have direct repercussions on the estimated levels of suburbanisation, decentralisation of economic functions, and segregation of urban land uses. What the results from the four study settlements have suggested were that both suburbanisation and decentralisation, although very much apparent, are only minor processes at work in the make-up of urban morphologies during the last decade. Instead, more pronounced variations in the characteristics of settlements are exerted by physical and planning constraints, and the juxtapositioning of urban land uses.

In retrospect this thesis has shown how key interactions between GIS and remote

sensing can produce measurements of different land uses that are amenable to routine analysis and insightful interpretation by fractal models. The ultimate quest perhaps is the formulation of classification algorithms that can further improve on the capture of intricate variabilities in the urban landscape, together with a deeper understanding of how urban processes lead to cities of different shapes and densities. For now, this thesis has demonstrated the active role of fractal models based on classified satellite data across both space and time. Because of this, urban geography has been reinvigorated by an approach that has produced a more flexible geometry of urban land use patterns, and one in which urban processes can be carefully monitored by reliable and consistent satellite-derived information.

7.4 Future Work

The immediate line of research that needs to be continued is the exploration of further means of linking socioeconomic information with remotely-sensed data within a GIS framework. This time perhaps, applying socioeconomic data to the classification of satellite imagery at the sub-pixel level, which employ techniques such as fuzzy set theory and neural networks. There is also the possibility of using socioeconomic-related data other than those from the Population Censuses. Possible alternative sources include postcodes from the Central Postcode Directory, digitised urban boundary data from the DoE Urban Database, and Address-point information from the Ordnance Survey.

On the fractal modelling side, there is as yet no formal theory as to how the fractal dimensions of individual land uses "add-up" to those of the whole. For instance, the four dwelling types defined from the 1991 data when aggregated, form the residential category. The question is 'how do the individual dimensions D_k, (k = detached, semi-detached terraced, and apartments) combine to produce $D_{residential}$?'

Further work is also foreseeable on the reconciliation of the scale at which image analysis takes place, and the scale at which models of urban morphology and land use are devised. Remotely-sensed images are themselves abstract models of real-world phenomena, which are deemed representative of land cover features at stated scales. Fractal analysis may be able to accommodate changes in the spatial resolution of these images in response to changes in the level of detail in land use categorisation

and the juxtapositioning of different land use types.

Finally, the ultimate combined quest of these areas of research must surely lie in the establishment of a comprehensive classification of morphologies based on a deeper understanding of how urban processes lead to cities of different shapes and densities.

BIBLIOGRAPHY

Alonso, W. (1964) *Location and Land Use : Toward a General Theory of Land Rent*, Harvard University Press, Cambridge, MA., USA.

Alperovich, G. and Deutsch, J. (1992) "Population density gradients and urbanisation measurement", *Urban Studies*, **29**, 1323-1328.

Anas, A. (1982) *Residential Location Markets and Urban Transportation: Economic Theory, Econometrics and Policy Analysis with Discrete Choice Models*, Academic Press, New York, NY., USA.

Anas, A. and Kim, I. (1992) "Income distribution and the residential density gradient", *Journal of Urban Economics*, **31**, 164-180.

Anderson, J.R., Hardy, E.E., Roach, J.T. and Witmer, R.E. (1972) "A land use and land cover classification system for use with remote sensor data", *U.S. Geological Survey*, circular **671**.

Arlinghaus, S.L. (1985) "Fractals take a central place", *Geografiska Annaler*, **67B**, 83-88.

_____ (1993) "Central place fractals: theoretical geography in an urban setting", in *Fractals in Geography*, Lam, N.S-N. and De Cola, L. (eds), Prentice-Hall, Englewood Cliffs, NJ, USA, 213-227.

Aronoff, S. (1982) "Classification accuracy: a user approach", *Photogrammetic Engineering and Remote Sensing*, **48**, 1299-1307.

Avery, G. (1963) "Measuring land use changes on USDA photographs", *Photogrammetric Engineering*, **29**, 620-624.

Barker, G.R. (1988) "Remote sensing: the unheralded component of geographic information systems", *Photogrammetic Engineering and Remote Sensing*, **54**, 195-199.

Barnsley, M.J., Barr, S.L. and Sadler, G.J. (1991) "Spatial re-classification of remotely-sensed images for urban land-use monitoring", *Proceedings of SPATIAL DATA 2000*, Christ Church, Oxford, UK. (Nottingham Remote Sensing Society) 106-117.

Barnsley, M.J., Sadler, G.J. and Shepherd, J.W. (1989) "Integrating remotely sensed images and digital map data in the context of urban planning", *Proceedings of the 15th Annual Conference of the Remote Sensing Society*, University of Bristol, UK. (Nottingham Remote Sensing Society), 25-32.

Barnsley, M.J., Barr, S.L., Hamid, A., Muller, J-P., A. L., Sadler, G.J. and Shepherd, J.W. (1993) "Analytical tools to monitor urban areas", in *Geographical Information Handling - Research and Applications*, Mather, P.M. (ed), Wiley, Chichester, UK, 147-184.

Barr, S.L. (1992) "Object-based re-classification of high resolution digital imagery for urban land-use monitoring", *Proceedings of the XXIV Conference of the International Society for Photogrammetry and Remote Sensing (ISPRS'92)*, 2-14. International Archives of the Photogrammetry and Remote Sensing: Commission 7, Washington D.C., USA, 969-976.

Barton, H. (1992) "City transport: strategies for sustainability", in *Sustainable Development and Urban Form*, Breheny, M.J. (ed), Pion, London, UK, 197-

216.

Bassett, K. (1991) *Economic Structuring and Political Changes in the "M4-corridor": Studies of Bristol and Swindon*, PhD Thesis, Department of Geography, University of Bristol.

Batty, M. (1976) *Urban Modelling: Algorithms, Calibrations, Predictions*, Cambridge University Press, Cambridge, UK.

Batty, M. and Kim, K.S. (1992) "Form follows function: reformulating urban population density functions", *Urban Studies*, **29**, 1043-1070.

Batty, M. and Longley, P.A. (1987) "Urban shapes as fractals", *Area*, **19**, 215-221.

_____ (1988) "The morphology of urban land use", *Environment and Planning B*, **15**, 461-488.

_____ (1994) *Fractal Cities; A Geometry of Form and Function*, Academic Press, London, UK. and San Diego, CA., USA.

Batty, M. and Xie, Y. (1994a) "Urban analysis in a GIS environment: population density modelling using ARC/INFO", in *Spatial Analysis and GIS*, Fotheringham, A.S. and Rogerson, P. (eds), Taylor and Francis, London, UK. and Bristol, PA., USA, 189-220.

_____ (1994b) "Preliminary evidence for a theory of the fractal city", *Environment and Planning A* (in press).

_____ (1994c) "New technologies, land use analysis and urban form: modelling land use from remote imagery, digital data sources and ARC/INFO coverages", *Paper presented at a conference on Geographic Information and Land Use Analysis*, Birkbeck College, London, UK, 17 June.

Batty, M., Fotheringham, A.S. and Longley, P.A. (1989) "Urban growth and form: scaling, fractal geometry and diffusion-linked aggregation", *Environment and Planning A*, **21**, 1447-1472.

Battey, P. and Brown, P. (1995) "From human ecology to customer targeting: the evolution of geodemographics", in *GIS for Business and Service Planning*, Longley, P.A. and Clarke, G. (eds), Longman, Harlow, UK. (forthcoming).

Bayes, T. (1763) "An essay towards solving a problem in the doctrine of chances", *Philosophical Transactions of the Royal Society of London*, **53**, 370-418. (Reproduced in Barnard, G.A. (1958) "Studies in the history of probability and statistics, IX", *Biometrika*, **45**, 293-315.

Berger, J.O. (1985) *Statistical Decision Theory and Bayesian Analysis*, Springer-Verlag, New York, NY., USA.

Bernstein, R. (1983) "Image geometry and rectification", in *Manual of Remote Sensing*, Colwell, R.N. (ed), American Society of Photogrammetry, Falls Church, VA., USA, vol **1**, 875-881.

Blackledge, J.M. (1993) "On the synthesis and processing of fractal signals and images", in *Applications of Fractals and Chaos*, Crilly *et al.* (eds), Springer-Verlag, Berlin Heidelberg, Germany, 81-99.

Bolstad, P.V., and Lillesand, T.M. (1991) "Rapid maximum likelihood classification", *Photogrammetric Engineering and Remote Sensing*, **57**, 67-74.

Bracken, I. (1994) "Towards improved visualisation of socio-economic data", in *Visualization in Geographical Information Systems*, Hearnshaw, H.M. and

Unwin, D.J. (eds), Wiley, Chichester, UK, 76-84.

Bracken, I. and Martin, D.J. (1989) "The generation of spatial population distributions from census centroid data", *Environment and Planning A*, **21**, 537-543.

_____ (1993) "Surface representation of social change 1981-1991", *Paper presented at Research on the 1991 Census*, University of Newcastle-upon-Tyne, UK, 13 September.

Bristol City Council (1988) *The Role of Bristol City Council and Avon County Council in Economic Development*, Research Report **242**, Bristol City Council Planning Department, 41pp.

Bristol Development Corporation (1993) *A Balanced Transport Strategy for Bristol / A proposal by Bristol Development Corporation*, 18pp.

Brooner, W.G., Haralick, R.M., and Dinstein, I. (1971) "Spectral parameters affecting automated image interpretation using Bayesian probability techniques", *Proceedings of the Seventh International Symposium on Remote Sensing of Environment*, ERIM, Ann Arbor, MI, USA, 1929-1948.

Bryant, N.A., McLeod, R.G., Zorbrist, A.L., and Johnson, H.E. (1979) "California desert resource inventory using multispectral classification of digitally mosaicked Landsat frames", *Proceedings of 1979 Symposium on Machine Processing of Remotely-Sensed Data*, Purdue University, IL., USA, 69-79.

Burgess, E.W. (1925) "The growth of the city: an introduction to a research project", in *The City*, Park, R.E. and Burgess, E.W. (eds), Chicago, IL., USA.

Burrough, P.A. (1986) *Principles of Geographical Information Systems for Land Resources Assessment*, Monographs on Soil Resources Survey **12**, Oxford University Press, Oxford, UK.

Campbell, J.B. (1983) *Mapping the Land: Aerial Imagery for Land Use Information*, Association of American Geographers, Washington, D.C., USA.

_____ (1987) *Introduction to Remote Sensing*, Guildford Press, New York, NY., USA.

Carter, H. (1982) *The Study of Urban Geography*, Edward Arnold, Baltimore, MD., USA.

Cherry, G.E. (1974) *The Evolution of British Town Planning*, Leonard Hill, Beds, UK.

Clark, C. (1951) "Urban population densities", *Journal of the Royal Statistical Society (Series A)*, **114**, 490-496.

Cohen, J. (1960) "A coefficient of agreement of nominal scales", *Educational and Psychological Measurement*, **20**, 37-46.

Curran, P.J. (1985) *Principles of Remote Sensing*, Wiley, New York, NY., USA.

Curran, P.J. and Williamson, H.D. (1986) "Sample size for ground and remotely-sensed data", *Remote Sensing of Environment*, **20**, 31-41.

Dale, A., and Marsh, C. (1993) *The 1991 Census User's Guide*, HMSO, London, UK.

Davis, F.W. and Simonett, D.S. (1991) "GIS and remote sensing", in *Geographical Information Systems: Principles and Applications*, Maguire, D.J., Goodchild, M.F. and Rhind, D.W. (eds), Longman, London, UK., 191-213.

Davis, F.W., Quattrochi, D.A., Ridd, M.K., Lam, N.S-M., Walsh, S.J., Michaelsen, J.C., Franklin, J., Stow, D.A., Johannsen, C.J. and Johnston, C.A. (1991)

"Environmental analysis using integrated GIS and remotely-sensed data: some research needs and priorities", *Photogrammetric Engineering and Remote Sensing*, **57**, 689-697.

De Cola, L. (1989) "Fractal analysis of a classified Landsat scene", *Photogrammetric Engineering and Remote Sensing*, **55**, 601-610.

_____ (1993) "Multifractals in image processing and process imaging", in *Fractals in Geography*, Lam, N.S-N. and De Cola, L. (eds), Prentice-Hall, Englewood Cliffs, NJ., USA, 228-241.

De Jong, S.M. (1993) "Fractal analysis of digital images to classify land cover types", *Paper presented at the 25th International Symposium, Remote Sensing and Global Environment Change*, Graz, Austria, 4-8 April.

Dendrinos, D.S. (1992) *The Evolution of Cities*, Routledge, London, UK.

Dillon, W.R. and Goldstein, M. (1984) *Multivariate Analysis: Methods and Applications*, Wiley, New York, NY., USA.

DoE (Department of Environment) (1991) *Rates of Urbanisation in England 1981-2001*, Planning Research Programme, HMSO, London, UK.

_____ (1992) *Land Use Change in England No 7*, Statistical Bulletin (**92**) 4, Middlesex, UK.

Dreyer, P. (1993) "Classification of land cover using optimized neural nets on SPOT data", *Photogrammetric Engineering and Remote Sensing*, **59**, 617-621.

Dunn, C. and Boyle, P. (1991) "Point-based representations of socioeconomic data", in *New Ways of Representing Socioeconomic Data*, Martin, D.J. and Bracken, I. (eds), 24-34.

Dymond, J.R. (1993) "An improved Skidmore/Turner classifier", *Photogrammetric Engineering and Remote Sensing*, **59**, 623-626.

Edmonston, B., Goldberg, M.A. and Mercer, J. (1985) "Urban form in Canada and the United States: an examination of urban density gradients", *Urban Studies*, **22**, 209-217.

Ehlers, M., Edwards, G. and Bedard, Y. (1989) "Integration of remote sensing with geographic information systems: a necessary evolution", *Photogrammetric Engineering and Remote Sensing*, **55**, 1619-1627.

Ehlers, M., Greenlee, D. Smith, T., and Star, J.L. (1991) "Integration of remote sensing and GIS: data and data access", *Photogrammetric Engineering and Remote Sensing*, **57**, 669-675.

EOSAT (1990) *Sample Thematic Mapper Floppy Disk Data products*, Landsat Products Service, Sioux Falls, SD., USA, 25-26.

ERDAS Inc. (1991) *ERDAS (version 7.4) User's Manual*, Earth Resources Data Analysis Systems, Atlanta, GA., USA.

ERDAS Inc (1994) *ERDAS Imagine (8.1) User's Manual*, Earth Resources Data Analysis Systems, Atlanta, GA., USA.

ESRI Inc. (1990) *Understanding GIS: The Arc/Info Method*, Environmental Systems and Research Institute, Redland, CA., USA.

Estes, J.E., Hajic, E.J. and Tinney, L.R. (1983) "Fundamentals of image analysis of visible and thermal infrared data", in *Manual of Remote Sensing*, Colwell, R.N. (ed), American Society of Photogrammetry, Falls Church, VA., USA,

987-1124.

Evans, A.W. (1985) *Urban Economics: An Introduction*, Basil Blackwell, Oxford, UK. and New York, NY., USA.

Eyton, J.R. (1993) "Urban land use classification and modelling using cover-type frequencies", *Applied Geography*, **13**, 111-121.

Faust, N.L., Anderson, W.H. and Star, J.L. (1991) "Geographic information systems and remote sensing future computing environment", *Photogrammetric Engineering and Remote Sensing*, **57**, 655-668.

Fisher, P.F. and Pathirana, C. (1990) "The evaluation of fuzzy membership of land cover classes in the suburban zone", *Remote Sensing of Environment*, **34**, 121-132.

Fitzpatrick-Lins, K. (1980) "The accuracy of selected land use and land cover maps at scales of 1:250,000 and 1:100,000", *Journal of Research*, **6**, 169-173.

Foody, G.M. (1992) "A fuzzy sets approach to the representation of vegetation continua from remotely-sensed data: an example from lowland heath", *Photogrammetric Engineering and Remote Sensing*, **58**, 221-225.

Foody, G.M. and Campbell, N.A., Trodd, N.M. and Wood, T.F. (1992) "Derivation and applications of probabilistic measures of class membership from the maximum-likelihood classification", *Photogrammetric Engineering and Remote Sensing*, **58**, 1335-1341.

Forster, B.C. (1980) "Urban residential ground cover using Landsat digital data", *Photogrammetric Engineering and Remote Sensing*, **46**, 547-558.

_____ (1983) "Some urban measurements from Landsat data", *Photogrammetric Engineering and Remote Sensing*, **49**, 1693-1707.

_____ (1985) "An examination of some problems and solutions in monitoring urban areas from satellite platforms", *International Journal of Remote Sensing*, **6**, 139-151.

_____ (1993) "Coefficient of variation as a measure of urban spatial attributes, using SPOT HRV and Landsat TM data", *International Journal of Remote Sensing*, **14**, 2403-2409.

Foster, J.L. and Parkinson, C.L. (1993) "Indications and effects of human activities", in *Atlas of Satellite Observations Related to Global Change*, Gurney, R.J., Foster, J.L. and Parkinson, C.L. (eds), Cambridge University Press, Cambridge, UK, 425-447.

Fotheringham, A.S., Batty, M. and Longley, P.A. (1989) "Diffusion-limited aggregation and the fractal nature of urban growth", *Papers of the Regional Science Association*, **67**, 55-69.

Frankhauser, P. (1994) *La Fractalite des Structures, Urbaines*, Collection Villes, Anthropos, Paris, France.

Franklin, S.E. and Peddle, D.R. (1990) "Classification of SPOT-HRV imagery and texture features", *International Journal of Remote Sensing*, **11**, 551-556.

Gahegan, M. (1994) "A consistent user-model for a GIS incorporating remotely-sensed data", in *Innovations in GIS*, Worboys, M.F. (eds), Taylor and Francis, London, UK, 65-75.

Gong, P. and Howarth, P.J. (1990) "An assessment of some factors influencing

multispectral land-cover classification", *Photogrammetric Engineering and Remote Sensing*, **56**, 597-603.

Goodchild, M.F. and Mark, D.M. (1987) "The fractal nature of geographic phenomena", *Annals of the Association of American Geographers*, **77**, 265-278.

Goodchild, M.F., Anselin, L. and Deichmann, U. (1993) "A framework for the areal interpolation of socioeconomic data", *Environment and Planning A*, **25**, 383-397.

Goodenough, D.G. (1988) "Thematic Mapper and SPOT integration with geographic information system", *Photogrammetric Engineering and Remote Sensing*, **54**, 167-176.

Green, E.J., Strawderman, W.E. and Airola, T.M. (1993) "Assessing classification probabilities for thematic maps", *Photogrammetric Engineering and Remote Sensing*, **59**, 635-639.

Gurney, C.M. and Townshend, J.R.G. (1983) "The use of contextual information in the classification of remotely sensed data", *Photogrammetric Engineering and Remote Sensing*, **49**, 55-64.

Haack, B., Bryant, N. and Adams, S. (1987) "An assessment of Landsat MSS and TM data for urban and near-urban land-cover digital classification", *Remote Sensing of Environment*, **21**, 201-213.

Haggett, P., Cliff, A.D. and Frey, A. (1977) *Locational Analysis in Human Geography 1: Locational Models*, Arnold, London, UK.

Haig, R.M. (1926) "Toward an understanding of the metropolis", *Quarterly Journal of Economics*, **40**, 421-433.

Haralick, R.M. and Fu, K. (1983) "Pattern recognition and classification", in *The Manual of Remote Sensing*, Colwell, R.N. (ed), American Society of Photogrammetry and Remote Sensing, Falls Church, VA., USA.

Harris, C.D. and Ullman, E.L. (1945) "The nature of cities", *Annals of the Association of American Academy of Political and Social Science*, **242**, 7-17.

Harris, R. (1985) "Contextual classification post-processing of LANDSAT data using a probabilistic relaxation model", *International Journal of Remote Sensing*, **6**, 847-866.

Harrison, A.R. and Richards, T.S. (1987) *An Evaluation of General Purpose Classification Techniques for the Discrimination of Urban Land Use in SPOT Panchromatic and Multispectral Data*, Report to M.P.S.I. Systems Ltd., Bristol, UK.

He, C. (1989) "Development of remote sensing in China", *Space Policy*, **5**, 65-74.

Hill, J. and Megier, J. (1988) "Regional land cover and agricultural area statistics and mapping in the Department Ardeche, France, by use of Thematic Mapper data", *International of Remote Sensing*, **9**, 1573-1595.

Hixson, M.M., Scholz, D. and Fuhs, N. (1980) "Evaluation of several schemes for classification of remotely-sensed data", *Photogrammetric Engineering and Remote Sensing*, **46**, 1547-1553.

Hord, R.M. (1982) *Digital Image Processing of Remotely Sensed Data*, Academic, New York, NY., USA.

Hoyt, H. (1939) *The Structure and Growth of Residential Neighbourhoods in American Cities*, Washington, USA.

Hutchinson, C.F. (1982) "Techniques for combining Landsat and ancillary data for digital classification improvement", *Photogrammetric Engineering and Remote Sensing*, **48**, 123-130.

Huxhold, W.E. (1991) *An Introduction to Urban Geographic Information Systems*, Oxford University Press, New York, NY., USA.

Iisaka, J. and Hegedus, E. (1982) "Population estimation from Landsat imagery", *Remote Sensing of Environment*, **12**, 259-272.

Isard, W. (1956) *Location and Space Economy*, Massachusettes Institute of Technology, Cambridge, MA., USA.

Iversen, G.R. (1984) *Bayesian Statistical Inference*. Quantitative Applications in the Social Sciences, **43**, Sage, Beverley Hills, CA., USA, and London, UK.

Jackson. M.J., Carter, P., Smith, T.F. and Gardner, W.G. (1980) "Urban land mapping from remotely-sensed data", *Photogrammetric Engineering and Remote Sensing*, **46**, 1041-1050.

Janssen, L.L.F., Jaarsma, M.N. and Van Der Linden, E.T.M. (1990) "Integrating topographic data with remote sensing for land cover classification", *Photogrammetic Engineering and Remote Sensing*, **56**, 1503-1506.

Jensen, J.R., ed (1983) "Urban/suburban land use analysis", in *Manual of Remote Sensing*, Colwell, R.N. (ed), American Society of Photogrammetry, Falls Church, VA., USA, 1571-1666.

_____ (1986) *Introductory Digital Image Processing*, Prentice-Hall, Englewood Cliffs, NJ., USA.

_____ (1989) "Remote sensing in geography", in *Geography in America*, Gaile, G. and Williams, C.J. (eds), Merrill, Columbus, OH., USA, 746-775.

Jensen, J.R., Toll, D.L. (1982) "Detecting residential land-use development at the urban fringe", *Photogrammetric Engineering and Remote Sensing*, **48**, 629-643.

Kent, M., Jones, A. and Weaver, R. (1993) "Geographical information systems and remote sensing in land use planning: an introduction", *Applied Geography*, **13**, 5-8.

Kraus, S.P., Senger, L. and Ryerson, J.M. (1974) "Estimating population from photographically determined residential land use types", *Remote Sensing of Environment*, **3**, 35-42.

Lam, N. S-M. (1990) "Description and measurement of Landsat TM images using fractals", *Photogrammetric Engineering and Remote Sensing*, **56**, 187-195.

_____ (1993) "Spatial interpolation methods: a review", *American Cartographer*, **10**, 129-149.

Langford, M., Maguire, D.J. and Unwin, D.J. (1991) "The areal interpolation problem: estimating population using remote sensing in a GIS framework", in *Handling Geographical Information: Methodology and Potential Applications*, Masser, I. and Blakemore, R. (eds), 55-77.

Langford, M., Unwin, D.J. and Maguire, D.J. (1990a) "Generating improved population density maps in an integrated GIS", *Proceedings of the First*

European Conference on Geographical Information Systems, EGIS Foundation, Utrecht, The Netherlands.

_____ (1990b) "Mapping the density of population: continuous surface representations as an alternative to choroplethic and dasymetric maps", *Midlands Regional Research Laboratory, Research Report* **8**, University of Leicester, UK.

Latham, R.P. and Yeates, M. (1970) "Population density growth in metropolitan Toronto", *Geographical Analysis*, **2**, 177-185.

Lauer, D.T., Estes, J.E., Jensen, J.R. and Greenlee, D.D. (1991) "Institutional issues affecting the integration and use of remotely-sensed data and geographic information systems", *Photogrammetric Engineering and Remote Sensing*, **57**, 647-654.

Lillesand, T.M. and Kiefer, R.W. (1987) *Remote Sensing and Image Interpretation*, John Wiley and Sons, New York, NY., USA.

Lloyd, P.E. and P. Dicken (1977) *Location in Space: A Theoretical Approach to Economic Geography*, Harper & Row, New York, NY., USA.

Lo, C.P. (1986) *Applied Remote Sensing*, Longman, Harlow and London, UK.

_____ (1989) "A raster approach to population estimation using high-altitude aerial and space photographs", *Remote Sensing of Environment*, **27**, 59-71.

Lo, C.P. and Wu, C.Y.M. (1984) "New town monitoring from sequential aerial photographs", *Photogrammetric Engineering and Remote Sensing*, **50**, 1145-1158.

Longley, P.A., Batty, M. and Shepherd, J.W. (1991) "The size, shape and dimension of urban settlements", *Transactions, Institute of British Geographers, NS*, **16**, 75-94.

Lunetta, R.S., Congalton, R.G, Fenstermaker, L.K., Jensen, J.R., McGwire, K.C. and Tinney, L.R. (1991) "Remote sensing and geographic information system data integration: error sources and research issues", *Photogrammetric Engineering and Remote Sensing*, **57**, 677-687.

Mandelbrot, B.B. (1967) "How long is the coast of Britain? Statistical self-similarity and fractional dimension", *Science*, **156**, 636-638.

_____ (1983) *The Fractal Geometry of Nature*, W.H. Freeman and Company, San Francisco, CA., USA.

Marble, D.F. (1981) "Some problems in the integration of remote sensing and geographic information systems", *Proceedings of the Second Australasian Remote Sensing Conference*, Canberra, Australia.

Marble, D.F. and Peuquet, D.J. (1983) "Geographic information systems and remote sensing", in *The Manual of Remote Sensing*, Colwell, R.N. (ed), American Society of Photogrammetry and Remote Sensing, Falls Church, VA.

Marshall, J.U. (1989) *The Structure of Urban Systems*, University of Toronto Press, Toronto, Canada.

Martin, D.J. (1988) "An approach to surface generation from centroid-type data", *Technical Reports in Geo-information Systems, Computing and Cartography*, **5**, Wales and South West Regional Research Laboratory, Cardiff, UK.

_____ (1989) "Mapping population data from zone centroid locations",

Transactions, Institute of British Geographers, **14**, 90-97.

_____ (1991) *Geographic Information Systems and their Socioeconomic Applications*, Routledge, London, UK.

_____ (1994) "Using GIS to look at population change 1981-1991", *Paper presented at the Annual Conference of the British Geographers*, Nottingham, UK, 3-6 January.

Martin, D.J. and Bracken, I. (1991) "Techniques for modelling population-related raster databases", *Environment and Planning A*, **23**, 1069-1075.

Maselli, F., Conese, C., Petkov, L. and Resti, R. (1992) "Inclusion of prior probabilities derived from a nonparametric process into the maximum-likelihood classifier", *Photogrammetric Engineering and Remote Sensing*, **58**, 201-207.

Maselli, F., Conese, C., Zipoli, G. and Pittau, M.A. (1990) "Use of error probabilities to improve area estimates based on maximum likelihood classifications", *Remote Sensing of Environment*, **31**, 155-160.

Mason, D.C., Corr, D.G., Cross, A, Hoggs, D.C., Lawrence, D.H., Petrou, M. and Tailor, A.M. (1988) "The use of digital map data in the segmentation and classification of remotely-sensed images", *International Journal of Geographical Information Systems*, **2**, 195-215.

Mather, P.M. (1985) "A computationally-efficient maximum likelihood classifier employing prior probabilities for remotely-sensed data", *International Journal of Remote Sensing*, **6**, 369-376.

MCC (1992) *SASPAC User Manual: Parts 1 and 2*, Manchester Computing Centre, University of Manchester, UK.

McDonald, J.F. (1989) "Econometrics of urban population density: a survey", *Journal of Urban Economics*, **26**, 361-385.

McKeown, D.M., Harvey, W.A. and McDermott, J. (1985) "Rule-based interpretation of aerial imagery", *Proceedings of the IEEE Transactions on Pattern Analysis and Machine Intelligence*, **7**, 570-580.

Meakin, P. and Tolman, S. (1989) "Diffusion-limited aggregation: recent developments", in *Fractals' Physical Origins and Properties*, Pietronero, L. (ed), Plenum Press, New York, NY., USA, 137-168.

Mesev, T.V. (1991) *Suitability of Ancillary Data for Improving Post-image Classification of Mixed Hardwoods*, Unpublished Master's research paper, Geography Department, The Ohio State University, OH., USA.

_____ (1992) "Integration between remotely-sensed data and population surface models", *Paper presented at the Regional Science Association*, Dundee, UK, 15-18 September.

_____ (1993) "Population prior probabilities in urban image classification", *Paper presented at the Annual Meeting of the Association of American Geographers*, Atlanta, GA., USA, 6-10 April.

Mesev, T.V., Batty, M., Longley, P.A. and Xie, Y. (1995) "Morphology from imagery: detecting and measuring the density of urban land use", *Environment and Planning A* (in press).

Michalak, W.Z. (1993) "GIS in land use change analysis: integration of remotely-

sensed data into GIS", *Applied Geography*, **13**, 28-44.

Mills, E.S. (1970) "Urban density functions", *Urban Studies*, **7**, 5-20.

_____ (1992) "The measurement and determinants of suburbanisation", *Journal of Urban Economics*, **32**, 377-387.

Mills, E.S. and Tan, J.P. (1980) "A comparison of urban population density functions in developed and developing countries", *Urban Studies*, **17**, 313-321.

Morris, F.B. and Pyle, G.F. (1971) "The social environment of Rio de Janeiro in 1960", *Economic Geography*, **47**, 286-299.

Muth, R. (1969) *Cities and Housing: The Spatial Pattern of Urban Residential Land Use*, University of Chicago Press, Chicago, IL., USA.

Newcomer, J.A. and Szajgin, J. (1984) "Accumulation of thematic map error in digital overlay analysis", *American Cartographer*, **11**, 58-62.

Nordbeck, S. (1971) "Urban allometric growth", *Geografiska Annaler*, **53B**, 54-67.

OPCS (1984) *Key Statistics for Urban Areas*, Office of Population Censuses and Surveys, HMSO, London, UK.

OPCS (1991) *1991 Census User's Guides*, **1-45**, Office of Population Censuses and Surveys, General Register Office for Scotland, UK.

Openshaw, S. (1984) "The modifiable areal unit problem", *Concepts and Techniques in Modern Geography*, **38**, Geobooks, Norwich, UK.

Parr, J.B. (1985a) "A population-density approach to regional spatial structure", *Urban Studies*, **22**, 289-303.

_____ (1985b) "The form of the regional density function", *Regional Studies*, **19**, 535-546.

Peuquet, D.J. and Boyle, A.R. (1990) "Interactions between the cartographic document and the digitizing process", in *Introductory Readings in Geographic Information Systems*, Peuquet, D.J. and Marble, D.F. (eds), Taylor and Francis, Bristol, PA., USA, 215-221.

Piwowar, J.M., LeDrew, E.F. and Dudycha, D.J. (1990) "Integration of spatial data in vector and raster formats in geographical information systems", *International Journal of Geographical Information Systems*, **4**, 429-444.

Quarmby, N.A. and Cushnie, J.L. (1989) "Monitoring urban land cover changes at the urban fringe from SPOT HRV imagery in south-east England", *International Journal of Remote Sensing*, **10**, 953-963.

Quarmby, N.A., Cushnie, J.L. and Saull, R.J. (1988) "Remote sensing for real world applications", *Proceedings of Image Processing '88*, Blenheim Online, London, 151-162.

Raper, J., Rhind, D.W. and Shepherd, J.W. (1992) *Postcodes: The New Geography*, Longman, London, UK.

Rhind, D.W. (1983) *A Census Users Handbook*, Methuen, London, UK.

Richards, J.A., Landgrebe, D.A. and Swain, P.H. (1982) "A means for utilizing ancillary information in multispectral classification", *Remote Sensing of Environment*, **12**, 463-477.

Richter, D.M. (1969) "Sequential urban change", *Photogrammetric Engineering*, **35**, 764-770.

Robinson, A.H., Sale, R., Morrison, J. and Muehrcke, P. (1985) *Elements of*

Cartography, Wiley, Chichester, UK.

Rosenfield, G.H. and Fitzpatrick-Lins, K. (1986) "A coefficient of agreement as a measure of thematic classification accuracy", *Photogrammetric Engineering and Remote Sensing*, **52**, 223-227.

Sadler, G.J. and Barnsley, M.J. (1990) "Use of population density data to improve classification accuracies in remotely-sensed images of urban areas", *South East Regional Research Laboratory*, Working Report Number **22**, Birkbeck, London, UK.

Sander, L.M. (1987) "Fractal growth", *Scientific American*, **256**, 82-88.

Schmitt, S.A. (1969) *Measuring Uncertainty: An Elementary Introduction to Bayesian Statistics*, Addison-Wesley, Reading, MA., USA.

Schowengerdt, R.A. (1983) *Techniques for Image Processing and Classification in Remote Sensing*, Academic Press, New York, NY., USA.

Shepherd, J.W. and Congdon, P. (1990) "Small town England: an investigation into population change among small and medium-sized urban areas", *Progress in Planning*, **33**, 1-111.

Shelton, R.C. and Estes, J.E. (1981) "Remote sensing and geographical information systems: an unrealised potential", *Geo-Processing*, **1**, 395-420.

Shimoda, H., Fukue, K., Yamguchi, R., Zhang, Z. and Sakata, T. (1988) "Accuracy of land cover classification of TM and SPOT data", *Proceedings of IGARS Symposium*, Edinburgh, UK, ESA SP-284, 529-535.

Schlien, S. and Smith, A. (1975) "A rapid method to generate spectral theme classification of LANDSAT imagery", *Remote Sensing of Environment*, **4**, 67-77.

Sibley, D. (1971) "Density gradients and urban growth", *Urban Studies*, **8**, 294-297.

Skidmore, A.K. and Turner, B.J. (1988) "Forest mapping accuracies are improved using a supervised nonparametric classifier with SPOT data", *Photogrammetric Engineering and Remote Sensing*, **54**, 1415-1421.

Smeed, R.J. (1961) "The traffic problem in town", *Manchester Statistical Society Papers*, Norbury Lockwood, Manchester, UK.

Snedecor, G.W. and Cochran, W.G. (1967) *Statistical Methods*, Iowa State University Press, Ames, IO.

Stamp, L.D. (1962) *The Land of Britain, Its Use and Misuse*, Longman, London, UK.

Star, J.L., Estes, J.E. and Davis, F. (1991) "Improved integration of remote sensing and geographic information systems: a background to NCGIA initiative 12", *Photogrammetric Engineering and Remote Sensing*, **57**, 643-645.

Strahler, A.H. (1980) "The use of prior probabilities in maximum likelihood classification of remotely-sensed data", *Remote Sensing of Environment*, **10**, 135-163.

Strahler, A.H., Logan, T.L. and Bryant, N.A. (1978) "Improving forest cover classification accuracy from Landsat by incorporating topographic information", *Proceedings of the Twelfth International Symposium on Remote Sensing of Environment*, Environmental Research Institute of Michigan, MI., USA, 927-942.

Sui, D.Z. (1993) "Integrating neural networks with GIS for spatial decision making",

Operational Geographer, **11**, 13-20.

Swain, P.H. and Davis, S.M. (1978) *Remote Sensing: The Quantitative Approach*, McGraw-Hill, New York, NY.

Tatsuoka, M.M. (1971) *Multivariate Analysis: Techniques for Educational and Psychological Research*, Wiley, New York, NY., USA.

Thomas, I.L., Benning, V.M. and Ching, N.P. (1987) *Classification of Remotely-Sensed Images*, IOP, Bristol, UK.

Toll, D.L. (1984) "An evaluation of simulated TM data and Landsat MSS data for determining suburban and regional land use and land cover", *Photogrammetric Engineering and Remote Sensing*, **50**, 1713-1724.

Tomlin, C.D. (1990) *Geographic Information Systems and Cartographic Modeling*, Prentice-Hall, Englewood Cliffs, NJ., USA.

Treitz, P.M., Howarth, P.J. and Gong, P. (1992) "Application of satellite and GIS technologies for land-cover and land-use mapping at the rural-urban fringe: a case study", *Photogrammetric Engineering and Remote Sensing*, **58**, 439-448.

UMRCC (1989) *SASPAC User's Manual: volumes 1 and 2*, University of Manchester Regional Computer Centre, Manchester, UK.

Urban Renewal Administration, Housing and Home Finance Agency, and Bureau of Public Roads (1965) *Standard Land Use Coding Manual: A Standard System for Identifying and Coding Land Use Activities*, Washington D.C., USA.

Vicsek, T. (1989) *Fractal Growth Phenomena*, World Scientific Company, Singapore.

Wagner, D.F. (1989) *A Comparison and Evaluation of Three Polygon Overlay Algorithms*, GIS Technical Services, **TR 89-01**, Department of Geography, The Ohio State University, Columbus, OH., USA.

Walmsley, D.J. and Lewis, G.J. (1984) *Human Geography: Behavioural Approaches*, Longman, London, UK.

Wang, F. (1990) "Fuzzy supervised classification of remote sensing images", *IEEE Transactions on Geoscience and Remote Sensing*, **28**.

Wang, F., Treitz, P.M. and Howarth, P.J. (1992) "Road network detection from SPOT imagery for updating geographical information systems in the rural-urban fringe", *International Journal of Geographical Information Systems*, **6**, 141-157.

Webster, C.J., Oltof, W. and Berger, M. (1991) "Exploring the discriminating power of texture statistics in interpreting a SPOT satellite image of Harare", *Technical Report in Geo-Information Systems, Computing and Cartography*, **36**, Wales and South West Regional Research Laboratory, Cardiff, UK.

Welch, R. (1982) "Spatial resolution requirements for urban studies", *International Journal of Remote Sensing*, **3**, 139-146.

Witten, T.A. (1981) "Diffusion-limited aggregation, a kinetic critical phenomenon", *Physical Review Letters*, **47**, 1400-1403.

Witten, T.A. and Sander, L.M. (1981) "Diffusion-linked aggregation", *Physical Review B*, **27**, 5686-5697.

Wrigley, N. (1985) *Categorical Data Analysis for Geographers and Environmental Scientists*, Longman, New York, NY., USA.

Zhou, Q. (1989) "A method for integrating remote sensing and geographic information systems", *Photogrammetric Engineering and Remote Sensing*, **55**, 591-596.

Zielinski, K. (1979) "Experimental analysis of eleven models of population density", *Environment and Planning A*, **11**, 629-641.

_____ (1980) "The modelling of urban population density: a survey", *Environment and Planning A*, **12**, 135-154.